January 2020

Development Of A Novel Cardiac Ischemia-Reperfusion Model In The Axolotl

Jeremy Tolentino Llaniguez
Wayne State University, jllaniguez@gmail.com

DEVELOPMENT OF A NOVEL CARDIAC ISCHEMIA-REPERFUSION MODEL IN THE AXOLOTL

by

JEREMY (JAY) TOLENTINO LLANIGUEZ

DISSERTATION

Submitted to the Graduate School

of Wayne State University,

Detroit, Michigan

in partial fulfillment of the requirements

for the degree of

DOCTOR OF PHILOSOPHY

2018

MAJOR: BIOMEDICAL ENGINEERING

Approved By:

_____

Advisor: Juri G. Gelovani, MD, PhD Date

_____

Mai T. Lam, PhD Date

_____

Tara M. Cotroneo, DVM Date

_____

Ryan Thummel, PhD Date

DEDICATION

This body of work is dedicated to my parents, Carson Austria Llaniguez and Nora Tolentino Llaniguez; and my sister, Ronnylyn Tolentino Llaniguez; for their continual support during my MD/PhD training. Even though we have been located countries and states apart, respectively, their love is felt as if they are here with me in the heart of Detroit. I must also mention my two grandmothers – Barbara Austria Llaniguez and Fe Seril Tolentino. Although they unfortunately passed away much too early, they were the bows to me – the arrow. They were formative in pointing me in the right direction – continually pushing me to find my purpose and meaning in life.

My extended family, the Urfanos and my adopted family from the Pangan clan and the entire tribe including the Rojases, Sankers, et al. spread everywhere from California, Oregon, Washington, and Tennessee. Although your Kuya has not always been around, whenever I see your beautiful faces, it is like I never left home. Your support has maintained me as I have pursued my academic endeavors from Berkeley, Cambridge, and now Detroit.

ACKNOWLEDGMENTS

Scientists should axolotl good questions that are testable by science-driven, hypothesis-based experiments. My mentors have been instrumental in helping me think critically about problems to axolotl questions. I would like to thank my advisor Dr. Juri G. Gelovani with helping me develop this project with early *gedankenexperiments*; the members of my dissertation committee – Dr. Mai T. Lam, Dr. Tara M. Cotroneo, and Dr. Ryan Thummel; Dr. DiCarlo and his insight into cardiovascular physiology and his masterful rodent surgeon Dr. Lujan; the research staff of DLAR at Wayne State University, Dr. Voss and the Muzinics of the Ambystoma Genetic Stock Center at the University of Kentucky; Dr. Jeffrey Nelson from Dr. James Thomson's laboratory at the University of Wisconsin – Madison.

My peers in medical school, graduate school, and the American Medical Association have been instrumental in making me feel human while I tackled this ambitious research project. Their support is appreciated and will never be forgotten. They have kept me grounded, reminded me of my purpose – to disrupt healthcare and be a change agent for patients, and have framed my efforts as a stepping stone to making an impact in the field of medicine. Thank you all.

All work towards earning my MD and PhD degrees has been generously powered by: Dessert Oasis Coffee Roasters, Great Lakes Coffee Roasting Company, ASHE Supply Co, and Avalon International Breads. Many thanks to the amazing staff that have keep me fueled and awake to pursue my passions.

TABLE OF CONTENTS

LIST OF FIGURES

LIST OF TABLES

CHAPTER 1: PROJECT INTRODUCTION

The leading cause of death in the US and worldwide result from cardiovascular diseases such as myocardial infarction (MI), that due to the lack of cardiac tissue regeneration or repair often leads to death. In contrast to the tissue response in humans and other mammals after injury, non-mammalian vertebrate species such as the axolotl (*Ambystoma* mexicanum) and zebrafish (*Danio rerio*) exhibit increased regenerative capacity for limbs and other organs, including the heart. With the recognized limitations of pharmacotherapy of myocardial infarction (MI) in human patients, cell-based therapies have been undergoing rapid development and clinical testing. However, there is still no consensus about cell types, delivery routes, dosing and treatment schedules and pretreatment conditioning of cells prior to administration. This lack in understanding the mechanisms behind the cell-cycle of cardiomyocytes and or cardiac progenitor cells, both during times of normal homeostasis and after pathologic insults, is central to the lack of progress in stimulating the regeneration of cardiac tissue. To understand the differences in cardiac tissue response after an MI, developing a true model of ischemia-reperfusion injury in an animal known for epimorphic regeneration in the adult life stage will help reframe the direction of research in the field of tissue engineering and regenerative medicine in the realm of cardiology.

CHAPTER 2: PROJECT SUMMARY & HYPOTHESIS

Multiple studies using non-mammalian vertebrates have been published showing cardiac tissue regeneration and remodeling after traumatic cardiac injury, but the methods described to induce cardiac tissue trauma and necrosis do not recapitulate the cellular mechanisms that are well-known in ischemia-reperfusion injury. With challenging access to coronary arteries in the zebrafish (Hu et al., 2001) to the lack of coronary arteries in salamanders (Francis, 1934), surrogate injury modalities have been used to injury the heart in these laboratory animals. The more commonly used injury methods include: cryoinjury, conditional genetic ablation, and ventricular (apical) resection. Although these injuries can occur in human patients, the conclusions from these experiments cannot be broadly applied to all cardiac injuries. Thus, with the literature published to date, it is yet to be concluded whether an adult vertebrate animal can recover from an ischemia-reperfusion injury to the heart.

Although little to no publications on cardiac tissue response after ischemia-reperfusion injuries are available in non-mammalian vertebrates, there is overwhelming evidence regarding the regeneration capabilities of salamanders. Salamanders are known to regenerate almost any organ or limb throughout their lifespan(Roy and Gatien, 2008). From these conclusions, the following hypothesis is proposed:

> "The axolotl, an animal capable of healing damaged organs and limbs throughout its lifespan through the process of epimorphic regeneration, can regenerate a cardiac ischemia-reperfusion injury as an adult."

To understand how the axolotl heart responds to an ischemia-reperfusion injury that recapitulates a myocardial infarction, this research project focused on two Specific Aims,

discussed in CHAPTER 3: SPECIFIC AIMS. The results of the two Specific Aims show that following an ischemia-reperfusion injury, the axolotl heart can clear necrotic cardiac tissue from the injury site and replace it with nascent myocardium. The spatiotemporal process that is observed in histological preparations show an evolving injury that is unlike the repair and regeneration process described in zebrafish and mammals. These findings provide new and exciting avenues of exploration to elucidate the molecular signaling mechanisms responsible for cardiac repair in the axolotl with the goal of translating these findings to human patients.

CHAPTER 3: SPECIFIC AIMS

From the late 1950s, the age-adjusted death rate due to diseases of the heart has fallen from almost 600 deaths per 100,000 U.S. residents to just over 190 deaths per 100,000 U.S. residents today. With the recognized limitations of pharmacotherapy of myocardial infarction (MI), cell-based therapies have been undergoing rapid development and clinical testing. However, there is still no consensus about: 1) the most appropriate cell type; 2) the most appropriate delivery routes; 3) the effective doses and treatment schedules; and 4) genetic modifications and/or pretreatment conditioning of cells (e.g. drugs, growth factors, cytokines) prior to administration. Furthermore, several fundamental questions about cardiac tissue regeneration remain unanswered. Specifically, what is the reason for the poor capacity for tissue regeneration and remodeling in humans (mammals in general), as compared to robust regeneration seen in non-mammalian vertebrates, such as the axolotl (*Ambystoma mexicanum*) and zebrafish (*Danio rerio*)? Can cellular processes and regulatory mechanisms involved in axolotl heart regeneration be exploited and reactivated in the injured human myocardium to treat sequelae of MI? The lack of understanding cell-cycle regulation governing cardiomyocyte growth, division, and proliferation, both in normal and pathologic states, is a major hurdle in understanding the regenerative potential in cardiac tissue. By comparing the response to injury in animals that show a robust regenerative response, details behind cardiomyocyte and cardiac progenitor biology in mammals can be dissected. *The central hypothesis that continues to remain unanswered in the field of cardiac regenerative biology is can an ischemic cardiac injury be fully regenerated in an adult vertebrate animal, without the aid of external genetic manipulation or administration of cell-based therapies.*

Observations from recent pre-clinical animal studies and clinical trials of stem cell-based therapies of MI have so far left unchanged conclusions made in the late 1970s by Dr. Pavel P. Rumyantsev: “The lack of unanimity concerning the extent of cardiac muscle regeneration and its mechanisms in orthodox histological studies obliges us to describe in more detail data based on the use of modern cytological methods”. Therefore, the major goal and innovative aspect of this project is to determine if a true ischemic cardiac injury can be fully regenerated in an adult animal that is capable of epimorphic regeneration. To this end, we will pursue the following Specific Aims:

Specific Aim 1: Develop a cardiac injury model in the axolotl that mimics the pathophysiology of a myocardial infarction in the mammalian heart. Past studies in zebrafish and axolotls have used cardiac injury models that do no recapitulate cardiac ischemia. We will pursue the development of a true ischemic cardiac injury model in the axolotl that, when performed in a mammalian model, produces similar pathology to a left anterior descending artery ligation. As part of the surgical procedure development, all pre-, peri-, and post-operative animal care and welfare must be established.

Specific Aim 2: Determine the spatiotemporal progression of axolotl cardiac tissue histopathology over time. Following the development of the pre-, peri-, and post-operative procedures to enable appropriate animal welfare after major survival surgery, long-term follow-up experiments will provide information on the spatiotemporal processes that occur after an ischemic cardiac event in the axolotl. Non-invasive, functional imaging will allow periodic tracking of cardiac function over time.

CHAPTER 4: BACKGROUND AND LITERATURE REVIEW

Background and Significance of Cardiovascular Disease

In spite of the steady improvement in heart failure therapy (Jakob and Landmesser, 2013), cardiovascular disease still ranks as the number one cause of death in the US (Murphy et al., 2013; Xu et al., 2016) and worldwide (Organization, 2017). With the recognized limitations of current pharmacological supportive care for myocardial infarction (MI), cell-based therapies have been undergoing rapid laboratory bench work development and clinical bedside testing.

Initial work in cell therapy started with the transplantation of skeletal myoblasts in rats and rabbits (Murry et al., 1996; Taylor et al., 1998; Taylor et al., 1997). However, since skeletal muscle cell ultrastructure (Kijima et al., 1993) and physiology (Lilly, 2011) greatly differs from that of cardiomyocytes, such as the requirement in cardiomyocytes of an extracellular influx of calcium to promote calcium-induced calcium release (CICR) excitation-contraction coupling (Fabiato and Fabiato, 1979), problems of arrhythmogenesis damped progress (Abraham et al., 2005; Fernandes et al., 2006; Menasche et al., 2008). Excitement for cell-based therapy reemerged in 2001 (Jackson et al., 2001; Orlic et al., 2001) after it was reported that in mouse models of myocardial ischemia cardiac side population cells [a subtype of cardiac stem cells (Ellison et al., 2010; Jackson et al., 2001)] and bone marrow cells (Orlic et al., 2001) generate new myocardium *de novo* by differentiating into cardiomyocytes (CMs). Extending this excitement was modern histological confirmation for human cardiomyocyte proliferation after myocardial infarction (MI) (Beltrami et al., 2001). These studies provided the basis of using adult stem cells as a new mode of therapy for repairing pathologic cardiac tissue either by stem cells differentiating into new cardiomyocytes or facilitating the self-repair of damaged

cardiomyocytes. The safety and feasibility of using adult stem cells to stimulate cardiac regeneration in animal models of myocardial ischemia led to the first in-man feasibility study documented in a case report in 2001, proving that intracoronary administration of autologous bone marrow cells could be used to regenerate myocardium after an MI (Strauer et al., 2001).

Contrasting these results, other studies soon pointed out that these hematopoietic stem cells adopt mature hematopoietic fates in damaged myocardium (Balsam et al., 2004; Murry et al., 2004); transdifferentiation of bone marrow stem cells does not unanimously account for cardiac tissue regeneration. Other mechanisms proposed for cardiac regeneration through cell-based therapy include: nuclear reprogramming of damaged tissue by fusion (Nygren et al., 2004; Yang et al., 2012) or the rescue of damaged tissue by paracrine factors (Gnecchi et al., 2008; Segers et al., 2007). Conversely, other studies found that facilitating the repair of damaged tissue is not the mechanism, rather the stimulation of endogenous cardiac precursors to create new myocardium leads to cardiac repair (Limana et al., 2007; Loffredo et al., 2011).

The lack of consensus for the mechanisms behind cardiac repair (Lovell and Mathur, 2010) as a barrier to progress is not a new insight. The idea that cardiac tissue can regenerate was first observed in rabbits and frogs in 1875 by Zielonko (Zielonko, 1875). Recent studies in 1-day versus 7-day old neonatal mice (Haubner et al., 2012; Porrello et al., 2011) reconfirmed experiments from the early 1900s [reviewed in (Rumyantsev, 1977)] that cardiac damage can be perfectly remodeled when performed on neonatal animals. However, if the same injuries are performed on slightly older animals, the heart reverts to healing by scarring mechanisms found in adults. Thus, the argument can be made that the genetic programs for cardiac repair exist within adult mammalian DNA, but are somehow repressed. Although this is a logical deduction, what has not

been confirmed is that early, adult vertebrate animals can completely regenerate their hearts through epimorphosis, fully recovering the original structure and function of the heart. Although prior studies in non-mammalian vertebrates like zebrafish and newts have given researchers hope that cardiac injuries can fully recovery after severe injury, studies to date have not confirmed this ability in a true model of cardiac ischemia.

Is Cardiac Tissue Regeneration and Repair in Humans Even Possible?

The proverbial "elephant in the room" in cardiovascular disease research is the argument that the heart is a post-mitotic organ, incapable of healing itself after it is injured. In this discussion of the background and literature review on cardiac muscle repair, discussing this long-held dogma will take priority before delving into the clinical relevance of regenerating native human heart tissue.

The heart has traditionally been considered a post-mitotic organ (Anversa et al., 1986; Anversa et al., 1990; Barja and Herrero, 2000; Korecky and Rakusan, 1978; Pollack et al., 2002), mainly due to the historical acceptance that little or no cardiac tissue is replaced during normal aging, or repaired after injury or secondary to cardiac dysfunction (e.g. cardiac myopathies). If heart tissue inherently lacks the ability to divide, proliferate, or show any other signs of cellular dynamics, then advancing research within the field of regenerative medicine for cardiac tissue would not be realistic or rational. However, since the first question arouse about the post-mitotic state of the mammalian heart in the early 1990s (Rumyantsev and Carlson, 1991), evidence has been accumulating that the mammalian heart retains the capability to renew cardiomyocytes during the life of the animal; otherwise, any remaining cardiomyocytes in the heart would be present from birth, be the same age as the individual, and any cardiomyocytes lost with age or

as a consequence of disease would not be replaced. Still, although the evidence has been identified, the magnitude of cardiomyocyte cellular dynamics in rodents and human is highly debated, ranging from less than a 1% rate of cardiomyocyte renewal per year in adult mammals up to a rate of 40% in humans or 80% in mice [reviewed in (Bergmann and Jovinge, 2014)].

The debate behind the rate of cardiomyocyte renewal revolves around the assumptions made about cardiomyocyte cellular dynamics, the methodologies used to identify proliferating and dividing cardiomyocytes, and the origin of new cardiomyocytes (if new cardiomyocytes are even formed). Supporting the idea that the heart is a dynamic organ was the identification of apoptotic (Cheng et al., 1995; Narula et al., 1996; Olivetti et al., 1997; Olivetti et al., 1996) and necrotic myocytes (Collinson and Gaze, 2007; Kajstura et al., 1996; Mahajan and Jarolim, 2011; Omland et al., 2009) in aging and failing hearts. In relation to cellular dynamics, to quantify the extent of cardiomyocyte turnover, what is required is the frequency of cell death and the duration of the apoptosis-necrosis cell phenotype. The wide range in estimates of cellular turnover are exacerbated by the ongoing disagreement concerning the frequency of occurrence of apoptosis, necrosis, oncosis, and autophagy within the heart (Anversa and Kajstura, 1998; Kostin et al., 2003). Additionally, there is currently no consensus on the timeframe of the apoptosis-necrosis sequence in cardiomyocytes, with estimates ranging from a few hours to a few days (Bergmann and Jovinge, 2014; Rodriguez and Schaper, 2005).

Compounding the lack of consensus in cardiomyocyte cellular dynamics, the biochemical methods used to quantify the number of cells proceeding through various cellular phenotypes have also been heavily criticized. DNA fragmentation during apoptosis can be identified through DNA gel electrophoresis, the TUNEL (**T**erminal Deoxynucleotidyl Transferase d**U**TP **N**icked-**E**nd

Labeling) assay, or the Taq polymerase-mediated in situ ligation assay (Takemura et al., 2013). However, DNA fragmentation in and of itself is not a specific indicator of apoptosis; necrosis and aspects of normal cellular behavior such as DNA repair and RNA synthesis result in oligonucleosomal DNA fragmentation or DNA nicks (Bergmann and Jovinge, 2014; Takemura et al., 2013). Similarly, caspases are important signals in the apoptosis cascade (Cohen, 1997; Earnshaw et al., 1999) and measuring their activation can quantify the magnitude of apoptosis. However, caspases also function as secondary signals in cellular proliferation, cellular differentiation, cell-cycle regulation, and cell-survival pathways (Takemura et al., 2013). To date, no biochemical markers definitively pinpoint a cell undergoing apoptosis with complete specificity; only morphological observations of the cellular phenotype can incontrovertibly identify an apoptotic cardiomyocyte. Surprisingly, since the identification of apoptotic myocytes in the mid-1990s (Cheng et al., 1995; Narula et al., 1996; Olivetti et al., 1997; Olivetti et al., 1996), not one cardiomyocyte expressing the ultrastructural morphology that defines apoptosis has been identified in a failing human heart or in animal models of heart failure (Takemura et al., 2013).

In parallel to the problems of published methods to biochemically assess apoptosis, controversies remain when assessing the extent of cardiomyocyte proliferation. The most common tools used to study cardiomyocyte proliferation are immunohistochemical markers of DNA synthesis using antibodies against the Ki-67 nuclear and nucleolar protein (Duchrow et al., 1995; Endl and Gerdes, 2000; Gerdes et al., 1984; Scholzen and Gerdes, 2000) or the phosphorylation of Ser^{10} on histone 3 (H3 phosphorylation into pH3) (Goto et al., 1999; Gurley et al., 1973; Hendzel et al., 1997). However, taking snapshots of a cell cycle with an unknown

timescale and preparing slices of tissue with an unknown frequency of proliferating cells in the organ at large are major *a priori* limitations in estimating the frequency and magnitude of proliferating cells. Additionally, it is not guaranteed, based on the presence of these proliferation markers, if the cell will divide into two daughter diploid cardiomyocytes or form a single polyploid or multinucleated cardiomyocyte (Bergmann and Jovinge, 2014; Bergmann et al., 2015). Furthermore, if renewed cardiomyocytes are partially (or fully) derived from the differentiation of cardiac stem or progenitor cells, the proliferating cell population that eventually will contribute to mature cardiomyocytes will not be identified by the co-staining used to identify cycling cells within the heart that express a cardiomyocyte lineage. This will severely underestimate the rate of cardiomyocyte cellular dynamics. In this regard, rather than indicating a phase in mitosis [e.g. Ki-67 for G1, S, G2 and M-phase or phosphorylated histone 3 for M-phase (Senyo et al., 2014)] birth markers that are incorporated into the newly synthesized DNA of proliferating cardiomyocytes or cardiomyocyte progenitors are required to "chase" the lineage commitment of the daughter cell, prompting the use of thymidine analogs to prospectively label proliferating cells. Thymidine analogs such as tritiated thymidine, halogenated bromodeoxyuridine (BrdU), and iododeoxyuridine (IdU) are commonly used in animal models, but their use in humans outside of sensitizing tumors to radiation therapy (BrdU and IdU) (Kinsella et al., 1987; Kinsella et al., 1984) is challenging. Although these birth-marker experiments have provided insight into cardiomyocyte cellular dynamics in model animals and humans (as a consequence of the treatment of underlying cancers), the use of halogenated pyrimidine analogs are not immune from confounds relying upon the detection of a fluorescent signal from a secondary antibody against the specific, primary antibodies against BrdU and IdU; the autofluorescence of

myocardium complicates any method relying upon fluorescence detection (Steinhauser and Lee, 2011). Furthermore, although these birth markers label more than just a phase of the cardiomyocyte in mitosis, they still label a subset of cells within the heart that rarely undergo cellular proliferation, making the choice of tissue section an important aspect in determining dynamics on the cellular level. Finally, the use of nucleotide analogs to label cells undergoing DNA synthesis is not specific to the process of semiconservative DNA replication – it also occurs during DNA repair. Semiconservative DNA replication is also not specific to one process – only an indicator of S-phase cell cycle progression. Without additional markers, nucleotide incorporation assays cannot differentiate between cells undergoing polynucleation, polyploidization, or cells that will simply stop at the G2/M checkpoint (Leone et al., 2015).

More recently, a novel method has been established to retrospectively birth-date cardiomyocytes by comparing levels of ^{14}C within their DNA to atmospheric levels of ^{14}C. This method, relying upon the spike of atmospheric ^{14}C levels from above-ground testing of nuclear weapons prior to the Treaty Banning Nuclear Weapon Tests in the Atmosphere, in Outer Space and under Water (abbreviated as the Partial Test Ban Treaty) of 1963, treats the time of increased nuclear testing as the DNA labelling pulse with the period following the ban as the "chase" (Spalding et al., 2005). The levels of ^{14}C since 1963 have been carefully studied, and given the half-life of ^{14}C ($t_{½}$ = 5730 years), the decrease in [^{14}C] is attributed not to its radioactive decay, but its diffusion into the biosphere. A seminal study of the application of this technique to cardiomyocytes was first published in 2009 (Bergmann et al., 2009) and extended with the addition of stereologic techniques in 2015 (Bergmann et al., 2015), concluding that cardiomyocyte turnover decreases exponentially with age – young children were shown to have

cardiomyocyte birth rates of 4-5% per year, while by 20 years of age, adults were shown to have a turnover rate of <1% per year. However, although this technique relies on the stability of DNA after a cell has performed its last cellular division (Bergmann et al., 2009; Spalding et al., 2005), cell preparation for analysis can lead to confounding factors. To analyze cardiomyocyte nuclei using the method developed by Spalding et al. (Spalding et al., 2005), tissue must be digested and the cardiomyocyte nuclei sorted using fluorescence-activated cell sorting (FACS) technology. Not only do the aforementioned issues of using appropriate lineage markers to identify proliferating cardiomyocytes and/or cardiac progenitors and the autofluorescence of elastin, collagen, and lipids (Marcu, 2010) found in the matrix of myocardial tissue (Sullivan et al., 2014) affect this approach, but any contamination that remains after the digestion and isolation of cardiomyocyte nuclei can introduce bias into the analysis (Steinhauser and Lee, 2011).

In addition to the controversy over the rate of cardiomyocyte dynamics within the adult mammalian heart, there is an ongoing debate about the cellular source responsible for cardiomyocyte turnover in adult mammals, with groups publishing data championing on the one hand cardiac stem or progenitor cells (Bollini et al., 2011; Ellison et al., 2013; Hsieh et al., 2007; Mayfield et al., 2014; Nadal-Ginard et al., 2014; Smart et al., 2011) and on the other hand pre-existing cardiomyocytes (Ali et al., 2014; Engel, 2005; Mollova et al., 2013; Porrello et al., 2013; Senyo et al., 2013; van Berlo et al., 2014; van Berlo and Molkentin, 2014; Zacchigna and Giacca, 2014). Reviews assessing the literature at large attribute the disparate experimental materials and methods as an underlying cause of the ongoing controversy, with groups using different animals and dissimilar approaches for performing the genetic-fate mapping studies to discern the origin of cardiomyocyte renewal (Milasinovic and Mohl, 2015; van Berlo and Molkentin,

2014). Recently, a new consensus is beginning to emerge, allowing for the contribution of both sources of cells to play a role in cardiomyocyte cellular dynamics; during homeostasis, cardiomyocyte turnover may occur predominantly through the proliferation of pre-existing cardiomyocytes, while after injury, cardiac stem and progenitor cells are engaged alongside pre-existing cardiomyocytes to repair lost or damaged myocardium (Bergmann and Jovinge, 2014; Malliaras et al., 2013; Senyo et al., 2014).

Although the field is slowly converging, what is clear from the literature is that the heart can no longer be viewed as a post-mitotic organ full of quiescent cardiomyocytes, an idea called into question decades ago (Rumyantsev and Carlson, 1991) and proven with modern cytological studies. What can be concluded is that the low-rates of cardiomyocyte turnover are insufficient to repair the approximately one billion cardiomyocytes that are typically lost after an MI (Frangogiannis, 2015; Laflamme and Murry, 2005). With clear evidence of full regeneration after extensive injury in the hearts of non-mammalian vertebrates [such as zebrafish and newts (Becker et al., 1974; Oberpriller and Oberpriller, 1974; Poss et al., 2002)] and neonatal mice (Haubner et al., 2012; Porrello et al., 2011), momentum is moving the field of cardiac regeneration towards the promise that the adult mammalian heart can endogenously repair itself with functioning, well-integrated, *de novo* cardiomyocytes. In summary, the adult mammalian heart shows dynamic cell turnover, so therefore it is rational and realistic to continue to foray into the field of regenerative medicine for cardiac tissue, elucidating the mechanisms behind the cell-cycle control of both healthy and damaged cardiac tissue to provide a better understanding on how to enable the self-repair of damaged myocardium.

Cardiac Injury Models

Salamanders, including axolotls, have been extensively studied as model organisms for tissue regeneration (Brockes, 1997; Cano-Martinez et al., 2010; Chalkley, 1954; Hay and Fischman, 1961; Khattak et al., 2013; Monaghan and Maden, 2012; Neff et al., 1996; Rose, 1948; Rose and Rose, 1952; Roy and Gatien, 2008; Simon, 2012; Singh et al., 2010; Sobkow et al., 2006; Voss et al., 2009; Whited and Tabin, 2010; Whited et al., 2013). Older studies observed gross changes in anatomy and histology (Chalkley, 1954; Hay and Fischman, 1961; Rose, 1948) ; more recently, regeneration has been examined using modern molecular tools (Khattak et al., 2013; Monaghan and Maden, 2012; Sobkow et al., 2006; Whited et al., 2012; Whited et al., 2013). The standard approach to induce repeatable and reproducible ischemic damage in a rodent is to perform a left anterior descending (LAD) coronary artery ligation to effectively recapitulate the pathogenesis of an atherosclerotic infarction in a human (Salto-Tellez et al., 2004; Wang et al., 2006). However, performing the same procedure is impossible in amphibians. Phylogenetically less evolved, amphibians have trabeculated ventricular myocardium (Stocum, 2006). Instead of relying upon coronary arteries to nourish the beating ventricular myocardium, oxygen and nutrients in the blood infiltrate the numerous sinuses formed by the myocardial trabeculations (Reese et al., 2002; Stocum, 2006). Therefore, for purposes of translating the findings in the axolotl to mammalian species, developing an identical approach to inducing myocardial ischemia in both animals is paramount to the success of this plan of work.

To induce cardiac injury in model animals without coronary arteries, methods such as cryoinjury/cryoablation (Gonzalez-Rosa et al., 2011; van den Bos et al., 2005), diphtheria-toxin conditional genetical ablation (Akazawa et al., 2004; Wang et al., 2011), or apical resection

(Porrello et al., 2011; Poss et al., 2002) have been implemented. Although these approaches result in serious cardiac tissue trauma or reduction in cardiac function, the injury processes do not recapitulate the pathogenesis of cellular dysfunction akin to ischemia-induced or ischemia-reperfusion-induced cardiac tissue necrosis. Although gross tissue histology may not dramatically differ from healing infarcted tissue, signaling mechanisms responsible for cell death are different.

Injury Due to Ischemia and Ischemia-Reperfusion

The principle cellular locations and biochemical mechanisms responsible for cellular injury that lead to necrosis or apoptosis are: 1) mitochondrial damage leading to reductions in adenosine triphosphate (ATP) production and increases in the production of reactive oxygen species (ROS); 2) loss of calcium-ion (Ca^{2+}) homeostasis leading to mitochondria damage and inappropriate activation of cellular enzymes; 3) loss of plasma and lysosomal membrane integrity leading to extracellular outflow of intracellular components through the damaged plasma membrane or the enzymatic degradation of intracellular components from the leakage of acid hydrolases normally sequestered in lysosomes; and 4) protein misfolding and DNA damage due to the loss of homeostatic intracellular conditions (Robbins et al., 2010). These general mechanisms of cell death are interrelated and injurious stimuli may simultaneously trigger multiple mechanisms, making it difficult to assign cell injury in a setting to a single dominant biochemical derangement or intracellular locale. However, in ischemia, the fundamental cause of necrosis is reduction of ATP levels (Robbins et al., 2010), causing multiple downstream effects.

Depletion of ATP and Rise of AMP/ADP Levels

The loss of blood flow to the heart in ischemia affects ATP levels in two fundamental ways: 1) a reduction in oxygen levels (hypoxia) necessary for oxidative phosphorylation of adenosine

diphosphate (ADP) in mitochondria and 2) a reduction in nutrients that can be oxidized by functioning mitochondria or processed through anaerobic glycolysis in the cytoplasm of myocardium. Energy stored in the phosphate of ATP is required for almost all transport mechanisms, biochemical syntheses, and component turnover/degradation processes within the cell. Unlike most tissues in the body, the heart cannot increase oxygen extraction from hemoglobin in the blood on demand using physics behind the oxygen-hemoglobin dissociation curve – at rest, left ventricular myocardial oxygen consumption is high with very efficient oxygen extraction (~75%) resulting a low coronary venous oxygen tension (~18 mmHg) (Tune et al., 2004). ATP levels begin to fall within 1-2 minutes of cardiac ischemia and within 10 minutes of cardiac ischemia, ATP levels have dropped to 50% of normal (Lilly, 2011); notably a 5-10% drop in normal ATP levels lead to widespread derangements in many critical cellular systems (Robbins et al., 2010).

As ATP levels begin to wane, the activity of primary active transport systems is affected. Reduced activity of the sodium-potassium ATPase (ouabain-sensitive Na^+, K^+-ATPase) allows sodium ions diffusing into the cell through to accumulate and simultaneously fails to replace intracellular levels of potassium ions that have diffused out of the cell. In addition to these two cations, decreased ATP levels affect two primary active transporters that lead to the intracellular accumulation of calcium ions: the plasma-membrane calcium ATPase (PMCA) becomes less effective at moving calcium ions back to the external environment while the sarcoplasmic/endoplasmic reticulum calcium ATPase (SERCA) becomes less responsive in sequestering Ca^{2+} in the sarcoplasmic reticulum (for the next cycle of calcium-induced calcium release that links electrical excitation and physical contraction). Furthermore, calcium ions are

further trapped inside the cytoplasm as ATP levels drop since the major calcium exporter in the cell is the sodium-calcium exchanger (NCX), an antiporter transport protein that exchanges three sodium ions for each calcium ion. Since NCX exchanges ions in opposite directions based only on concentration gradients, as ATP levels fall and sodium concentrations are impaired and reversed due to the reduced activity of the sodium-potassium ATPase, the NCX begins to import calcium into the cell instead of export calcium to the extracellular environment – the increased [Ca^{2+}] also further activates ATPases exacerbating ATP depletion. From the standpoint of impaired non-penetrating solute handling, the net gain of non-penetrating solute is followed by isosmotic movement of water, causing cellular swelling and dilation of the endoplasmic reticulum (ER).

Failing to produce ATP results in increases in rising levels of less energetic nucleotides within the cell. Without oxygen acting as the final electron receptor in oxidative phosphorylation (which also prevents the Krebs cycle from operating since it requires aerobic conditions - coenzymes NADH and $FADH_2$ generated in the Krebs cycle need to be oxidized in oxidative phosphorylation, or else the falling [NAD^+]/[NADH] ratio inhibits the Krebs cycle (Nelson et al., 2017)), levels of adenosine monophosphate (AMP) and ADP begin to rise. In conjunction with the lack of glucose substrate delivery due to ischemia, glycogenolysis is enhanced as AMP stimulates glycogen phosphorylase *a* and *b* activity to break down glycogen stores. Furthermore, in combination with increasing levels of powerful agonists (AMP, ADP and inorganic phosphate) and decreasing levels of strong antagonists (ATP and citrate), the activity of phosphofructokinase is heavily activated and eventually becomes autocatalytic as its reaction product (fructose 1,6-bisphosphate) is itself an antagonist of ATP and citrate inhibition of phosphofructokinase. In the aerobic-anaerobic transition, the rate of glycolysis increases 15- to 20-fold (Williamson, 1966).

Furthermore, without the Krebs cycle to consume pyruvate generated in glycolysis, pyruvate is reduced to lactate by lactate dehydrogenase. Lactate is the ionized form of lactic acid, so in solution, an increased level of lactate results in an increased equilibrium level of hydrogen ions, reducing the pH level inside the cell. The increasingly acidic intracellular environment leads to chromatin clumping, reduced enzymatic activity, and denaturation of proteins (Robbins et al., 2010). This last mechanism can also stimulate further cell injury and even cell death due to the unfolded protein response (Robbins et al., 2010).

An additional consequence of depleting ATP levels in the cell is a decrease in protein synthesis. A common pool of ribosomal subunits freely floats in the cytoplasm. For any mRNA that encodes a cytosolic-bound protein, the ribosomal subunits assemble into complete ribosomes around the freely-floating mRNA. However, for polypeptide chains to form and elongate, tRNA must be activated through ATP hydrolysis to load the correct amino acid, forming an aminoacyl-tRNA that can then be used in protein translation (Alberts, 2002). Furthermore, for proteins that are destined for secretion or function in the lumens of the endoplasmic reticulum (ER), Golgi apparatus, lysosomes, or the biogenesis of membrane proteins for peroxisomes, the nucleus and the plasma membrane, the proteins must be synthesized while bound to the ER and translocated into the ER lumen (Walter and Johnson, 1994; Zimmermann et al., 2006) or translated into the cytosol while the ribosome remains attached to the ER translocon (Cooper, 2000). Once the appropriate, nascent polypeptide sequence emerges from a ribosome that needs to be bound to the ER, the signal recognition particle (SRP) binds to both the polypeptide and ribosome, pausing translation while homing to the SRP receptor, an ER membrane protein (Walter and Johnson, 1994). From here, the ribosome and its nascent polypeptide are transferred

to the protein translocase for translocation across the ER membrane. The translocase protein consists of the heterotrimeric SEC61 membrane protein complex (α-, β-, and γ-subunits), the SEC62 membrane protein, and two J-domain transmembrane proteins ERj1 and SEC63. The SEC61 complex provides the pore for the protein to translocate, SEC62 is a stabilizing protein, while the two J-domain transmembrane proteins interact with the luminal protein BiP (for binding protein) (Zimmermann et al., 2006). BiP exhibits ATPase activity through regulation of two (SIL1 and GRP170) nucleotide exchange factors (NEF), effectively functioning as a ratcheting mechanism to pull the translating polypeptide through the translocon pore (Zimmermann et al., 2006). Furthermore, it is proposed that ATP is required to assemble the membrane-bound translocase protein. Therefore, depletion of ATP in the cell reduces protein synthesis in the cytosol and leads to the disassembly of translocase proteins, reduced BiP ATPase activity, and detachment of ribosomes from the ER. Fundamentally, the synthesis of proteins for intracellular and extracellular use are affected when ATP levels are depleted during an ischemic event. The multiple effects of cell injury following ATP depletion are outlined in Figure 1, adapted from (Lilly, 2011).

Mitochondrial Damage

As the main supply of ATP to sustain cellular processes, mitochondria play a critical role in signaling cell injury and death by multiple pathways (Robbins et al., 2010). As ATP levels drop even 5-10% below normal, multiple changes occur to many critical cellular systems that affect the normal function of mitochondria. Cellular swelling due to non-penetrating solute imbalances and acidification of the intracellular environment are major contributors to an environment that can damage mitochondria and lead to cell death.

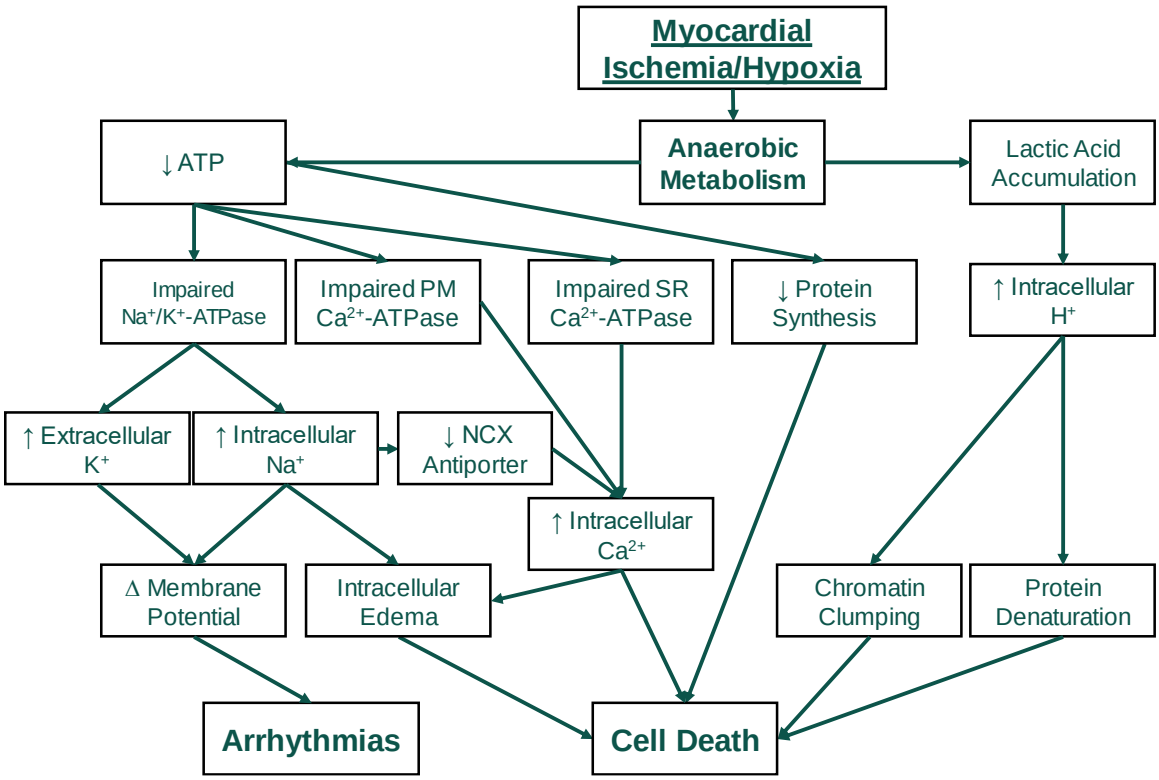

Figure 1: Signaling cascade, resulting from anaerobic metabolism, leading to cell death in ischemia.
An abbreviated list of downstream signaling mechanisms following myocardial ischemia and/or hypoxia leading to the reduced availability of oxygen to the working cardiac tissue.

The $[Ca^{2+}]$ in the mitochondrial matrix compartment is controlled by multiple ion transporters and the proton pumps of the respiratory chain in oxidative phosphorylation. The transport cycle consists of the Ca^{2+} uniporter moving calcium ions from the intermembrane space into the mitochondrial matrix, the Na^{+}/Ca^{2+} exchanger (NCX), and the Na+/H+ exchanger of the inner membrane. This transport cycle relays changes in cytosolic $[Ca^{2+}]$ to changes in $[Ca^{2+}]$ in the mitochondrial matrix. Calcium ions in the range of 0.2 – 10 µM are important for the regulation of Ca^{2+}-sensitive enzymes like key regulators of oxidative metabolism – pyruvate dehydrogenase, oxoglutarate dehydrogenase, and isocitrate dehydrogenase. If ATP levels are within 75% of normal levels in cardiac cells, even with >100-fold increases in mitochondrial $[Ca^{2+}]$, the cells remain viable.

In the absence of ATP, the overload of cytosolic [Ca^{2+}] (due to increased intracellular [Na^{+}] and [H^{+}]) and the presence of high levels of inorganic phosphate, Pi (due to reduced production of ATP), leads to the opening of a pore in the inner membrane of the mitochondria, one component in a protein complex called the permeability transition (PT) pore. With an estimated diameter of 2.0 – 2.6 nm, the PT pore is large enough to allow transport of most metabolites produced in the mitochondrial matrix and hydrated inorganic ions including Ca^{2+}. First thought to be a method to regulate [Ca^{2+}] overload in the mitochondria matrix, it is now established that PT pore opening is involved in the pathogenesis of necrotic cell death (Crompton, 1999). Additionally, opening of the PT pore, a high-conductance channel, leads to loss of mitochondrial inner membrane potential, further inhibiting oxidative phosphorylation and progressive depletion of ATP. A vicious cycle begins since PT pore opening leads to ATP breakdown rather than synthesis, which leads to additional [Ca^{2+}] deregulation, which leads to further PT pore opening, and so forth. Once past a point of phosphorylation potential for adenine nucleotides and regulation of [Ca^{2+}], the cell undergoes necrosis.

The portion of the PT pore protein complex on the inner membrane, adenine nucleotide translocase (ANT), can also contact the voltage-dependent anion channel (VDAC) protein, on the outer membrane creating the full PT pore protein, enabling a continuous connection from the cytosol to the matrix of the mitochondria. Additionally, swelling of the highly folded inner membrane from ANT opening can lead to matrix expansion and outer-membrane rupture. Individually or in combination, these phenomenon can contribute to leakage of pro-apoptotic proteins from the intermembrane space or mitochondrial matrix and help mediate cellular apoptosis as well (Crompton, 1999).

Loss of Calcium Ion Homeostasis

Thus far, the loss of calcium ion homeostasis and regulation has been a consequence of depleting ATP levels to mediate cellular injury (cellular swelling through reduced active ion transport and mitochondrial damage through PT pore formation). Increases in intracellular calcium ion concentration due to a lack of calcium ion regulation can lead to cell injury through more direct biochemical means – promotion of Ca^{2+}-activated effector mechanisms. A non-exhaustive list of calcium-sensitive enzyme classes and processes include: Ca^{2+}-activated binding proteins (e.g. calmodulin); synthases (e.g. NO synthase); protein kinases (e.g. myosin light chain kinase [MLCK]); protein phosphatases (e.g. calcineurin); transglutaminases (e.g. transglutaminase 2); catabolic enzymes targeting DNA (e.g. endonucleases), proteins (e.g. calpain), and lipids (phospholipase A_2); energy-dependent processes (e.g. ATPases); and transcription regulation (e.g. cyclic AMP response element-binding protein [CREB]) (Berridge et al., 2003). Ca^{2+} is an activator of numerous enzymes involved in the turnover of proteins, phospholipids, and nucleic acids in the cell. Sustained increases in homeostatic intracellular [Ca^{2+}] can lead to unmitigated breakdown of cellular macromolecules important to cell function. As cardiomyocyte injury occurs within minutes of ischemia, the focus will be on enzymes and processes that result in more immediate cellular changes and injury and discussions of derangements in transcription will not be included. The preceding list of enzymes and processes can then be grouped into two categories: 1) the activation of Ca^{2+}-dependent catabolic enzymes and 2) the alteration of cytoskeletal integrity.

Homeostatic protein turnover is essential in all cells. In every tissue, the majority of intracellular proteins are degraded through the ubiquitin/proteasome pathway (UPP) (Lecker et

al., 2006). Interestingly, large protein complexes like intact myofibrils cannot be degraded by UPP – specific interactions between individual proteins of the myofibril (e.g. actin, myosin, and troponin) protect the myofibril from UPP processing (Solomon and Goldberg, 1996). Thus, to degrade myofibrils, the complex must be pre-processed before entering the UPP. Pre-disassembly of the myofibril is attributed to calpains, a Ca^{2+}-activated neutral protease. Since optimum activity of calpains is at normal intracellular pH, calpains are not sequestered in lysosomes, remaining freely solubilized in the cytosol (Nicotera et al., 1992). Studies in transgenic mice that overexpress calpain lead to widespread myocytolysis and a robust inflammatory response eventually leading to heart failure – these results support the idea that calpain overactivation, either through transgenic upregulation of calpain protein production or increased activation from elevated levels of intracellular [Ca^{2+}] contribute to myocardial injury (Galvez et al., 2007). The degradation of the contractile machinery in myocardium eventually is irreversible, leading to cell death.

Phospholipases are important enzymes for generating signaling molecules from phospholipid sources. For example, phospholipase C (PLC), is an important plasma membrane protein that catalyzes phosphatidylinositol 4,5-bisphosphate into diacylglycerol (DAG) and inositol 1,4,5-triphosphate (IP_3). Although PLC is not a catabolic enzyme of structural phospholipids per se, it is important in calcium ion mobilization and its overstimulation creates an autocatalytic loop to release additional Ca^{2+} from the sarcoplasmic reticulum and other non-mitochondrial stores from IP3 signaling (Berridge et al., 2003; Nicotera et al., 1990), while also upregulating activity of a specific Ca^{2+}-activated isoform of PLC, PLCδ, to create additional IP3. Furthermore, elevated [Ca^{2+}] activates a different phospholipase that does have the ability to

catabolize structural phospholipids – phospholipase A_2 (PLA_2). PLA_2 regulates the production of arachidonic acid from phospholipids to regulate cellular process (e.g. $[Ca^{2+}]$ levels) and for eicosanoid biosynthesis (Leslie, 1997; Nicotera et al., 1992). Not only is PLA_2 a Ca^{2+}- and calmodulin-dependent enzyme, calcium ion is also necessary for binding PLA_2 to the plasma membrane to carry out its enzymatic function (Leslie, 1997). Thus, when supranormal levels of $[Ca^{2+}]$ are present in the cell, PLA_2 activity is increased and its localization to the plasma membrane is enhanced, resulting in extensive plasma membrane breakdown and in the possible generation of toxic metabolites from arachidonic acid byproducts (Nicotera et al., 1992). These mechanisms contribute to additional cell injury that are eventually irreversible, leading to cell death.

Nucleic acid repair and turnover is tightly regulated for appropriate cell function. Normally, DNA compaction by chromatin binding protects it from sources of extracellular damage (e.g. radiation (Takata et al., 2013)) and blocks access to active sites for various enzymes targeted to DNA(Alberts, 2002). Ca^{2+} overload and calpain activation has been shown to affect the integrity of the nuclear membrane, decreasing the ability to regulate nucleocytoplasmic transport, creating a subsequent rise of $[Ca^{2+}]$ in the nucleoplasm to match elevated $[Ca^{2+}]$ in the cytoplasm (Zhivotovsky and Orrenius, 2011). A consequence of Ca^{2+} influx into the nucleus is chromatin unfolding by redistributing histones or activating topoisomerase II (Nicotera et al., 1994). With DNA more accessible due to increased $[Ca^{2+}]$, it is now more susceptible to endogenous DNase activity or increased catabolism from Ca^{2+}-activated enzymes like endonucleases (Nicotera et al., 1994). Additionally, topoisomerase II activated by calcium to enable chromatin unfolding can, at elevated $[Ca^{2+}]$, be locked into a conformation that cleaves, but does not religate, DNA, further

leading to DNA damage (Nicotera et al., 1992). With conditions tipping the balance towards DNA damage without methods for repair, the accumulating DNA damage is eventually irreversible, leading to cell death.

The intracellular cytoskeleton is composed of three different fibers, differentiated by size, protein composition, activity and function (Nicotera et al., 1992). These fibers, in order of size are: microfilaments, intermediate filaments, and microtubules. Given the different compositions, activities, and functions of cytoskeleton proteins, the disruption of these different classes of proteins due to increased [Ca^{2+}] can occur from multiple mechanisms, which can be grouped into two distinct processes: 1) modifications of cytoskeleton protein interactions and binding or 2) catabolism of cytoskeleton proteins.

Microfilaments are predominantly composed of actin and various actin-binding proteins (ABPs). The ABPs modulate actin polymerization state, the self-assembly of actin to form actin bundles, and the association of actin bundles to link to protein anchors in the plasma-membrane (Nicotera et al., 1992). ABPs that mediate interactions of actin bundles to the plasma membrane require Ca^{2+} homeostasis to mediate normal activity. At supranormal levels of [Ca^{2+}], alpha-actinin dissociates from the assembled actin arrays, delinking actin arrays from the plasma membrane. Additionally, because of ATP depletion, actin depolymerization occurs and the actin-myosin network breaks down, further leading to further cytoskeletal damage (Nicotera et al., 1992). Microtubule structure and distribution are also controlled by interactions of microtubule-associated proteins (MAPs) and their modulation by Ca^{2+}. In the presence of calmodulin, studies in fibroblasts show that microtubule disassembly occurs at the millimolar instead of the micromolar range of unbound [Ca^{2+}]. Lastly, the phosphorylation state of cytoskeleton proteins

is important in regulating their interactions with other proteins. Ca^{2+}-calmodulin-dependent protein kinases play a role in regulating cytoskeleton-protein phosphorylation states and studies where kinases and phosphatases are irregularly inhibited can induce abnormal protein interactions, leading to cell injury and death (Nicotera et al., 1992).

Ca^{2+}-dependent proteases catabolize numerous cytoskeletal proteins including spectrin, fodrin, caldesmon, adducin, and tubulin (Nicotera et al., 1992). An important striated muscle protein that anchors alpha-actinin to the cell's sarcolemma, is vinculin (Zemljic-Harpf et al., 2009). Vinculin is a preferred substrate for Ca^{2+}-dependent proteases (Nicotera et al., 1990) so increases in free cytosolic [Ca^{2+}] leads to increased vinculin degradation, unlinking the sarcomeres from the plasma membrane, preventing myofibril force generation from being translated to surrounding myocardium, thereby reducing the pumping function of the heart.

Additional Damage in Ischemia-Reperfusion

Thus far, the discussion has focused on the pathophysiology of injury due to ischemia. To limit the size of the area at risk due to the loss of blood flow and possibly salvage cells that have not sustained irreversible damage, the timely reestablishment of blood flow is paramount. However, the reperfusion of ischemic myocardium can independently promote further cell injury and death through multiple mechanisms. These include: drawbacks from activating and facilitating innate immunity; consequences of restarting cellular processes in dysfunctional cellular machinery from the resupply of required components for cellular function and washout of waste products; and exacerbations of ischemia from paradoxical microvascular obstruction (Hausenloy and Yellon, 2013).

The innate immune system is always poised to eliminate damaged cells. After reestablishing blood flow to areas of the heart damaged from ischemia, endothelial cells become activated, release cytokines, and increase expression of adhesion proteins to promote neutrophil and monocyte activation, homing, and adherence to the affected area. The influx of neutrophils and monocytes causes the generation of harmful reactive oxygen species (ROS) due to the presence of NADPH oxidase assembled in a multiprotein plasma membrane complex (Robbins et al., 2010) and the release of proteolytic enzymes from these leukocytes, contributing to vascular and myocardial damage (Piper et al., 2003). The complement system is another component of innate immunity activated after ischemia-reperfusion. The anaphylatoxins (C3a, C4a, and C5a) are preferentially cleaved from their corresponding complement components leading to histamine release and increased vascular permeability (Robbins et al., 2010); C5a acts as a chemoattractant for leukocytes exacerbating ROS production and proteolysis; and an increase in the formation and deposition of the membrane attack complex in cell membranes leads to further plasma membrane damage and increased cell permeability, further contributing to cell injury. Thus, two components of the innate immune system that are normally protective are stimulated after reperfusion and contribute to additional myocardial cell injury (Moens et al., 2005).

The return of fresh blood to ischemic areas delivers much needed oxygen and fuel substrates (i.e. glucose and fatty acids), refreshes extracellular levels of non-penetrating ions, and washes away waste metabolites like carbon dioxide and lactate. With the return of oxygen and substrates to feed the Krebs cycle and oxidative phosphorylation in mitochondria, a burst of oxidative stress is produced. This occurs because enzymes in the electron transport chain are not

necessarily inhibited, just unlinked from respiration. For example, complex I activity continues to produce superoxide anions (O_2^-) from oxygen, using the NADH produced by the Krebs cycle in aerobic glycolysis (Kowaltowski et al., 2009; Tompkins et al., 2006). With enzyme dysfunction due to inappropriate phosphorylation state or environmental pH inside the mitochondria, the superoxide anion may react to form hydroxyl radicals (OH^-) another damaging reactive species (Kowaltowski et al., 2009). Furthermore, oxidative stress has been shown to upregulate endothelial NOS (eNOS) and inducible NOS (iNOS) *in vitro* with human coronary artery endothelial cells grown in culture and *in vivo* with experimental rats (Zhen et al., 2008), creating the nitric oxide (NO) free radical. The reaction of NO and O_2^- generates the highly reactive nitrogen species peroxynitrite ($ONOO^-$) that freely crosses mitochondrial membranes (Marla et al., 1997) which can oxidize multiple substrates like membrane phospholipids (Radi et al., 1991) directly contributing to cytotoxicity. Peroxynitrite is also known to mediate protein tyrosine nitration, a recognized pathological pathway. Of importance in ischemia-reperfusion injury, a notable enzyme that loses function upon protein nitration is the mitochondrial matrix enzyme manganese superoxide dismutase (MnSOD). Upon nitration of Tyr-34 by a Mn-catalyzed process, the enzyme is completely inactivated (Radi, 2004). The loss of this specific dismutase allows for the accumulation of superoxide anion produced by complex I that is uncoupled from oxidative phosphorylation, thereby increasing oxidative stress in the mitochondria (Kowaltowski et al., 2009).

The intracellular and extracellular [Ca^{2+}] is normally 10^{-3} mM and 10^{1} mM respectively, a difference of four orders of magnitude (Nicotera et al., 1992). Refreshing the extracellular calcium ion depot reestablishes a tremendous concentration gradient between the exterior

versus interior of affected tissues. With the plasma membrane of affected areas already damaged from ischemia, the reperfusion of fresh blood to areas at risk in the infarcted heart lead to further intracellular Ca^{2+} overload (Hausenloy and Yellon, 2013). Consequently, the cell injury mechanisms mentioned in the section about the loss of calcium ion homeostasis are stimulated with prolonged calcium overload inducing additional PT pore opening in mitochondria, exacerbating mitochondrial damage (Halestrap et al., 2004).

Ischemia promotes intracellular anoxia, lactate formation, and ATP depletion, leading to acidosis (conditions below physiological pH of 7.4 found in normal blood) inside the cell. Although acidosis is generally viewed as detrimental to cellular functions, especially regarding proper protein folding and how it affects enzyme activity, the acidotic environment may provide a protective mechanism during ischemia, hypoxia, and toxic stress (Bond et al., 1994; Lemasters et al., 1996). In studies of cultured rat cardiomyocytes, acidosis ($pH \leq 7.0$) during anoxia and hypoxia resulted in losses of less than 25% of cells over a 4.5-hour period. However, if a pH of 7.4 is maintained in the anoxic and hypoxic infusion media, more than 95% of cells are lost after 4.5 hours (Bond et al., 1994). The picture becomes grimmer after reperfusion. After 4 hours of anoxia, cultured rat cardiomyocytes were reperfused under three different conditions: 1) normal [O_2] and pH (pH = 7.4); 2) anoxic with normal pH; and 3) normal [O_2] with acidic pH (pH = 6.2). After one hour of reperfusion, the first two conditions resulted in about 50% cell death. However, reperfusion with oxygenated, yet acidotic media led to minimal cell losses of about 5% (Bond et al., 1994). This is particularly interesting since oxygen status did not play a role in determining cell viability at physiological pH, whereas the return of pH from acidotic to physiologic precipitated the observations in cell culture, creating a “pH paradox”. The working hypothesis

from this group is that the acidic environment following ischemia inhibits the function of degradative enzymes like phospholipases, proteases, and endonucleases that are activated from Ca^{2+} overload after ATP depletion (Bond et al., 1994; Lemasters et al., 1996). Many of these enzymes have optimum shape and confirmation at neutral to slightly alkaline conditions – a range covered by the pH of normal blood (Alberts, 2002). Thus, acidosis in ischemia reduces the activity of these destructive enzymes, while restoring pH during reperfusion by washing out lactate and other waste metabolites releases this inhibition, accelerating cellular injury in multiple compartments, ultimately tipping the scale towards cell death (Bond et al., 1994; Lemasters et al., 1996).

Ischemia not only affects cardiomyocytes, it also affects all supporting and connective tissue. Following ischemia-reperfusion injury, coronary endothelial cells become dysfunctional, showing impaired vasodilatory and anti-thrombotic functions (Moens et al., 2005) while physically swelling and taking a plump appearance (Hausenloy and Yellon, 2013). Instead of producing potent vasodilators like endothelium-derived hyperpolarizing factor (Lilly, 2011), prostacyclin (Moens et al., 2005), and NO (Moens et al., 2005), dysfunctional endothelium produce potent vasoconstrictors like endothelin-1 and ROS (Lilly, 2011; Moens et al., 2005). Additionally, dysfunctional endothelium become sensitive to thrombin and its ability to stimulate vasoconstriction (Moens et al., 2005). This functional reduction in coronary artery caliber is combined with physical obstructions to block blood flow during reperfusion. In combination with the swelling of cardiomyocytes that produce external capillary compression, the swollen endothelial cells physically reduce the capillary lumen diameter (Moens et al., 2005). The impaired release of prostacyclin and NO, themselves inhibitors of platelet aggregation, lead to

the formation of micro-thrombi (Lilly, 2011). Finally, the activated endothelium that attracts leukocytes to the area to marginate, roll, and adhere to the endothelium during inflammation create leukocyte plugs that impede flow (Hausenloy and Yellon, 2013). The functional and physical blockage of blood flow during reperfusion is called microvascular obstruction (MVO) that can vary in severity from "no-flow" to "low-flow" (Moens et al., 2005). In patients that have therapeutic interventions following a myocardial infarction, the presence of MVO is associated with a larger area at risk, a lower ejection fraction after recovery, adverse left ventricle remodeling, and worse clinical outcomes (Hausenloy and Yellon, 2013).

Injury Due to Cryoinjury or Cryoablation

The field of low-temperature cellular biology and cryobiology is a richly diverse field covering topics such as how freezing temperatures can preserve cell and tissue function for long-term, low temperature storage (Mazur, 1984) to how it can be used for targeted injury and destruction of pathologic tissues (Gage and Baust, 1998). The discussion for cardiac injury here will focus on cryobiology processes that pertain to cryoinjury and cytoablative applications. Given the tiny volumes of water inside cells and the colligative properties of the dissolved proteins and electrolytes in plasma, the intracellular solution generally exhibits a eutectic freezing point range of 0 to –40°C. Given the electrolyte and protein make up of specific cells, some even have a eutectic freezing point as low as –55°C. Once frozen, the duration of freezing plays a role in the amount of tissue damage that is induced. However, *in vitro* and *in vivo* tests have found that cooling below the eutectic freezing point can eliminate the need for sustained dwell times. Thus, to repeatably and reproducibly induce cell damage, achieving tissue temperatures colder than –50°C for any duration ensures cellular freezing damage (Gage and Baust, 1998).

As the local tissue environment drops towards the eutectic freezing point for the cell, ice crystal formation first occurs in the extracellular space (Mazur, 1984). When this occurs, the remaining extracellular solution becomes hyperosmotic. If the cooling rate is slow enough, the cell has sufficient time to move water out of the cell by osmosis, concentrating the intracellular solutes to maintain the chemical potential of intracellular water in equilibrium with the chemical potential of extracellular water, preventing the formation of ice crystals (Mazur, 1984). Thus, to induce ice crystal formation inside the cell and ensure physical, intracellular injury, cooling must occur fast enough to prevent water movement by osmosis. A clinical target is to achieve a cooling rate of at least –50°C/minute (Gage and Baust, 1998). Once properly frozen, the destruction of cells and tissue by freezing are mediated by at least two processes: direct cell and tissue injury and ischemia/anoxia from vascular stasis.

Direct cell and tissue injury from freezing occurs by two linked biochemical and biophysical changes: solute concentration derangements and ice crystal formation (Gage and Baust, 1998). As ice crystals form intracellularly and desiccate the cell, solute concentrations inside the cell begin to rise. The high concentration of solutes is thought to induce cell injury by changing the conformation of numerous proteins, damaging enzymatic machinery and destabilizing organelle and cellular membranes (Hoffmann and Bischof, 2002). The ice crystals themselves are thought to mechanically pierce or shear organelles and the cell membrane, practically ensuring cell death through mechanical trauma. Furthermore, overall tissue macrostructure and organ function is impaired since the shearing forces from ice crystal formation in the supporting and connective tissue around tightly packed cells cause gross tissue damage (Gage and Baust, 1998).

The suggested clinical freezing point and cooling rate to achieve cryoinjury not only freezes cells and tissue, it leads to circulatory stagnation as blood in the vasculature freezes. This reduction and/or complete loss of blood flow while tissue is frozen is the textbook definition of ischemia. In this case, the expectation would be that derangements in the section describing ischemic would occur in cryoinjury. The complete and clear demarcation of cellular necrosis in cryogenic lesions with damaged yet viable cells in the periphery of the affected area convince many investigators that ischemia and "the vascular effect" dominate cryoinjury (Gage and Baust, 1998; Hoffmann and Bischof, 2002), but many of the mechanisms described in the section on ischemia-induced injury require intact organelles and dysfunctional, yet viable cells. Conversely, others argue that the uniformity of cell death and the contours of the necrotic area matching the shape of the cooling probe is evidence of direct cell injury due to ice crystal formation dominating cryoinjury (Mazur, 1984). Without a clear consensus, it can only be concluded that vascular stagnation during freezing is not a protective mechanism, but it may play a role to cause further cell injury.

Freezing is not the only damaging feature of cryoinjury; the thawing process can induce further damage to affected areas. As the damaged tissue and frozen blood thaw, microvascular obstruction and further cell rupture can occur. The freezing process damages the endothelium lining the vessels that perfuse the heart, leading to MVO as described in ischemia-reperfusion (Gage and Baust, 1998) once blood begins to flow. Thus, unaffected tissues surrounding the necrotic lesion from cryoinjury may be affected by ischemic damage since tissue perfusion does not immediately resume upon tissue thawing. Finally, as ice crystals first melt in the extracellular spaces during tissue thawing, the environment surrounding the cells is briefly hypotonic in

comparison. As a result, water enters the cell and its organelles through their mechanically-damaged membranes, causing them to swell even further and potentially rupture (Hoffmann and Bischof, 2002).

Injury Due to Conditional Genetic Ablation

Toxinogenic strains of *Corynebacterium diphtheriae* produce diphtheria toxin (DT), a single polypeptide chain of about 62 kilodaltons (Pappenheimer, 1977). DT contains two distinct fragments with separate functions, the enzymatically active (DT-A) domain and the receptor binding (DT-B) domain. DT enters the cell when DT-B binds to the DT receptor on the cell surface, a protein identified as a precursor to heparin-binding EGF-like growth factor (HB-EGF) (Akazawa et al., 2004), and is internalized into the cell as endosomes by receptor-mediated endocytosis (Falnes and Sandvig, 2000). In the late stages of the endosome lifecycle, the late endosomes containing DT fuse with lysosomes, acidifying the DT-containing late endosome (Huotari and Helenius, 2011). This hydrolyzes DT, unfolding the protein to expose the hydrophobic interior that immediately interacts with membrane lipids, causing the rapid translocation of DT-A into the cytosol (Draper and Simon, 1980; Sandvig and Olsnes, 1980).

Once present in the cytosol, it is commonly accepted that DT-A leads to cell death by inactivating elongation factor 2 (EF-2) in ribosomes, inhibiting protein synthesis (Pappenheimer, 1977; Saito et al., 2001; Van Ness et al., 1980a, b). Without protein turnover, cell death is guaranteed, with most researchers attributing cell death to apoptosis (Komatsu et al., 1998), while some believe cell death from DT occurs also by autophagy (Akazawa et al., 2004). In either regard, cell death follows a structured program, normally eliciting little to no inflammation (Robbins et al., 2010). However, although both apoptosis and autophagy should not induce

inflammation, inflammatory cells and cytokines were detected when DT was used in a conditional genetic ablation model for heart failure (Akazawa et al., 2004). This may have occurred since almost 20% of cardiomyocytes were induced to die at the same time, requiring an inflammatory response to clear all the cellular debris. Finally, some researchers have reported that DT exhibits DNase activity, leading to apoptosis induced by internucleosomal DNA cleavage (Chang et al., 1989). However, this may just be part of the spectrum of programmed cellular death since other laboratories have claimed that DNA fragmentation seen from DT is simply a consequence of apoptosis induced by EF-2 inactivation (Kochi and Collier, 1993).

Injury Due to Apical Resection

The classical and most popular cardiac resection technique is apical resection. This model involves the gross, mechanical removal of the ventricular apex (Porrello et al., 2011; Poss et al., 2002), although some newt researchers have also removed lateral aspects of the ventricle (Witman et al., 2011). In mammals, if the resection does not penetrate either ventricular chamber and bleeding is controlled, survival rates in neonatal P1 mice are about 90%, although survival in P7 mice is much worse (Porrello et al., 2011). This parallels survival rates in zebrafish (Poss et al., 2002) and salamanders(Cano-Martinez et al., 2010), although less care is required when resecting ventricular tissue since clotting in these non-mammalian vertebrates is more robust (Cano-Martinez et al., 2010; Wang et al., 2011) and their systemic blood pressures are much lower (Hu et al., 2001; Shelton and Jones, 1968).

Except for different methodologies to exteriorize or retract the heart for resection in neonatal mice (Bryant et al., 2015), the cardiac resection injury model only damages the cells and tissues directly at the cut border. Once bleeding is stopped (from natural hematoma formation

or by applied pressure from surgeon) and a stable clot has formed, acute inflammatory processes secondary to gross tissue damage and trauma are the main cellular-response mechanisms. Some important mediators of acute inflammation, along with their actions include: vasoactive amines (increase vascular permeability); arachidonic acid metabolites (leukocyte chemoattractant); and cytokines (leukocyte chemoattractant and activator). Outcomes of acute inflammation include resolution/regeneration (clearance of injurious stimuli, replacement of cells and resumption of normal function), healing (formation of abscess or remodeling through fibrosis), or progression (to chronic inflammation) (Robbins et al., 2010).

Molecular Signaling Pathways Mediating Cardiac Repair

In highly regenerative animals, the restoration of lost tissue, regardless of cause, is generally believed to follow reactivated pathways of embryogenesis and development such as Hippo, BMP, FGF, PDGF, Wnt, Notch, Hedgehog, retinoic acid (Castellan and Meloni, 2018; Han et al., 2014). While this may be true for non-mammalian vertebrates, the situation is not well understood in mammals. The variability in responses in mammals may derive from the improper reactivation of developmental pathways or evolutionary changes to intrinsic cellular processes that have decreased the regenerative ability of developmental pathways in juvenile and mature mammals (or a combination of both) (Vivien et al., 2016). However, what is clear from the numerous studies in the field of regenerative medicine is that the molecular processes of cardiac repair and regeneration are age-related (Castellan and Meloni, 2018), species-dependent (Judd et al., 2016; Vivien et al., 2016), tissue-specific (Iismaa et al., 2018), and injury-driven (Andersen et al., 2014; Bryant et al., 2015; Darehzereshki et al., 2015; Jesty et al., 2012; Konfino et al., 2015; Polizzotti et al., 2016; Strungs et al., 2013). The following review summarizes signaling pathways

that are candidates for manipulating the repair process to perfectly restore tissue lost due to cardiac injury.

Injury Due to Ischemia and Ischemia-Reperfusion

Non-mammalian Vertebrates

Coronary vessels are not found in all organisms with a heart. For instance, most amphibians such as newts, salamanders, and frogs have no coronary vessels (Reese et al., 2002). Consequently, journal database searches rarely reveal any cardiac regeneration studies in amphibians using ischemia or ischemia-reperfusion injury models. Thus, mechanisms guiding heart regeneration in amphibians after cardiac ischemia/ischemia-reperfusion injuries remain to be investigated and elucidated.

The presence of coronary vessels in fish are variable, usually found in large predatory fish or fish that live in environments of low oxygen tension. These fish have coronary arteries in the epicardium that perfuse coronary vessels located only in the outer compact ventricular myocardium (Moore et al., 1976). Interestingly, not only do zebrafish have coronary arteries on the epicardium of the dorsal and ventral ventricular surfaces, coronary vessels are also found throughout the compact myocardium of the ventricle, with coronary capillaries terminating at the subtrabecular layer adjacent to the compact layer (Hu et al., 2001). Although zebrafish do have coronary vessels supplied by a coronary artery, the size limitations of their gross cardiac anatomy make producing ischemia and ischemia-reperfusion injuries very difficult. Zebrafish coronary arteries are 10-15 µm in diameter (Hu et al., 2001), making it very difficult to produce a localized ligation to induce ischemia or ischemia-reperfusion injuries. Therefore, like amphibians,

mechanisms guiding heart regeneration in fishes after cardiac ischemia or ischemia-reperfusion injuries remain to be investigated and elucidated.

Mammals

The tissue response after a myocardial infarction follows an exquisitely orchestrated and complex set of events. These processes occur, with or without reperfusion, and can be grouped into the inflammatory, reparative, and maturation phases (Prabhu and Frangogiannis, 2016). Once cells begin to die from ischemia, cell death mechanisms are activated, primarily driven by necrosis, secondarily by apoptosis, and to a lesser degree by autophagy (Eltzschig and Eckle, 2011; Frangogiannis, 2012; Hotchkiss et al., 2009). Additional damage from reperfusion injuries augment the damage-based activation of inflammation.

Necrotic, apoptotic, stressed, and injured parenchymal and stromal cells after myocardial infarction release damage-associated molecular patterns (DAMPs) that are the major inflammatory phase ligands. Examples of DAMPs involved in the inflammatory response during cardiac ischemia and ischemia-reperfusion injuries are high-mobility group box 1 (HMGB1), S100 proteins, ATP, heat shock proteins, complement, among others (de Haan et al., 2013; Eltzschig and Eckle, 2011). These substances bind to related pattern recognition receptors (PRRs) such as membrane-bound toll-like receptor (TLRs), cytosolic nucleotide-binding oligomerization domain-like receptors (NLRs), and cell-surface receptors for advanced glycation end products (RAGEs) on surviving parenchymal cells and infiltrating leukocytes. Binding of DAMPs on PRRs robustly activate the endpoint signaling cascades of inflammation such as mitogen-activated protein kinases (MAPKs) that mediate transcription of inflammatory mediators through the phosphorylation and regulation of transcription factors, coregulatory proteins and chromatin

proteins (Whitmarsh, 2007) and nuclear factor kappa-light-chain-enhancer of activated B cells (NF-κB) signaling that acts as a transcription factor that activates gene transcription for multiple inflammatory mediators (Newton and Dixit, 2012).

The reparative phase inhibits and resolves the inflammatory phase, involving the control of multiple inflammatory cells that have migrated to the injury site. Molecular signals that inhibit inflammation include cytokines like IL-10 (suppresses synthesis of proinflammatory cytokines and chemokines in macrophages through STAT3 signaling) (Prabhu and Frangogiannis, 2016), a member of the TGF-β family [growth differentiation factor-15 (GDF-15)/macrophage inhibitory cytokine-1(MIC-1)] (counteracts leukocyte integrin activation by blocking chemokine signaling] (Kempf et al., 2011), and lipid-derived pro-resolving mediators (e.g. lipoxins resolvins, protectins, and maresins) (Serhan, 2014). Signals that resolve inflammation and promote the transition to fibrosis and stimulate the conversion of fibroblasts to myofibroblasts include: inducing and activating a different member of the TGF-β family (e.g. TGF-β1); modifying the extracellular matrix (ECM) by the secretion and deposition of matricellular proteins (thrombospondin-1 and the osteopontin family); and globally upregulating of the renin-angiotensin-aldosterone system (Booz and Baker, 1995) (mediated by TGF-β signaling) (Prabhu and Frangogiannis, 2016) and bolstering it by the local generation of angiotensin II at the site of infarction (Sun and Weber, 1996). Other mediators of myofibroblast activation include members of the PDGF and FGF families along with proteases derived from mast cells (tryptase and chymase) (Prabhu and Frangogiannis, 2016). The conversion of fibroblasts to the myofibroblast phenotype (i.e. fibroblasts with stress fibers like α-smooth muscle actin and contractile proteins like the embryonal isoform of smooth muscle myosin (Rohr, 2011; Santiago et al., 2010)) results in

increased proliferative activity and matrix stabilization, quickly producing stable structural tissue to withstand the mechanical forces in the heart. Delays in resolving inflammation, a greater initial inflammatory response, and large regions at risk are predictors of progressive compensatory ventricular remodeling (Prabhu and Frangogiannis, 2016). The importance of macrophages in the reparative phase are elegantly shown in a negative-control experiment. When macrophages are depleted from the healing heart by serial injections of clodronate-containing liposomes, the lack of TGF-β and vascular endothelial growth factor-A (VEGF-A) secretion resulted in the ongoing presence of cellular debris for four weeks after injury, whereas the untreated hearts allowed macrophage to rapidly remove necrotic cellular debris to allow granulation tissue formation (van Amerongen et al., 2007).

The maturation phase involves the deactivation of reparative cells (e.g. fibroblasts and myofibroblasts) and their clearance from the injury site by apoptosis. Additionally, matrix proteins secreted during the reparative phase begin to cross-link and form a more cohesive network to provide added structural integrity to the injured area. The signaling mechanisms that lead to the deactivation of reparative cells, their clearance by apoptosis, and the cross-linking of matrix proteins remains unknown (Prabhu and Frangogiannis, 2016).

Injury Due to Cryoinjury or Cryoablation

Non-mammalian Vertebrates

A review of the literature supports the notion that cardiac development-signaling pathways are essential for adult zebrafish heart regeneration (Vivien et al., 2016). Additionally, secondary to tissue damage, DAMPs trigger an inflammatory response responsible for tissue repair. Prior studies in non-mammalian vertebrates using cryoinjury or cryoablation techniques

provide evidence that these two signaling pathways play a role in cardiac tissue regeneration in these animals.

Cardiac cells are derived from embryonic precursors found in the anterior lateral plate mesoderm. These embryonal cells differentiate into mature cardiac cells through the control of homeobox transcription factors from the Nk2 family, specifically *nkx2.5*. The regulation of *nkx2.5* expression is accomplished by the secretion of transforming growth factor β (TGFβ) (Stainier, 2001). Similarly, the T-Box family (*tbx*) of transcription factors are important regulators of the differentiation of embryonic mesoderm. First cloned in the mouse, *Tbx18* is found to be highly expressed in the developing epicardium of the heart (Kraus et al., 2001). Cloning and expression studies of the paralog *tbx18* in zebrafish show that this gene is expressed starting at 36 hours post fertilization in the epicardium covering the sinus venosus, atrium and ventricle (Begemann et al., 2002). Lastly, a gene essential to the formation of an intact epicardium is the paralogous Wilms tumor suppressor-1 zebrafish gene, *wt1*. Conserved across vertebrate species, this gene is expressed as early as 4 days post-fertilization in zebrafish (Serluca, 2008). In summary, the developmental control of epicardium is essential to regulate cardiomyocyte proliferation and organization during embryogenesis (Sucov et al., 2009).

Transcript and protein expression analysis identified TGFβ to be activated during the cardiac regeneration process after cryoinjury in zebrafish hearts. To directly attribute this signaling pathway as necessary for regeneration, the investigators blocked the type I TGFβ receptor with a specific inhibitor (SB431542). Blocking the downstream effects of the TGFβ signaling pathway impaired heart regeneration (Chablais and Jaźwińska, 2012). In another study, researchers used prior results of epicardial activation after apical resection injury in the zebrafish

(Lepilina et al., 2006) (discussion below) to scope their investigation of gene expression changes after cryoinjury. After inducing cryoinjury, fluorescence in heart sections were visualized in transgenic zebrafish (*wt1b*:EGFP^{li1}) expressing GFP under control of the Wilms tumor 1 paralog (*wt1b*) promoter. Additionally, the heart sections were co-labeled with *in situ* hybridization techniques using RNA probes against *tbx18*. The histologic preparations show that *tbx18*-postitive and GFP-positive cells are found after 3-days post injury (dpi), the expression is limited to the epicardium, and the two different signals overlap. These results indicate that cryoinjury induces expression of developmental pathways in epicardium. Using immunofluorescence staining, the GFP-positive epicardial cells were labeled with anti-PCNA (proliferating cell nuclear antigen) antibodies. At 3 dpi, the injury-activated epicardial cells were proliferating and by 7 dpi, these cells had migrated through the wound area (Schnabel et al., 2011). The researchers also measured cardiomyocyte proliferation after cryoinjury using a different transgenic zebrafish line expressing GFP under control of the cardiac myosin light chain 2 (myosin light chain7) [*cmcl2* / *myl7*] promoter that was also co-stained with anti-PCNA antibodies. At 1 dpi, no increase of PCNA-positive cardiomyocytes was detected. However, *cmcl2*:GFP-positive cells were positive for PCNA at 3 dpi. The data from Schnabel et al. suggest that there is activation of a developmental gene program (*tbx18* and *wt1a/wt1b*) that activates epicardial cells and increases cellular proliferation in the epicardium. However, although these epicardial cells migrate throughout the wound area, it is unknown if the cardiomyocytes in the injured area are induced to proliferate by the activated epicardial cells or if the two events are simply correlated.

Developmental pathways are not the only signaling mechanisms involved in zebrafish heart regeneration after cryoinjury. After inducing massive cellular death, Chablais et al. notes a

progressively-healing injury response: thrombosis, inflammation, fibroblast accumulation, and collagen deposition. Following the heart for 60 days after cryoinjury, it was found that the scar tissue at the site of injury is progressively remodeled into functioning myocardium. Immunohistochemical techniques show that scar tissue undergoing remodeling is associated with fibroblasts that are positive for vimentin (VIM) secretion and the presence of ECM containing the protein tenascin-C (TNC) (Chablais et al., 2011). Previously thought to only be an intracellular intermediate filament, vimentin is secreted by activated macrophages; the anti-inflammatory cytokine interleukin-10 (IL-10) blocks macrophage secretion of vimentin (Mor-Vaknin et al., 2003). Vimentin plays roles in cell adhesion, cell migration, and cellular signaling especially in processes common to inflammation (Ivaska et al., 2007). However, it is not clear if vimentin itself stimulates regeneration or if it simply signals the pro-inflammatory, reparative and proliferative phase of inflammation. On the other hand, tenascin-c is found to play a direct role in tissue repair. Compared to levels in normal tissue, TNC expression is induced during tissue remodeling, vasculogenesis, and wound healing (Jones and Jones, 2000). In contrast to ECM proteins that provide structural support, TNC and other matricellular proteins (matrix proteins that can regulate cell function (Bornstein, 2001)) maintain a state of intermediate adhesion, allowing for cellular migration and actin stress fiber reorganization, supporting an environment for tissue remodeling and repair (Bornstein and Sage, 2002; Jones and Jones, 2000).

Mammals

Like many injuries, inflammation plays a role in healing the mammalian heart after cryoinjury. A differential regeneration and scarring response after cryoinjury in neonatal mice was reported that was dependent upon the severity of the cryoinjury. In animals that received a

transmural injury, scarring persisted twenty-one, sixty, and one-hundred twenty days after surgery, whereas animals that received a less severe, non-transmural cryoinjury could heal with minimal scarring when inspected by histology at the same time points. After examining protein samples from mice three and seven days after injury for evidence of biomarkers or factors that mediate fibrosis or inflammation, it was found that there was a difference in expression of plasminogen activator inhibitor 1 (PAI-1) between transmural (10.2-fold increase over control) and non-transmural injury groups (3.1-fold increase over control) (Darehzereshki et al., 2015). PAI-1 is a protease inhibitor that limits tissue digestion during the inflammatory phase (Prabhu and Frangogiannis, 2016) and degradation of ECM that is laid down during the reparative phase by fibroblasts and myofibroblasts (Christia and Frangogiannis, 2013). Thus, insufficient remodeling of connective tissue and plasmin due to the increase expression of PAI-1 in the animals with transmural cryoinjury could play a role in mediating the repair of this injury type in mammals.

In addition to inflammatory pathways, cell cycle and proliferation pathways have been studied to further elucidate healing differences between neonatal mammals and slightly older, juvenile mammals after cryoinjury. When administered to adult mice, recombinant neuregulin-1 (rNG1) stimulates the regeneration of cardiomyocytes (Polizzotti et al., 2015). Therefore, the same group hypothesized that administration of rNRG1 to neonatal mice after cryoinjury would be more effective since their cardiac cellular plasticity and new cardiomyocyte birthrate is much greater at this point in development (Bergmann et al., 2009; Bergmann et al., 2015). The results from that study suggest that the earlier administration of rNRG1 leads to better outcomes for the injured hearts. rNRG1 expression activates the ErbB/PI3K/Akt, ERK, and GSK3β/β-catenin

signaling pathways that lead to CM hypertrophy, dedifferentiation and proliferation (Bersell et al., 2009; Cai et al., 2016; D'Uva et al., 2015; Ebner et al., 2013; Wadugu and Kuhn, 2012). Although the experiments described by Polizzotti et al. are not the naturally-driven injury response to cryoinjury, the concept that the more proliferation-competent cardiomyocytes in neonatal and younger animals can have their natural expression of proliferation overdriven by rNRG1 and the downstream signals it activates.

Injury Due to Conditional Genetic Ablation

Non-mammalian Vertebrates

Developmental pathways have been identified to play a role in the rescue of zebrafish hearts injured by cardiac conditional genetic ablation. Taking the results of retinoic acid production following cardiac resection injuries in zebrafish, Wang et al. evaluated retinoic acid production following cardiomyocyte-specific ablation. In short, this specific injury induced retinoic acid production by non-myocardial cells, including endocardium and epicardium, that eventually lead to the full regeneration of destroyed cardiomyocytes (Wang et al., 2011). Thus, signaling from dying cardiomyocytes engaged neighboring cells to express developmental pathways to regenerate myocardium.

Continuing with other developmental pathways involving epicardium, another study showed the importance of this tissue layer as a source of paracrine signals important for cardiomyocyte survival and proliferation. By Want et al. extended the genetic ablation technique to also include the epicardium. When the epicardium was ablated along with myocardium injury, cardiomyocyte proliferation was inhibited and regeneration delayed. The epicardium has a high endogenous renewal capacity, with Sonic hedgehog signaling playing a major role in mediating

epicardial regeneration (Wang et al., 2015). Thus, the Sonic hedgehog signaling pathway can play an important role in mediating neighboring tissue health to support cardiomyocyte regeneration after injury.

Finally, the Notch pathway has been implicated as playing a role in cardiac repair after genetic ablation. Unlike the paracrine signaling from neighboring cells that promote cardiomyocyte renewal, an atrial-to-ventricular transdifferentiation of muscle cells was found to follow massive genetic ablation of ventricular muscle in zebrafish embryos. In this study, Notch signaling played a key role in mediating this transdifferentiation and blocking Notch signaling prevented cardiac regeneration (Zhang et al., 2013).

Mammals

No studies to date have used cardiac genetic ablation in neonatal mice as an injury model to study cardiac regeneration. Based on the diphtheria toxin mechanism of action, cell death is likely due to apoptosis based on the observation of DNA fragmentation in studies using cell lines (Kochi and Collier, 1993) or through autophagy due to the observation of up-regulated lysosomal markers and the presence of increased numbers of autophagosomes. There is no additional damage to surrounding tissue since these genetic mouse models use the α-myosin heavy chain promoter to enable cardiac-specific cardiomyocyte cell ablation. A generalized inflammatory response was noted after cardiomyocyte cell death.(Akazawa et al., 2004). Methods to mediate inflammation mentioned in previous sections on mammalian studies may play a role in mediating regeneration if this model is used to study cardiac regeneration in mammals.

Injury Due to Apical Resection

Non-mammalian Vertebrates

The signaling mechanism involved in repairing gross tissue loss in the heart is not completely understood, but a review of the literature on apical resection in non-mammalian and mammalian vertebrates, the most likely mechanism is the Hippo signaling pathway. The Hippo signaling pathway is a highly-conserved organ-size control pathway, first discovered in *Drosophila* genetic screens, controlling heart growth my promoting apoptosis and inhibiting cellular proliferation (Heallen et al., 2011; Zhao et al., 2010). When the Hippo pathway is stimulated, the transcription cofactor Yes-associated protein (YAP) and its associated transcriptional coactivator with PDZ-binding motif, Taz, are phosphorylated through a chain of kinases that prevent YAP/Taz from entering the nucleus – this promotes cell death and reduces cell proliferation. The opposite is true when the Hippo pathway is inhibited – YAP/Taz enter the nucleus to prevent cell death and increase cell proliferation (Ikeda and Sadoshima, 2016). Although the evolutionarily-conserved mechanism plays a role in organ size, precisely controlling the heart during fetal, neonatal, adolescent, and adult developmental stages, the intrinsic regulation of heart size outside of developmental programs is not well understood.

Mammals

In parallel with non-mammalian vertebrate studies, assessing multiple genetic mouse models also suggests the Hippo pathway mediate regeneration after mechanical resection (Zhou et al., 2015). Conditional knockout mouse models of various proteins involved in the Hippo pathway promote the possibility that the Hippo pathway also plays a role in the repair and regeneration of the heart. As published in a previous study, apical resection at P1 in the neonatal

mouse lead to complete regeneration, whereas the same surgery in a P7 neonatal mouse lead to extensive scarring, as expected in adult mice (Porrello et al., 2011). Investigating Hippo signaling during neonatal development shows that phosphorylated YAP (pYAP) levels low in P2 mice, suggesting a state favoring cellular proliferation, but increases sharply in P10 and P12 mice, suggesting a state favoring cellular apoptosis (Heallen et al., 2013). Using this information, conditional knockout mice were developed. Deletion of an upstream scaffold protein, Salvador (SAV), that stabilizes one of the earlier kinases that eventually lead to the phosphorylation of Yap, leads to a constitutively suppressed Hippo signal. In this case, YAP/Taz enters the nucleus to stimulate cell proliferation. The results of the tamoxifen-induced knockout of SAV starting at P7, with the apical resection surgery at P8, lead to a reduction in scar size when compared to control animals (Heallen et al., 2013). In the case of organ size mismatch after apical resection in the heart, it is proposed that mechanical stresses and mechanotransduction signaling through cytoskeleton and junctional proteins may regulate the Hippo pathway in this condition (Zhou et al., 2015).

Implications to the Field of Cardiac Regenerative Medicine

Repeatable and reproducible ischemic damage in a rodent is achieved via LAD coronary artery ligation to mimic the pathogenesis of a myocardial infarction. To replicate the clinical sequalae of a patient treated to unblock the thrombus, the LAD ligation can be removed to induce ischemia-reperfusion injury. Regeneration after ischemia-reperfusion injury in mammals has only be identified in neonatal animals. Furthermore, there have been no published studies that show complete regeneration after ischemia-reperfusion injury in any adult vertebrates, particularly since non-mammalian vertebrates do not have coronary arteries to ligate.

To study cardiac regeneration in adult animals, other cardiac injury models have been performed in zebrafish and salamanders, and translated and validated in laboratory rodents. These include approaches such as cryoinjury (Gonzalez-Rosa et al., 2011; van den Bos et al., 2005), DT conditional genetical ablation (Akazawa et al., 2004; Wang et al., 2011), or apical resection (Porrello et al., 2011; Poss et al., 2002). Cryoinjury protocols for zebrafish (González-Rosa and Mercader, 2012) and mice (Polizzotti et al., 2016) are available and use the same technique – application of a metal probe cooled using liquid nitrogen. For DT conditional ablation, studies in zebrafish and mice use different approaches. Wild-type mice and rats are normally insensitive to DT-A since the rodent cell-surface receptor (heparin-binding EGF-like growth factor, or HB-EGF) for DT-B cell-binding moiety does not recognize DT-B (Saito et al., 2001). To induce diphtheria-toxin-receptor conditional ablation, transgenic mice are designed to express human or monkey HG-EGF in a tissue-specific manner using an appropriate gene promoter. To target the heart, Akazawa et al. used the α-myosin heavy chain promoter and simply injected DT by intramuscular injection (Akazawa et al., 2004). Zebrafish also do not have a DT receptor. To facilitate a DT cardiomyocyte ablation model in zebrafish, two different transgenic zebrafish lines were crossed to create a Cre-lox animal: *cmlc2:CreER; bactin2:loxp-mCherry-STOP-loxp-DTA*. This zebrafish, called Z-CAT (zebrafish cardiomyocyte ablation transgenes), then proceeds to ablate cardiomyocytes by administering 4-hydroxy tamoxifen (4-HT) (Wang et al., 2011) to excise the STOP signal, and induce production of DT-A. Finally, multiple studies of apical resection in non-mammalian vertebrates and rodents have been published, with details for zebrafish (Poss et al., 2002) and mice (Mahmoud et al., 2014) available, with removal of ≤20% of the apex suggested for improved animal survival rates.

The adoption of surrogate cardiac injury models in non-mammalian vertebrates provides evidence that animals capable of epimorphic regeneration can resolve specific cardiac injuries as adults. However, as described here, the signaling mechanisms for each substitute injury model do not fully replicate the pathophysiology due to ischemia and ischemia-reperfusion injuries. The injury model that best approaches ischemia-reperfusion is cryoinjury, having a stage of reperfusion after blood in the vasculature thaws. Although producing microvascular obstruction after blood begins to reflow, other injury mechanisms after traditional ischemia-reperfusion require viable cells to produce cellular injury by calcium overload, ROS-species overproduction, and acidosis reversal. Cryoinjury as applied in these model systems tend to mechanically rupture cells and organelles immediately upon freezing, ensuring cell death before gross tissue and blood begin to thaw.

Although providing inspiration to the field of cardiac regenerative medicine and the possibilities of healing serious heart injuries, the surrogate models used to date have not provided evidence that adult vertebrate animals can successful regenerate from clinically-relevant ischemia and ischemia-reperfusion injuries that plagues many human patients worldwide. Answering this question will provide information to inform how the field proceeds and prioritizes tissue engineering and regenerative medicine approaches to address ischemic heart disease.

CHAPTER 5: RESEARCH STRATEGIES

This section details the specific approaches to address the Specific Aims. Developing a technique to induce an ischemic cardiac injury in the axolotl that recapitulates a myocardial infarction in mammals is paramount to this project.

Choice of Model Animals

Zebrafish (*Danio rerio*) have been extensively studied as a model for cardiac regeneration (Jopling et al., 2010; Poss, 2007; Raya et al., 2004; Zhang et al., 2013) due to its many advantages in modeling human disease (Chico et al., 2008; Dooley and Zon, 2000; Kari et al., 2007). However, the zebrafish heart is much more primitive than mammalian hearts: zebrafish have two-chambered hearts that currently lack any evidence of secondary heart field derivatives (Lieschke and Currie, 2007). With their three-chambered hearts, amphibians also exhibit physiological traits in common with all vertebrates including mammals (Burggren and Warburton, 2007). Compared to zebrafish, the closer developmental ancestry of amphibians to mammals suggest they are more suitable models for modeling mammalian and human diseases (Burggren and Warburton, 2007; Voss et al., 2011); despite anatomical differences with higher mammals, the embryonic development from the anterior lateral plate mesoderm (induced by the pharyngeal mesoderm) mirrors development in other vertebrates (Easton et al., 1994; Jacobson and Sater, 1988). Also, epicardium development in the axolotl (*Ambystoma mexicanum*) is similar to the general pattern described for higher vertebrates (Fransen and Lemanski, 1990). Additionally, axolotls also have been evaluated as models for cardiac regeneration (Cano-Martinez et al., 2010; Roy and Gatien, 2008).

Observations of axolotl regeneration have been attributed to its neotenic development (Roy and Gatien, 2008). Robust axolotl regeneration during juvenile stages of development is corroborated by observations that *Xenopus* species lose the ability to regenerate when they begin to metamorphose into an adult (Roy and Gatien, 2008; Whited et al., 2012). Moving past observations, the overall goal of this proposal is to elaborate a mechanistic explanation of differences between regeneration between non-mammalian vertebrates and higher mammals. Past studies have detailed robust myocardium regeneration in higher mammals, albeit only in very young animals (Haubner et al., 2012; Porrello et al., 2011; Rumyantsev, 1977). These studies confirm genetic programs for cardiac repair exist within mammalian DNA, but are somehow quickly suppressed after the neonatal and juvenile stages of development.

For comparisons to a higher mammal, the mouse has been chosen due to the wide use of this animal in cardiovascular disease research (Battey et al., 1999). Protocols detailing cardiac procedures for inducing cardiac injury such as MI are widely published (Bayat et al., 2002; Jackson et al., 2001; Klocke et al., 2007; Michael et al., 1995; Murry et al., 2004; Orlic et al., 2001; Salto-Tellez et al., 2004; Tarnavski et al., 2004; Wang et al., 2006; Yue et al., 2013) and the novel model of cardiac ischemia can be piloted while using well-established approaches to expose the heart for survival surgery.

Specific Aim 1

Overview of Specific Aim 1

Develop a cardiac injury model in the axolotl that mimics the pathophysiology of a myocardial infarction in the mammalian heart.

Analyzing cellular characteristics around the mechanically-clamped apex will provide the spatial mapping of necrotic, perinecrotic, and penumbral areas. Studying the labeling indices of cardiomyocyte proliferation [using bromodeoxyuridine (BrdU) or equivalent] uptake in these defined spatial regions will result in the temporal mapping of DNA synthesis activity, like those depicted in Figure 2.

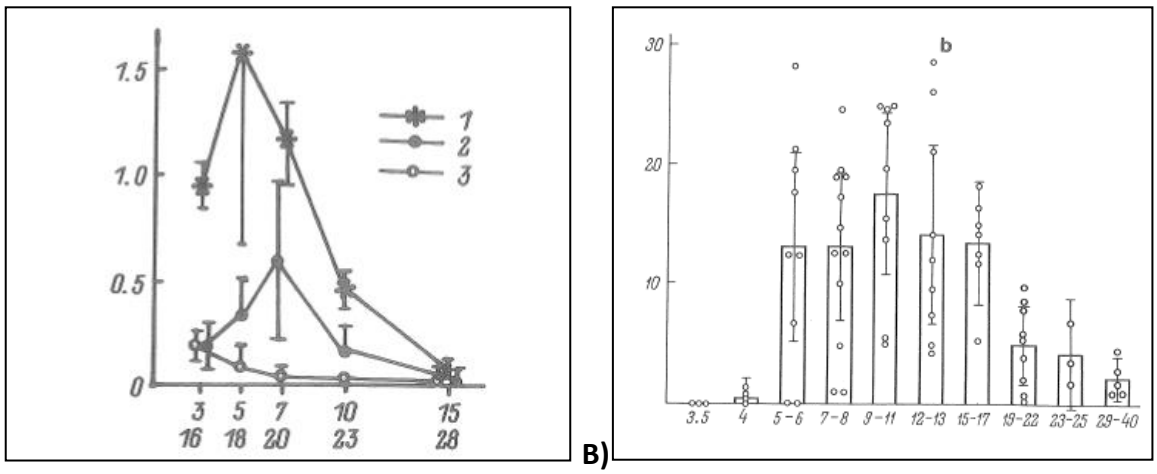

Figure 2: Pulse ^{3}HTdR labeling after ventricular injury.
A) Data from 13-day-old rats and **B)** in frog myocyte nuclei from perinecrotic myocardium. Vertical Axis – Labeling Index, Horizontal Axis – Days after injury [Upper number in (a)]

Specifically, using appropriate nuclei staining of cardiomyocytes to track DNA synthesis and cardiomyocyte proliferation; cardiomyocyte immunohistochemistry for stem cell markers and/or myofibril precursors, to ascertain the differentiation stage of any proliferating cardiomyocytes; and visualizing sarcomeric morphology to pinpoint mature cardiomyocytes will provide cellular characteristics in different zones within the regenerating heart. Analyzing the temporal response of nucleic-acid synthesis activity from BrdU (or equivalent) labeling in the proliferating zone of hearts in axolotls will also help to reconfirm past studies of cell-cycle kinetics during regeneration (Rumyantsev, 1977; Rumyantsev and Carlson, 1991) [Figure 2, adapted (Rumyantsev and Carlson, 1991)] in higher vertebrates. Elucidating the clinically relevant

spatiotemporal patterns of tissue characteristics is important since studies in the regenerating axolotl limb show varied patterns of gene expression by region and time within the regenerating limb blastema (Jhamb et al., 2011; Stewart et al., 2013).

Rationale of Specific Aim 1

Salamanders, including axolotls, have been extensively studied as model organisms for tissue regeneration (Brockes, 1997; Cano-Martinez et al., 2010; Chalkley, 1954; Hay and Fischman, 1961; Khattak et al., 2013; Monaghan and Maden, 2012; Neff et al., 1996; Rose, 1948; Rose and Rose, 1952; Roy and Gatien, 2008; Simon, 2012; Singh et al., 2010; Sobkow et al., 2006; Voss et al., 2009; Whited and Tabin, 2010; Whited et al., 2013). Older studies observed gross changes in anatomy and histology (Chalkley, 1954; Hay and Fischman, 1961; Rose, 1948) ; more recently, regeneration has been examined using modern molecular tools (Khattak et al., 2013; Monaghan and Maden, 2012; Sobkow et al., 2006; Whited et al., 2012; Whited et al., 2013). As stated in the overview to Specific Aim 1, the goal of this study is to understand the fundamental cardiomyocyte biology following ischemic injury. The standard approach to induce repeatable and reproducible ischemic damage in a rodent is to perform a left anterior descending (LAD) coronary artery ligation to effectively recapitulate the pathogenesis of an atherosclerotic infarction in a human (Salto-Tellez et al., 2004; Wang et al., 2006). However, performing the same procedure is impossible in amphibians. Phylogenetically less evolved, amphibians have trabeculated ventricular myocardium (Stocum, 2006). Instead of relying upon coronary arteries to nourish the beating ventricular myocardium, oxygen and nutrients in the blood infiltrate the numerous sinuses formed by the myocardial trabeculations (Reese et al., 2002; Stocum, 2006). Therefore, for purposes of translating the findings in the axolotl to mammalian species,

developing an identical approach to inducing myocardial ischemia in both animals is paramount to the success of this plan of work.

To induce cardiac injury in model animals without coronary arteries, methods such as cryoinjury (van den Bos et al., 2005), diphtheria-toxin-receptor conditional ablation (Akazawa et al., 2004), or apical resection (Porrello et al., 2011; Poss et al., 2002) have been implemented. Although these approaches result in serious cardiac tissue trauma or cardiac function, the injury processes do not recapitulate the pathogenesis of cellular dysfunction akin to ischemia-induced cardiac tissue necrosis. This leads to tissue histology that is dramatically different from healing infarcted tissue. First and foremost, ischemia is not the main factor in the previously mentioned techniques; subjecting at-risk and surrounding tissue to a state of normoxia will lead to different profiles of gene expression and signaling cascades versus tissues in an environment of ischemia-induced hypoxia. Additionally, each approach causes cell death in different manners. In cryoinjury-induced trauma, cells experience acute cell death immediately upon freezing due to the formation of intracellular and extracellular ice crystals that pierce the plasma membrane (Mazur, 1970). Wild-type mice and rats are normally insensitive to diphtheria-toxin fragment A (DT-A) since the rodent cell-surface receptor (heparin-binding EGF-like growth factor, or HB-EGF) for the diphtheria-toxin fragment B (DT-B) cell-binding moiety does not recognize DT-B (Saito et al., 2001). Therefore, in diphtheria-toxin-receptor conditional ablation, transgenic mice are designed to express human or monkey HG-EGF in a tissue-specific manner using an appropriate gene promoter. Once able to enter the cell of interest, DT-A inactivates elongation factor 2 (EF-2) inhibiting protein synthesis (Saito et al., 2001) and consequently cleaving the internucleosomal DNA (Chang et al., 1989) leading to cell death. In both instances, the cellular response to these

forms of cellular injury are drastically different from the cascade of cellular death in ischemia-induce necrosis [see Figure 1, adapted (Lilly, 2011)]. Therefore, the concept of mechanically clamping the apex of the heart is proposed to prevent perfusion of cardiac tissue to recapitulate an ischemic environment (inadequate blood flow to the beating ventricular myocardium) for the desired pathogenesis (ischemia-induced cellular necrosis) and tissue pathology (myocardial infarction).

General Approach of Specific Aim 1

The concept of mechanically clamping the apex of the heart is proposed to prevent the local perfusion of cardiac tissue. This should recapitulate an ischemic environment (inadequate blood flow to the beating ventricular myocardium) for the desired pathogenesis (ischemia-induced cellular necrosis) and tissue pathology (myocardial infarction). Prior studies on cardiac regeneration in axolotls do not contain complete details on performing open thoracotomies (Cano-Martinez et al., 2010) in these animals and the pre-, peri-, and post-operative care that is required to ensure animal welfare following major survival surgery. Additionally, since this is a novel technique, no prior guidance is available on the appropriate tools and technique to perform a mechanically-induced cardiac ischemic injury.

While developing surgical procedures to induce a myocardial infarction in axolotls, guidance on analgesics in amphibians for appropriate animal welfare was lacking. Federally funded animal research must adhere to the Public Health Service Policy on Humane Care and Use of Laboratory Animals, which states that “procedures that may cause more than momentary or slight pain or distress to animals will be performed with appropriate sedation, analgesia, or anesthesia” unless the procedure is justified for scientific reasons in writing by the investigator

(National Research Council (U.S.). Committee for the Update of the Guide for the Care and Use of Laboratory Animals. et al., 2011). Given the nature of regenerative medicine research, animals are frequently subjected to surgical injury to observe the healing process. Potential experimental confounders include the impact of opioids on wound healing (Chrastil et al., 2013) and the effects of stress, pain, and pain-induced stress on immune function.

Mexican salamanders (axolotls), *Ambystoma mexicanum*, require simple husbandry and straightforward maintenance to keep animals well and healthy. In addition to their ease of care, their versatility as a research model to study developmental biology and tissue regeneration has led to their active use in laboratory research since the 1860s (Farkas and Monaghan, 2015). Over the years, much has been published about the general anatomy, biology, and behavior of axolotls. However, while being used for more than 150 years in regeneration studies, regularly involving painful procedures like limb amputation, guidance is lacking on the use of analgesics in amphibians to provide appropriate animal welfare.

Although amphibians are specifically excluded from guidelines in the Animal Welfare Act (AWA) (States, 2013), their status as vertebrates subjects their use in research activities to be regulated by Public Health Service (PHS) policy (Alworth and Harvey, 2007). Under the umbrella of PHS policy, the following documents require that every opportunity to minimize pain and distress are explored: the 1985 U.S. Government Principles for the Utilization and Care of Vertebrate Animals Used in Testing, Research, and Training (Committee, 1985); the 2011 *Guide for the Care and Use of Laboratory Animals* (Council, 2011); and the 2015 reprint of PHS Policy on Humane Care and Use of Laboratory Animals (Welfare, 2015). Furthermore, not only is animal welfare a concern, but pain, stress, and pain-induced stress have been known to affect overall

health and wound healing in animal and human patients (Christian et al., 2006; Glaser and Kiecolt-Glaser, 2005; Godbout and Glaser, 2006; Guo and Dipietro, 2010; McGuire et al., 2006; Soon and Acton, 2006; Vileikyte, 2007). Many diseases such as cardiovascular disease, cancer, diabetes, and compromised wound healing can be traced to dysregulation of the immune system, mediated by the hypothalamic-pituitary-adrenal (HPA) and sympathetic-adrenal medullary (SAM) / sympathetic nervous system (SNS) (Glaser and Kiecolt-Glaser, 2005; Guo and Dipietro, 2010). Therefore, to maintain animal welfare and minimize confounds in studying tissue regeneration in axolotls, appropriate analgesia is crucial.

Opioid receptor activation leads to a variety of effects, including analgesia, euphoria, feeding, hormone secretion, respiratory depression, reduction in gastrointestinal mobility, anxiolysis, and immune system modulation (Waldhoer et al., 2004). Focusing on tissue repair and the immune system, morphine, the prototypical μ-opioid receptor (OP_3) agonist, increases corticosteroid secretion and decreases natural killer cell activity (Hugunin et al., 2010; Odunayo et al., 2010). Overall, morphine administration leads to a dose-dependent suppression of T-cell proliferation with an increase in proinflammatory cytokines and a decrease in anti-inflammatory cytokines (Odunayo et al., 2010). However, studies have demonstrated that buprenorphine can be safely used in models of sepsis in mice (Hugunin et al., 2010) since buprenorphine has been shown to have less of an impact on the immune system compared with other opioid analgesics (morphine). However, this relationship has not been established in amphibians. Since it has been demonstrated that the immune response is directly involved in healing and regeneration in axolotls (Godwin et al., 2013; Godwin and Rosenthal, 2014), the impact of the dose-dependent use of opioids on tissue regeneration should be elucidated. Furthermore, not only can opioid

signaling play a role in tissue regeneration through immune system mechanisms, opioids have been known to directly provide cardioprotective effects through μ-opioid receptor stimulation. Multiple published studies in rats and rabbits regarding morphine preconditioning and postconditioning show that this opioid attenuates infarct size after ischemia-reperfusion injuries. (Chen et al., 2008; Groban et al., 2004).

Available studies covering analgesia use in amphibians have used frogs (*Xenopus laevis* and *Lithobates pipiens*) and newts (*Notophthalmus viridescens*). However, a recent book chapter (Farkas and Monaghan, 2015) cautioned the direct application of amphibian protocols and findings in different species for procedures used on axolotls, citing that although they are all amphibians, the different species are not closely related. Frogs are distantly related to urodeles (any order of amphibians that have a tail throughout life such as salamanders), diverging from a common ancestor about 260 million years ago (Farkas and Monaghan, 2015). Similarly, although newts and axolotls are both urodeles with similar superficial anatomy, they diverged from a common ancestor about 145 million years ago (Farkas and Monaghan, 2015). This divergence is evidenced by the fact that newt regeneration and axolotl regeneration after limb injury is driven by different mechanisms (Sandoval-Guzman et al., 2014). With sufficient differences in physiology, a study on the appropriate analgesia and their administration (dosage and frequency) in axolotls is warranted.

This study aimed to elucidate two objectives: 1) determine an appropriate dosage and frequency of administration between two commonly studied analgesics in amphibians - an injected (intracoelomic route) mixed partial opioid-receptor agonist-antagonist [buprenorphine (Lutfy and Cowan, 2004)] with a transcutaneously-delivered mixed partial opioid-receptor

agonist-antagonist [butorphanol (Schnellbacher, 2010)] to provide pain relief after noxious somatic and/or visceral stimuli; and 2) determine whether, and to what degree, opioid analgesics affect tissue healing and regeneration in an axolotl surgical model. Literature searches reveal few, published scientific studies investigating general signs of pain or distress in axolotls. Thus, to achieve the study objectives, methods to objectively and subjectively characterize behavior after noxious stimuli were also developed.

Animals

Mouse (Mus musculus):

Mice are housed per Wayne State University (WSU) Institutional Animal Care and Use Committee (IACUC) and WSU Division of Laboratory Animal Resource (DLAR) standard operating procedures. For details, please see APPENDIX B: IACUC & DLAR DOCUMENTATION – ANIMAL PROCEDURES.

Axolotl (Ambystoma mexicanum):

Male, adult, breeding and non-breeding wild-type axolotls (>60g) were purchased from the Ambystoma Genetic Stock Center (University of Kentucky; Louisville, KY). The animals are individually housed in open top polypropylene, static, mouse cages (19.0" X 10.5" X 6.125"). For environmental enrichment purposes, a single commercial rodent tunnel or 2" schedule 40 PVC pipe (~ 6-8" in length) is placed in the cage; enough 50% Holtfreter's solution (Armstrong and Malacinski, 1989; Hamburger, 1942) (5-6 liters) is added to cover the rodent tunnel to allow the axolotls free ability to swim into and hide in the tunnel. Tap water is treated using Kordon® water conditioner NovAqua® Plus™ and ammonia detoxifier AmQuel® Plus™ (Kordon LLC; Hayward, CA). The 50% Holtfreter's solution is made by mixing the appropriate amounts of salts (1.75 g

NaCl, 0.050 g $CaCl_2$, 0.025 g KCl, and 0.100 g $NaHCO_3$ to each liter of treated tap water) using a 55-gallon drum mixer in a clean container (e.g. commercial 44-gallon trash can) with the treated tap water, allowing the solution to age at least 24-hours to allow the Kordon® products to condition the tap water and allow chlorine to outgas (container was kept partially uncovered ~24 hours to allow chlorine outgassing). Before using, the quality of each batch of 50% Holtfreter's solution is checked using EasyStrips™ 6-in-1 Aquarium Test Strips and Ammonia Test Strips (Tetra; Blacksburg, VA). The animals are housed in a windowless room to prevent exposure to natural light that facilitates algae growth, instead using a 12:12-h artificial light:dark cycle (using standard fluorescent lighting) with an ambient temperature between 15-19°C (~59-66°F). Animals are fed ad libitum a diet of sinking Soft-Moist Salmon Diet (Rangen; Buhl, ID) three days a week (Monday, Wednesday, and Friday), allowing up to 2 hours for the animals to feed as adult axolotls exhibit low levels of activity when left undisturbed. Immediately after feeding, animals are transferred to new plastic rodent cages; tunnels are rinsed and replaced weekly. All axolotls are checked daily for overall health, inspecting the condition of gills and dorsal fin for signs of stress, along with observing for the presence of feces to ensure appropriate GI function. All animals are acclimated to laboratory conditions for 5 days before performing any experimental procedures. All animal use was approved by WSU's IACUC.

Mechanically-Induced Ischemia

Approach to Clamping of Cardiac Apex

The original IACUC A 02-02-14 Protocol and updated eProtocol 16-12-173 (see APPENDIX B: IACUC & DLAR DOCUMENTATION – ANIMAL PROCEDURES) provide general details concerning

the approach and methodologies to mechanically clamp the heart. As a novel approach to model ischemia in an animal without coronary arteries, further details are provided here.

No animals will undergo more than one major surgical procedure. All animal use was approved by Wayne State University's (WSU) Institutional Animal Care and Use Committee (IACUC). Under the guidance of WSU's veterinarians and Division of Laboratory Animal Research (DLAR), research was conducted in compliance with the Animal Welfare Act (States, 2013), principles stated in the *Guide for the Care and Use of Laboratory Animals* (Council, 2011) and other federal statutes and regulations relating to vertebrate animals and experiments involving vertebrate animals. WSU is fully AAALAC-accredited and NIH/PHS-accredited.

Mouse (Mus musculus):

Thoracotomies are commonly performed in mice. The steps listed in IACUC Protocol A 02-02-14 and eProtocol 16-12-173 are taken from various publications (Azhar et al., 1999; Bernal et al., 2009; Yang et al., 2002). The novel portion in this research project is the mechanical clamping of the apical portion of the mouse heart. Once the thoracotomy is performed and the ribs are retracted to expose the mouse's heart, the same setup using a single microvascular clamp described for the axolotl is used in the mouse. Male and female mice were used for pilot studies. To confirm development of pathology, if the mouse survived the ischemic event, at least five days elapsed before euthanasia and harvesting the heart for histological studies. Male and female mice were used for pilot studies. To confirm development of pathology, if the mouse survived the ischemic event, at least five days elapsed before euthanasia and harvesting the heart for histological studies. Please see Figure 3 for an overview of how the surgical instruments are arranged during the described surgery.

The difficulty in replicating the same injury in the mouse was finding a clamp that could produce sufficient force to grasp the compact myocardium of the mammalian heart, yet was gentle enough for the spongy, trabeculated myocardium of the axolotl. Additionally, it was found that grasping too much of the apex of the mouse's heart lead to fatal arrhythmias about 15-18 minutes into the procedure, a few minutes shy of the 20 minutes of ischemia needed for irreversible myocardial cell damage and cell death in mammalian hearts(Robbins et al., 2010). Thus, various trials of clamping methods and clamp types were completed with unsuccessful results. The microvascular clamp from Fine Science Tools (Cat. No. 00398-02), produced successful results in the mouse. This allowed us to pursue experiments in the axolotl.

A)  **B)** 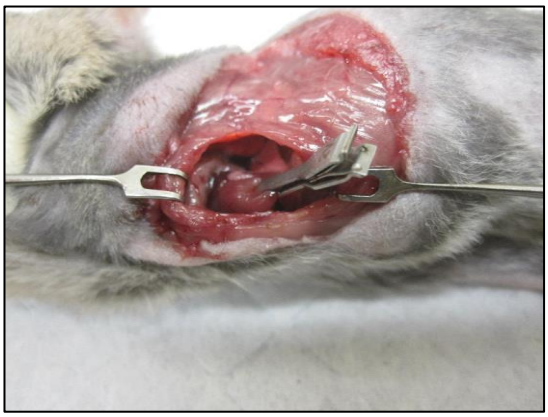

Figure 3: Layout of surgical instruments for mechanically clamping the heart in a mouse. **A)** General view of instrument layout. **B)** Slightly zoomed in view of surgical site. Rib spreaders allow visualization and access to apex of the heart. Lightly wiping the apex with a cotton applicator allows microvascular clamp to more easily grasp heart.

Axolotl (Ambystoma mexicanum):

Animals are fasted for at least 24 hours to avoid emesis during anesthesia induction. About one hour prior to inducing anesthesia, 0.5 – 0.75 mg/L of butorphanol is administered directly into the 50% Holtfreter's solution in the animal's cage to provide analgesia. Anesthesia is induced by placing the axolotl in a bath of 0.1% tricaine methanesulfonate (MS-222 or Tricaine-

S; Western Chemical, Inc., Ferndale, WA) dissolved in 50% Holtfreter's solution. After reaching a surgical plane of anesthesia, anesthesia is maintained by covering the animal in gauze sponges or Kimwipe™ laboratory tissues moistened with the same 0.1% MS-222 in 50% Holtfreter's solution. Every 10 minutes during the surgical procedure, an additional 3 – 5 mL of 0.1% tricaine methanesulfonate are squirted onto the gauze or tissues and on the animal's gills. Animals are kept in place in a dorsal recumbent position using rolled paper towels held to their shape using surgical tape. The rolled paper towel "chocks" keep the animal from rolling to either side during surgery.

Once a surgical plane of anesthesia is maintained, the ventral surface of the thorax is disinfected by placing gauze soaked in chlorhexidine solution (0.75%) or benzalkonium solution (2 mg/L) for 3 – 5 minutes at the intended site of incision followed by irrigation with sterile water or amphibian saline (0.63% NaCl). The concentration of amphibian saline was calculated from the plasma osmolarity of the axolotl (Hronowski and Armstrong, 1977). With the animal in a dorsal-recumbent position, a 10 – 15mm paramedian ventral thorax-area incision will be made with a #22 blade (amphibian integument is thin, but very tough (Wright, 2000)) on the animal's right or left side to prevent damaging the pectoral girdle. Advance the cut about 10 mm caudal to the gular fold (line of fusion between the larval gill cover and the skin, providing a demarcation between head and pectoral region(Francis, 1934)). A skin flap is made by using microsurgical scissors to create two cuts perpendicular to the ends of the initial incision to a similar landmark on the animal's lateral side, providing access to the pectoral girdle. The skin flap is made large

enough such that it lays open strictly due to gravity and surgical tools or clamps are not needed to maintain access. Please see Figure 4 for an example of how the animal presents after this step.

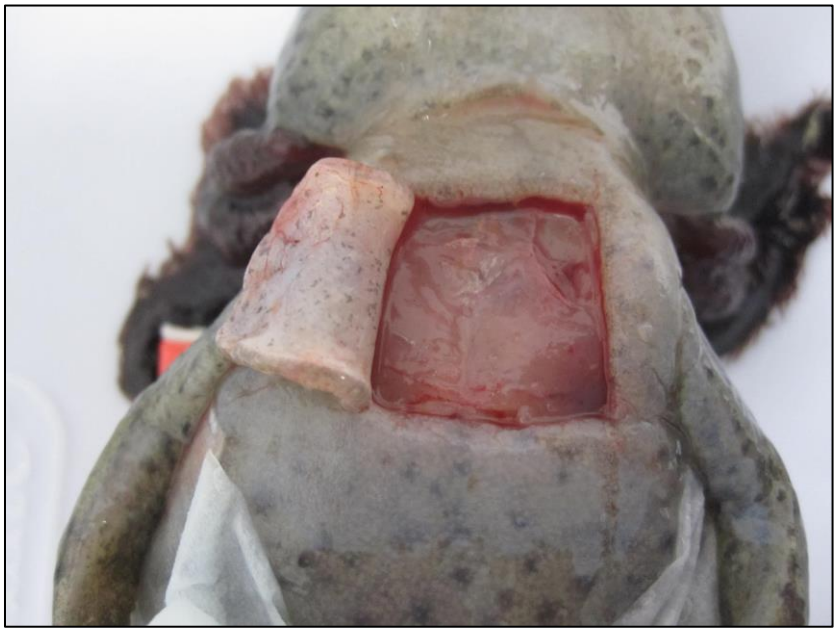

Figure 4: Access to axolotl pectoral cavity
Creation of skin flap provides access to underling coracoid cartilage.

The coracoid region, the largest portion of the pectoral girdle, consists of right and left aspects of coracoid cartilage [see Figure 5 (Francis, 1934)]. These flaps extend across two-thirds of the width of the axolotl's body from the attached forelimb, thereby overlapping each other in the middle. Either left or right aspect can be superficial or deep to its respective counterpart. Forming a semi-circular plate, with its convex side facing ventrally, the coracoid region forms a "breastplate" to protect the animal's pectoral region. The connective tissue that attach the left and right aspects of the coracoid cartilages can be bluntly dissected away with micro scissors, allowing each coracoid cartilage to be rotated out of the way to expose the animals rostral portion of its ventral trunk. After rotating the coracoid cartilages out of the way, they can be held

open using ultra fine hemostats (Fine Science Tools, Cat. No. 13021-12, or equivalent); compression of the cartilage will occur but this will not affect clinical outcomes.

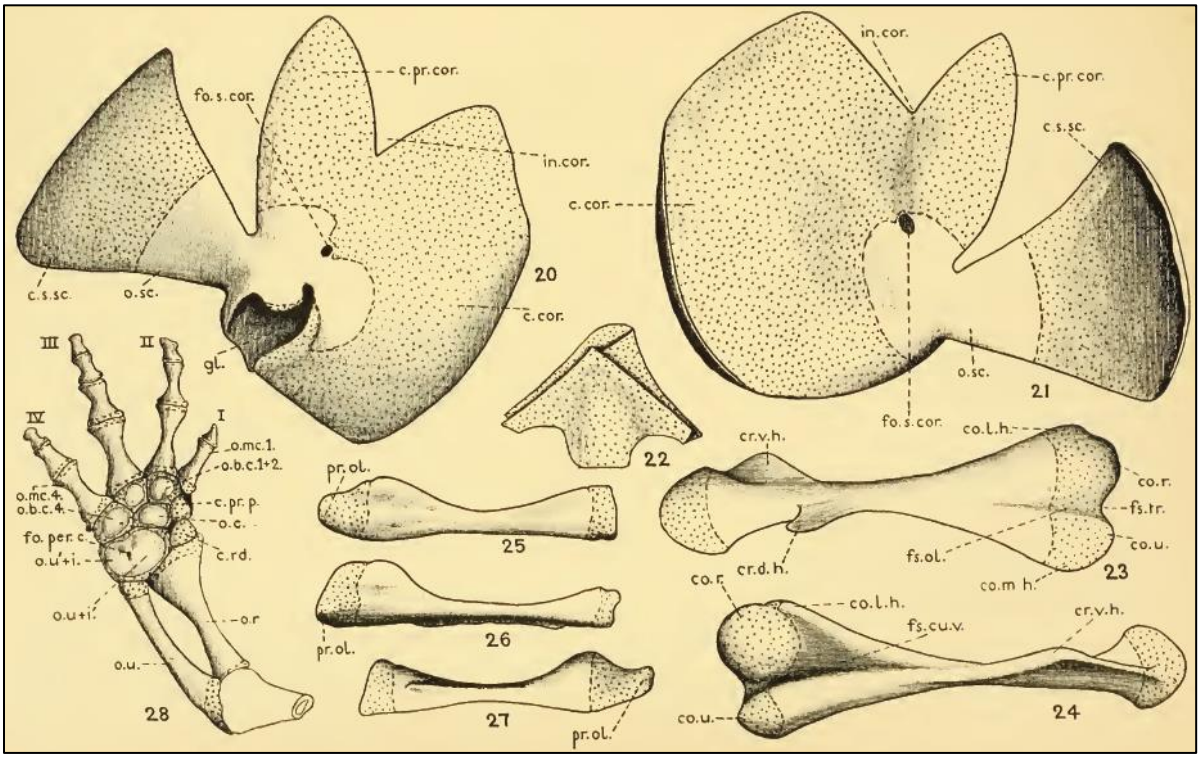

Figure 5: Anatomy of axolotl pectoral girdle.
From Plate IV in *The Anatomy of the Salamander* (Francis, 1934). Important features include: c.cor = coracoid cartilage and c.pr.cor = procoracoid cartilage.

After the left and right aspects of coracoid cartilage are rotated out of the way, the animal's pectoral cavity is exposed. Retraction of the two aspects of coracoid cartilage can be accomplished using curved forceps (Fine Science Tools, Cat. No. 11017-17, or equivalent) placed between the ultrafine hemostats (insert forceps in the closed position) with the natural opening tension sufficient to retract the two aspects of coracoid cartilage. Within this cavity, the pericardium is immediately visible, a tough, fibrous, and semi-transparent membrane that forms a pericardial cavity around the heart. Grasp the pericardium with fine forceps and hold it away from the beating heart to prevent damaging the heart while creating incision into pericardium. Using fine or microsurgical scissors, an incision is made in the pericardium to provide access to

the axolotl's heart. To provide retraction of the incision, curved forceps (Fine Science Tools, Cat. No. 11017-17, or equivalent) can be placed into the incision (insert forceps in the closed position) with the natural opening tension sufficient to retract the pericardium. With the heart now visible, a single microvascular clamp (Fine Science Tools, Cat. No. 00398-02, or equivalent) is carefully placed to clamp the apical portion of the heart. The heart tissue should immediately blanch, indicating a lack of blood flow to the area. This approach of clamping the heart to mechanically induce ischemia is adapted from a method to stabilize the heart during surgeries to repair penetrating cardiac wounds (Grabowski et al., 1995). Please see Figure 6 for an overview of how the surgical instruments are arranged during the described surgery.

A) 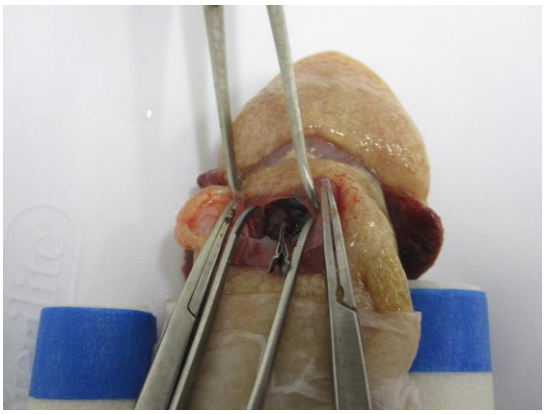 **B)** 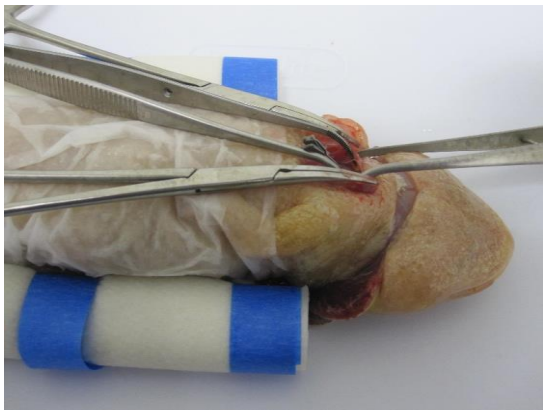

Figure 6: Layout of surgical instruments for mechanically clamping the heart in an axolotl. **A)** Ultra-fine hemostats hold the two coracoid cartilage structures in positions rotated away from the pericardial cavity. The curved forceps at the top and bottom of the figure provide traction on the pericardium, allowing unobscured access to the heart. The base of the heart is clamped with an S&T vascular clamp. **B)** A side view of the surgical procedure showing a different view of the surgical instruments and the vascular clamp in place.

After sustaining ischemia for the recommended amount of time, rinse the cardiac cavity as necessary with sterile amphibian saline or sterile Lactated Ringer's solution and approximate and close the pericardial sac with one loop of a 6-0 monofilament, non-absorbable suture tied with a simple surgeon's knot. Best results with closing surgical sites during the development of this surgical protocol were obtained with Novafil™ sutures (Monofilament Synthetic Polybutester

Suture; Covidien, New Haven, CT) for acute procedures or Biosyn™ sutures (Monofilament Synthetic Glycomer™ 631 Suture; Syneture, Norwalk, CT) for chronic procedures. Moisten the pectoral cartilage that is held with the ultra-fine hemostats to prevent tearing the cartilage from the hemostat's jaws. For acute procedures, the skin is closed using an everting suture pattern (to prevent keratin cysts (Gentz, 2007; Wright, 2000)) with non-absorbable, monofilament sutures. For chronic procedures, the skin is closed using absorbable, monofilament sutures.

Though aseptic surgical techniques are used, after closing the animal, a single dose (5 mg/kg) of enrofloxacin (Baytril®; Bayer DVM, Shawnee Mission, KS) is administered post-operatively as amphibian procedures are considered "clean-contaminated" at best. The enrofloxacin is diluted to 5 mg/mL using sterile amphibian saline. Additionally, post-operative fluids (sterile amphibian saline) are administered at a dose of 10 mL/kg (Gentz, 2007). Animals are thoroughly rinsed in fresh 50% Holtfreter's solution and then returned to their home cage to continue exposure to butorphanol as the animal recovers from anesthesia. Post-operative analgesia continues for 48-72 hours.

Post-operative care and procedures:

Food is offered starting on postoperative day 1 (surgical procedure is day 0). The surgical wound is assessed daily for any complications. For 3-5 days following surgery (as allowed by each experimental schedule), the animals are assessed for signs of stress and infection. Additional injections of enrofloxacin are provided if signs of stress or infection are present. Most animals show no signs of post-surgical infection as Holtfreter's solution helps inhibit the growth of bacteria, fungi, and parasites (Wright and Whitaker, 2001).

For nuclei labeling index studies to detect cardiomyocyte proliferation and turnover, each animal is injected with BrdU [250 mg/kg, intracoelomic] (Cano-Martinez et al., 2010) at least three hours prior to euthanasia and heart collection. BrdU is soluble in water up to 10 mg/mL without the use of heat. To dissolve BrdU, it is suggested to use sterile amphibian saline for injection into axolotls.

Time for Ischemic Damage:

The length of time needed to induce ischemic damage in the axolotl heart to recapitulate a myocardial infarction and the subsequent ischemia-reperfusion injury is unknown. As part of developing this novel cardiac injury model, experiments will start with inducing a 20-minute ischemic event prior to euthanizing the animal. Depending upon the histopathologic results from simple stains like H&E and Gomori's/Masson's trichrome stains (Gomori's usually counterstains collagen green, Masson's usually counterstains collagen blue), the amount of time for ischemia will be adjusted upward.

GLAS Experiment 1 – Validate Quantitative Methods to Evaluate Nociception in Naïve Animals

While there are several demonstrated differences between frogs, newts, and salamanders, it has been shown that A- and C-nociceptive fibers are present in most vertebrate animals, including amphibians (Coble et al., 2011; Hamamoto and Simone, 2003; Sneddon, 2014). Although axolotls are classified in a different family and order from newts and frogs respectively, it is expected that pain receptors are likely conserved within the class. However, nociceptor fiber distribution and number may vary (Sneddon, 2014). Previous studies in frogs (*Rana pipiens and Xenopus laevis)* have described mechanical (manual von Frey [vF] aesthesiometers), thermal, and

chemical (acetic acid test [AAT]) methods to assess pain and analgesic efficacy (Willenbring and Stevens, 1996). A recent study in newts (Koeller, 2009) (*Notophthalmus viridescens*) used qualitative behavioral observations to show the efficacy of opioids (buprenorphine and butorphanol) after limb amputation. Therefore, qualitative quantitative assessment methods and can be used in axolotls, but will likely need to be modified to produce a repeatable result within this species. Preliminary studies were conducted with a small number of axolotls using vF aesthesiometers (Touch Test Sensory Evaluator; Stoelting, Wood Dale, IL) and acetic acid testing to evaluate response to noxious mechanical and chemical stimuli (see APPENDIX A: PILOT STUDIES AND SUPPLEMENTARY INFORMATION for further details on Quantitative Pain Assessments). These studies have shown a clear, behavioral response to noxious stimuli and demonstrated the technical feasibility of adapting vF evaluators and the AAT to axolotls. Based upon these preliminary results, quantitative measurements will be used to optimize an opioid analgesic regimen to use in a surgical model in axolotls.

For this experiment, the two different quantitative techniques will be evaluated in naïve axolotls to determine which method produces more consistent responses. Each technique (vF or AAT) will be evaluated with the same group of six animals. The animals' response to noxious mechanical and chemical stimulation will be measured to establish a baseline response. The nociception threshold is defined as the weakest force or concentration that elicits a behavioral response. The quantitative method which produces the most repeatable measurements will determine which technique will be utilized in subsequent experiments. Details of how each quantitative test are performed can be found in the Quantitative Pain Assessments section of APPENDIX A: PILOT STUDIES AND SUPPLEMENTARY INFORMATION.

GLAS Experiment 2 – Determine Optimized Analgesia

The effects of different doses of butorphanol and buprenorphine on qualitative behavioral parameters and quantitative pain assessments to noxious stimuli was evaluated before and after the use of analgesia. The schedule of assessments is outlined in Table 1 (see APPENDIX A: PILOT STUDIES AND SUPPLEMENTARY INFORMATION for details on Quantitative Pain Assessments and Behavioral Assessments). Six animals were assigned to each analgesic group, buprenorphine or butorphanol, at three different doses (low [L], medium [M], or high [H] dosage). Buprenorphine (Penro Specialty Compounding; Colchester, VT) is administered at one of three doses (Low = 25 mg/kg, Medium = 50 mg/kg, High = 75 mg/kg) as an intracoelomic (IC) injection every 24-hours for 48 hours. Butorphanol (MWI Veterinary Supply; Boise, ID) shall be administered at one of three concentrations (Low = 0.25 mg/L, Medium = 0.50 mg/L, High = 0.75 mg/L) directly into the 50% Holtfreter's solution of the animal's cage every 24-hours for 48 hours. The medium dose is based upon a published dose that was effective in newts (Koeller, 2009) while the low and high doses are 50% lower or higher, respectively.

Following the study schedule outlined in Table 1, axolotls were subject to qualitative and quantitative tests to assess their behavior before and during administration of control (amphibian saline) or treatment drugs. Around 24-hours prior to administration of any study compounds, each group of six axolotls were tested for baseline behavioral and quantitative behavior. The next day, the study would commence with the operators (two for behavioral testing and one for quantitative testing) kept blind to the treatment.

Table 1: Study schedule for each dose (L, M, and H) in Experiment 2.

Test	Baseline	Analgesia	Assessments			Analgesia	Assessments			
	-24h	0h	1h	6h	12h	24h	25h	31h	36h	48h
Quantitative	✓		✓	✓	✓	✓	✓	✓		✓
Cageside	✓		✓	✓			✓	✓		
Video	✓ (x2)*		✓		✓	✓			✓	✓
Feeding	✓			✓				✓		

*Two measures in 24 hours

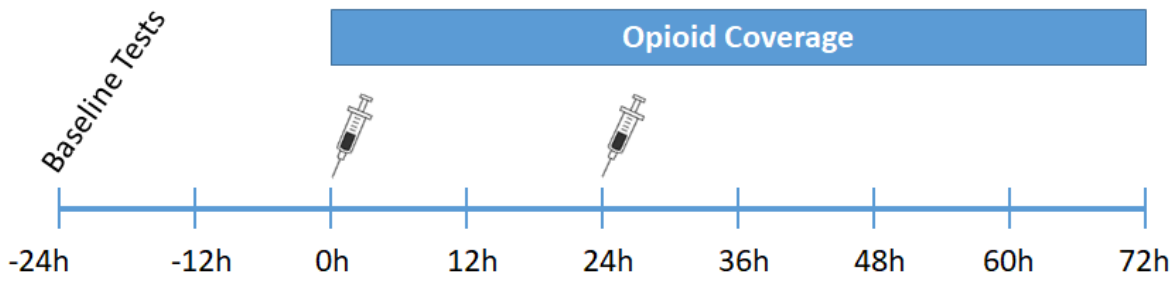

Figure 7: Goal of Analgesia Administration and Coverage
Analgesics were administered just prior to surgery and twenty-four hours later. Based on axolotl husbandry standard operating procedures, animals given butorphanol directly in the cage water were exposed up to seventy-two hours from surgery.

To keep the operators blinded to treatment, the study supervisor would draw and uniformly mark each syringe (e.g. with the identifying animal information), draw equal volumes of control or study drug for injection and control or study drug for immersion bath. Although each animal was only assigned one treatment, each animal received an injection of drug or control and administration of drug or control into the home tank. This was to ensure no operator knew if an animal was being treated with an injection- or immersion-based treatment.

GLAS Experiment 3 – Evaluate Optimal Analgesic Dose in a Surgical Model in Axolotls

Three surgical groups of animals (6 per group, receiving either butorphanol, buprenorphine, or no analgesic) will undergo mechanical induction of cardiac ischemia. Please see – ANIMAL PROCEDURES for specific details on performing the surgeries. Using data from Experiment 2, animals will receive optimized analgesic doses. The same evaluation criteria and

schedule (behavioral and quantitative methods) that were used in Experiment 2 will be used in Experiment 3 however the 0-hour time point will be designated as the point of recovery from anesthesia.

GLAS Experiment 4 – Evaluate Histologic Differences in Healing: Control & Analgesia

Three surgical experimental groups (buprenorphine, butorphanol, or no analgesia) of naïve axolotls will undergo mechanical induction of cardiac ischemia using the same doses utilized in Experiment 3. Please see APPENDIX B: IACUC & DLAR DOCUMENTATION – ANIMAL PROCEDURES for specific details on performing the surgeries. Each experimental treatment group will consist of 18 animals; 6 will be humanely euthanized at each of three post-operative time points (12 hours, 2 days, and 7 days). These time points were selected based upon observations from pilot studies we have performed examining cardiac histology in axolotls following mechanical ischemic injury. Following euthanasia, cardiac tissue will be collected for histologic processing and analysis. Quantitative and behavioral assessments will be performed as described in Table 1 for each group as allowed until the time of euthanasia.

Harvested hearts will be fixed in formaldehyde-zine fixative and sent to a third party for processing (Histowiz, Inc., Brooklyn, NY). Mounted sections will be stained using hematoxylin and eosin (H&E), Masson's Trichrome and Picrosirius Red methods. Staining times will be optimized by the third party to ensure good contrast in axolotl tissue. Cellular proliferation activity in the penumbra will be indexed by staining with antibodies specific for BrdU, while cell death will be tracked by proxy using TUNEL – these staining protocols will also be optimized by the third party. Studies of cardiac myofibrillogenesis describe the myofibril assembly process as a transition through three types of fibrils: premyofibrils containing non-muscle myosin IIB; nascent myofibrils

containing both non-muscle myosin IIB and muscle-specific myosin II; and mature myofibrils containing only muscle-specific myosin II (Rhee et al., 1994). All tissue samples will be stained with antibodies for proteins of myofibrillogenesis and stem cell markers; 10 high-powered views will be evaluated under microscopy to observe statistical differences in histology.

Histological Analysis

Histology sections will be viewed at various zooms. The reported results will exclude the 10X zoom of the eyepiece.

Statistical Analysis

The intraclass correlation coefficient statistical test can be used to assess the consistency of a measuring tool to quantify the same phenomenon under the same conditions. This statistical tests assesses how closely measurements of the same phenomenon on the same subject resemble each other (Shrout and Fleiss, 1979). The data regarding which mechanical probe or acetic acid vial produced a response was gathered by a single rater. Additionally, there is no dependence of order or score pairing on the outcome measures. Therefore, in SPSS, a one-way random model is used when calculating the intraclass correlation coefficient. Intraclass correlation coefficients (ρ) of $\rho = 1$ measures perfect test-retest reliability while a $\rho = 0$ suggests the measurement test has no reliability. An ANOVA within each test group is also run to make sure there are no outlier responses among the tested animals. Of note, an ANOVA assessment between the reliability measures between the von Frey evaluators and the acetic acid test is not applicable because this would be comparing means of two different outcome measures. An ANOVA is intended to compare means of the same outcome measure between different populations.

For the qualitative behavioral tests, animals were scored using a Likert-style system (0-3; no response, minor response, nominal response, and major response) for all measures except for feeding, which was simply dichotomous (yes or no), developed from observations during pilot studies. These observations are ordinal, except for feeding which is categorical. For the quantitative tests, the logarithmic dilutions of acetic acid were assigned vial codes. The logarithmic concentrations were mapped to an interval scale that includes 0 (0-15). Although the data are interval, since they are not normally distributed, a non-parametric statistical approach is used. When evaluating the efficacy of a control or treatment effect, the change (delta or Δ) in quantitative or qualitative response is referenced to the baseline measurement. Thus, the statistic that is being evaluated is change in response. Findings from qualitative testing, including change in feeding, are included to see if analgesics change behavior – they are not indicative of the efficacy of analgesia.

For pathology evaluations, multiple views for each section were inspected by an outside veterinary pathologist blind to treatment and time groupings. After gaining familiarity with the samples, a Likert-style ordinal scale was created to describe the histologic features under review. Only immunohistochemistry slides identifying TUNEL and BrdU and simple stains identifying heterophils, and lymphocytes were evaluated. Please see APPENDIX A: PILOT STUDIES AND SUPPLEMENTARY INFORMATION section for more information on the qualitative behavior and pathology scoring rubrics. In Kruskal-Wallis statistical testing, the test statistic used for hypothesis testing is the mean rank. This rank-based nonparametric approach is used to determine if there are statistically significant differences between two or more groups of an independent variable (e.g. treatment group) on an ordinal (or continuous) dependent variable

(e.g. pain assessment). The theory behind using mean ranks rather than the mean of the measured outcome is that the distribution of scores in each treatment group are not known a priori and are not assumed to be identical. Dependent outcomes are ranked, irrespective of the group, per the outcome's magnitude; small magnitudes have lower ranks while greater have higher ranks.

With the qualitative measurements and pathology assessments recorded as ordinal data along with the recoding of a non-normal (logarithmic) scale to an interval scale, the significance of treatment effects for qualitative and quantitative data at each time point are assessed by Kruskal-Wallis one-way analysis of variance (ANOVA) for unrelated samples. If the omnibus test shows significance, post-hoc comparisons are run using Mann-Whitney tests for qualitative and quantitative data on a succinct set of tests (compared to control treatment) to prevent inflation of Type-I error rates. For pathology assessments, a subset of hearts was sent for staining and immunohistochemistry processing (Histowiz, Inc., Brooklyn, NY), thus reducing the sample size compared to qualitative and quantitative testing. Post-hoc comparisons for pathology scores are evaluated using two-sample Kolmogorov-Smirnov Z testing. At most, two post hoc tests will be performed (Control to Treatment 1 and Control to Treatment 2) so the critical level of significance in post-hoc testing is corrected (for multiple comparisons) from $\alpha_{critical} = 0.05$ to $\alpha_{critical} = 0.05/2 = 0.025$. For feeding behavior, we have the independent nominal variable of treatment group (e.g. control versus treatment) and the dependent nominal variable of change in feeding behavior (e.g. positive change, negative change, or no change). To investigate associations between two nominal (and categorical) variables, the Goodman and Kruskal's λ (or lambda) test is used. This test is a nonparametric approach to measure the strength of association between two variables.

Using this approach, the ordering of time is ignored and each time point is viewed independent. IBM SPSS Statistics software (Version 23 & 24, IBM North America, New York, NY) was used for all analyses.

Benchmarks for Success of Specific Aim 1

GLAS Experiment 1: For this experiment two different quantitative techniques, von Frey fibers and a modified acetic-acid wiping test, will be evaluated in naïve axolotls to determine which method produces more consistent responses. Each technique (vF or AAT) will be evaluated with a different group of six animals. The animals' response to noxious mechanical and chemical stimulation will be measured with an electronic vF aesthesiometer or different concentrations of acetic acid, respectively, to establish a baseline response. The quantitative method which produces the most repeatable results will determine which technique will be utilized in subsequent experiments.

GLAS Experiment 2: We will evaluate the effects of different doses of butorphanol and buprenorphine on quantitative and behavioral parameters (see Table 1). Six animals will be assigned to each analgesic group, buprenorphine or butorphanol (low [L], medium [M], or high [H] dosage).

GLAS Experiment 3: Three surgical groups of animals (6 per group, receiving either butorphanol, buprenorphine, no analgesic) will undergo mechanical induction of cardiac ischemia. Using data from Experiment 2, animals will receive optimized analgesic doses. The same evaluation criteria and schedule (behavioral and quantitative methods) that were used in Experiment 2 will be used in Experiment 3 however the 0-hour time point will be designated as the point of recovery from anesthesia.

GLAS Experiment 4: Three surgical experimental groups (buprenorphine, butorphanol, and no analgesia) of naïve axolotls will undergo mechanical induction of cardiac ischemia using the same doses utilized in Experiment 3. Each experimental group will consist of 18 animals; 6 will be humanely euthanized at each of three post-operative timepoints (12 hr, 2 days, 7 days). These timepoints were selected based upon observations from pilot studies we have performed examining cardiac histology in axolotls following mechanical ischemic injury. Following euthanasia, cardiac tissue will be collected for histologic processing and analysis. Quantitative and behavioral assessments will be performed as described in Table 1 for each group as allowed until the time of euthanasia.

Potential Problems and Alternative Strategies for Specific Aim 1

GLAS Experiment 1: The current approach to elicit a nociceptive response in axolotls relies on stimulating the animal just lateral to the dorsal fin, in line with its forelimb. However, in the integumentary system of salamanders, in contrast to the cold/heat receptors and tactile receptors located in the epidermis, the pain and pressure receptors are situated in the dermis. Thus, the vF aesthesiometers may be stimulating tactile receptors and not pain receptors. Additionally, while several behaviors observed in newts may be useful in evaluating analgesic efficacy in that species, it is unclear whether these same behaviors will be useful in axolotls. Given the lack of any established pain related ethograms specific to axolotls, the published data in newts is the most promising starting point.

GLAS Experiment 2: Although a significant body of knowledge on pain control exists in newts and frogs, caution is advised when applying doses and schedules to axolotls that diverged from the closest common ancestor 145 and 260-million years ago, respectively. If no significant

differences are noted in somatic nociception, proceeding onto the next set of experiments is still warranted to determine if the drugs and doses tested provide antinociception to visceral pain. Also, with opioid receptor distributions that are predate the mammalian distribution patterns, common side effects of opioid use in mammals may arise in amphibians.

GLAS Experiment 3: Like Experiment 2, using drugs and doses from a distantly related cousin to the axolotl may not result in significant differences in antinociception compared to control animals. However, proceeding onto the next set of experiments is still warranted to determine if the drugs and doses tested affect tissue histopathology during healing and/or regeneration.

GLAS Experiment 4: The histopathology of healing and regenerating cardiac tissue after an ischemic injury is unknown. Histology staining optimization will be optimized by the third party. However, immunohistochemistry relies on compatible antibody binding. The best-available muscle myosin and non-muscle myosin antibodies will be used, but their compatibility to axolotl tissue is not guaranteed. Optimization by the third party will proceed at their expertise.

Potential Hazards of Specific Aim 1

Experiment 1: Undue pain and stress on the animals can result from the assessment of behavior from noxious stimuli. A stepwise approach from very mild to highly noxious will be used to elicit behavior, while closely monitoring animal welfare at each step throughout the experiments.

Experiment 2: Administration of one of the drugs requires injection. The injection site has been chosen to prevent damage to internal organs, while DLAR training of the users to handle injections in animals is a safeguard to safety of laboratory personnel. Additionally, injection of

animals under light sedation will increase safety to both animal and laboratory personnel during the procedure.

Experiment 3: Thoracotomies and survival surgeries are highly stressful to the animal and require surgeon skill to successfully complete. Multiple practice and pilot surgeries were performed to ensure constant sedation and animal welfare throughout the procedure. Constant monitoring of the animals while under a surgical plane of anesthesia is standard practice for all animal procedures.

Experiment 4: The euthanasia process proceeds with a stepwise approach from inducing anesthesia, performing primary euthanasia using a higher dose of anesthetic, followed by assurance of death using decapitation and pithing. Personnel safety is a potential hazard due to the use of scalpel and large-bore hypodermic needles. Multiple practice and pilot euthanasia attempts were successfully completed to ensure the welfare of the animal and establish competency of the process for laboratory personnel.

Specific Aim 2

Overview of Specific Aim 2

Determine the spatiotemporal progression of axolotl cardiac tissue histopathology over time after mechanically-induced ischemia-reperfusion injury.

After establishing the pre-, peri-, and post-operative procedures to induce a true ischemic injury in axolotls, monitoring gross functional recovery and the spatiotemporal development of histopathology in the damaged areas over time will enhance understanding of cardiomyocyte biology and lifecycle.

Rationale of Specific Aim 2

Urodele amphibians, which include axolotls, are the only vertebrates that have been shown to dedifferentiate their cells, recreating an "embryonic" environment from which they can regenerate injured body parts and internal organs. With the ability to "start over", this process of repair and regeneration leads to the perfect replacement of the lost or injured tissue via cellular dedifferentiation, subsequent cellular proliferation, followed by re-differentiation into the appropriate cell phenotypes, a process termed epimorphic regeneration (Roy and Gatien, 2008). Mammalian cells were shown to have the ability to dedifferentiate as well (Odelberg et al., 2000), but this was done under experimental conditions by the ectopic expression of the homeobox-containing transcriptional repressor *msx1*. *msx1* has been identified in the regenerating urodele limb blastema and the limb of a developing mammalian mouse embryo (Odelberg et al., 2000). Thus, unlike mammals, urodeles can regulate the signaling mechanisms that mediate cellular dedifferentiation, proliferation, and re-differentiation, allowing them to maintain their lifelong ability to regenerate [see Figure 8, adapted from (Roy and Gatien, 2008)]. Unfortunately, there have not been any studies to test this ability in urodeles in the heart using a model of ischemic injury. Furthermore, newts and axolotls have shown mechanistic differences in how they regenerate skeletal muscle injuries (Sandoval-Guzman et al., 2014). Thus, since the newt (*Notophthalmus viridescens*) is a neotene, whereas the axolotl (*Ambystoma mexicanum*) is an obligate neotene (Duellman and Trueb, 1994), cardiac injury regeneration in the newt

(Oberpriller and Oberpriller, 1974) may follow different mechanisms and produce different results compared to the axolotl, especially when using a true ischemic injury.

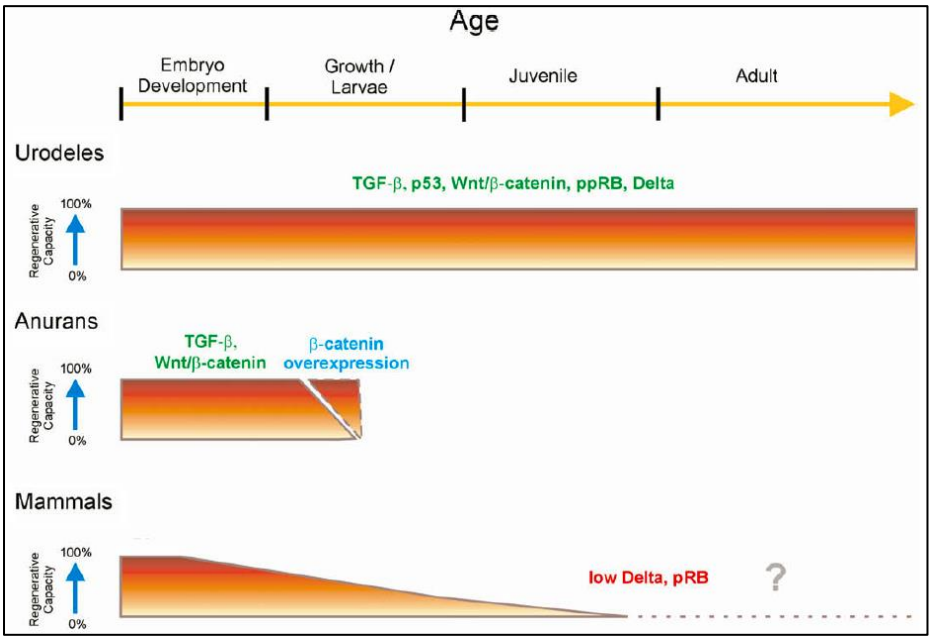

Figure 8: The relationship between the regenerative capacity of various species and the age of the organism.
Also shown are proposed molecules responsible for the regenerative capacity (or lack thereof) are shown.

General Approach of Specific Aim 2

Echocardiography

The first historical use of ultrasound to record moving images of the heart occurred on October 29, 1953 by Dr. Inge Edler and Dr. Hellmuth Hertz using the Siemens Ultrasound Reflectoscope (Singh and Goyal, 2007). Heralding the field of "ultrasound cardiography", their findings of M-mode ultrasound images were eventually published in the proceedings of the Royal Physiological Society in Lund in 1954 (Edler and Hertz, 2004). M-mode, which uses only one ultrasonic beam, is rarely used by itself in modern equipment, being a supplement to 2D scans with multiple ultrasonic beams transmitted through wide arcs, or Doppler imaging that allows for the detection of blood flow direction and velocity. These modern applications of ultrasound

waves, now referred to as echocardiography or cardiac ultrasound, provides a safe, non-invasive imaging modality that plays an essential role in the diagnosis and serial evaluation of cardiac pathologies (Lilly, 2011).

Development of Non-Invasive, Functional Cardiac Imaging

Axolotls are anesthetized in small mouse poly using 0.1% tricaine methanesulfonate (MS-222). Figure 9 shows the setup for conducting ultrasound scans. Scans are performed immediately after inducing a light plane of anesthesia and performed as quickly as possible to prevent a decrease in cardiac output due to prolonged anesthesia exposure.

Figure 9: Setup for Ultrasound Scans
After inducing anesthesia, axolotls can be held in place with rodent crocks or enrichment tunnels.

Access to a Verasonics Vantage 128™ (www. http://verasonics.com/vantage-systems/) high-resolution research ultrasound system was kindly provided by Dr. Mohammadreza Nasiriavanaki of the WSU Biomedical Engineering (BME) department. Controlled through a MATLAB® (https://www.mathworks.com/) interface, script modification is required to fit individual applications.

MathWorks®, the makers of MATLAB®, offer add-on suites to the base installation of MATLAB® to give end-users additional options for specific applications. Since the MATLAB® script templates from Verasonics do not modify the receive (RCV) signal before recording results to audio-video interleave (.avi) files, image post-processing is required to analyze images recorded by the Vantage 128™ system. The Image Processing Toolbox suite provides additional capabilities to image processing workflows. After individually captured frames are extracted from audio-video interleave files using the open-source software VirtualDub (Version 1.10.4, Build 35491: https://sourceforge.net/projects/virtualdub/), the images can be processed by MATLAB® using commands enabled by the Image Processing Toolbox suite. The pseudo code approach to image processing follows this simplified algorithm: 1) Convert image to grayscale color space, 2) enhance grayscale images, 3) manually define the region of interest (ROI), and 4) calculate the functional cardiac parameter of interest. Please refer to the section "MATLAB® Code for Image Post-Processing and Fractional Area Change Calculations" in APPENDIX A: PILOT STUDIES AND SUPPLEMENTARY INFORMATION for details on the development of the image post-processing script used to determine cardiac fractional area change (FAC) for the axolotls presented in CHAPTER 6: RESULTS.

Time Course for Follow-Up

Review of cardiac regeneration studies in zebrafish provide range of expected timescales for regeneration of different cardiac injuries. After cardiac resections with the removal of up to 20% of the ventricular apex, full regeneration has been shown after 2 months due to local cardiomyocyte proliferation. Following a cardiac injury from cryoablation, freeze damage of around 25% of the ventricle can be completely remodeled after 4 months with local

cardiomyocyte proliferation replacing collagen from the lesion that forms. After conditional genetic ablation of up to 60% of both atrial and ventricular cardiomyocytes, the zebrafish heart rapidly remodels within 1 month after injury from robust global cardiomyocyte proliferation (Choi and Poss, 2012). Given these time estimates of regeneration in the zebrafish, and without any guidance in how a true ischemic cardia injury in the axolotl will remodel, 1-, 2-, 3-, and up to 4-month follow-up time points for collecting heart specimens with regular (e.g. weekly or bi-weekly) echocardiograms to monitor functional recovery will be the approach in this study.

Animals

Adult, male and female, wild-type axolotls at ~7 years of age were gifted from the Dr. James Thomson laboratory (through Dr. Jeff Nelson, Regenerative Biology Laboratory, Morgridge Institute for Research). The animals were individually housed in plastic, static rodent cages without the use of the cage top – animals are identified by marking on their individual cage cards. For environmental enrichment purposes, a single rodent tunnel is placed in the cage; enough 50% Holtfreter's solution(Armstrong and Malacinski, 1989; Hamburger, 1942) is added to cover the rodent tunnel to allow the axolotls free ability to swim into and hide in the tunnel. Following pilot studies and GLAS Grant experiments, animals were kept in 50% Holtfreter's solution made from tap water treated using Kordon® water conditioner NovAqua® Plus™ and ammonia detoxifier AmQuel® Plus™ (Kordon LLC; Hayward, CA). After ectoparasites like *Ichthyobodo necator*, *Chilodonella uncinate*, and various species from the genus *Trichodina* were found from skin scrapings on multiple animals, deionized water from the research building's water processing plant (particulate filtration, reverse osmosis, UV treatment, and deionization) was used as the water source for 50% Holtfreter's solution. The change in water source occurred

before any surgeries were performed. The 50% Holtfreter's solution is made by mixing the appropriate amounts of salts (1.75 g NaCl, 0.050 g $CaCl_2$, 0.025 g KCl, and 0.100 g $NaHCO_3$ to each liter of treated tap water) in a clean, uncovered container (e.g. 44-gallon commercial trash can) with the building's deionized water. The 55-gallon drum mixer was cleaned with Contec™ Accel TB™ Ready-to-Use Disinfectant (active ingredient: 0.5% hydrogen peroxide) before inserting into the deionized water before mixing. Before using, the quality of each batch of 50% Holtfreter's solution is checked using EasyStrips™ 6-in-1 Aquarium Test Strips and Ammonia Test Strips (Tetra; Blacksburg, VA). Additionally, biological activity was checked with a Charm Sciences, Inc (Lawrence, MA) novaLUM luminometer which detects ATP residue from microorganisms. Test batches of 50% Holtfreter's solution made with clean containers, 55-gallon mixer, and deionized water showed no biologic activity for 72-hours after mixing. From this point onwards, all prepared 50% Holtfreter's solution was used within 72-hours or tested with the novaLUM to ensure zero biological activity.

The animals were housed in a windowless room to prevent exposure to natural light that facilitates algae growth, instead using a 12:12-h artificial light:dark cycle (using standard fluorescent lighting) with an ambient temperature between 15-19°C (~59-66°F). While observing feeding behaviors before surgeries, animals were fed ad libitum a diet of sinking Soft-Moist Salmon Diet (Rangen; Buhl, ID) three days a week (Monday, Wednesday, and Friday). However, after two animals became anorexic and were euthanized after two-weeks of inappetence, livers were tested and found positive for hypovitaminosis A. Animals were switched to a new diet, Amphibian & Carnivorous Reptile Gel (Mazuri, PMI Nutrition International LLC, Saint Louis, MO) on an every-other-day schedule. Animals are allowed up to 2 hours to feed as adult axolotls

exhibit low levels of activity when left undisturbed. If animals did not quickly acclimate to the new food source, the original Rangen Soft-Moist Salmon Diet was added to the cage. Immediately after feeding, animals are transferred to new plastic rodent cages; tunnels are rinsed and replaced weekly. All axolotls are checked daily for overall health, inspecting the condition of gills and dorsal fin for signs of stress, along with observing for the presence of feces to ensure appropriate GI function. All animals are acclimated to laboratory conditions for 5 days before performing any experimental procedures.

Since the axolotls from the University of Wisconsin showed some abnormal clinical behavior, female, adult, breeding and non-breeding wild-type axolotls (>60g) were purchased from the Ambystoma Genetic Stock Center (University of Kentucky; Louisville, KY). The animals were individually housed using the new method of Holtfreter's solution preparation and storage and were fed ad libitum the new diet, Amphibian & Carnivorous Reptile Gel (Mazuri, PMI Nutrition International LLC, Saint Louis, MO) on an every-other-day schedule. Animals were allowed up to 2 hours to feed as adult axolotls exhibit low levels of activity when left undisturbed. If animals did not quickly acclimate to the new food source, the original Rangen Soft-Moist Salmon Diet was added to the cage since the animals from the University of Kentucky were raised on this food source.

Experiment 1 – Development of Non-Invasive, Functional Cardiac Imaging

A 2017 publication studying cardiac cryoablation in axolotls used echocardiography to monitor cardiac morphology and function at various stages after cryoablation (Godwin et al., 2017a). The researchers in that study used a Vevo 2100 Imaging System (FUJIFILM/VisualSonics Inc., Canada), a commercial ultrasound solution for small animal imaging, with hardware and

software designed, assembled, and programmed for quick setup and ease of use by researchers. Without access to the same equipment and with the desire to look at raw ultrasound data from each channel, a collaborator at the home institution provided access and use of a research and development, high-frequency ultrasound machine, the Verasonics (Kirkland, WA) Vantage 128™. This development-only platform is run on proprietary Verasonics hardware with a user interface controlled by MATLAB® (MathWorks, Natick, MA).

Pilot scans were conducted with anesthetized animals in various configurations using ultrasound gel with animals out of the water, and directly on the skin while animals were submerged in anesthesia. Best results were found with direct application of the transducer to the submerged animal, and the transducer position was optimized to capture longitudinal ventricular cross sections. To enable consistency in capturing images, landmarks were found that applied to all animals. Underlying the dorsal surface of the heart is a mesocardial ligament (Francis, 1934) which anchors the heart to the dorsal surface of the pericardium. This provides a hyperechoic feature that allows for positioning the transducer. Furthermore, the transducer was rotated to capture the atrioventricular valves in the scan. Using these two landmarks help provide a repeatable approach to visualizing the axolotl heart.

After repeatable pilot scans of raw ultrasound data are captured, post-processing in MATLAB® is necessary to reduce noise and enhance features in the image. The MATLAB® software suite has robust image processing features and these are used to enhance images and to perform Fractional Area Change calculations (FAC). FAC should not be confused with ejection fraction (EF). When using ultrasound images, EF can be calculated by single-plane captures and tracing the appropriate images and applying the area-length method or modifications of

Simpson's rule (Quinones et al., 1981). These approaches extrapolate volumes based on well-defined ventricular chamber shape dictated by the compact myocardium in mammalian hearts, but can be improved using equations that incorporate velocity-time profiles of the outflow tract (Dumesnil et al., 1995). The trabeculated structure of the axolotl heart results in a poorly-defined ventricular chamber – thus, FAC is a way to estimate global ventricular function in amphibian hearts. The outer ventricular shape will be used to calculate FAC. Please see APPENDIX A: PILOT STUDIES AND SUPPLEMENTARY INFORMATION section for the details on the development of the post-processing algorithm and procedure to calculate FAC.

Experiment 2 – Long-Term Follow-up of Axolotl Hearts Following Ischemic Injury

Four surgical groups of animals (4-6 animals per group, for each endpoint for heart sampling) will undergo mechanical induction of cardiac ischemia. Using data from Aim 1, animals will receive optimized analgesic doses for 48-72 hours to provide for animal welfare and comfort. Please see APPENDIX B: IACUC & DLAR DOCUMENTATION – ANIMAL PROCEDURES for specific details on performing the surgeries.

Benchmarks for Success of Specific Aim 2

Experiment 1: After developing the algorithm to calculate FAC, comparison to the control values in the 2017 publication (Godwin et al., 2017a) will provide confidence to use approach developed by this laboratory.

Experiment 2: Induction of ischemia in the axolotls and survival until heart harvesting will be the endpoint for success in this experiment.

Potential Problems and Alternative Strategies for Specific Aim 2

Experiment 1: If the algorithm development cannot be achieved, other commercial, clinical ultrasounds that are ready for end-user applications are available at the home institution. A freely-accessible unit is a low-frequency, low-resolution unit, while a Vevo 2100 system is available from an imaging core at standard institutional-use fees. The Vevo 2100 system cannot be easily moved, making imaging the axolotls difficult, whereas the Verasonics Vantage 128™ is easily transportable and set up in the animal vivarium.

Experiment 2: Thoracotomies and survival surgeries are highly stressful to the animal and require surgeon skill to successfully complete. Multiple practice and pilot surgeries were performed to ensure constant sedation and animal welfare throughout the procedure. Constant monitoring of the animals while under a surgical plane of anesthesia is standard practice for all animal procedures. Multiple pilot survival surgeries have been performed to date with very few losses due to procedural errors during surgery (>95% survival rate to date). No potential problems are expected.

Potential Hazards of Specific Aim 2

Experiment 1: Imaging animals under light anesthesia does not pose any hazards.

Experiment 2: Multiple practice and pilot surgeries were performed to ensure surgeon skill with sharp instruments and familiarity with immersion anesthesia. Protective personal equipment requirements are outlined in approved protocols. Processes have been put in place and training has been provided to mitigate potential hazards.

CHAPTER 6: RESULTS

Specific Aim 1

Mechanically-Induced Ischemia

Mouse Pilot Studies

Using an appropriate microvascular clamp and carefully compressing only about 10-15% of the apical portion of the heart, attempts to mechanically-induce ischemia in the mouse were successfully completed without having to use antiarrhythmic drugs (e.g. dobutamine or dopamine) or emergency procedures (e.g. cardiac massage) to ensure animal survival. After 7

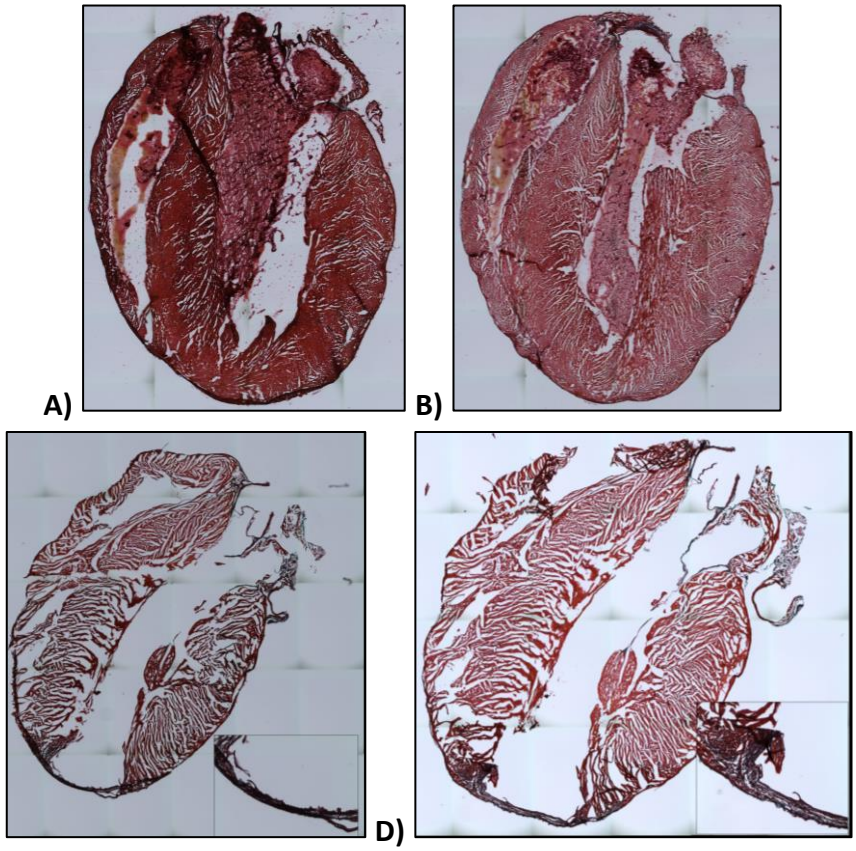

Figure 10: Histology of Mouse Hearts from Pilot Clamping Stides
Sections all stained with Gomori's Trichrome. **A)** and **B)** are hearts from naïve pilot animals. **C)** and **D)** are different sections from one animal that underwent mechanical induction of ischemia and shows evidence of ischemia-reperfusion injury. Inset pictures in the bottom row show additional details of thinned ventricular wall.

days, one animal was euthanized, the heart processed for histologic study, and stained with Masson's trichrome stain. As seen in Figure 10, the ventricular wall of the injured area shows evidence of thinning and slight chamber dilation, expected findings after a traditional myocardial infarction (Robbins et al., 2010).

Mechanically-Induced Ischemia: Axolotl Pilot Studies

After successful pilot results in mice, the same microvascular clamp and technique was used in axolotls. With no prior data on the time required to induce ischemia-reperfusion injuries, the appropriate time for ensuring ischemia-reperfusion injury was determined first by performing the mechanically-induced ischemic injury for 20 minutes and inspecting the histology of the injury site for signs of apoptosis and/or necrosis. Without any guidance on myocardial infarctions in salamanders, the 20-minute length of time was chosen as a starting point based on the clinical definition of human myocardial infarction (Robbins et al., 2010); 20 minutes of ischemia is the length of time needed for irreversible myocardial cell damage and cell death. A naïve heart from a group of pilot animals used to determine the required clamping-time for ischemia-reperfusion injuries in the axolotl is shown in Figure 11. This figure shows trabeculated cardiomyocytes with intact nuclei. After a 20-minute ischemic event, macroscopically, the clamped cardiac tissue resumed normal cardiac activity (contraction in time with surrounding myocardium) and microscopically, no signs of apoptosis or necrosis (e.g. pyknosis, karyolysis, or karyorrhexis) were evident after Masson's trichrome histology staining.

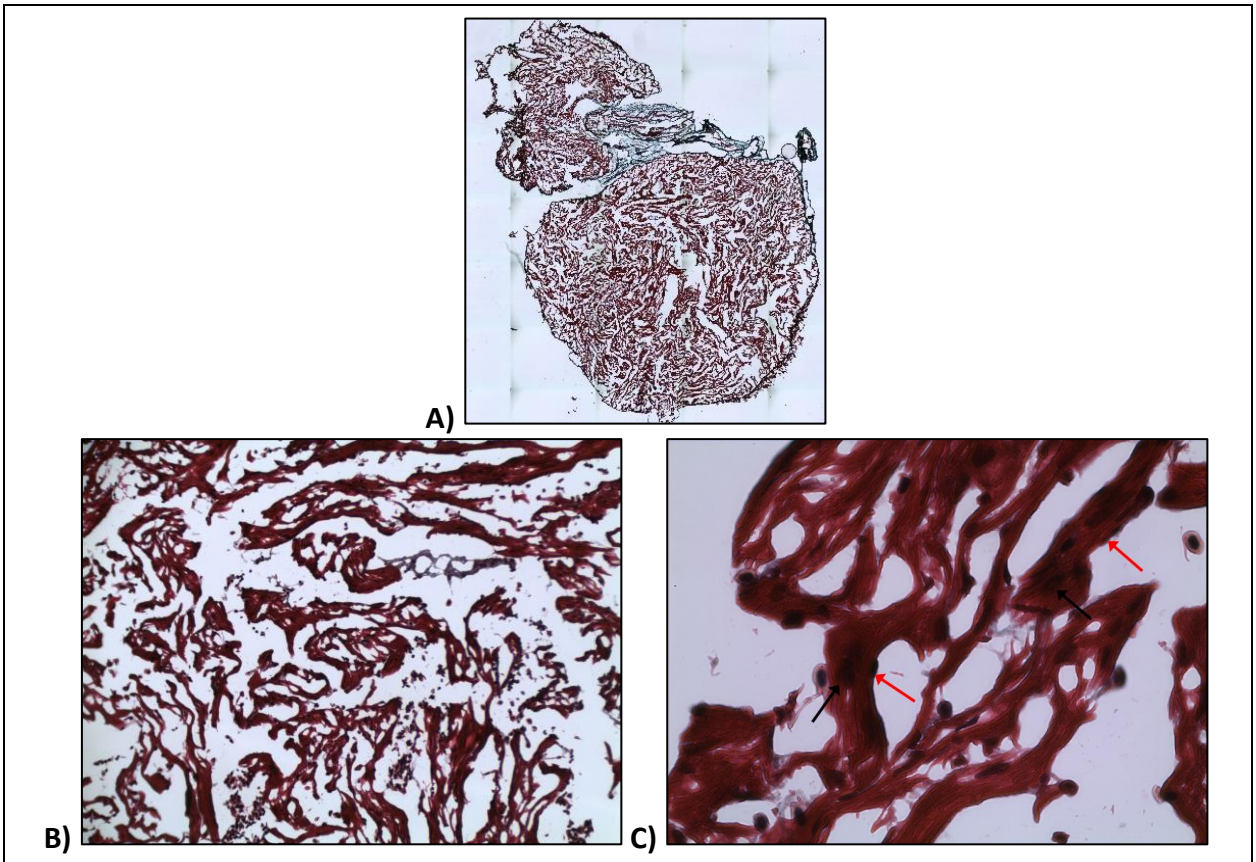

Figure 11: Heart of Naïve Animal for Clamping-Time Pilot Testing
A) Gross view of an axolotl heart from a naïve animal. Gomori trichrome sections of a naïve heart at **B)** 10X zoom view and **C)** 40X zoom view showing greater detail of the apex of the same heart. Normal cardiomyocytes and their nuclei (black arrows) are shown with flattened endothelial cells (red arrows) on the border of trabeculated tissue. Scale bars not shown.

Histology of various hearts subject to 20 minutes of ischemia and sacrificed 1-day, 2-days, 7-days, and 30-days status-post surgery are shown in Figure 12. Although some of the sections are slightly over stained, there is visual evidence A 30-minute ischemia-induction procedure was performed with results to Figure 12. Consequently, additional pilot surgeries were performed and the time for mechanically-induced ischemia was increased by increments of 15-30 minutes until there was macroscopic evidence of akinetic cardiac muscle after clamp removal. Consistent, clear physical and histological signs of apoptosis and necrosis were first determined after 120 minutes of mechanically-induced ischemia as shown in Figure 13.

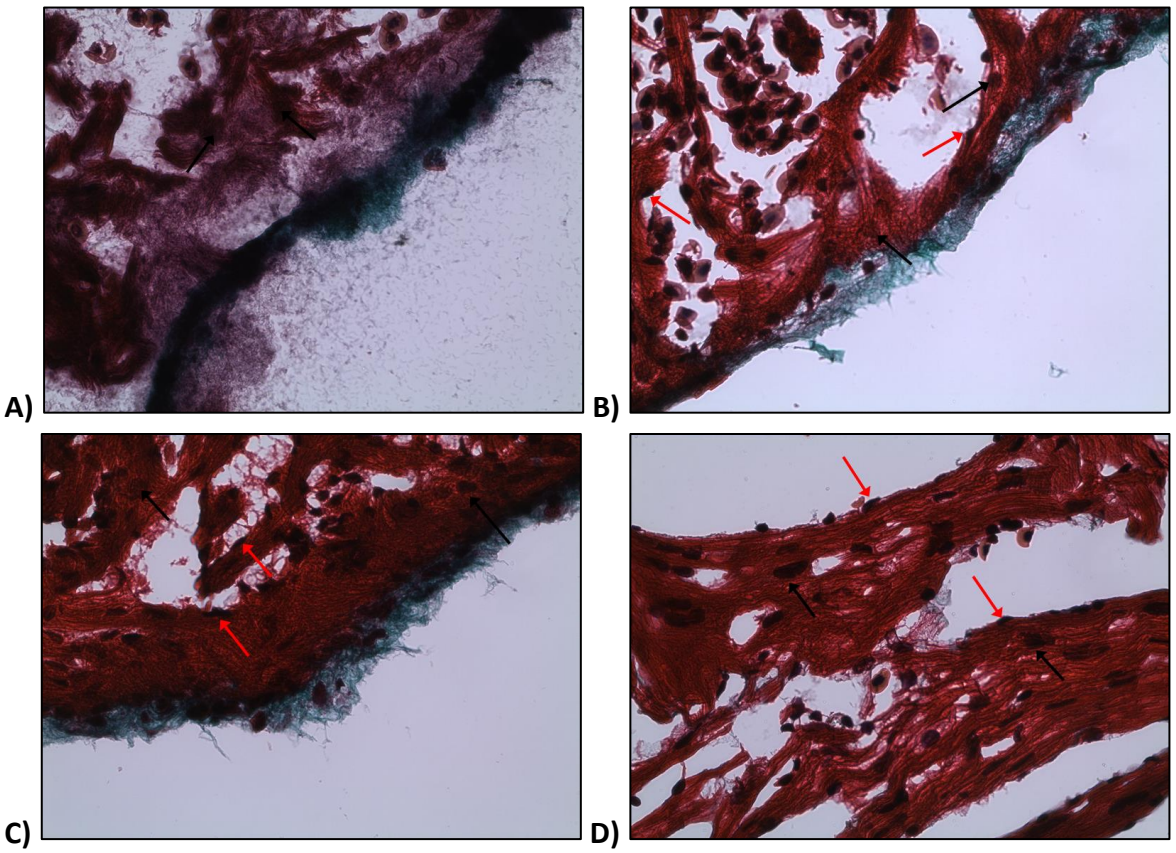

Figure 12: Pilot Hearts After 20 Minutes of Ischemia
Gomori's trichrome used to stain tissue. Pictures denote different days after surgery that induced ischemia-reperfusion injury. **A)** Status-post 1 day. Tissue was slightly overstained. **B)** Status-post 2 days. **C)** Status-post 7-days. **D)** Status-post 30-days. Note that after 20-minutes of ischemia, normal cardiomyocytes and their nuclei (black arrows) and flattened endothelial cells (red arrows) on the border of trabeculated tissue are still present like naïve tissue. Scale bars not shown.

After determining the appropriate amount of time to induce ischemia-reperfusion injuries and refining heart harvesting procedures during the pilot phase of this project, a naïve heart from the animals used in the GLAS Grant studies, illustrated in Figure 14, shows the expected trabeculated myocardium. Evident are endocardium (cardiac endothelium), cardiomyocytes, and epicardium. Sinus cavities between bands of myocardium allow blood to perfuse the beating heart. Few red blood cells are evident as hearts were flushed with heparin (100 units/mL) flush solution and amphibian saline before fixation.

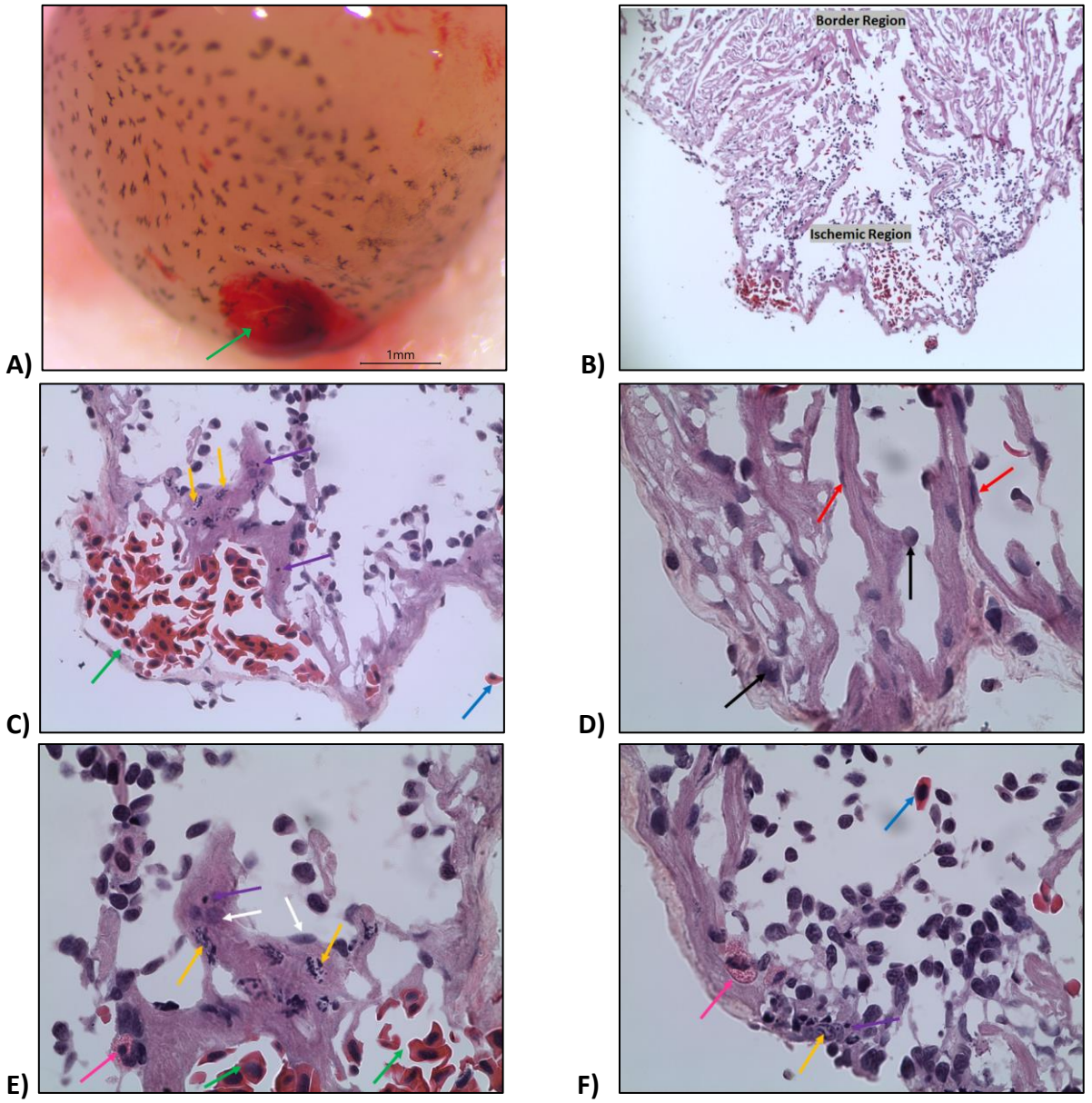

Figure 13: Pilot Hearts After 120 Minutes of Ischemia

A) Gross view of heart after 120 minutes of ischemia. After flushing the heart, the clamped area is clearly demarcated with a zone of hemorrhage (*green arrow*). **B)** 10X zoom view of a section containing the border and ischemic regions. **C)** 40X zoom view of ischemic region showing areas of hemorrhage (*green arrow*) full of RBCs (single RBC at *blue arrow*). The cardiomyocytes show different states of apoptosis such as karyorrhexis (*orange arrows*) and pyknosis (*purple arrows*). **D)** 60X zoom view of the border region showing normal cardiomyocytes (black arrows) with flattened endothelial cells (*red arrows*) on the border of trabeculated tissue. **E)** and **F)** 60X zoom view of the ischemic region showing cardiomyocytes in different states of apoptosis such as karyorrhexis, pyknosis, and karyolysis (*white arrows*). There is also evidence of necrotic cardiomyocytes with a hypereosinophilic cytoplasm (*pink arrows*).

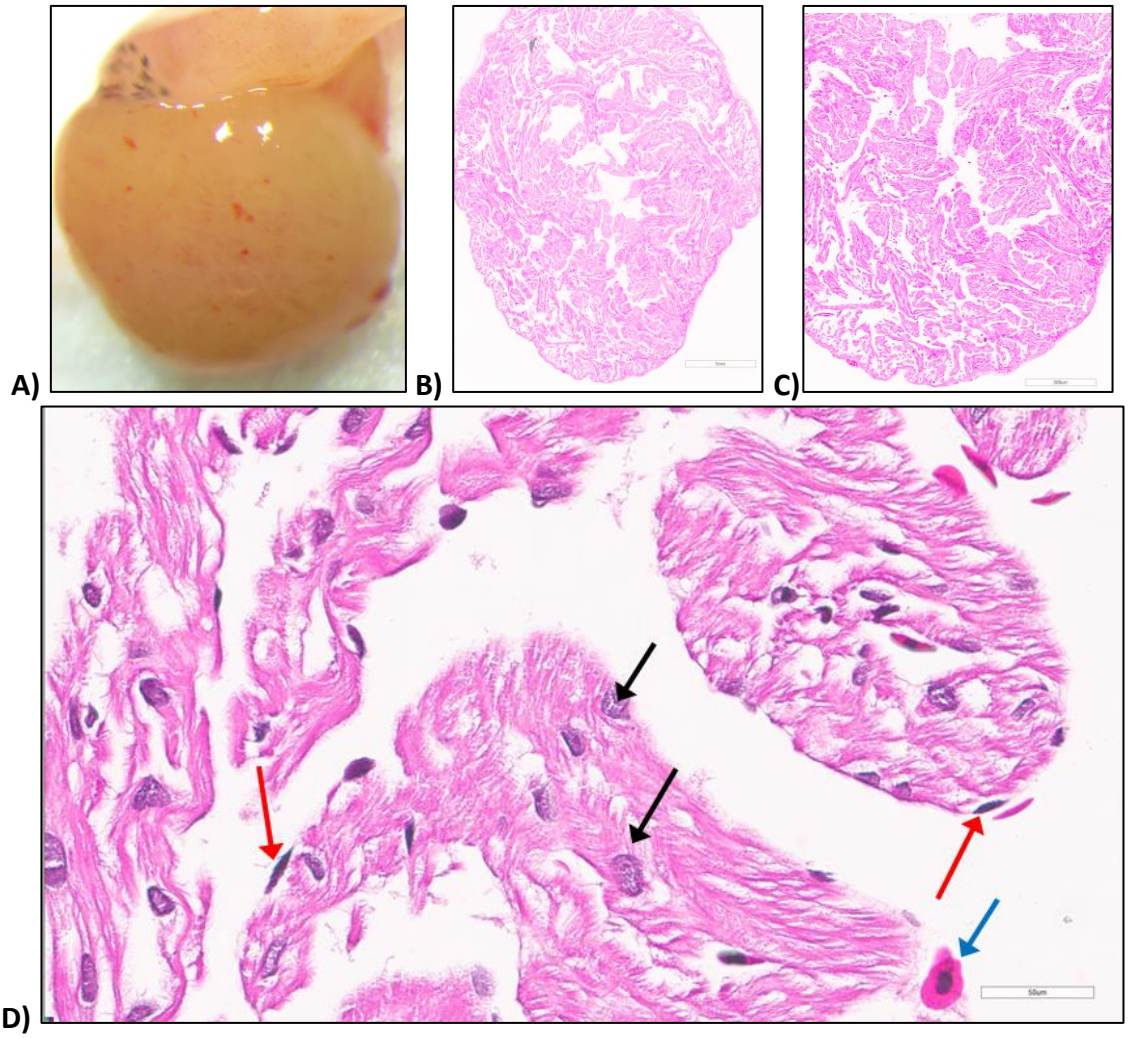

Figure 14: Heart from a Naïve Axolotl
A) Gross view of an axolotl heart from a naïve animal in the GLAS Grant group of experiments. **B)** H&E sections of a naïve heart at 2X zoom view and **C)** 4X zoom view showing greater detail of the apex of the same heart. **D)** Normal cardiomyocytes and their nuclei (black arrows) are shown with flattened endothelial cells (red arrows) on the border of trabeculated tissue. Scale bars show length scale at each zoom level.

To confirm that one-hundred twenty minutes of mechanically-induced ischemia and the return of blood flow results in ischemia-reperfusion, the procedure was performed on newly-acquired animas for works outlined under the GLAS Grant. After removing the clamp, the heart muscle was indeed akinetic. Hearts harvested from euthanized animals 12 hours (Figure 15) and 7 days (Figure 16) following the surgical procedure show a clearly demarcated area where the

clamp was placed. Following rinsing with heparin flush and amphibian saline, hemorrhaging into the injury site is clear. As expected following an ischemia reperfusion injury, histologic sections show the injured area contains inflammatory infiltrate and cytological evidence of hemorrhaging.

Acute (12 hours after injury, Figure 17) and chronic (7 days after injury, Figure 18) changes after mechanically-induced ischemia-reperfusion injury confirm mechanically-inducing ischemia for one-hundred twenty minutes results in gross tissue injury (hemorrhaging) and akinetic or dyskinetic muscle contraction of the injured area upon clamp removal. Microscopic evidence of ischemia-reperfusion injury includes the presence of necrotic cardiomyocytes, activation of endocardium, and infiltration of inflammatory cells (leukocytes). Cardiomyocyte nuclei that show evidence of pyknosis, karyorrhexis, and karyolysis in the bands of myocardium are evidence of apoptosis. Activated endocardium appear as swollen, “plump” endothelial cells that line trabeculated regions within the parenchyma of the heart. Lymphocytes and heterophils are the most common leukocytes in the injured region. Heterophils have a segmented nucleus and colorless cytoplasm that contain rod-shaped granules that are typically eosinophilic. Heterophils are highly phagocytic and play a role in clearing pathogens and cellular debris at sites of inflammation (Claver and Quaglia, 2009). Additional details of histologic features of H&E stains is found in the results section of GLAS Experiment 4: Evaluate Histologic Differences in Healing: Control & Analgesia.

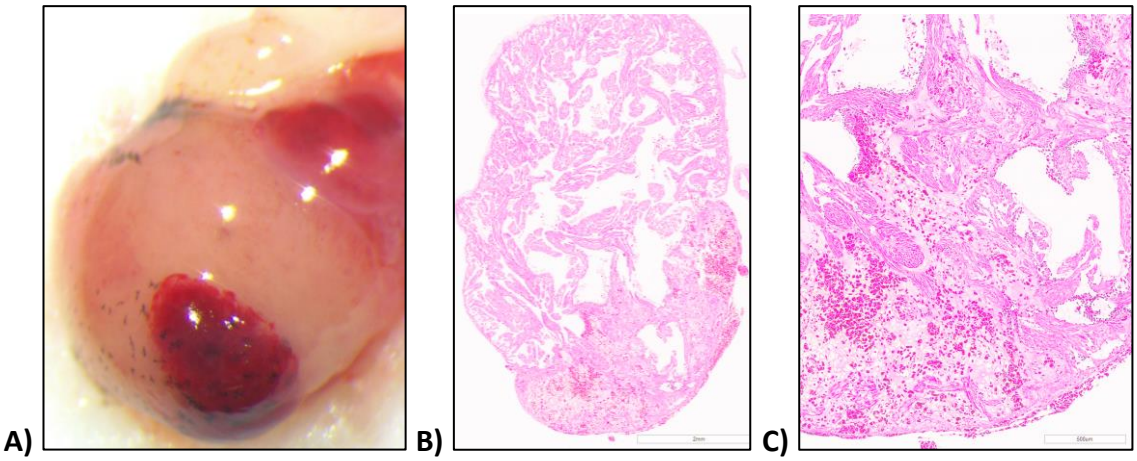

Figure 15: Heart from an Axolotl 12 Hours Post Injury

A) Gross view of an axolotl heart 12 hours post mechanical induction of ischemia-reperfusion injury. Hemorrhaging at the site of clamp application is evident after heart is rinsed with heparin lock solution and amphibian saline. H&E sections of injured heart at B) 2X zoom view and C) 4x zoom view showing greater detail of the apex of the same heart. Ischemia-reperfusion injury is evident in the sections, showing significant hemorrhage and loss of cardiomyocytes at the apex. Scale bars show length scale at each zoom level.

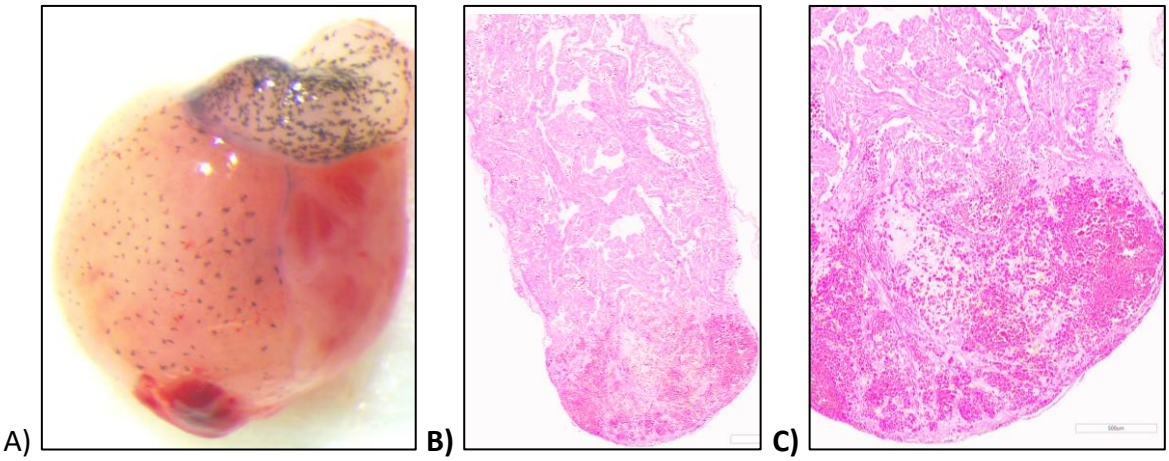

Figure 16: Heart from an Axolotl 7 Days Post Injury

A) Gross view of an axolotl heart 7 days post mechanical induction of ischemia-reperfusion injury. Hemorrhaging at the site of clamp application is evident after heart is rinsed with heparin lock solution and amphibian saline. H&E sections of injured heart at B) 2X zoom view and C) 4x zoom view showing greater detail of the apex of the same heart. Ischemia-reperfusion injury is evident in the sections, showing significant hemorrhage and loss of cardiomyocytes at the apex. Scale bars show length scale at each zoom level.

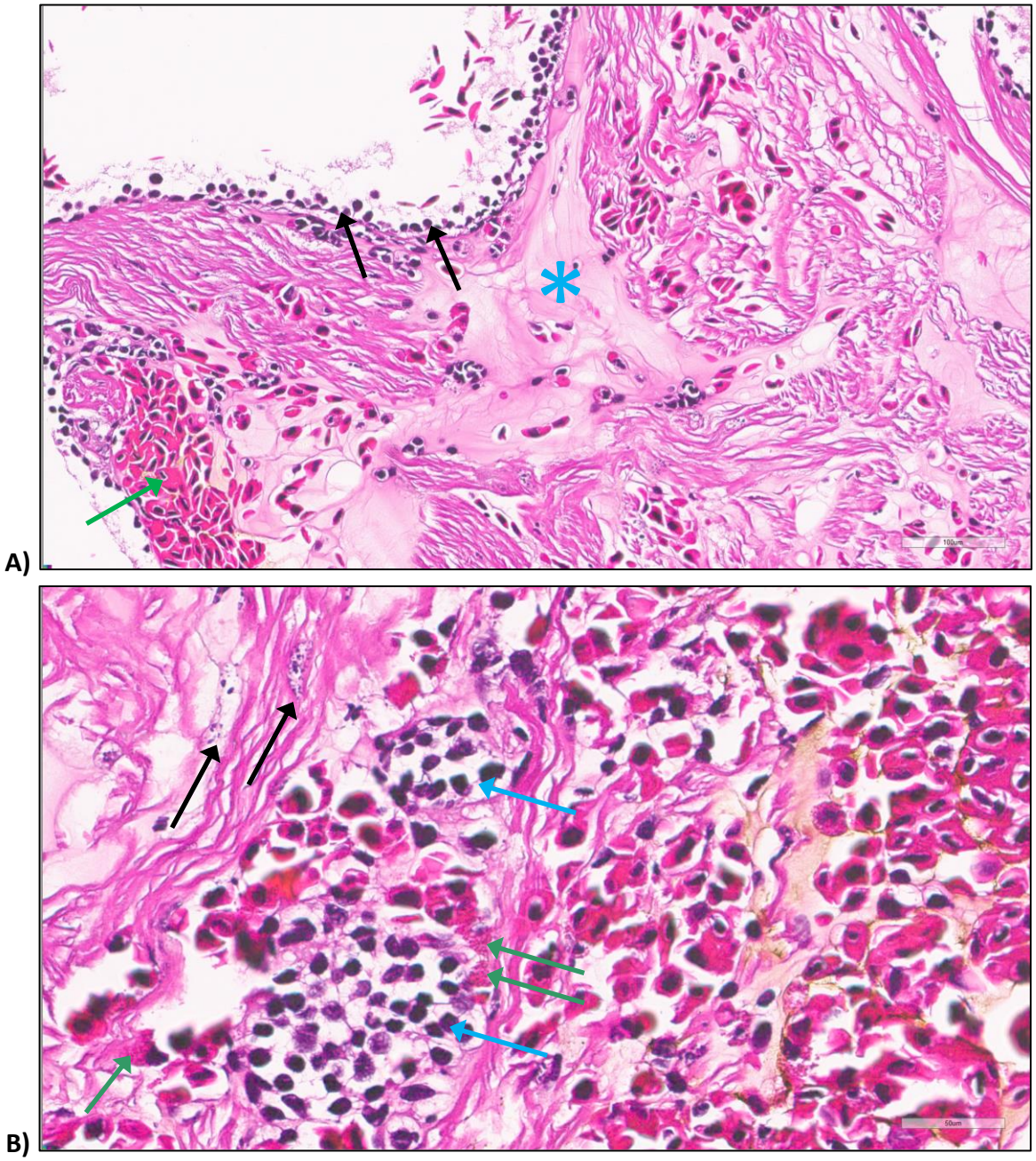

Figure 17: Histology of Injured Axolotl Heart 12 Hours After Injury.
A) 20X zoom view of an injured area of the heart. Activated endocardium (*black arrows*) line a trabeculated area while hemorrhage into the myocardial band is present (*green arrow*). Proteinaceous material (*blue asterisk*) from edematous or exudative fluid is also found within the myocardial bands. **B)** 40X zoom view of an injured area of the heart. Necrotic cardiomyocytes (*black arrows*) with hypereosinophilic cytoplasm are present. Lymphocyte aggregates (*light blue arrows*) and heterophils (*green arrows*) infiltrate the damaged myocardium.

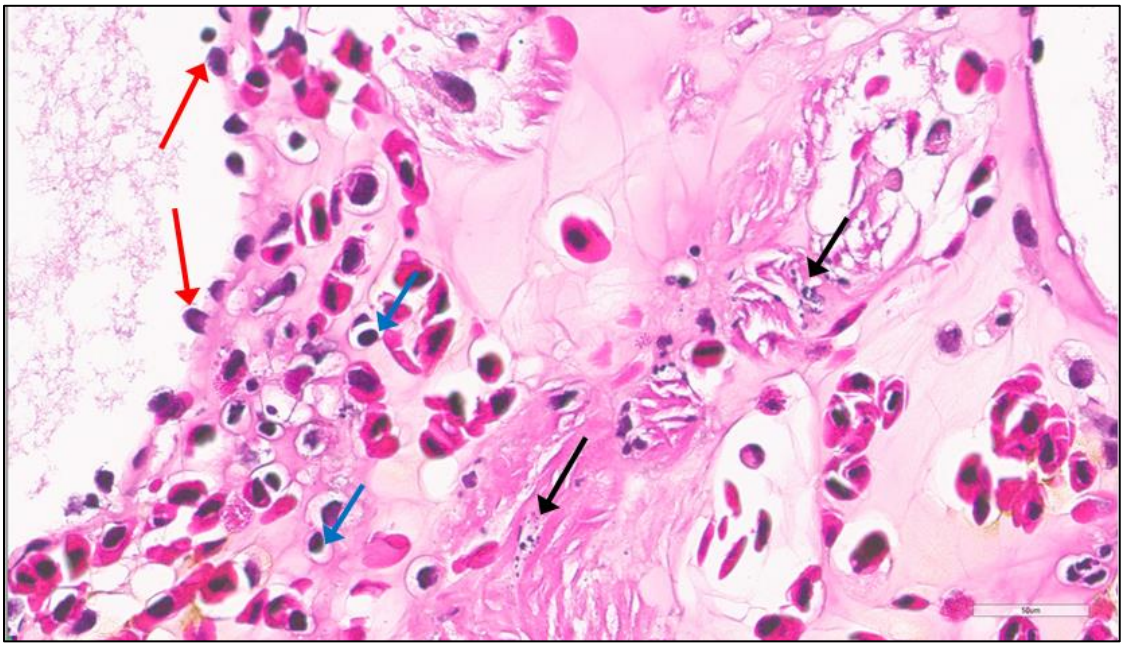

Figure 18: Histology of Injured Axolotl Heart 7 Days After Injury
(Top) 40X zoom view of a remote region of the heart away from the site of injury. Cardiomyocytes (*black arrows*) are normal and endocardium are flat (*red arrows*). A lone RBC is shown (*blue arrow*) outside of the bands of myocardium. (Bottom) 40X zoom view of an injured area of the heart. Necrotic cardiomyocytes (*black arrows*) with hypereosinophilic cytoplasm are present. The endocardium (*red arrows*) are activated, as noted by their "plump" appearance. Lymphocytes (light *blue arrows*) and red blood cells are evident within bands of myocardium.

GLAS Experiment 1: Validate Quantitative Methods to Evaluate Nociception in Naïve Animals

The National Institute of Standards and Technology (NIST) define repeatability as "closeness of the agreement between the results of successive measurements of the same measurand carried out under the same conditions of measurement"(Taylor and Kuyatt, 1994). Serial trials were performed using mechanical and chemical noxious stimuli. The data for the von Frey evaluators are found in Table 2 while the data for the acetic acid test are found in Table 3. Simple descriptive statistics are tabulated – the standard deviation of variations from the mean is used to quickly judge the repeatability of the testing method. For assessing the reliability of the

test, the intraclass correlation coefficient (ICC) is an appropriate test to determine test-retest reliability.

Table 2: Repeatability of Responses to Serial Testing Using von Frey Evaluators

Axolotl ID		17	18	19	20	21	22
vF Evaluator Code	Trial 1	6	7	7	7	9	4
	Trial 2	5	9	9	3	6	6
	Trial 3	8	8	8	5	7	12
Mean Response		6.3	8.0	8.0	5.0	7.3	7.3
Individual Variations		0.3	1.0	1.0	2.0	1.7	3.3
		1.3	1.0	1.0	2.0	1.3	1.3
		1.7	0.0	0.0	0.0	0.3	4.7
Mean of Individual Variation		1.1	0.7	0.7	1.3	1.1	3.1
SD of Individual Variation		0.69	0.58	0.58	1.15	0.69	1.68

Table 3: Repeatability of Responses to Serial Testing Using Acetic Acid

Axolotl ID		17	18	19	20	21	22
Acetic Acid Vial Code	Trial 1	6	4	6	6	7	5
	Trial 2	5	5	6	5	5	5
	Trial 3	6	5	5	6	5	5
Mean Response		5.7	4.7	5.7	5.7	5.7	5.0
Individual Variations		0.3	0.7	0.3	0.3	1.3	0.0
		0.7	0.3	0.3	0.7	0.7	0.0
		0.3	0.3	0.7	0.3	0.7	0.0
Mean of Individual Variation		0.4	0.4	0.4	0.4	0.9	0.0
SD of Individual Variation		0.19	0.19	0.19	0.19	0.38	0.00

Using SPSS, the intraclass correlation coefficient for the von Frey evaluators is $\rho = -0.050$ (95% confidence interval: -0.351 – 0.605), with an ANOVA assessment of $F(5,12) = 0.857$ ($p = 0.536$) suggesting there are no outlier animals. A negative value here for the intraclass correlation coefficient reflects a negative average covariance among the measurements. Using the same animal subjects, the acetic acid test shows an intraclass correlation coefficient of $\rho = 0.098$ (95%

confidence interval: -0.282 – 0.718), with an ANOVA assessment of $F(5,12) = 1.325$ ($p = 0.318$) suggesting there are no outlier animals. Given the upper bound of the 95% confidence interval, the acetic acid test shows a greater reliability than the von Frey evaluators.

In Table 2, the intraclass correlation coefficient results are illustrated using descriptive statistics. The nociception threshold using von Frey evaluators has much more variability between measurements. Although care is taken such that the flexible fiber is placed perpendicular to the site of evaluation before the force is applied, the shape of the animal (curved body lateral to dorsal fin) and the presence of its natural mucous coating sometimes makes it difficult to consistently apply the evaluator perpendicular animal's skin. Conversely, using a pipette, a small-caliber pipette tip, and a very small volume of acetic acid allows for the more precise application of this noxious stimulus.

As shown in Table 3, using the same axolotls from the von Frey evaluator assessment, the individual variation of the acetic acid test is smaller. From these simple descriptive statistics and the difficulty in consistently performing the measurements on axolotls, moving forward, the acetic acid test was used for all quantitative tests. A reproducibility ["closeness of the agreement between the results of measurements of the same measurand carried out under changed conditions of measurement"(Taylor and Kuyatt, 1994)] of the acetic acid test was performed in a different set of six axolotls. The intraclass correlation coefficient for this repeated test is $\rho = -0.117$ (95% confidence interval: -0.379 – 0.537) with an ANOVA assessment of $F(5,12) = 0.686$ ($p = 0.643$) suggesting there are no outlier animals. The descriptive statistics are shown in Table 4. When assessing all acetic acid tests across twelve different animals, the intraclass correlation

coefficient is ρ = -0.021 (95% confidence interval: -0.270 – 0.397) with an ANOVA assessment of F(11,24) = 0.938 (p = 0.523) suggesting there are no outlier animals.

Table 4: Reproducibility of Responses to Serial Testing Using Acetic Acid

Axolotl ID		23	24	25	26	27	28
Acetic Acid Vial Code	Trial 1	7	7	6	5	7	5
	Trial 2	6	6	5	6	6	6
	Trial 3	6	5	5	5	4	5
Mean Response		6.3	6.0	5.3	5.3	5.7	5.3
Individual Variations		0.7	1.0	0.7	0.3	1.3	0.3
		0.3	0.0	0.3	0.7	0.3	0.7
		0.3	1.0	0.3	0.3	1.7	0.3
Mean of Individual Variation		0.4	0.7	0.4	0.4	1.1	0.4
SD of Individual Variation		0.19	0.58	0.19	0.19	0.69	0.19

Although the variation is larger than the first series of serial acetic acid tests, it is still less than the variation of the von Frey evaluators. Furthermore, not only is testing more consistent with the acetic acid test (higher value of ρ using the 95% confidence interval when assessing the same set of animals between von Frey evaluators and acetic acid test), performing the acetic acid test is more easily accomplished by the operator or investigator.

Conclusion: For quantitative assessment of pain, AAT was found to be more consistent versus vF.

Study deviations: *None.*

Unanticipated findings: *None.*

Troubleshooting: *None.*

Future directions: Evaluate additional quantitative tools to measure analgesia response, such as thermal nociception.

GLAS Experiment 2: Determine Optimized Analgesia

The significance of treatment effects at each time point are assessed by Kruskal-Wallis one-way analysis of variance for unrelated samples. Quantitative tests were analyzed for the change in nociceptive threshold from baseline (Δ NT in graphs). Findings from qualitative testing are included to see if analgesics change behavior – they are not indicative of analgesia efficacy.

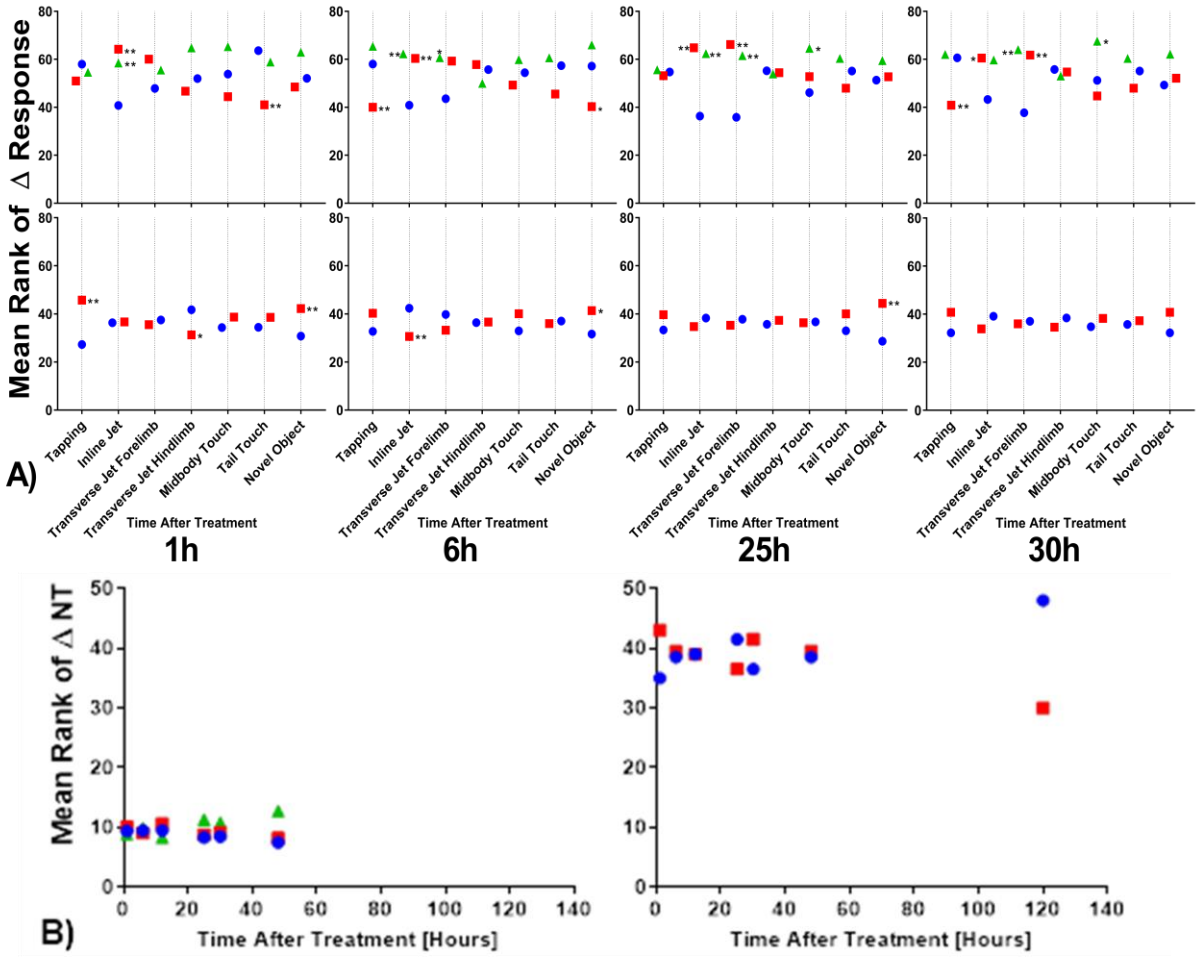

Figure 19: Results of Qualitative and Quantitative Testing in GLAS Experiment 2
A) Results of Experiment 2A (*Top*) and Experiment 2B (*Bottom*) qualitative testing.
B) Results of Experiment 2A (*Left*) and Experiment 2B (*Right*) quantitative testing.
Legend: ●Control; ■Butorphanol; ▲Buprenorphine
Significance: A) Top Row: ∗ $p < 0.025$, ∗∗ $p < 0.005$; Bottom Row: ∗ $p < 0.05$, ∗∗ $p < 0.025$.

All plots of quantitative and qualitative results for this experiment are shown in Figure 19.

In quantitative testing (*Left Panel*, Figure 19B), no significant difference exists between mid-dose

butorphanol or mid-dose buprenorphine compared to control. Evaluating the other behavioral tests in Experiment 2A no clear trend stands out between analgesic or time for either study drug.

An adverse effect was observed in two of six animals in the mid-dose buprenorphine group. Fecal output ceased after the completion of the first round of experiments, meeting criterion for euthanasia. Necropsy of the two affected animals demonstrated dark discoloration of the GI tract tissue (see Figure 20) near the site of injection with significant colon distension and fecal impaction. Although TUNEL staining is strong near the rectum, suggesting greater DNA damage, H&E results do not indicate any pathophysiology in this area. However, the TUNEL staining results could be due to increased GI epithelial turnover. The only clear clinical conclusion is that the fecal output was reduced. This finding could be caused by primary effect of opioids causing reduced GI motility or a local reaction to the IP injection of this buprenorphine formulation and concentration. Based on these findings, it was decided to eliminate buprenorphine from further use in this study and try another round of Experiment 2 tests (Experiment 2B) comparing high-dose butorphanol (0.75 mg/L) to control.

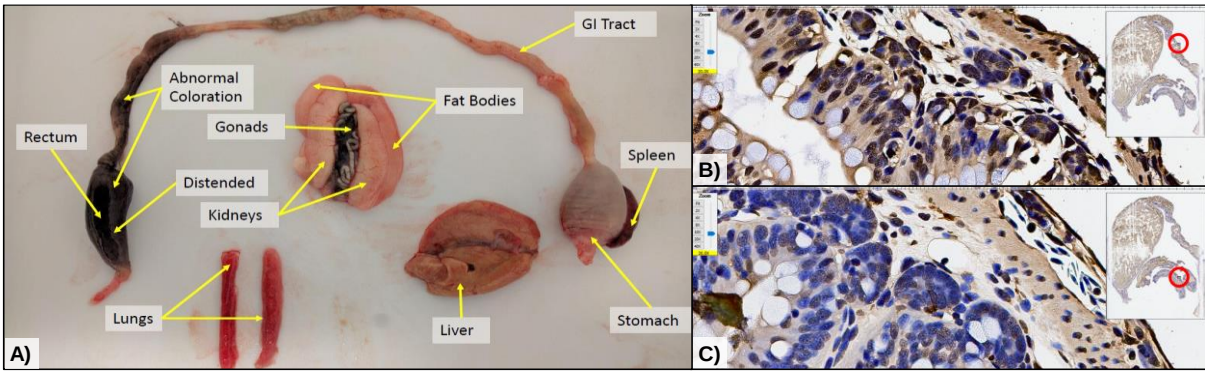

Figure 20: Adverse Effects Following Buprenorphine Injection
A) Gross necropsy findings B) TUNEL staining of affected and C) unaffected GI tract.

Qualitative and quantitative tests were repeated in Experiment 2B after waiting at least one-week to allow any study drugs to completely wash out of the animals' systems. In qualitative

testing (*Right Panel,* Figure 19B), no significant difference exists between high-dose butorphanol to control. Evaluating the other behavioral tests in Experiment 2B, no clear trend stands out with high-dose butorphanol over time.

Conclusion: Although no significant qualitative or quantitative trend is detected for controlling nociceptive, somatic pain when using the indicated treatments and doses in Experiment 2, the study continued using mid-dose and high-dose butorphanol.

Study deviations:

Although data on animal movement were recorded with pre-existing monitoring hardware from the institution's Division of Laboratory Animal Resources, video analysis software was not available and the data could not be analyzed for quantitative trends.

Unanticipated findings: Intracoelomic injections of mid-dose buprenorphine led to adverse effects related to reduced GI motility. Buprenorphine was dropped from further study.

Troubleshooting: *None.*

Future directions: Evaluate additional doses of butorphanol and different analgesic compounds. Evaluate animal movement data if software can be obtained.

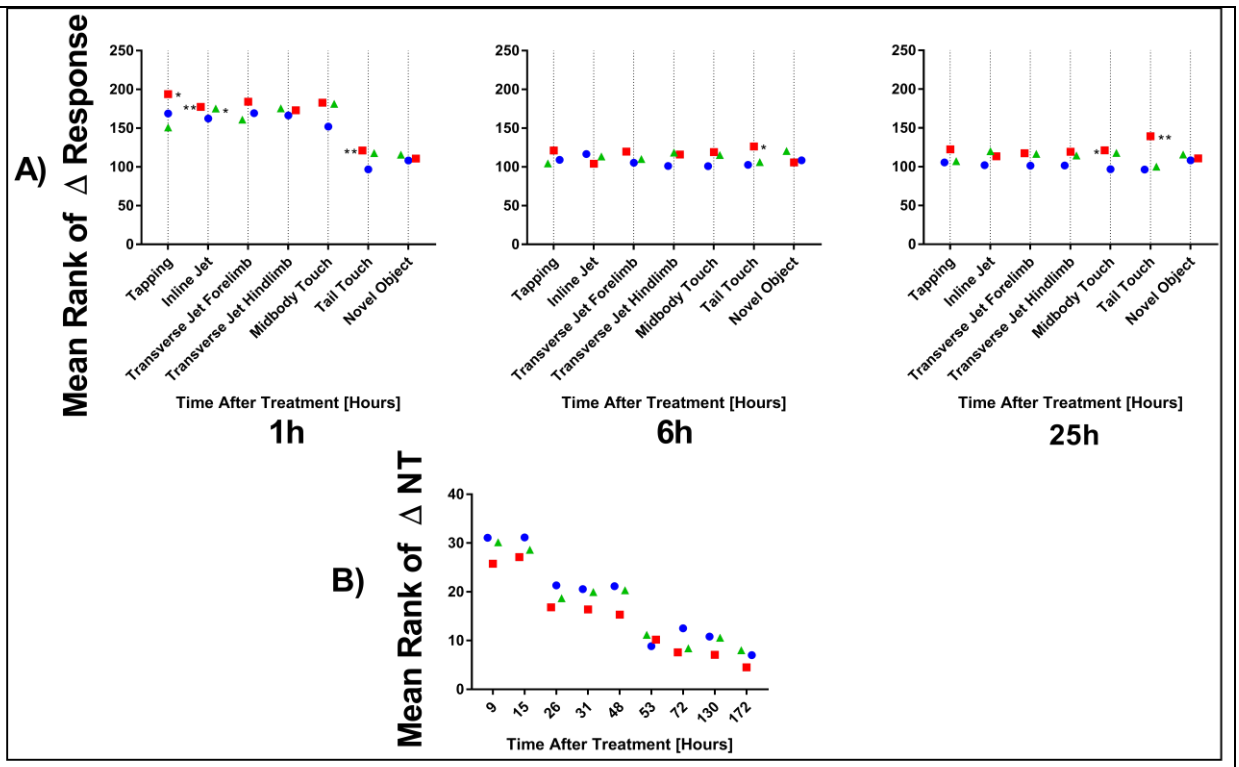

Figure 21: Results of Qualitative & Quantitative Testing in GLAS Experiment 3
A) Results of qualitative and B) quantitative testing.
Legend: ● Control; Butorphanol (■ Mid) and (◆ High)
Significance: ∗ $p < 0.025$, ∗∗ $p < 0.005$.

GLAS Experiment 3: Evaluate Optimal Analgesic Dose in a Surgical Model in Axolotls

The drugs and doses from the conclusion of Experiment 2 were used in Experiment 3 to test whether there would be measurable control of surgical (visceral) pain. All test outcomes are found in Figure 21. No statistical difference was measured in the quantitative tests, suggesting no significant analgesic effect with the drugs and doses tested.

Conclusion: No significant qualitative or quantitative trend is detected for controlling nociceptive, visceral pain when using the indicated treatments and doses in Experiment 3.

Study deviations: The time to recover from anesthesia after surgery varies, but all drugs are administered at the same time. For statistical comparisons, administration of study drug is used as 0-hour time point instead of time of anesthesia recovery.

Unanticipated findings: *None.*

Troubleshooting: *None.*

Future directions: Dose-escalation experiments are warranted to find the appropriate dose of butorphanol to provide pain relief. Evaluation of additional analgesics is warranted.

GLAS Experiment 4: Evaluate Histologic Differences in Healing: Control & Analgesia

After inducing mechanical ischemia, axolotls were euthanized at three different timepoints, hearts were flushed with heparin lock flush and then fixed in 4% formaldehyde/zinc. Fixed hearts were processed for staining (H&E, Masson's Trichrome, and picrosirius red; later acid fuchsin orange G) and immunohistochemistry (cardiac muscle myosin [Abcam AB50967], non-muscle myosin IIB [Abcam AB684], TUNEL, and BrdU) by Histowiz, Inc. (Brooklyn, NY), and pathology evaluated by Dr. Barry H. Rickman (VMD, PhD, DACVP, Sound VetPath, Edmonds, WA).

Surgical Outcomes

In total, fifty-eight operations (n = 58) were performed with one animal used as a naïve heart sample. Although experiments were design to have six groups per control and treatment group (medium- and high-dose butorphanol), due to surgical complications, there were twenty (n = 20) axolotls in the group euthanized twelve hours after ischemia-reperfusion injury and nineteen (n = 19) axolotls in the group euthanized forty-eight hours after ischemia-reperfusion injury. In the twelve-hour group, the left atrium was clamped instead of the ventricular apex and the vena cava posterior (i.e. inferior vena cava in humans) was nicked on one animal leading to profuse bleeding. In the forty-eight-hour group, the left atrium was accidentally damaged when opening the pericardial sac, leading to gross hemorrhage. Animals with surgical complications were removed from study.

Qualitative Assessments of Pathology

Simple Stains

Hematoxylin/Eosin Stain

Results of Mayer's hematoxylin/eosin (H&E) stains of a naïve axolotl heart are shown in Figure 14. Representative results of H&E staining in the ischemic region of damaged hearts are shown in Figure 22, Figure 23, and Figure 24 for animals sacrificed twelve hours (one-half day),

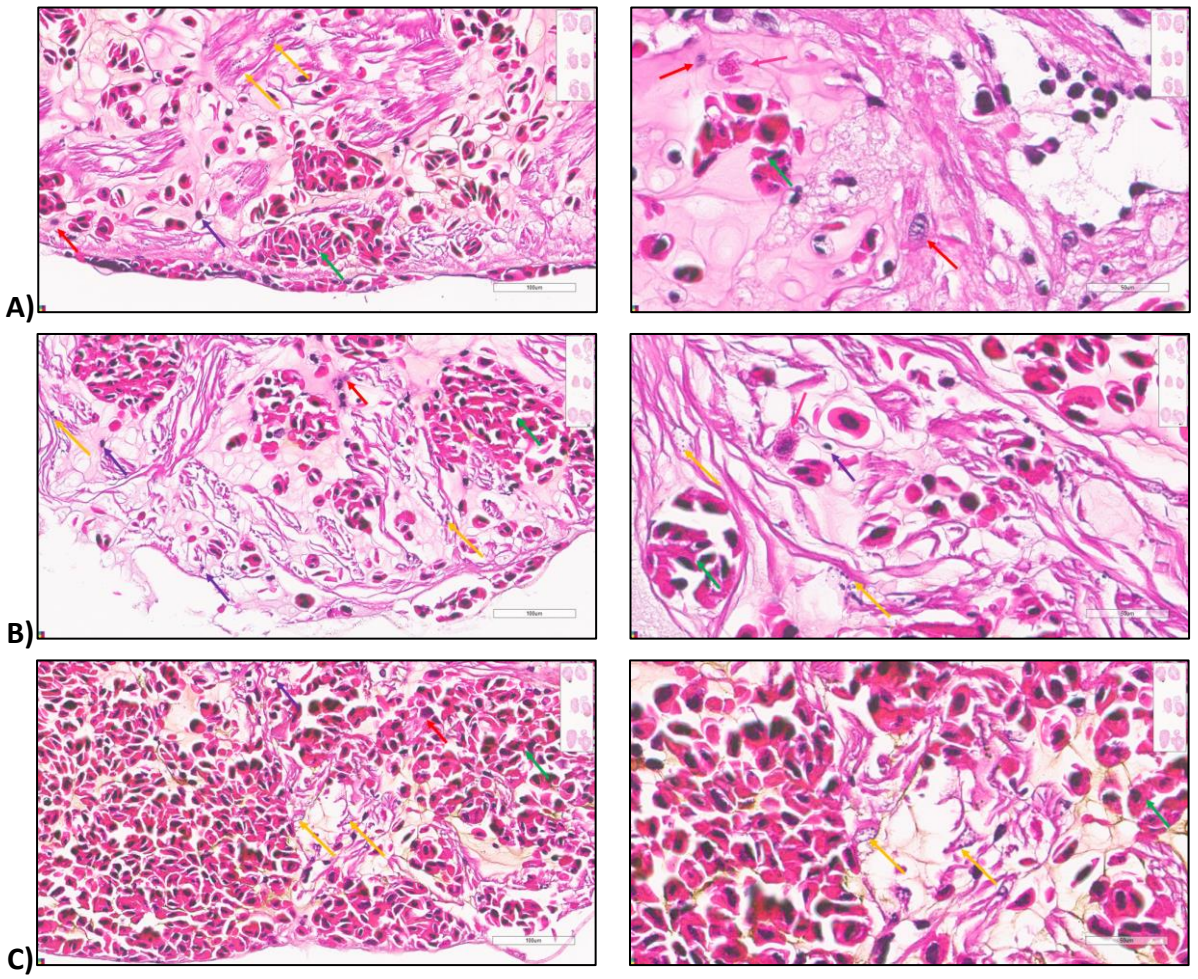

Figure 22: H&E Stains of Control and Treatment Groups 12 Hours After Injury
All views on the left are at 20X zoom while views on the right are at 40X zoom. **A)** Control animal. **B)** Animal treated with medium-dose butorphanol. **C)** Animal treated with high-dose butorphanol. Histology features: Hemorrhage (*green arrows*); karyorrhexis (*orange arrows*), pyknosis (*purple arrows*), karyolysis (*red arrows*) necrosis (*pink arrows*), heterophils (*blue arrows*). Not all views contain an instance of each histologic feature, each histologic feature not annotated. Scale bar included.

two days, and seven days after ischemia-reperfusion injury respectively. Evidence of microscopic ischemia-reperfusion injury such as necrotic and apoptotic cardiomyocytes, activation of endocardium, and infiltration of inflammatory cells (leukocytes) is present. Qualitatively, there is no characteristic pattern of staining neither between control or treatment groups nor temporally from twelve hours to seven days status-post injury.

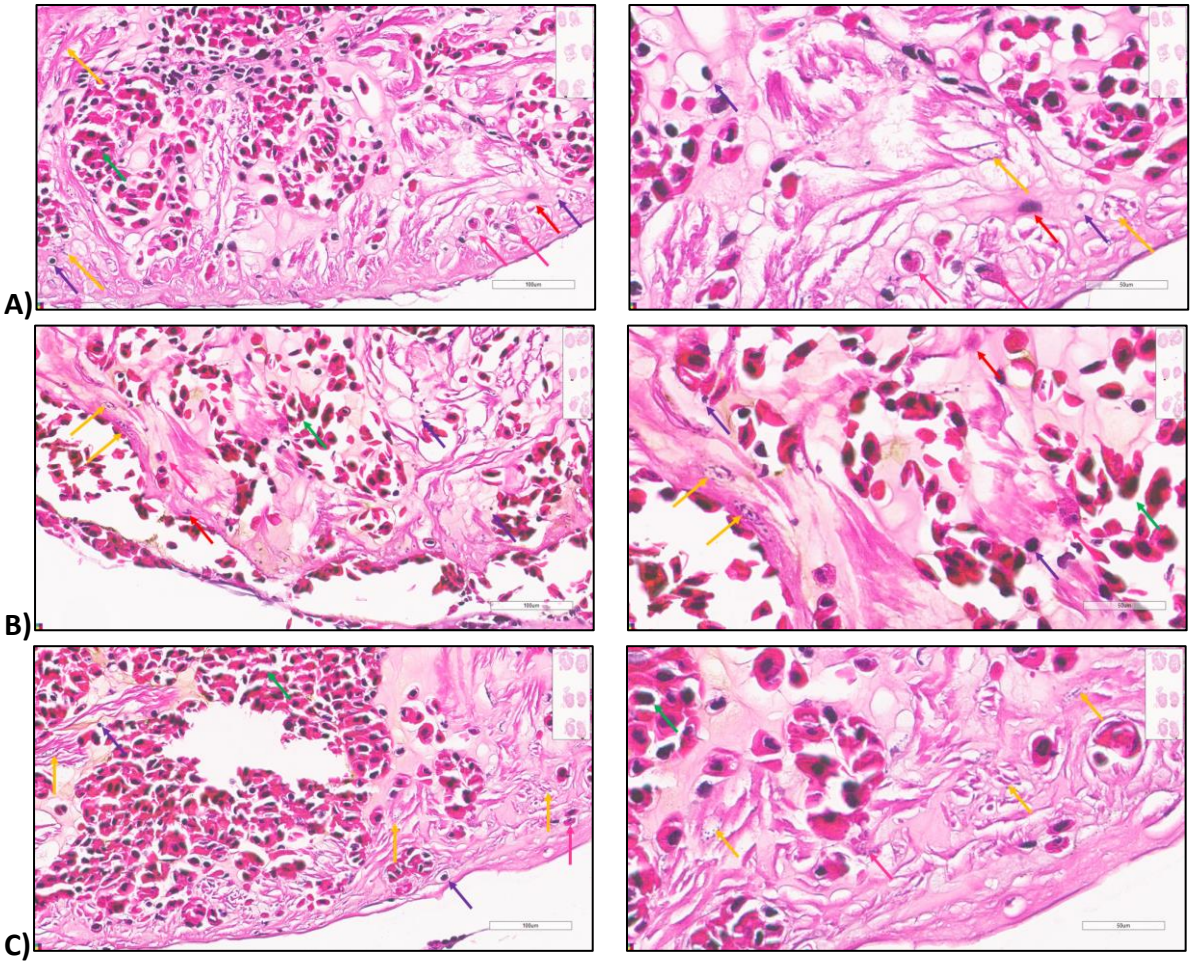

Figure 23: H&E Stains of Control and Treatment Groups 2 Days After Injury
All views on the left are at 20X zoom while views on the right are at 40X zoom. **A)** Control animal. **B)** Animal treated with medium-dose butorphanol. **C)** Animal treated with high-dose butorphanol. Histology features: Hemorrhage (*green arrows*); karyorrhexis (*orange arrows*), pyknosis (*purple arrows*), karyolysis (*red arrows*) necrosis (*pink arrows*), heterophils (*blue arrows*). Not all views contain an instance of each histologic feature, each histologic feature not annotated. Scale bar included.

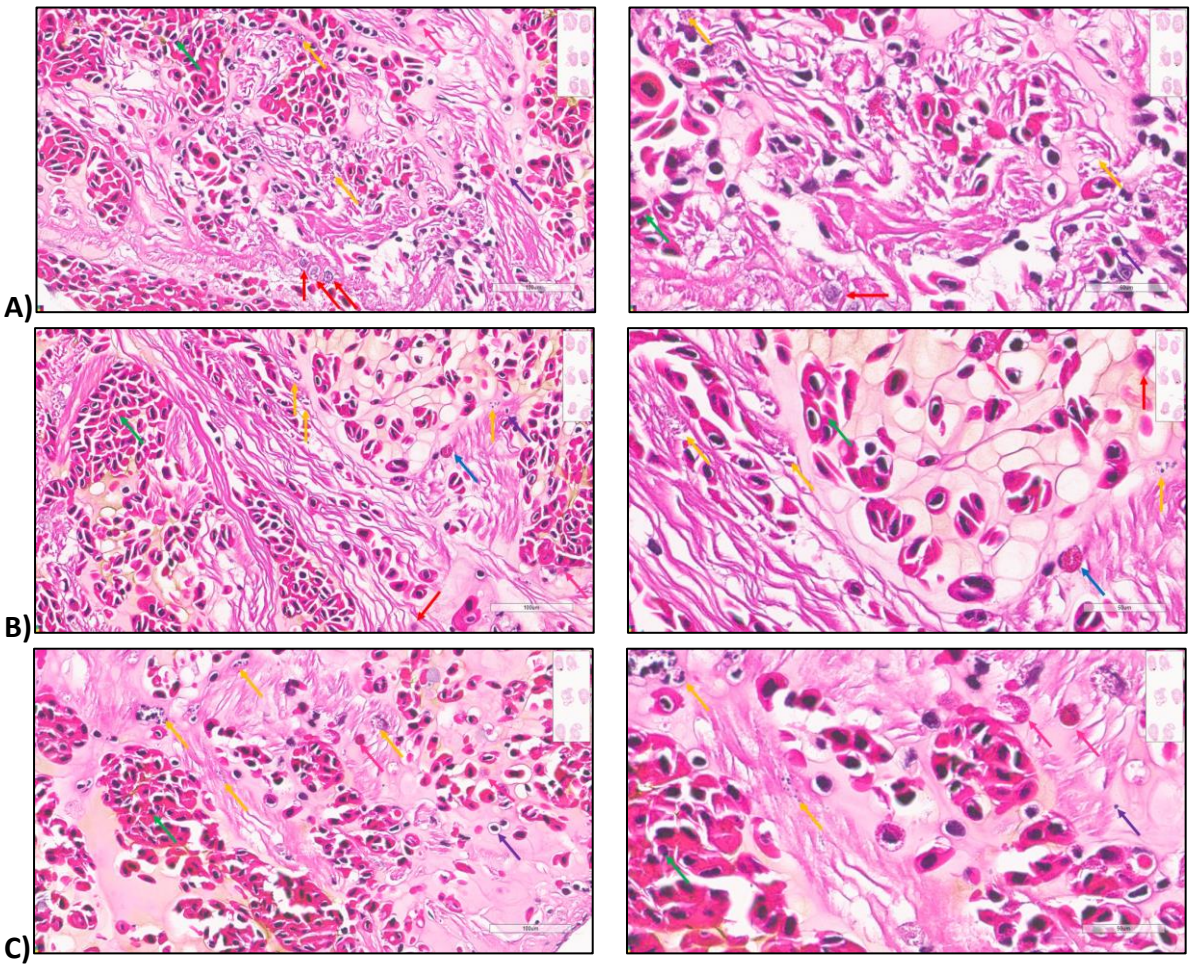

Figure 24: H&E Stains of Control and Treatment Groups 7 Days After Injury
All views on the left are at 20X zoom while views on the right are at 40X zoom. **A)** Control animal. **B)** Animal treated with medium-dose butorphanol. **C)** Animal treated with high-dose butorphanol. Histology features: Hemorrhage (*green arrows*); karyorrhexis (*orange arrows*), pyknosis (*purple arrows*), karyolysis (*red arrows*) necrosis (*pink arrows*), heterophils (*blue arrows*). Not all views contain an instance of each histologic feature, each histologic feature not annotated. Scale bar included.

First annotated in Figure 17A, there is evidence across control and treatment groups of eosinophilic (pink) edema or exudate in various tissue spaces of the injured myocardium. Eosin compounds are negatively-charged molecules and act as acidic dyes, staining basic (or acidophilic) structures red or pink. Eosin nonspecifically stains proteins, so in typical tissue, nuclei are stained blue by hematoxylin (by an incompletely understood reaction) while cytoplasm and extracellular matrix (ECM) have varying degrees of pink staining based on the type and

concentration of protein present (Fischer et al., 2008). Alternatively, the proteinaceous material may simply be components of the ECM that have been degraded by proteases present during the inflammatory cascade (Robbins et al., 2010).Thus, the only conclusion from H&E stains is that the edema or exudate is proteinaceous. Other stains are necessary to differentiate protein types.

Masson's Trichrome Stain

After confirming cardiac damage using H&E staining, additional simple stains were used to provide more details on the proteins present in axolotl histopathology following ischemia-reperfusion injury. Results of Masson's trichrome stains of a naïve axolotl heart are shown in Figure 25. Representative results from Masson's trichrome staining in the ischemic region of

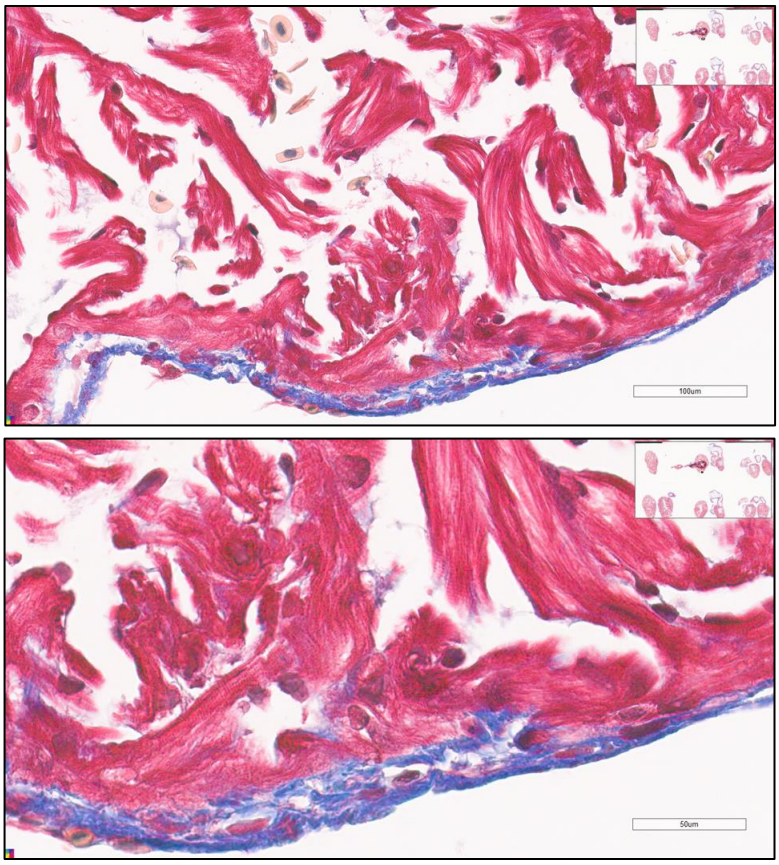

Figure 25: Masson's Trichrome Stains of Naïve Axolotl Heart
Views of naïve axolotl heart at **A)** 20X zoom and **B)** 40X zoom. Scale bar included.

damaged hearts are shown in Figure 26, Figure 27, and Figure 28 for animals sacrificed twelve hours, two days, and seven days after ischemia-reperfusion injury respectively.

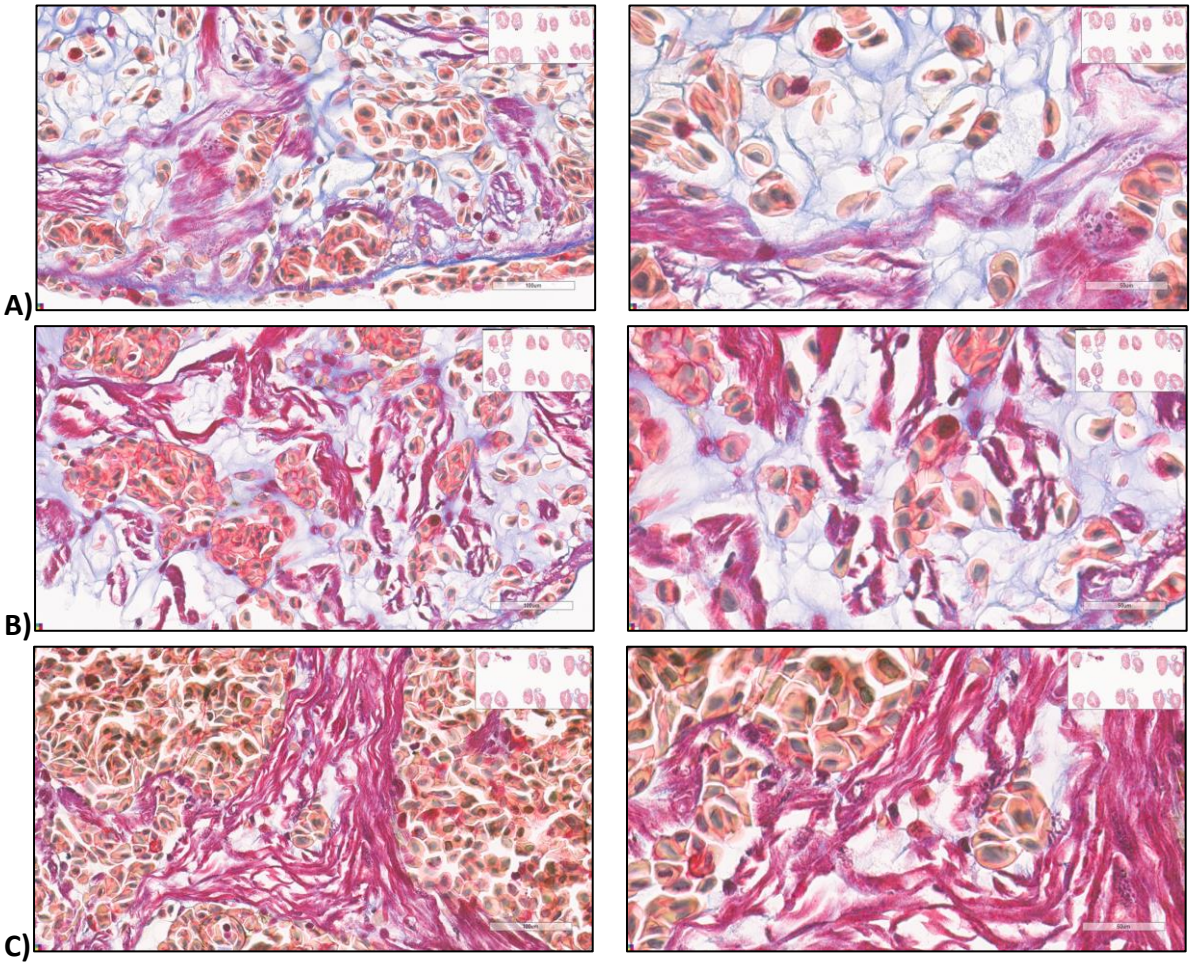

Figure 26: Masson's Trichrome Stains of Control and Treatment Groups 12 Hours After Injury All views on the left are at 20X zoom while views on the right are at 40X zoom. **A)** Control animal. **B)** Animal treated with medium-dose butorphanol. **C)** Animal treated with high-dose butorphanol. Scale bar included.

Like all trichrome methods, Masson's trichrome protocol extends the ability of the standard two-stain approach of H&E to further differentiate topology, specifically connective tissue. Masson's trichrome method combines the most precise hematoxylin preparations (iron hematoxylin by Heidenhain or Weigert) with a specific cytoplasmic stain (acid fuchsin with xylidine ponçeau) and a highly selective stain for connective tissue (fast green FCF or aniline blue) (Goldner, 1938). Connective tissue is a broad term and encompasses various cells, fibers and

amorphous ground substance. More specifically, connective tissues can be grouped into: connective tissue proper – includes loose or areolar, dense, regular and irregular adipose, and reticular; cartilage – hyaline elastic and fibrocartilage; bone – spongy or cancellous and dense or cortical; blood; and blood-forming – hematopoietic (Suvarna et al., 2012). In wound or injury repair, the most important connective tissue types are those that fill residual defects. These connective tissues are usually composed of cell types containing formed or fibrous intercellular substances (Robbins et al., 2010), providing great tensile strength to support damaged tissue (Suvarna et al., 2012). Formed elements in these structural connective tissues contain collagenic, reticular, and elastic-system fibers made up predominantly by collagen, reticulin, and elastic-system proteins respectively. The component proteins should not be confused with the structural features. The results of various staining protocols on different types of connective tissue are shown in Table 5 [adapted from (Suvarna et al., 2012)]. What is clear from Table 5 is that connective tissues appear as the same color or colors under the listed stains. Histowiz, Inc. uses the aniline blue dye in their Masson's trichrome protocol. Thus, areas stained light blue in Figure 26, Figure 27, and Figure 28 indicate areas of connective tissue.

Table 5: Results of Various Staining Protocols on Connective Tissue and Muscle

Tissue	Masson's Trichrome	van Gieson	Martius Scarlet Blue	Mallory's PTAH
Elastin	N/A	Yellow	Blue	Orange/Brown
Collagen	Blue/Green	Red	Blue	Blue
Reticulin	Blue/Green	Yellow	Blue	Orange/Brown
BM	Blue/Green	Yellow	Blue	Orange
Osteoid	Blue/Green	Red	Blue	Orange/Red
Cartilage	Varies	Varies	Varies	Varies
Fibrin	Red	Yellow	Red	Blue
Muscle	Red	Yellow	Red	Blue
Abbreviation: PTAH = Phosphotungstic Acid Hematoxylin; BM = Basement Membrane				

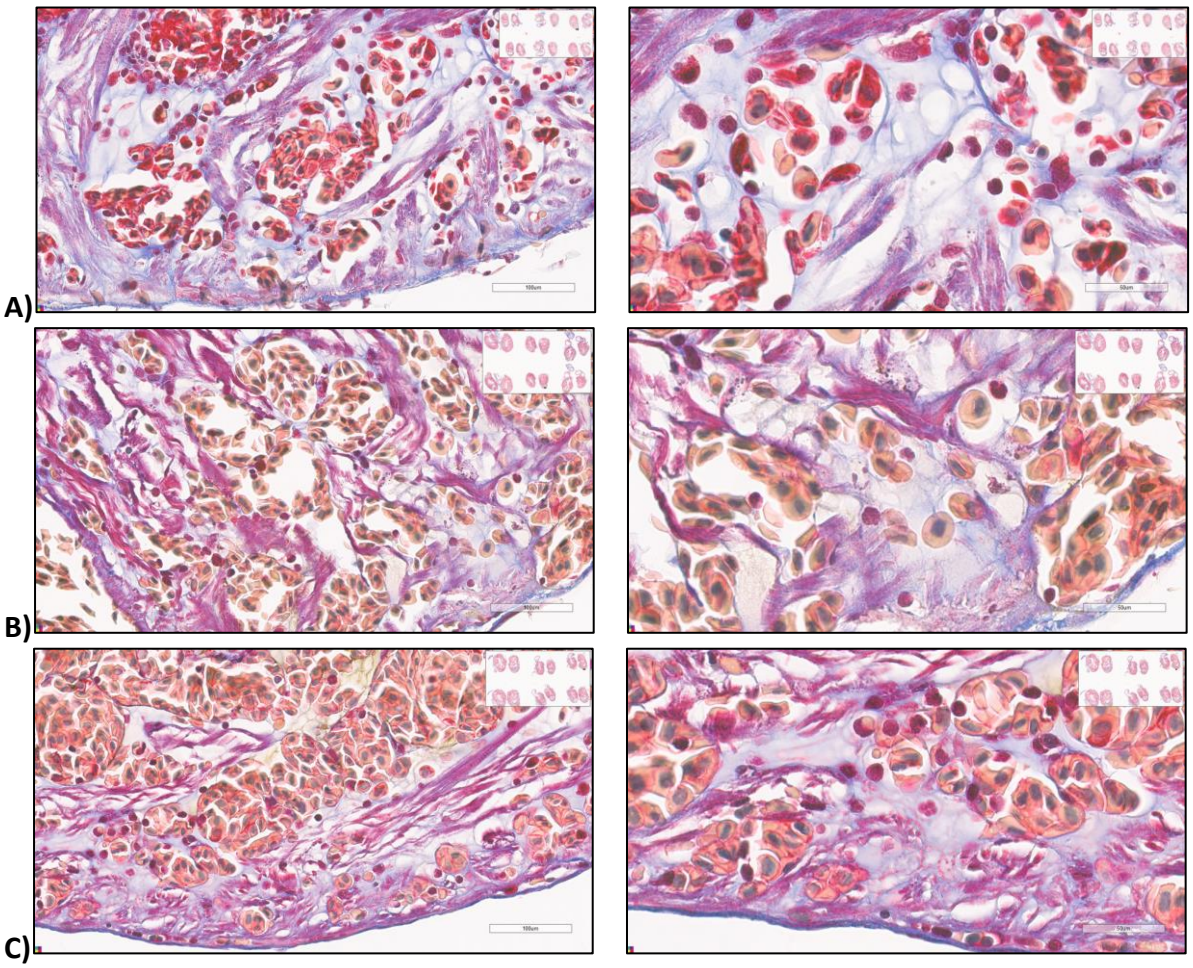

Figure 27: Masson's Trichrome Stains of Control and Treatment Groups 2 Days After Injury All views on the left are at 20X zoom while views on the right are at 40X zoom. **A)** Control animal. **B)** Animal treated with medium-dose butorphanol. **C)** Animal treated with high-dose butorphanol. Scale bar included.

The organization of structural connective tissues can help identify their type. Collagenic fibers occur as individual arranged in an open-weave pattern like in areolar tissue or collagen fibers can be clumped together as large bundles to form structures of high tensile strength like tendons. Individual collagenic fibers do not branch, but bundles of collagenic fibers frequently have branching morphology (Suvarna et al., 2012). Reticular fibers appear as fine, delicate fibers that are usually anchored to high-strength bundles of Type I collagen fibers. Reticular fibers are arranged in a three-dimensional network to provide a system of support even down to the

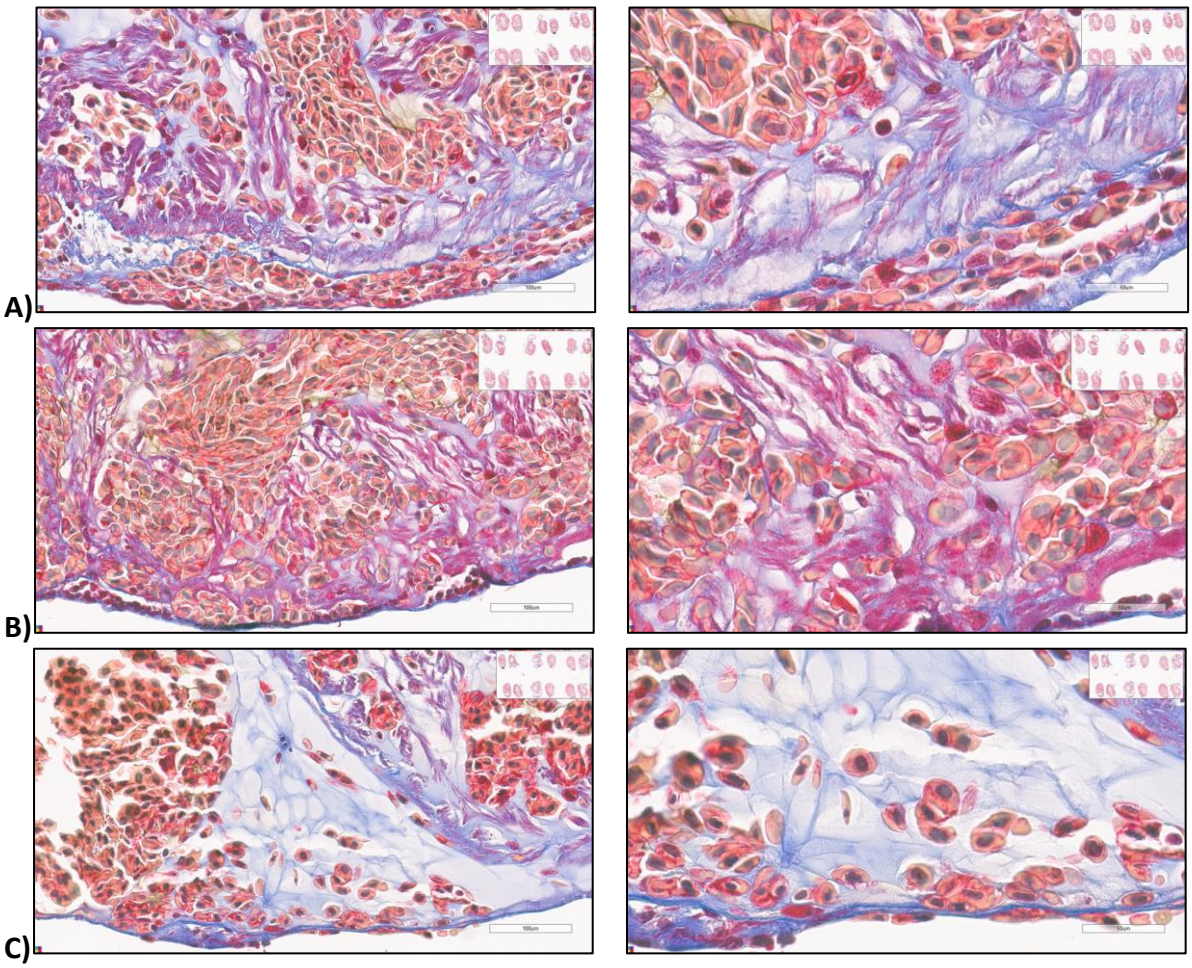

Figure 28: Masson's Trichrome Stains of Control and Treatment Groups 7 Days After Injury All views on the left are at 20X zoom while views on the right are at 40X zoom. **A)** Control animal. **B)** Animal treated with medium-dose butorphanol. **C)** Animal treated with high-dose butorphanol. Scales bar included.

individual cell level (Ushiki, 2002). The elastic-fiber system consists of oxytalan, elaunin, and elastic fibers with fibrillar, amorphous, or mixed structures, respectively. The three fibers represent different arrangements and compositions of elastin proteins and a microfibrillar scaffolding component termed elastic fiber microfibrillar protein (EFMP) (Suvarna et al., 2012). It is suggested that oxytalan and elaunin fibers contain immature elastin proteins, the differentiation between the two immature elastic-system fibers is the extent of elastin protein cross-linking (Schwartz and Fleischmajer, 1986).

Initial evaluations by Dr. Barry H. Rickman of slides stained by H&E suggested that the proteinaceous exudate may be flocculated proteins, possibly from degenerating muscle fibers. However, after assessing the slides stained by Masson's trichrome protocol, the lack of red dusting or staining (see Table 5) in these areas suggests it is unlikely that degenerating muscle fibers are contributing to this proteinaceous exudate. From the fact that there is no clear organization of fibers or connective tissue deposition in the areas of damage, the only conclusion from Masson's trichrome stains is that the proteinaceous exudate identified in H&E stains is some type of connective tissue. Other stains are necessary to differentiate protein types. Qualitatively, there is no characteristic pattern of staining neither between control or treatment groups nor temporally from twelve hours to seven days status-post injury.

Picrosirius Stain

Due to their fine structure, reticular fibers are difficult to see under light microscopy, especially when using H&E, but their argyrophilic proteoglycans produce dark stains when using any silver impregnation method (Suvarna et al., 2012). However, in cardiac tissue remodeling following injury, reticular fibers play little to no role in mediating repair (Robbins et al., 2010). Further investigations for reticular fibers were not explored. There are four major types of collagen protein, (Type I – Type IV) and several minor types. Type I collagen stains strongly with acid dyes (e.g. eosin) due to the presence of cationic groups on collagen protein. However, unlike collagen Type I, the other types of collagen are better differentiated through immunohistochemistry (Suvarna et al., 2012). Since validated axolotl antibodies are not commonly available, before moving to immunohistochemical methods to identify and/or

differentiate collagen in the area containing the proteinaceous exudate, a simple stain using the Sirius dye can help define connective tissue types.

The Sirius red dye intensely stains amyloid proteins and collagen fibers red under light microscopy (Suvarna et al., 2012). In addition to the deep color reaction, like the Congo red dye commonly used in amyloid pathology studies, Sirius red gives green birefringence under polarized light. This is attributed to the elongated structure of the Sirius red dye molecule that attaches to collagen fibers in such a way that their long axes are parallel (Vidal et al., 1982). Thus, Sirius red-positive collagen under aligned polarized light microscopy can appear red, orange, yellow, or green (the color change in order of decreasing thickness) (Rich and Whittaker, 2005). The use of circularly polarized light eliminates the requirement of aligning fibers to the transmission axis of the polarizing filter and allows visualizing all fibers simultaneously (Whittaker et al., 1994). Sirius red is sometimes used in solution with picric acid, as picrosirius solution (Sweat et al., 1964). The picric acid coagulates proteins and intensifies staining (Suvarna et al., 2012).

A review of picrosirius staining across 15 vertebrate species, representing the main vertebrate classes (fish, amphibians, reptiles, birds, and mammals) and using different organs from at least three specimens per class shows that all structures that stain red and exhibited signs of birefringency contain collagen (Junqueira et al., 1979). The study by Junqueira et al. does not outline which organs per vertebrate class were used or if the same organs were consistently stained for every specimen. Additionally, the study mentions three exceptions of structures that stain red that do not contain collagen: 1) keratohyaline granules of cornified epithelia; 2) mucus-producing glands; and 3) fish hearts. Although no mention of any exception to picrosirius staining is stated about amphibian hearts, since it is unknown if amphibian hearts were used in the study

and based on the similarity of heart development, morphology, and ultrastructure [adult fish and amphibians have trabeculated hearts (Hu et al., 2001; Lemanski, 1973a, b)] confirming the picrosirius stain in axolotls is necessary. In-house picrosirius staining was performed and a representative result is shown in Figure 29. This axolotl's heart was from the ischemia-induction time studies and was subject to thirty minutes of ischemia and the heart was sampled thirty days after the injury. Although an ischemia-reperfusion injury was not induced, collagen fibers are part of the normal axolotl heart structure, especially in the exterior wall. Exposing the heart sample to polarized light shows the presence of birefringent components, confirming picrosirius stains identify collagen in the axolotl heart.

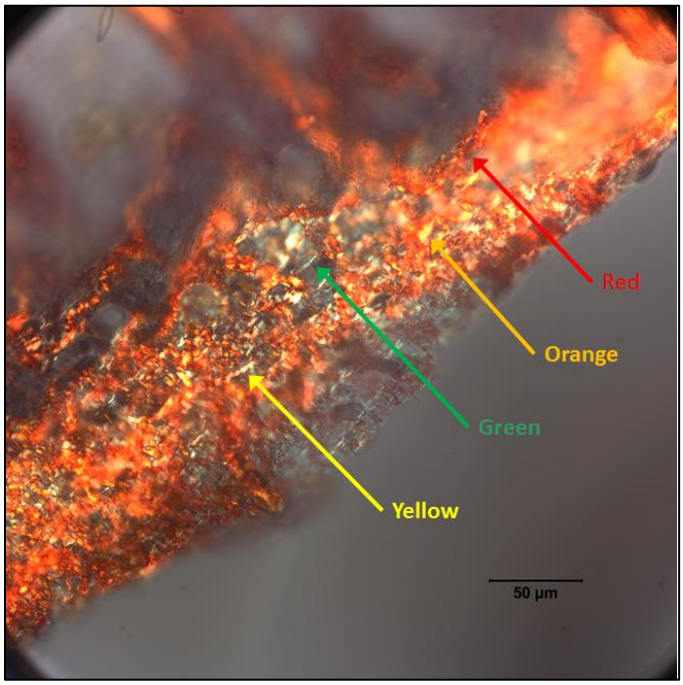

Figure 29: Picrosirius Staining of Axolotl Heart Viewed Under Polarized Light
Results of picrosirius staining done in-house showing axolotl collagen fibers reacting with Sirius red dye. The alignment of the dye along collagen fibers is evident as the birefringence characteristics (red to green color scale) apply to axolotl tissue.

Results of picrosirius stains of a naïve axolotl heart are shown in Figure 30. Representative results from picrosirius stains are shown in Figure 31, Figure 32, and Figure 33 for animals

sacrificed twelve hours, two days, and seven days after ischemia-reperfusion injury respectively. Like the test-run in-house, the samples processed by Histowiz, Inc. predominantly show positive Sirius red dye staining at the heart border with some scattered positive-staining collagen fibers appearing within the area of damage. However, the proteinaceous material does not stain red, suggesting that this exudate is less likely to be collagen. Qualitatively, there is no characteristic pattern of staining neither between control or treatment groups nor temporally from twelve hours to seven days status-post injury.

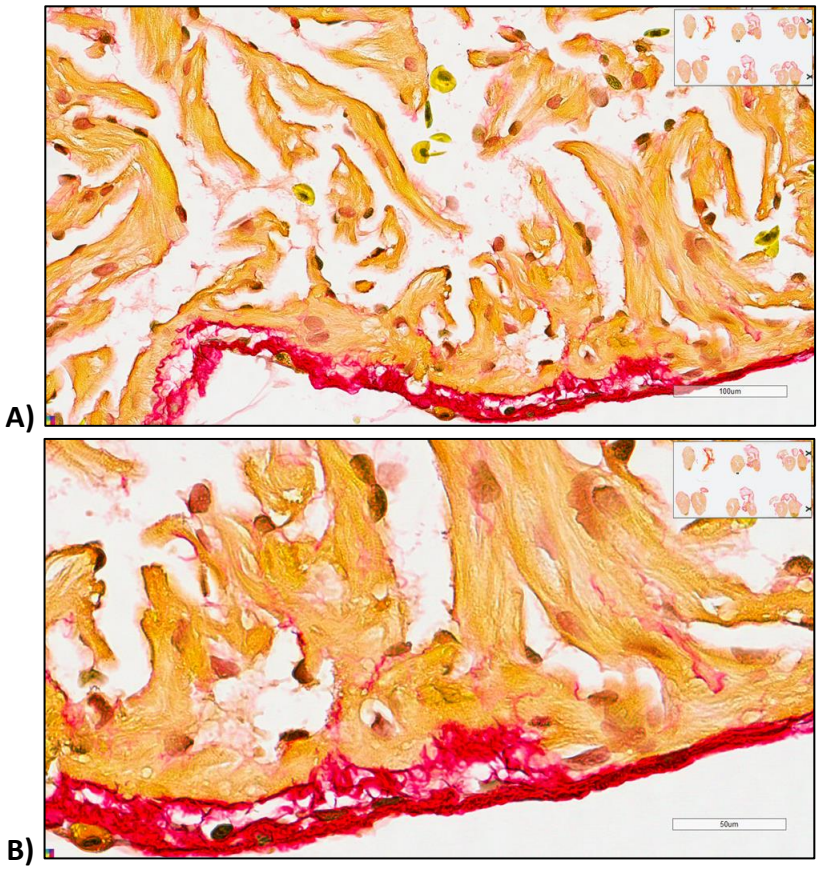

Figure 30: Picrosirius Stains of Naïve Axolotl Heart
Views of naïve axolotl heart at **A)** 20X zoom and **B)** 40X zoom. Scale bar included.

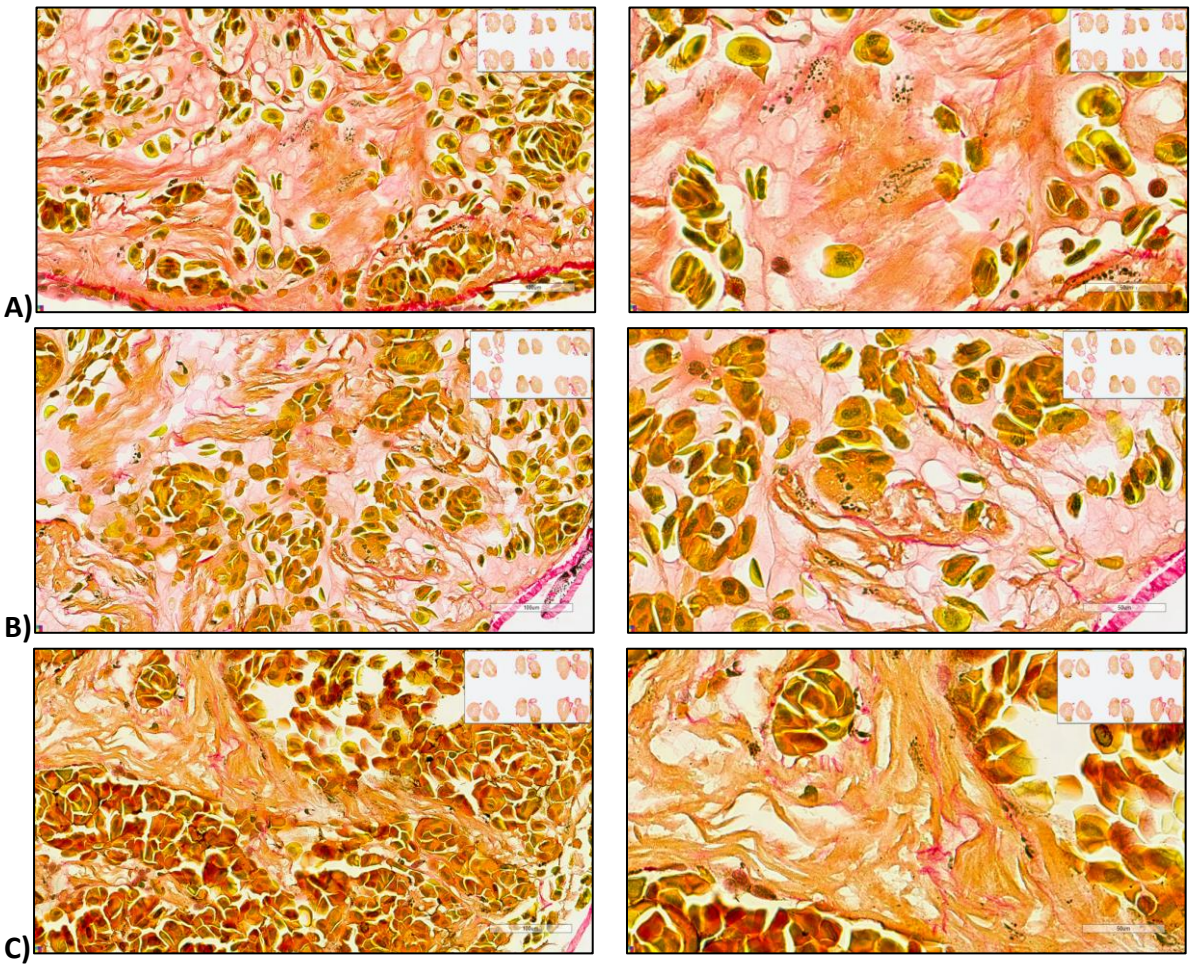

Figure 31: Picrosirius Stains of Control and Treatment Groups 12 Hours After Injury
All views on the left are at 20X zoom while views on the right are at 40X zoom. **A)** Control animal. **B)** Animal treated with medium-dose butorphanol. **C)** Animal treated with high-dose butorphanol. Scale bar included.

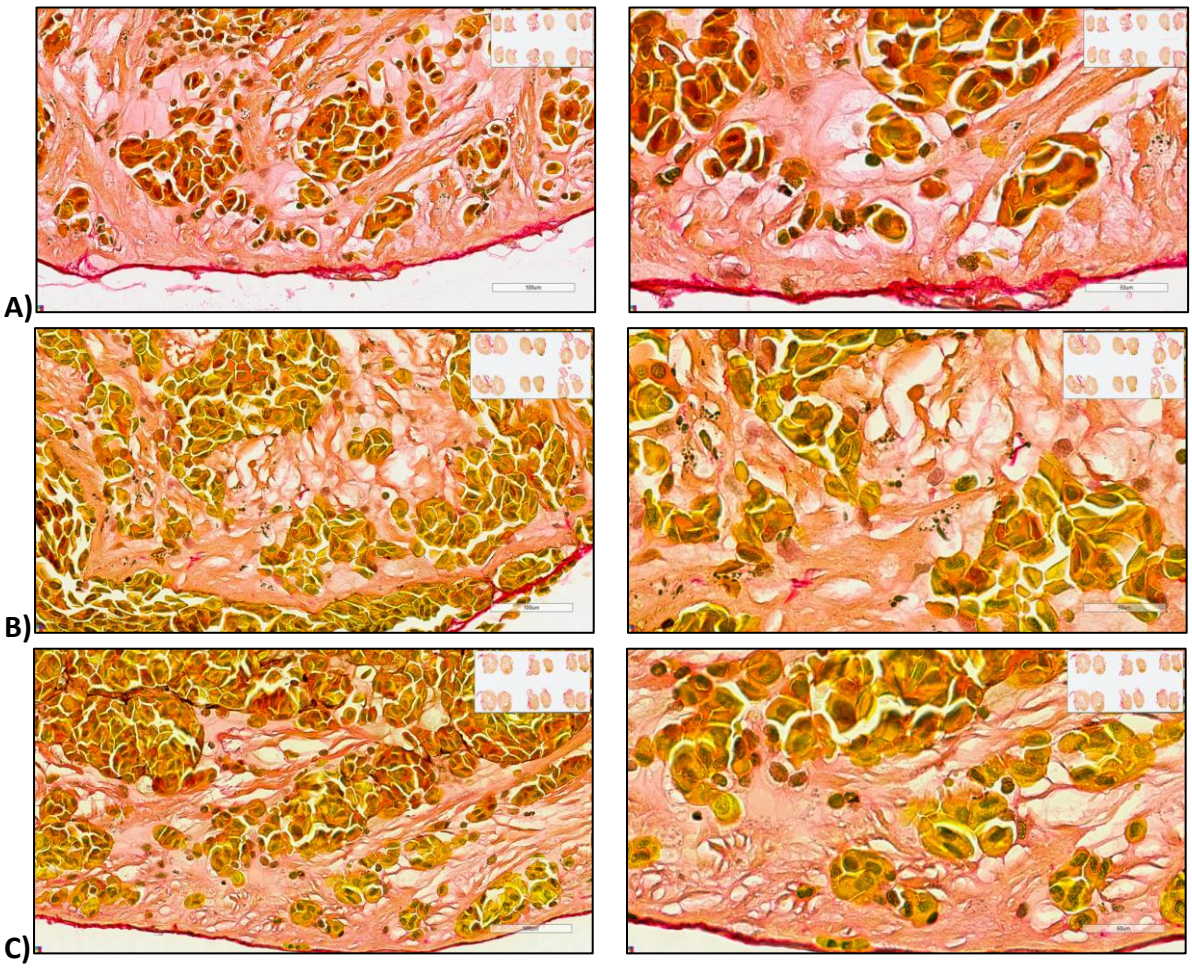

Figure 32: Picrosirius Stains of Control and Treatment Groups 2 Days After Injury
All views on the left are at 20X zoom while views on the right are at 40X zoom. **A)** Control animal. **B)** Animal treated with medium-dose butorphanol. **C)** Animal treated with high-dose butorphanol. Scale bar included.

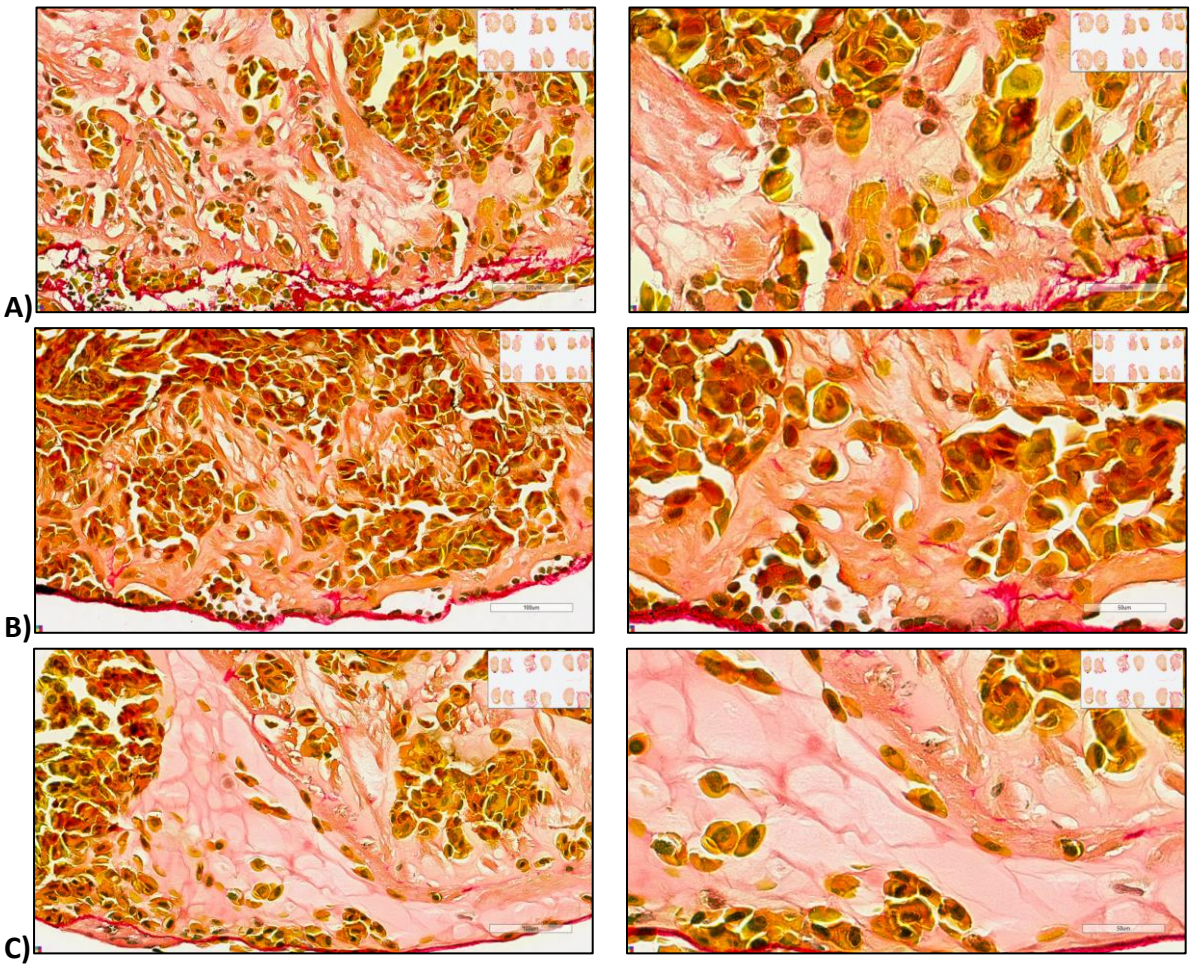

Figure 33: Picrosirius Stains of Control and Treatment Groups 7 Days After Injury

All views on the left are at 20X zoom while views on the right are at 40X zoom. **A)** Control animal. **B)** Animal treated with medium-dose butorphanol. **C)** Animal treated with high-dose butorphanol. Scale bar included.

Acid Fuchsin Orange G Stain

Using H&E and trichrome staining in cardiac regeneration studies of the zebrafish, healing after apical resection (Major and Poss, 2007; Poss et al., 2002) and cryoinjury (Chablais et al., 2011; Gonzalez-Rosa et al., 2011; Kikuchi et al., 2010; Schnabel et al., 2011) shows histopathology of cardiac remodeling with an acute-phase inflammatory exudate. In addition to fibrosis and scar tissue formation during inflammation, fibrin is an important constituent of this acute-phase inflammatory response and is found in areas of recent tissue damage (Suvarna et al., 2012). The

acid fuchsin orange G (AFOG) stain can be used to differentiate the protein content in the remodeling areas and can extend findings from Masson's trichrome stain. Developed in 1978 to study glomerular protein deposits in renal samples (Mihatsch and Bremer, 1978), staining results from that publication reveal protein deposits in glomerulus as: fibrin: red/deep red (fibrillar/threadlike appearance); serum: yellow to orange; amyloid: bluish-red; basement membrane: pale-blue; mesangial matrix: blue; cellular cytoplasm: grey to yellow-orange; cellular nuclei: orange-brown to black, collagen: blue; and erythrocytes: yellow-orange.

In a study with chronic follow-up over sixty days, AFOG staining in zebrafish subject to cardiac cryoinjury show a progressive evolution in the protein content within and bordering the injured cardiac tissue. Four days post cryoinjury (dpci), the injured myocardium is surrounded by non-muscle cells, most likely as a response to inflammation. By seven dpci, a border of fibrin has formed along the injured endocardium while loose, fibrillar collagen has infiltrated into the central portion of the injured area. At fourteen dpci, the outer edge of the fibrin layer has started to resolve and is beginning to be replaced by new cardiomyocytes while the central portion begins to form a mature network of collagen fibers. Twenty-one dpci, a new wall of cardiomyocytes has surrounded the injured area with fibrin almost completely resolved and the collagen network beginning to recede. By thirty dpci, no fibrin is present and the collagen network is markedly decreased. By sixty dpci, the infarct scar is nearly completely eliminated with rare collagen fibers scattered throughout the remodeled tissue (Chablais et al., 2011). This spatial and temporal Information about zebrafish cardiac tissue regeneration proceeds differently than the well-documented processes in mammalian cardiac tissue repair (Lilly, 2011; Robbins et al.,

2010) and regeneration (Haubner et al., 2012; Porrello et al., 2011), warranting further investigation using AFOG tissue staining in the axolotl.

Results of AFOG stains of a naïve axolotl heart are shown in Figure 34. Representative results from AFOG stains are shown in Figure 35, Figure 36, and Figure 37 for animals sacrificed twelve hours, two days, and seven days after ischemia-reperfusion injury respectively. Unlike zebrafish heart regeneration that shows the appearance of intensely red flocculated fibrin aggregates and fibrous fibrin structures that are eventually cleared and replaced first by collagen fibers and eventually new cardiomyocytes (Schnabel et al., 2011), the results of the axolotl heart pathophysiology after AFOG staining indicate the proteinaceous exudate (AFOG staining: light- to pale-blue) exhibits basement membrane proteins. Furthermore, the lack of any red hue or

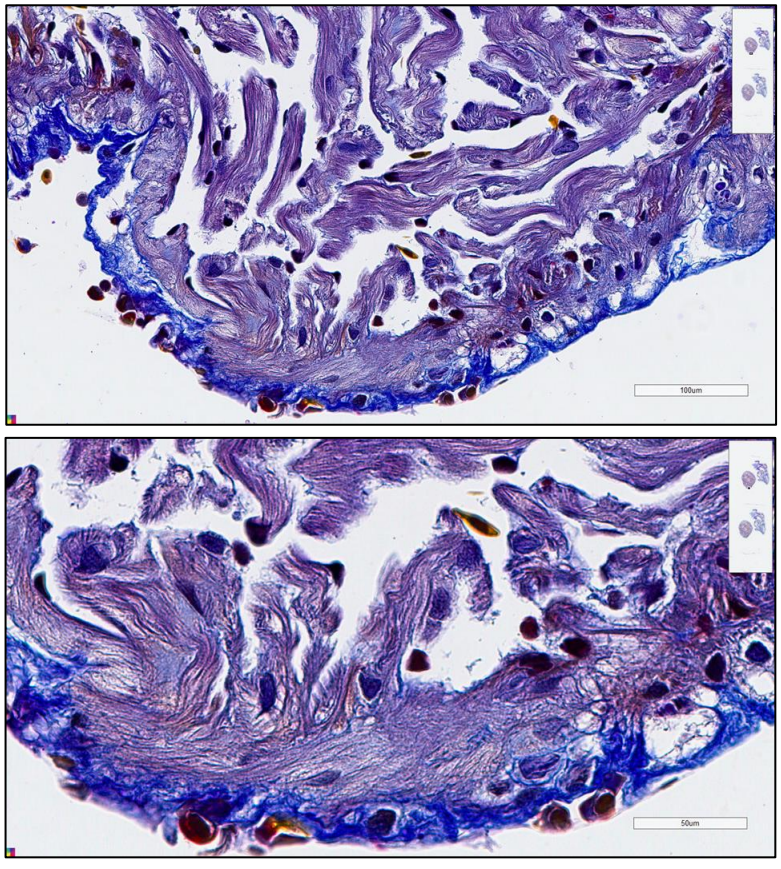

Figure 34: AFOG Stains of Naïve Axolotl Heart
Views of naïve axolotl heart at **A)** 20X zoom and **B)** 40X zoom. Scale bar included.

dusting in the proteinaceous exudate of the damaged axolotl tissue after AFOG staining make it unlikely that there is any fibrinoid material in this area. Fibrinoid is an eosinophilic material, regarded as a mixture of fibrin and other plasma-protein constituents, that stains identically to fibrin (Suvarna et al., 2012). Qualitatively, there is no characteristic pattern of staining neither between control or treatment groups nor temporally from twelve hours to seven days status-post injury.

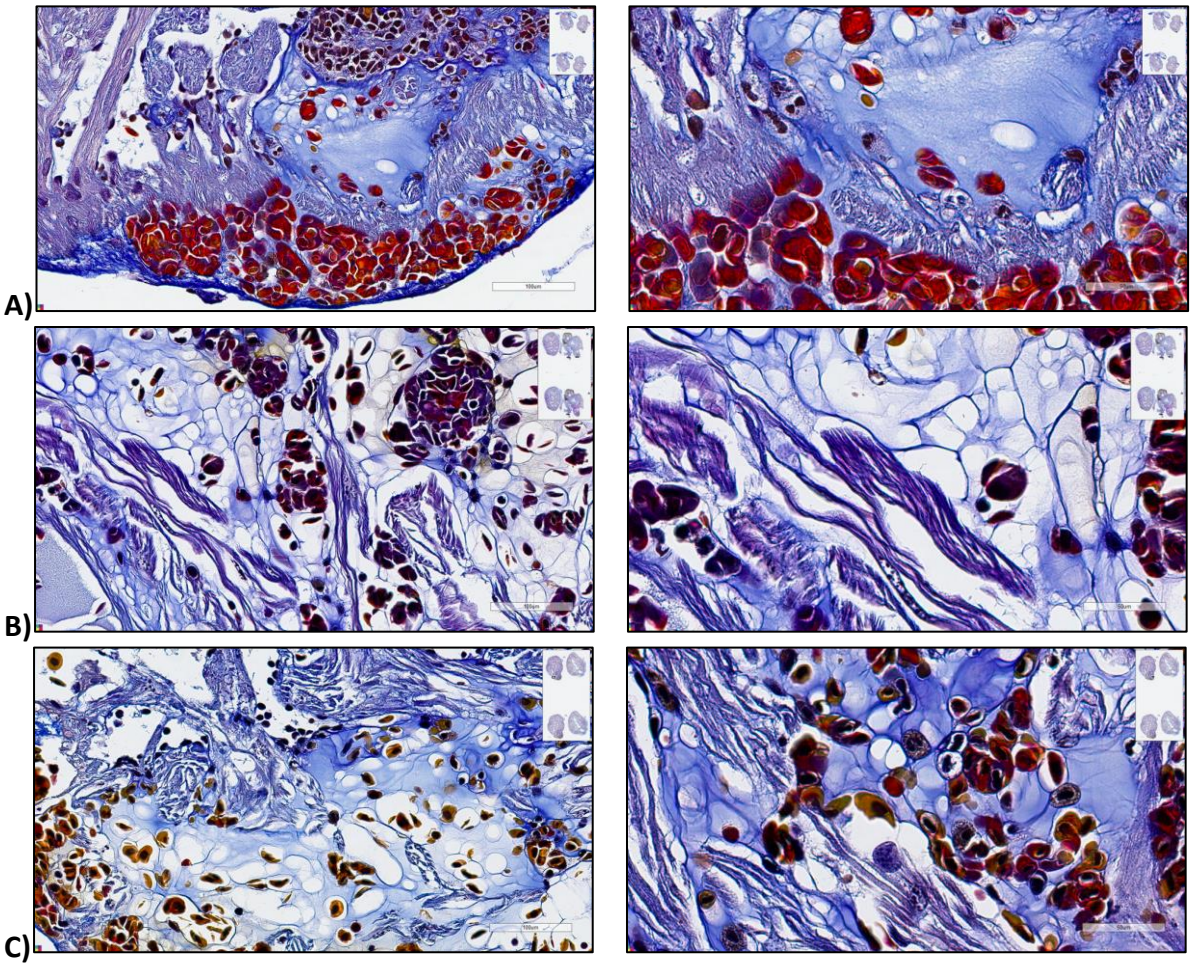

Figure 35: AFOG Stains of Control and Treatment Groups 12 Hours After Injury
All views on the left are at 20X zoom while views on the right are at 40X zoom. **A)** Control animal. **B)** Animal treated with medium-dose butorphanol. **C)** Animal treated with high-dose butorphanol. Scale bar included.

Regardless of location in the body, all basement membranes contain a common set of proteins that include laminin, collagen Type IV, various heparan sulfate proteoglycans, and entactin/nidogen (Martin and Timpl, 1987). Light microscopy with immunofluorescence or immunohistochemical enhancement lacks the resolving power to resolve subtle differences in the distribution of these components within intact basement membranes or to differentiate basement membrane from immediately adjacent tissue (Martinez-Hernandez and Chung, 1984). Follow-up studies have relied upon immunoelectron microscopy (electron immunohistochemistry) to identify and differentiate laminin and entactin within basement membrane tissue (Laurie et al., 1982b; Madri et al., 1980), finding that the four commonly-found proteins in basement membrane do not occur as separate layers, but are integrated into a common structure (Laurie et al., 1982a; Martin and Timpl, 1987). Since the proteinaceous exudate does not appear to have any structural organization (e.g. fibrous structures or cross-linking networks of fibrillar components), the basement membrane proteins identified by pale-blue staining using the AFOG protocol may be proteins soluble in plasma.

Heparan sulfate proteoglycans (HSPGs) are glycoproteins that can be divided into three types: membrane HSPGs (e.g. syndecans and glypicans); secreted ECM HSPGs (e.g. agrin and perlecan); or secretory vesicle proteoglycans (e.g. serglycin). Membrane-bound and secreted HSPGs can bind cytokines, chemokines, growth factors, and morphogens to protect these molecules from degradation by proteolysis. Alternatively, HSPGs can bind proteases or protease inhibitors directly to mediate protein metabolism and turnover (Sarrazin et al., 2011).

As discussed in the section titled “Molecular Signaling Pathways Mediating Cardiac Repair”, pathways of embryogenesis and development are generally believed to be activated

after tissue injury. Growth factors such as PDGF and FGF play a crucial role in the spatiotemporal control of cellular movement in development and repair. The exact mechanisms of how these cues are regulated are areas of intense research. Interestingly, it is suggested that heparan sulfates bound to proteins of the ECM modulate PDGF (Symes et al., 2010) and FGF (Ornitz and Itoh, 2001) function.

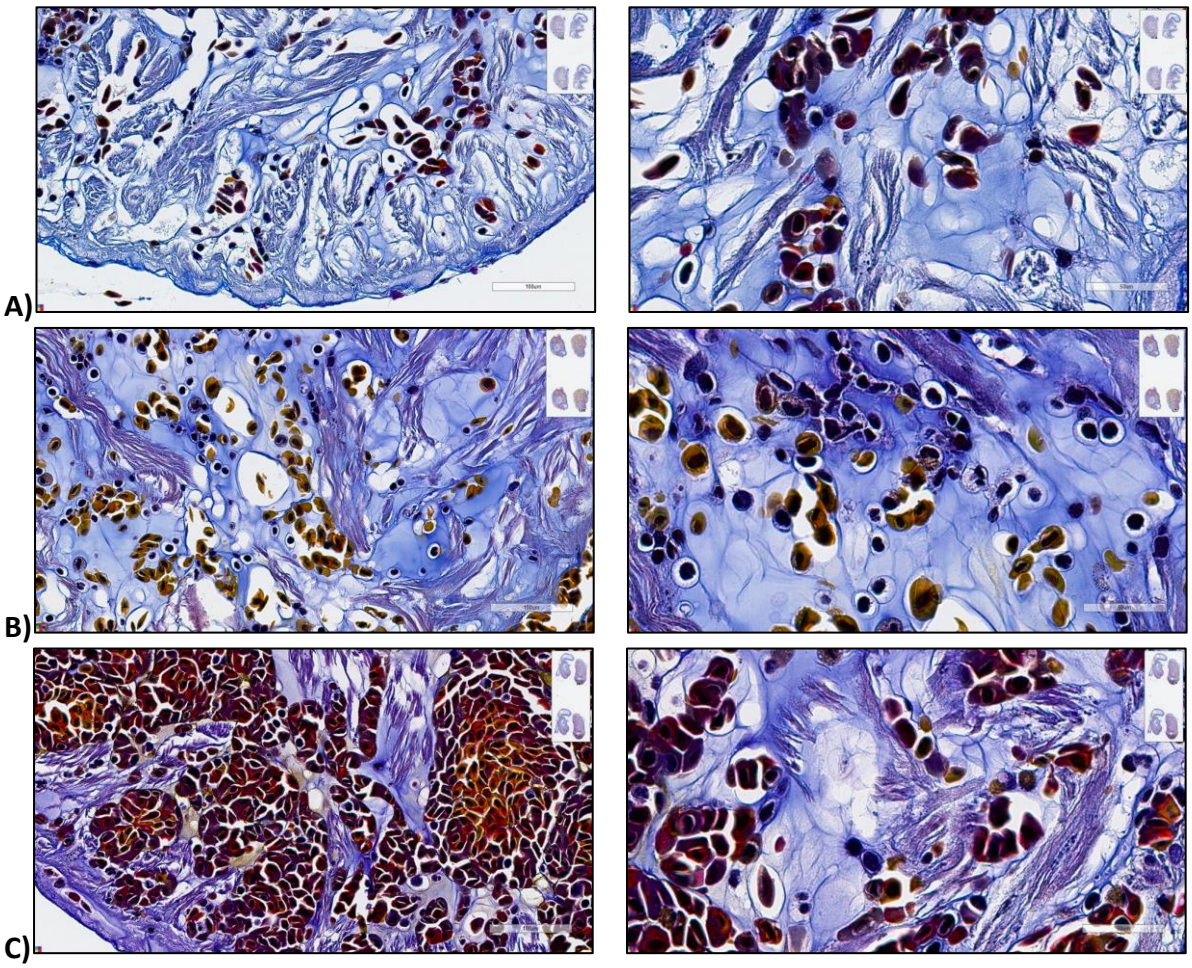

Figure 36: AFOG Stains of Control and Treatment Groups 2 Days After Injury
All views on the left are at 20X zoom while views on the right are at 40X zoom. **A)** Control animal. **B)** Animal treated with medium-dose butorphanol. **C)** Animal treated with high-dose butorphanol. Scale bar included.

In contrast to HSPGs bound to ECM proteins, the ectodomain of the syndecan family of transmembrane HSPGs, specifically syndecan-1 and syndecan-4 were found to be constitutively shed from cultured cells, with shedding accelerated by epidermal growth factor and thrombin (a

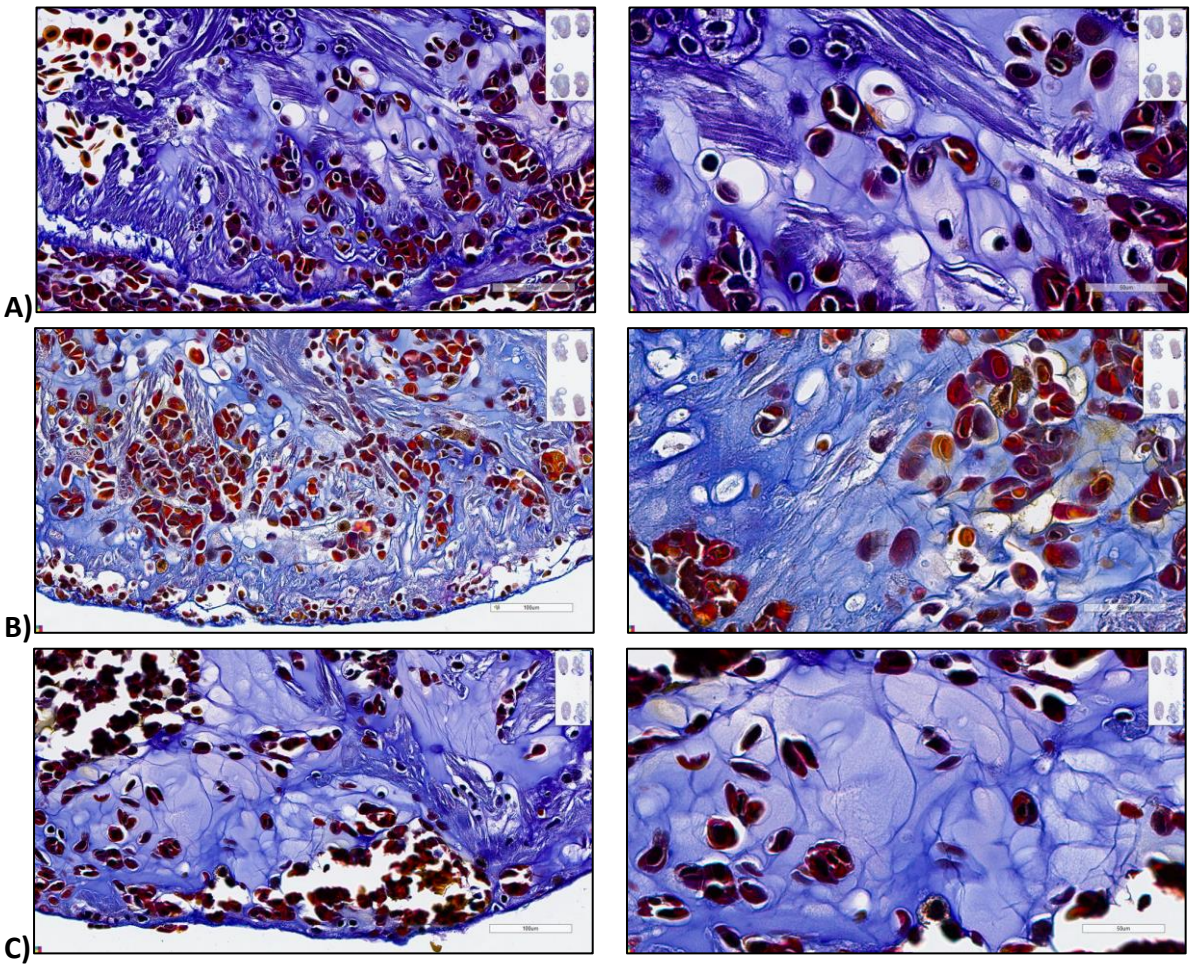

Figure 37: AFOG Stains of Control and Treatment Groups 7 Days After Injury
All views on the left are at 20X zoom while views on the right are at 40X zoom. **A)** Control animal. **B)** Animal treated with medium-dose butorphanol. **C)** Animal treated with high-dose butorphanol. Scale bar included.

protease) (Subramanian et al., 1997). These factors are known to be upregulated during inflammation and wound repair (Robbins et al., 2010). Plasma levels of syndecan-4 were measured in normal human subjects and human patients after an acute MI. Like the results in cultured cells, two-weeks after suffering an acute MI, peak levels of plasma syndecan-4 were about one-hundred times greater than levels in normal subjects, attributed to the accumulation of proteases from leukocytes and growth factors induced through inflammation. Furthermore, immunohistochemical analyses of heart samples from autopsied patients using the specific anti-

human syndecan-4 antibody (anti-ryudocan) stained newly injured tissues undergoing repair while old infarct scars and undamaged areas were left unstained (Kojima et al., 2001). Kojima et al. hypothesize in their study that the increased plasma syndecan-4 originates from the inflammatory fluid of cardiac tissues injured by myocardial infarction. Syndecan-4 has been shown to have specific binding affinities to heparin-binding growth factors such as basic FGF (bFGF) and VEGF (Woods et al., 1998), factors important for tissue repair and angiogenesis, respectively (Robbins et al., 2010). Considering the large number of cytokines, chemokines, growth factors, morphogens, proteases and protease inhibitors, soluble syndecan-4 may function as a tissue-repairing molecule. Its localization in healing hearts from autopsied patients also suggest that it can play a specific role in mediating cardiac tissue repair.

The unidentified protein identified as a homogenous, glassy, and pink substance in H&E staining is best characterized as hyaline change. This widely-used descriptive term applies to any alteration within cells or the extracellular space and is used more to capture general appearances, rather than as an indicator of cellular or tissue injury. This histological characterization denotes a spectrum of changes and not a specific pattern of protein secretion or accumulation (Robbins et al., 2010). Examples of intracellular accumulations of hyaline protein are found in alcoholic liver disease, Kaposi's sarcoma, and malignant fibrous histiocytoma. Hyaline accumulations found extracellularly are found predominantly in adenoid cystic carcinomas, endodermal sinus tumors, and diabetic glomerular nodular sclerosis (Barsky and Hannah, 1987).

Using highly specific antibodies to Type IV collagen and laminin, Barsky et al. tested the immunoreactivity of hyaline bodies found extracellularly in six disease processes and compared

results to hyaline bodies found intracellularly in three disease processes. The results showed a clear difference: all hyaline bodies found in extracellular settings displayed strong immunoreactivity for the basement membrane components of type Iv collagen and laminin, while the hyaline bodies found intracellularly were unreactive to the antibodies. This suggest a common origin of proteins for hyaline bodies found extracellularly that is markedly different from the histologic origin of hyaline bodies found intracellularly. The pathophysiologic implications points to the stimulation of hyperactive production of basement membrane protein synthesis by cells that normally produce and secrete basement membrane proteins. However, as many cell types synthesize type Iv collagen and laminin [see (Timpl and Dziadek, 1986) for a partial listing], the major contributor of hyaline change proteins in the regenerating axolotl heart following ischemia-reperfusion injury remains to be elucidated.

In summary, H&E, Masson's trichrome, picrosirius, and AFOG staining results of axolotl hearts healing after ischemia-reperfusion injury show characteristics that are unique to this animal. The exact make up of inflammatory infiltrate in the region of injury is unknown, but is likely to be a protein involved in hyaline change. Follow-up studies with axolotl-specific antibodies to connective tissue proteins and visualization using high-resolution electron microscopy can help identify the components involved in cardiac tissue repair following ischemia-reperfusion injury in the axolotl.

Immunohistochemistry

Negative control results for BrdU staining using a naïve axolotl heart are shown in Figure 38. A BrdU-positive cardiomyocyte is shown in the 40X view, evidence of nucleotide incorporation due to DNA synthesis is occurring in uninjured hearts. Representative results from

BrdU immunohistochemistry (IHC) stains are shown in Figure 39, Figure 40, and Figure 41 for animals sacrificed twelve hours, two days, and seven days after ischemia-reperfusion injury respectively. Slight-positive/lightly-dusted and strong BrdU-positive nuclei are present. There is very strong background staining evident, including a large portion of RBCs, in all areas of myocyte damage and hemorrhage, along with positive edge effects. The remote region containing undamaged tissue has lower background staining. RBCs can be differentiated from CMs by the presence of a translucent plasma membrane bordering the RBCs.

A)

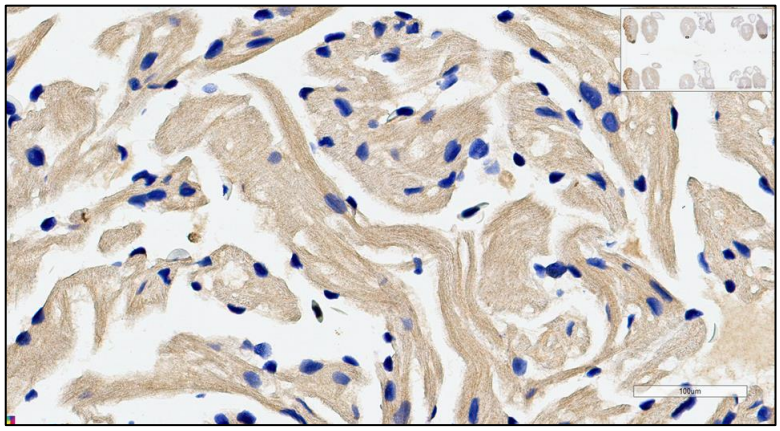

B)

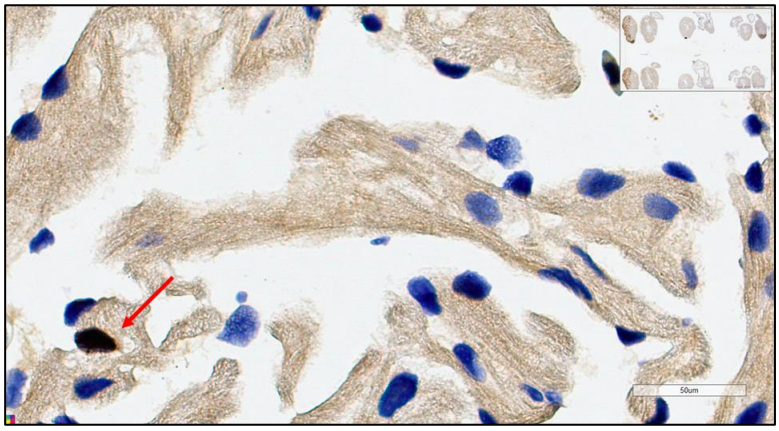

Figure 38: BrdU Immunohistochemistry of Naïve Axolotl Heart
Views of naïve axolotl heart at **A)** 20X zoom and **B)** 40X zoom. Histology features: BrdU-positive nuclei (*red arrow*). Not all views contain an instance of each histologic feature, each histologic feature not annotated. Scale bar included.

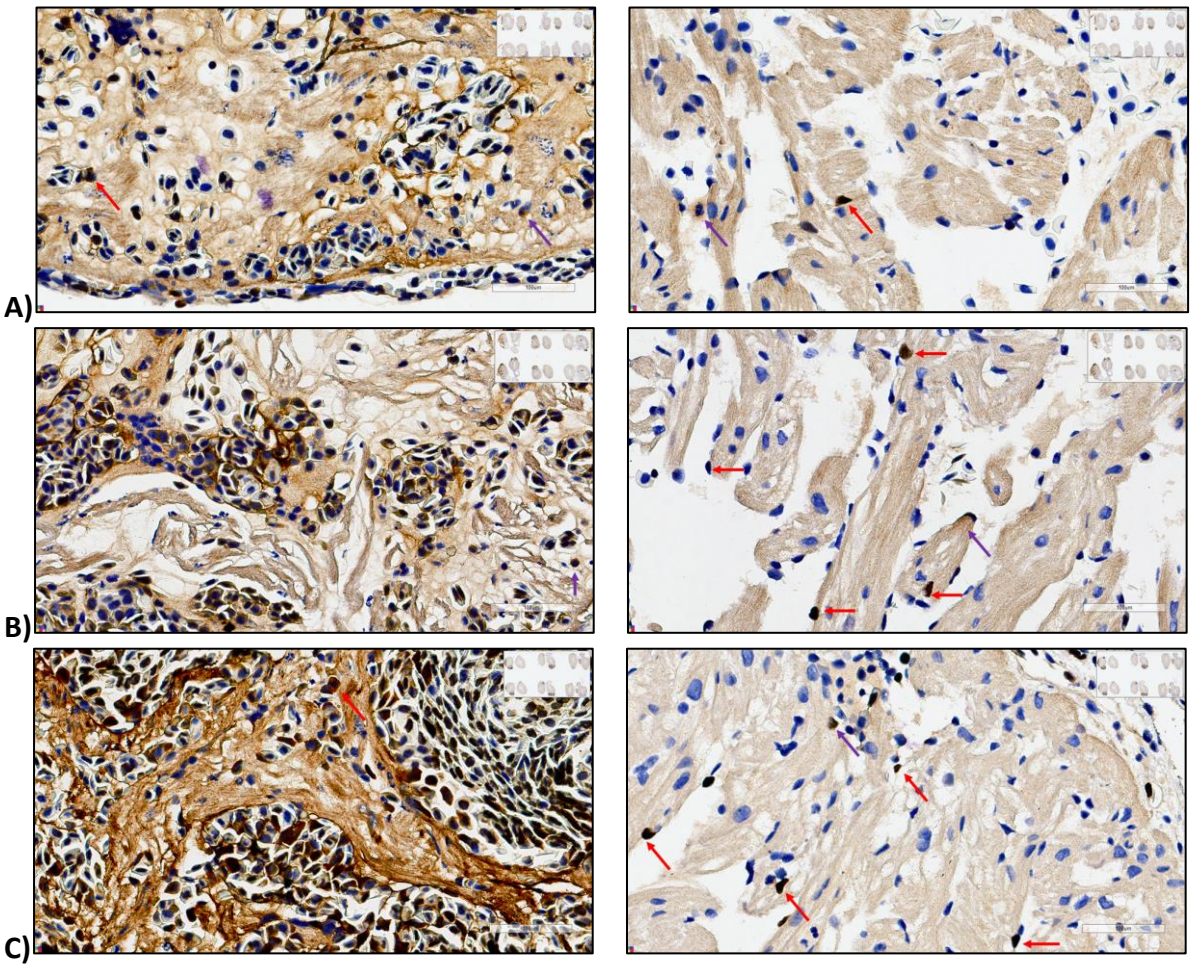

Figure 39: BrdU Immunohistochemistry of Control and Treatment Groups 12 Hours After Injury

All views are at 20X zoom with the left-hand views are from a field in the ischemic region while the right-hand views are from a field in the remote region. **A)** Control animal. **B)** Animal treated with medium-dose butorphanol. **C)** Animal treated with high-dose butorphanol. Histology features: BrdU-positive nuclei (*red arrows*) and slight-positive/lightly-dusted BrdU-positive nuclei (*purple arrows*). Not all views contain an instance of each histologic feature, each histologic feature not annotated. Scale bar included.

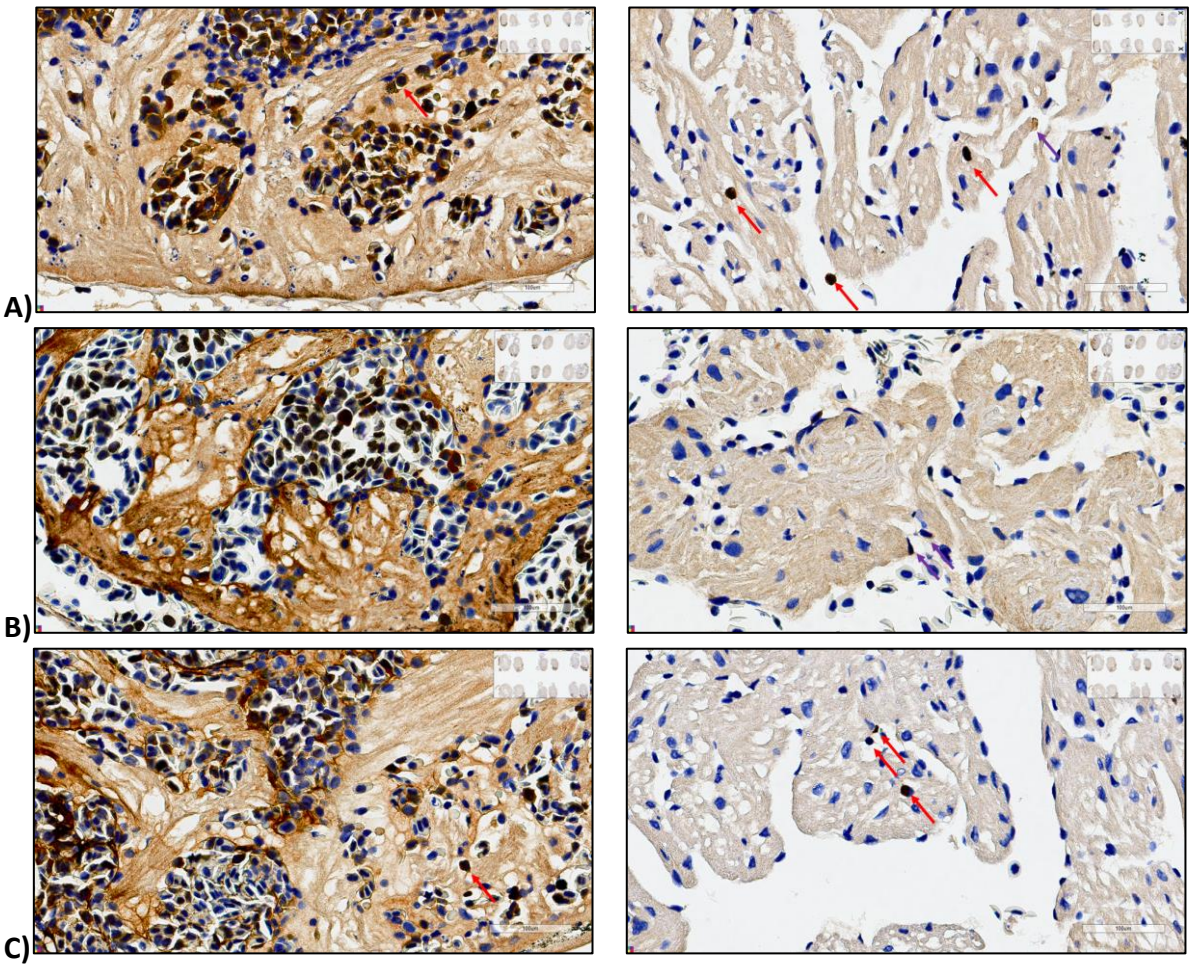

Figure 40: BrdU Immunohistochemistry of Control and Treatment Groups 2 Days After Injury All views are at 20X zoom with the left-hand views are from a field in the ischemic region while the right-hand views are from a field in the remote region. **A)** Control animal. **B)** Animal treated with medium-dose butorphanol. **C)** Animal treated with high-dose butorphanol. Histology features: BrdU-positive nuclei (*red arrows*) and slight-positive/lightly-dusted BrdU-positive nuclei (*purple arrows*). Not all views contain an instance of each histologic feature, each histologic feature not annotated. Scale bar included.

The BrdU nucleotide incorporation assay is a common approach to determine the extent of cardiomyocyte proliferation, using the fact that nucleotide analogs are incorporated into the DNA strands during DNA synthesis, thus labeling cells during the S-phase of the cell cycle. However, caution must be applied as DNA synthesis takes place because of multiple cellular events. DNA synthesis not only occurs during semiconservative DNA replication, but also during DNA repair. Furthermore, a cell may stop cell-cycle progression after S-phase: nucleotide-

progression assays do not indicate if a cell will continue to divide or undergo G2/M arrest, polyploidization, or polynucleation. Without additional proliferation assays to distinguish other stages of the cell cycle, cytokinesis, or karyokinesis, qualitatively, the 250 mg/kg BrdU single-bolus injection labels cardiac cell activity. Differences between control or treatment groups and temporally from twelve hours to seven days status-post injury are assessed in the section titled "Quantitative Assessments of Pathology".

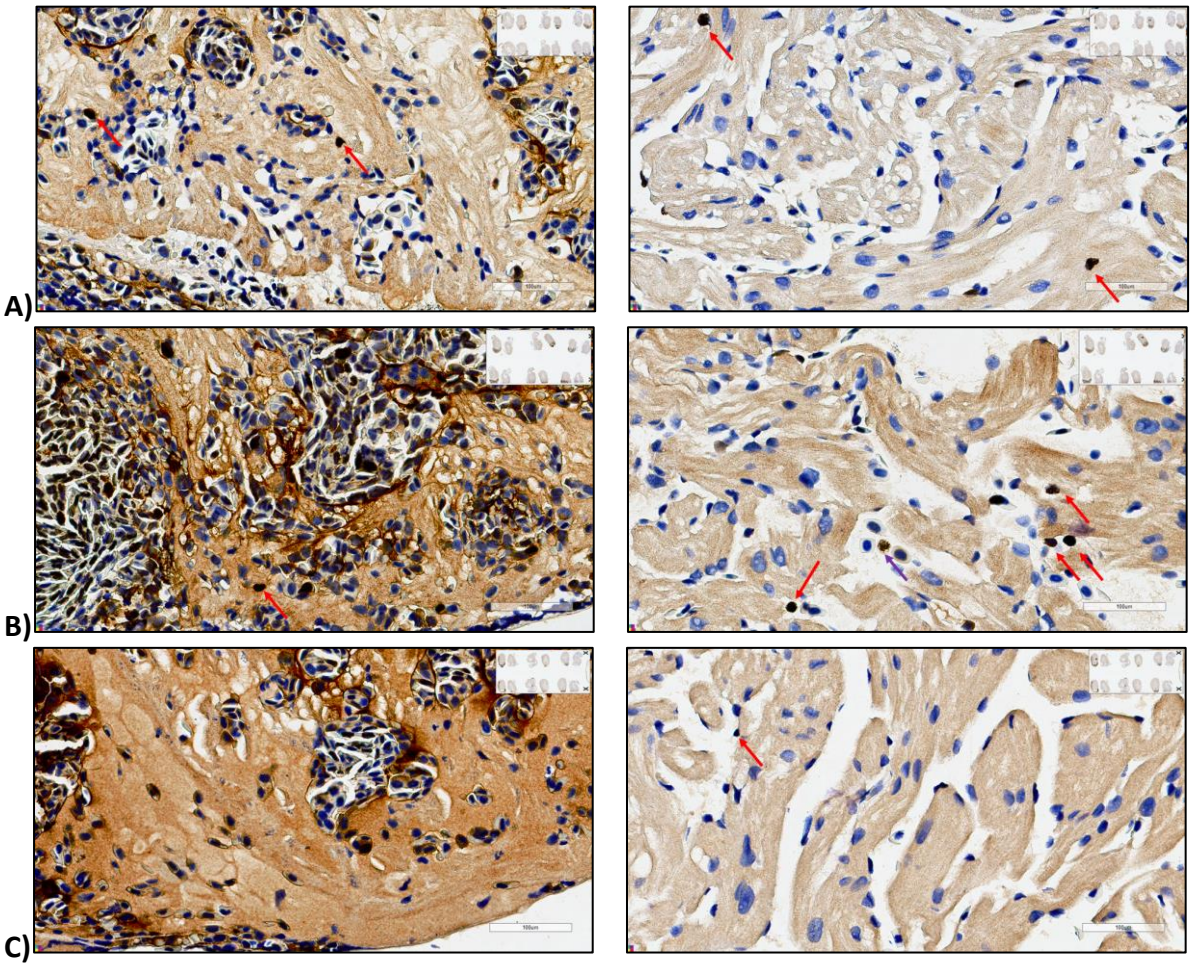

Figure 41: BrdU Immunohistochemistry of Control and Treatment Groups 7 Days After Injury All views are at 20X zoom with the left-hand views are from a field in the ischemic region while the right-hand views are from a field in the remote region. **A)** Control animal. **B)** Animal treated with medium-dose butorphanol. **C)** Animal treated with high-dose butorphanol. Histology features: BrdU-positive nuclei (*red arrows*) and slight-positive/lightly-dusted BrdU-positive nuclei (*purple arrows*). Not all views contain an instance of each histologic feature, each histologic feature not annotated. Scale bar included.

Negative control results for TUNEL staining using a naïve axolotl heart are shown in Figure 42. No evidence of light dusting or strong-positive TUNEL cardiomyocytes are present. Representative results from TUNEL immunohistochemistry stains are shown in Figure 43, Figure 44, and Figure 45 for animals sacrificed twelve hours, two days, and seven days after ischemia-reperfusion injury respectively. The background staining varies but is always stronger at the region of ischemia. Only cardiomyocytes with nuclei that are TUNEL-positive and have not started the process of apoptosis (pyknosis, karyorrhexis, or karyolysis) or necrosis are annotated in the figures. Differences between control or treatment groups and temporally from twelve hours to seven days status-post injury are assessed in the section titled "Quantitative Assessments of Pathology".

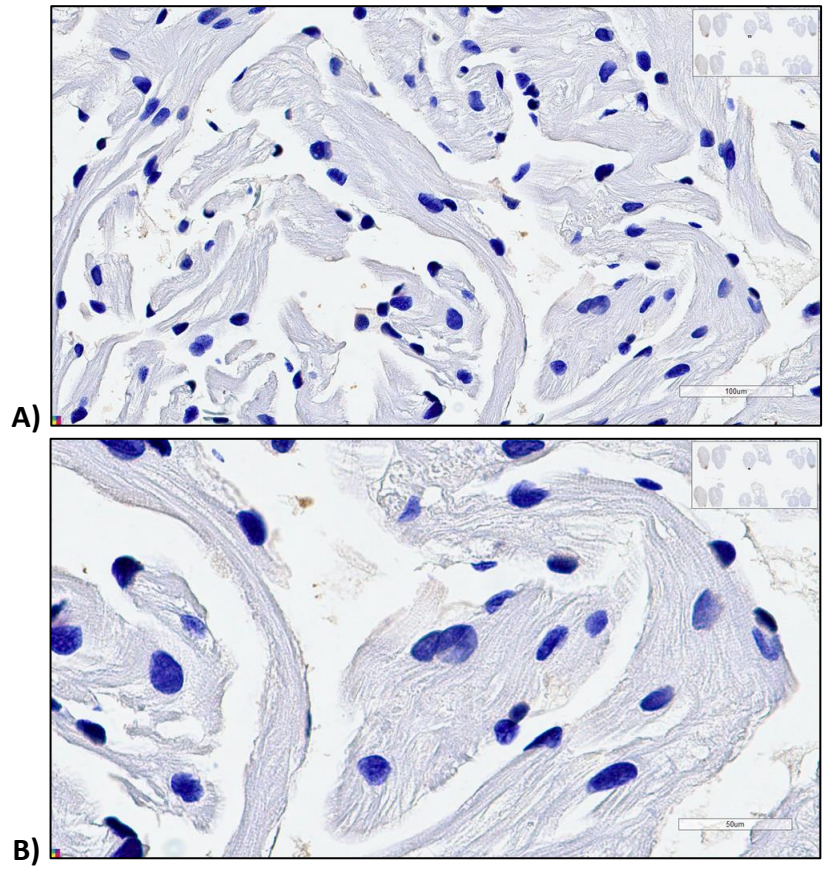

Figure 42: TUNEL Immunohistochemistry of Naïve Axolotl Heart
Views of naïve axolotl heart at **A)** 20X zoom and **B)** 40X zoom. Scale bar included.

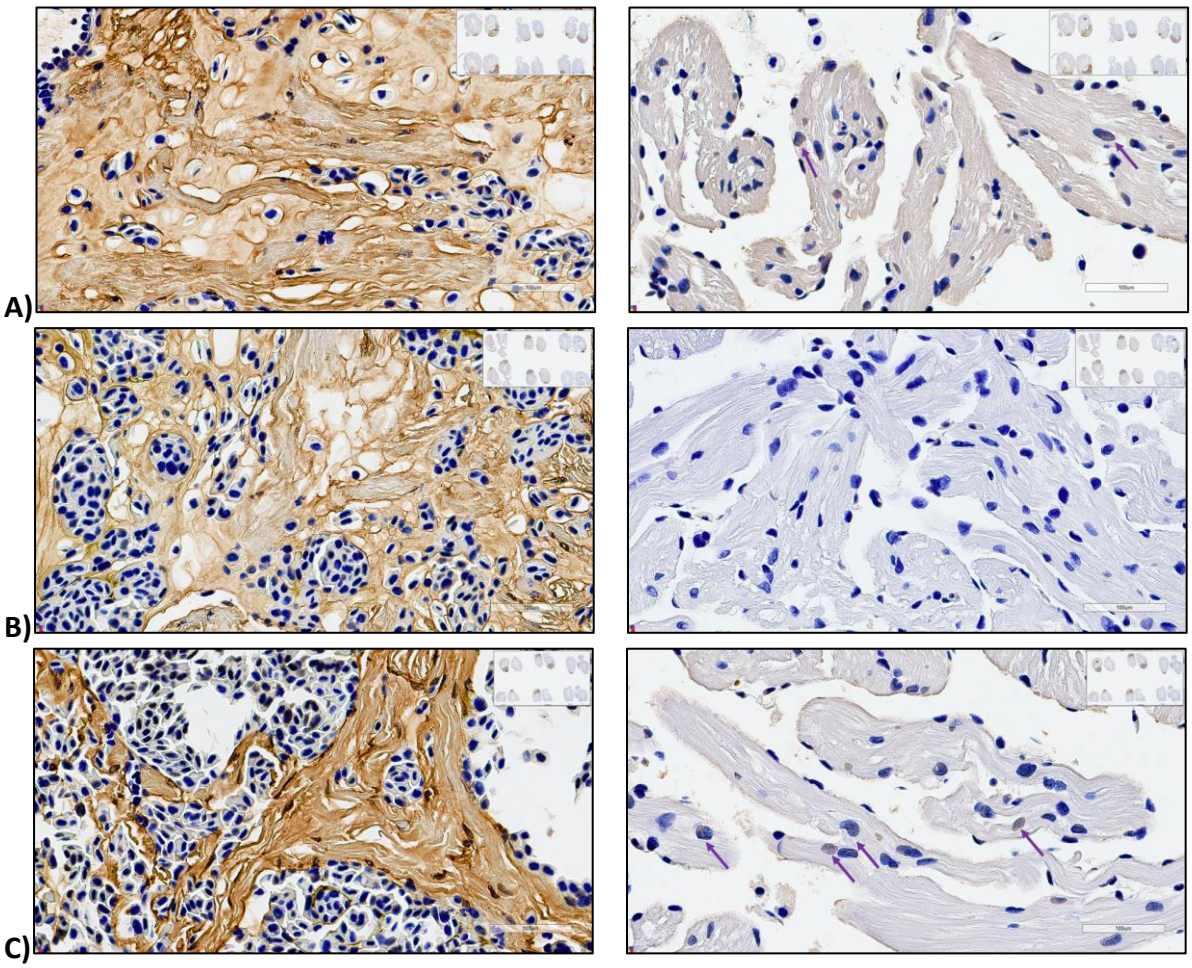

Figure 43: TUNEL Immunohistochemistry of Control and Treatment Groups 12 Hours After Injury

All views are at 20X zoom with the left-hand views are from a field in the ischemic region while the right-hand views are from a field in the remote region. **A)** Control animal. **B)** Animal treated with medium-dose butorphanol. **C)** Animal treated with high-dose butorphanol. Histology features: TUNEL-positive nuclei (*red arrows*) and slight-positive/lightly-dusted TUNEL-positive nuclei (*purple arrows*). Not all views contain an instance of each histologic feature, each histologic feature not annotated. Scale bar included.

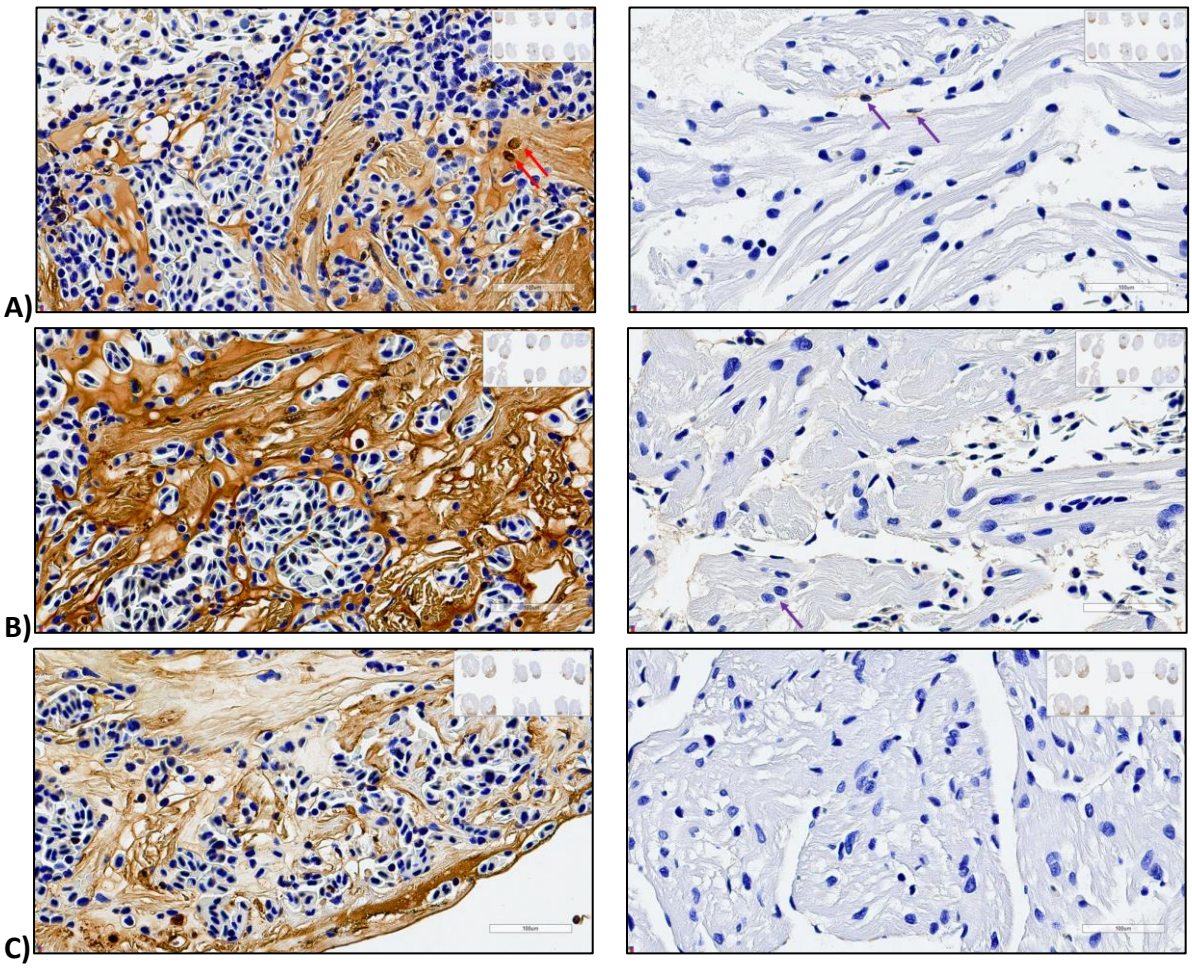

Figure 44: TUNEL Immunohistochemistry of Control and Treatment Groups 2 Days After Injury

All views are at 20X zoom with the left-hand views are from a field in the ischemic region while the right-hand views are from a field in the remote region. **A)** Control animal. **B)** Animal treated with medium-dose butorphanol. **C)** Animal treated with high-dose butorphanol. Histology features: TUNEL-positive nuclei (*red arrows*) and slight-positive/lightly-dusted TUNEL-positive nuclei (*purple arrows*). Not all views contain an instance of each histologic feature, each histologic feature not annotated. Scale bar included.

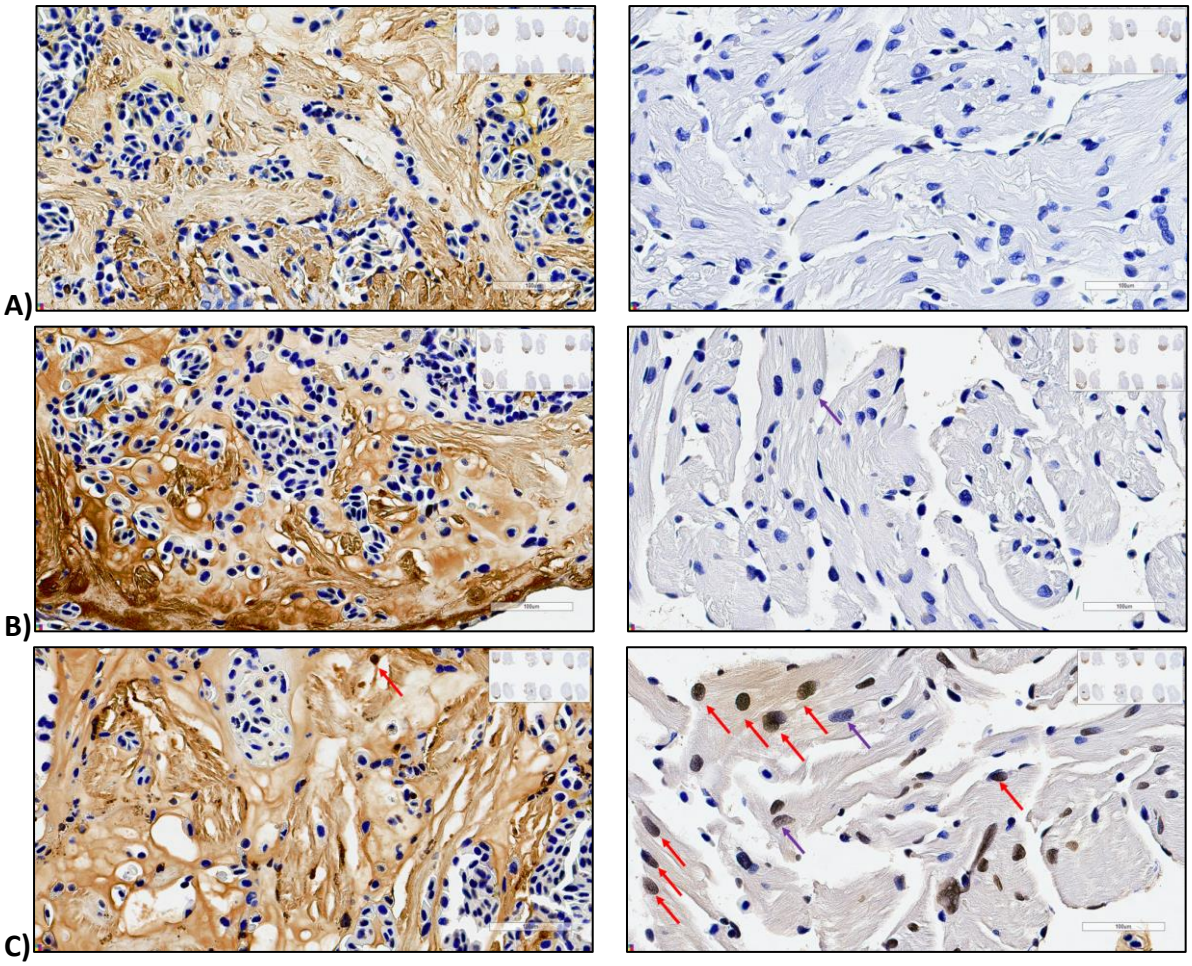

Figure 45: TUNEL Immunohistochemistry of Control and Treatment Groups 7 Days After Injury

All views are at 20X zoom with the left-hand views are from a field in the ischemic region while the right-hand views are from a field in the remote region. **A)** Control animal. **B)** Animal treated with medium-dose butorphanol. **C)** Animal treated with high-dose butorphanol. Histology features: TUNEL-positive nuclei (*red arrows*) and slight-positive/lightly-dusted TUNEL-positive nuclei (*purple arrows*). Not all views contain an instance of each histologic feature, each histologic feature not annotated. Scale bar included.

For cardiac muscle myosin, initial optimizations were performed with a commercially-available antibody (Abcam AB185967). Although amphibian or axolotl reactivity is not listed on the manufacturer's website, a simple analysis using basic local alignment search tool (BLAST) on the www.ambystoma.org website suggest sequence overlap of MYH7 (myosin heavy chain, cardiac muscle beta isoform) between mouse and axolotl genes. However, results for Abcam

AB185967 showed only light positive dusting of RBC nuclei at 1:100 and 1:200 dilution ratios and not features of myosin chains in the intracellular environment of cardiomyocytes. Another commercially-available antibody (Abcam AB50967) was used, showing light background staining in the injured areas, but most light positive dusting is again in the nuclei of RBCs and some cardiomyocytes – expected staining of myosin features in the intracellular environment of cardiomyocytes is not present.

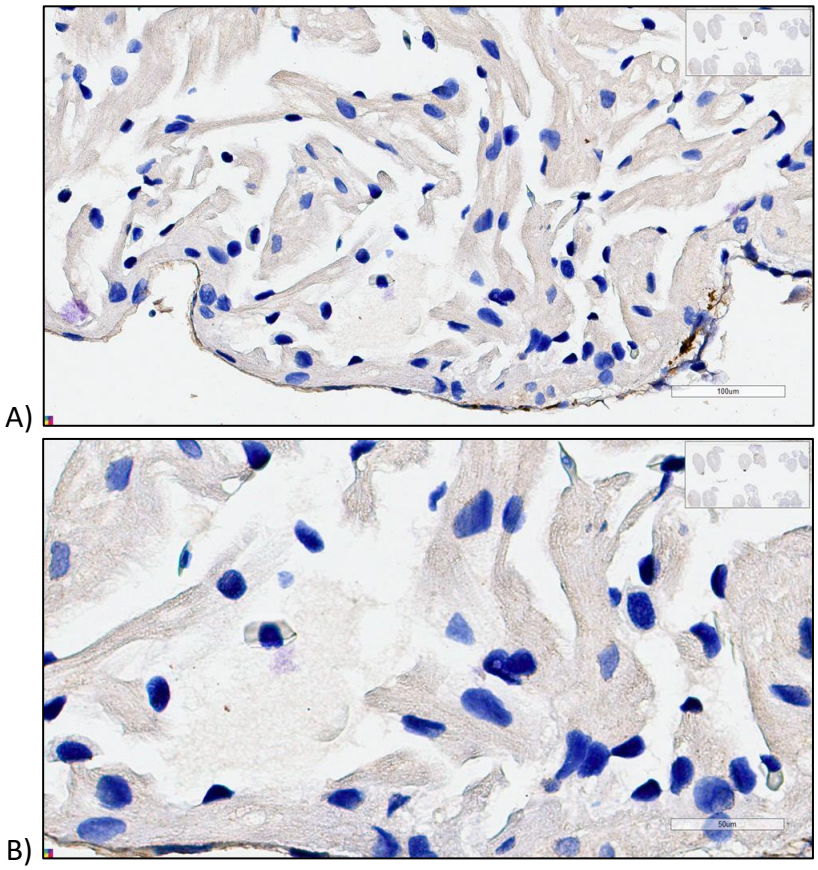

Figure 46: Cardiac Muscle Myosin Immunohistochemistry of Naïve Axolotl Heart
Views of naïve axolotl heart at **A)** 20X zoom and **B)** 40X zoom. Scale bar included.

Negative control results for cardiac muscle myosin staining using a naïve axolotl heart are shown in Figure 46. Representative results from cardiac muscle myosin (Abcam AB50967) immunohistochemistry stains are shown in for animals sacrificed twelve hours, two days, and seven days after ischemia-reperfusion injury respectively. Cardiac muscle myosin is negative

compared to control with dusting in the cytoplasm of a few cardiomyocytes, endothelium, and RBCs while other cardiomyocytes show strong intracellular staining while the area of ischemia has edge artifacts. There is no specificity or consistency to cell type or cellular feature. The expectation of cytoplasmic staining of intact myofibrils is not present – the tested antibodies do not cross-react with axolotl cardiac muscle myosin. Further quantitative assessments are not performed.

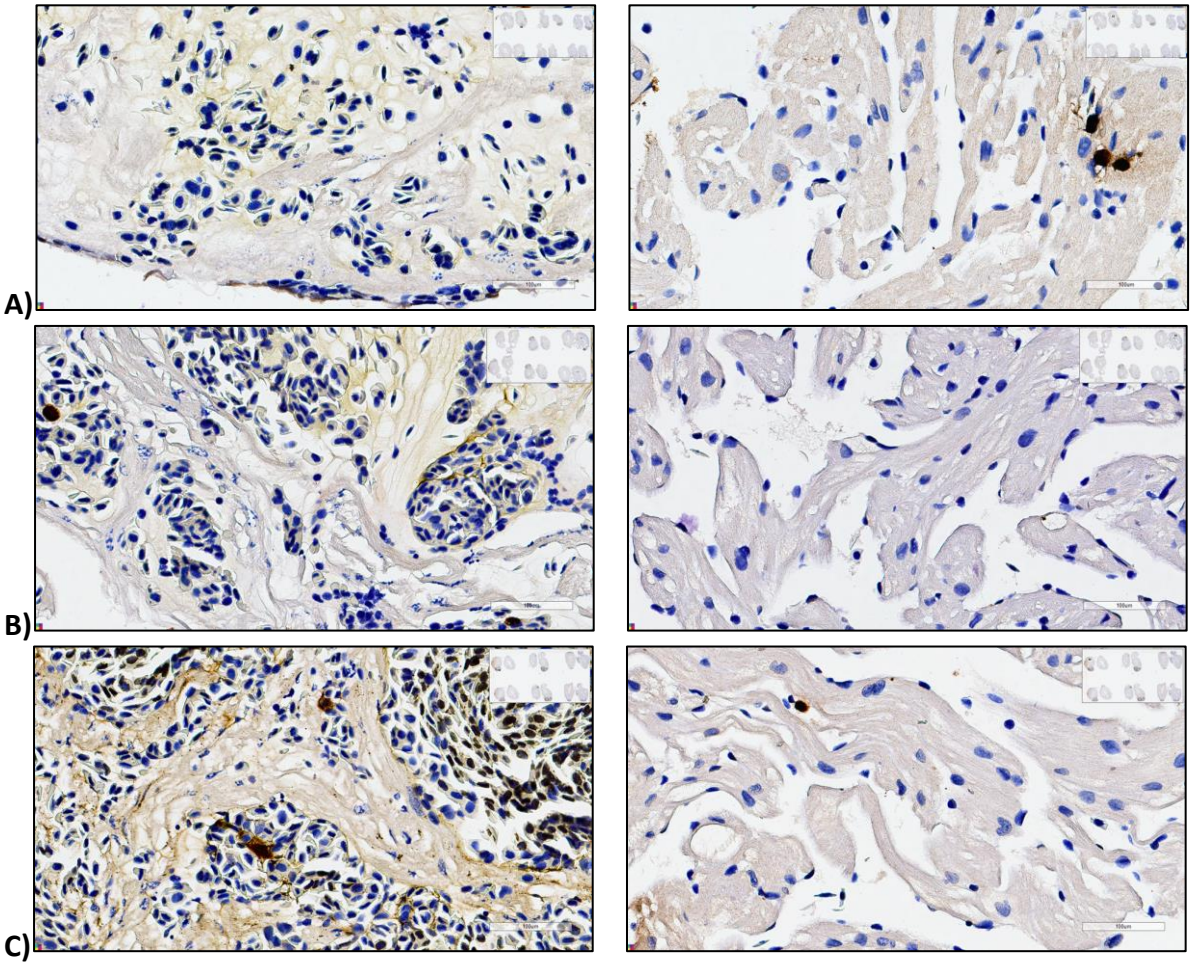

Figure 47: Cardiac Muscle Myosin Immunohistochemistry of Control and Treatment Groups 12 Hours After Injury

All views are at 20X zoom with the left-hand views are from a field in the ischemic region while the right-hand views are from a field in the remote region. **A)** Control animal. **B)** Animal treated with medium-dose butorphanol. **C)** Animal treated with high-dose butorphanol. Not all views contain an instance of each histologic feature, each histologic feature not annotated. Scale bar included.

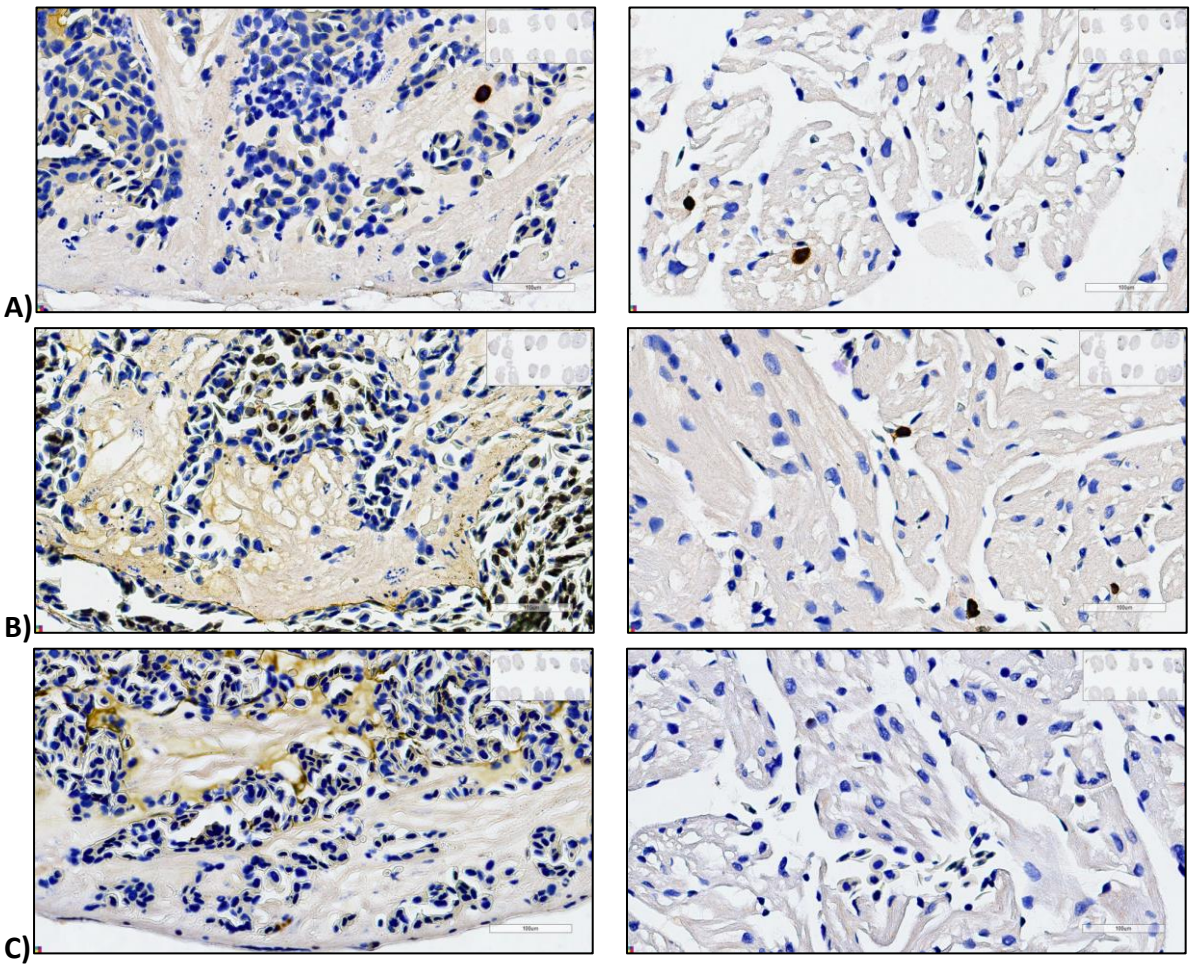

Figure 48: Cardiac Muscle Myosin Immunohistochemistry of Control and Treatment Groups 2 Days After Injury

All views are at 20X zoom with the left-hand views are from a field in the ischemic region while the right-hand views are from a field in the remote region. **A)** Control animal. **B)** Animal treated with medium-dose butorphanol. **C)** Animal treated with high-dose butorphanol. Not all views contain an instance of each histologic feature, each histologic feature not annotated. Scale bar included.

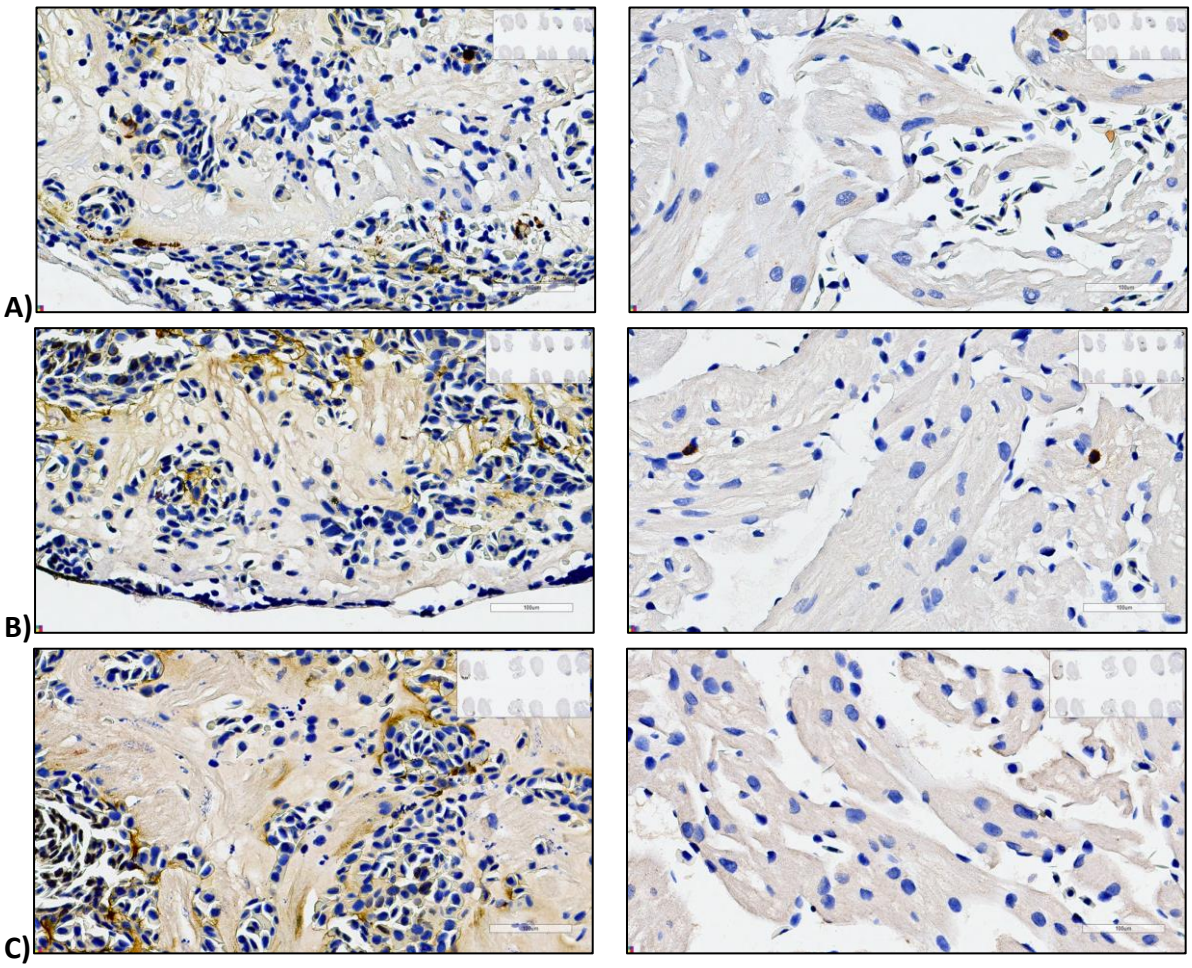

Figure 49: Cardiac Muscle Myosin Immunohistochemistry of Control and Treatment Groups 7 Days After Injury

All views are at 20X zoom with the left-hand views are from a field in the ischemic region while the right-hand views are from a field in the remote region. **A)** Control animal. **B)** Animal treated with medium-dose butorphanol. **C)** Animal treated with high-dose butorphanol. Not all views contain an instance of each histologic feature, each histologic feature not annotated. Scale bar included.

For non-muscle myosin IIB, initial optimizations were performed with a commercially-available antibody (Abcam AB684). Although amphibian or axolotl reactivity is not listed on the manufacturer's website, a simple analysis using basic local alignment search tool (BLAST) on the www.ambystoma.org website suggest sequence overlap of MYH10 (non-muscle myosin II heavy chain-B) between mouse and axolotl genes. After a test run of dilutions from 1:200 to 1:8000, results of 1:5000 showed the best results.

A)

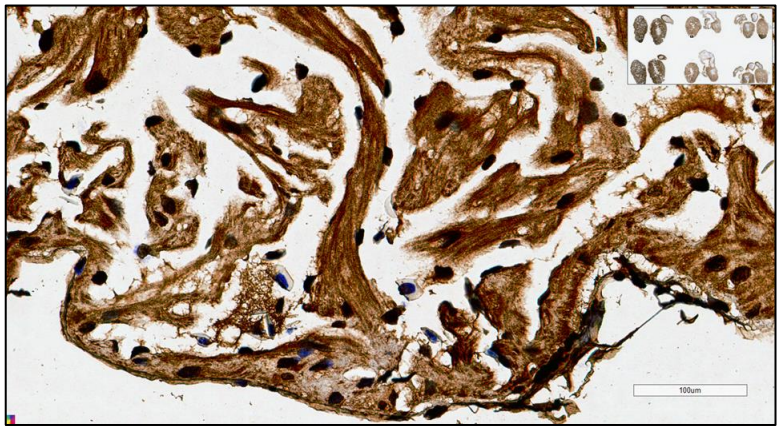

B)

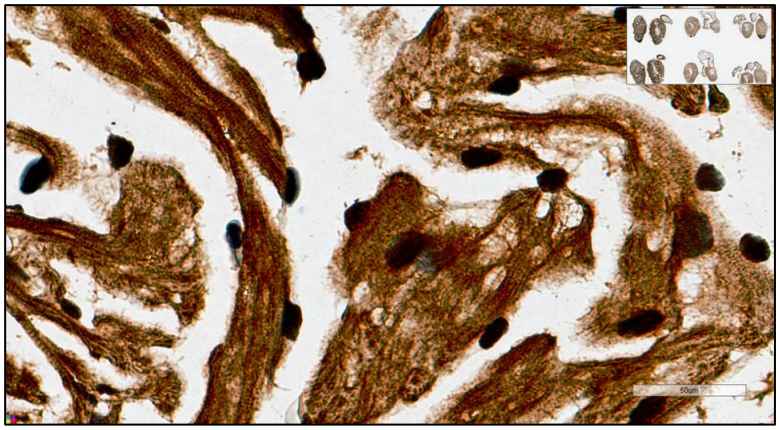

Figure 50: Non-Muscle Myosin Immunohistochemistry of Naïve Axolotl Heart
Views of naïve axolotl heart at **A)** 20X zoom and **B)** 40X zoom. Scale bar included.

Negative control results for non-muscle myosin staining using a naïve axolotl heart are shown in Figure 50. Representative results from non-muscle myosin IIB (Abcam AB684) immunohistochemistry stains are shown in for animals sacrificed twelve hours, two days, and seven days after ischemia-reperfusion injury respectively. Proteinaceous exudate is positive. Very weak (possibly background) to strongly positive staining of ischemic region, with no pattern evident to treatment type. There is no specificity or consistency to cell type or cellular feature. The expectation of cytoplasmic staining of nascent myofibrils is not present – the antibody tested reacts with multiple axolotl proteins. Further quantitative assessments are not performed.

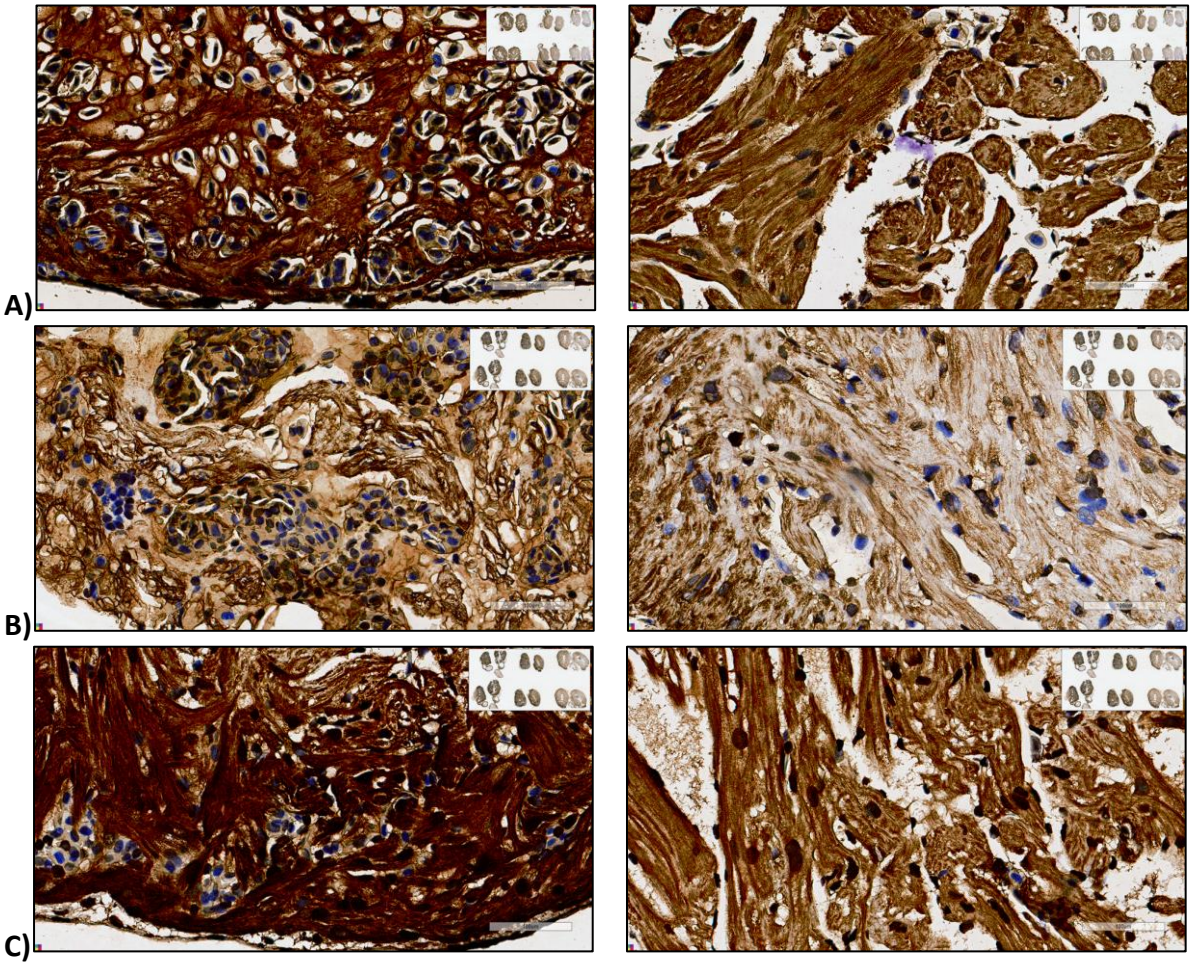

Figure 51: Non-Muscle Myosin Immunohistochemistry of Control and Treatment Groups 12 Hours After Injury

All views are at 20X zoom with the left-hand views are from a field in the ischemic region while the right-hand views are from a field in the remote region. **A)** Control animal. **B)** Animal treated with medium-dose butorphanol. **C)** Animal treated with high-dose butorphanol. Not all views contain an instance of each histologic feature, each histologic feature not annotated. Scale bar included.

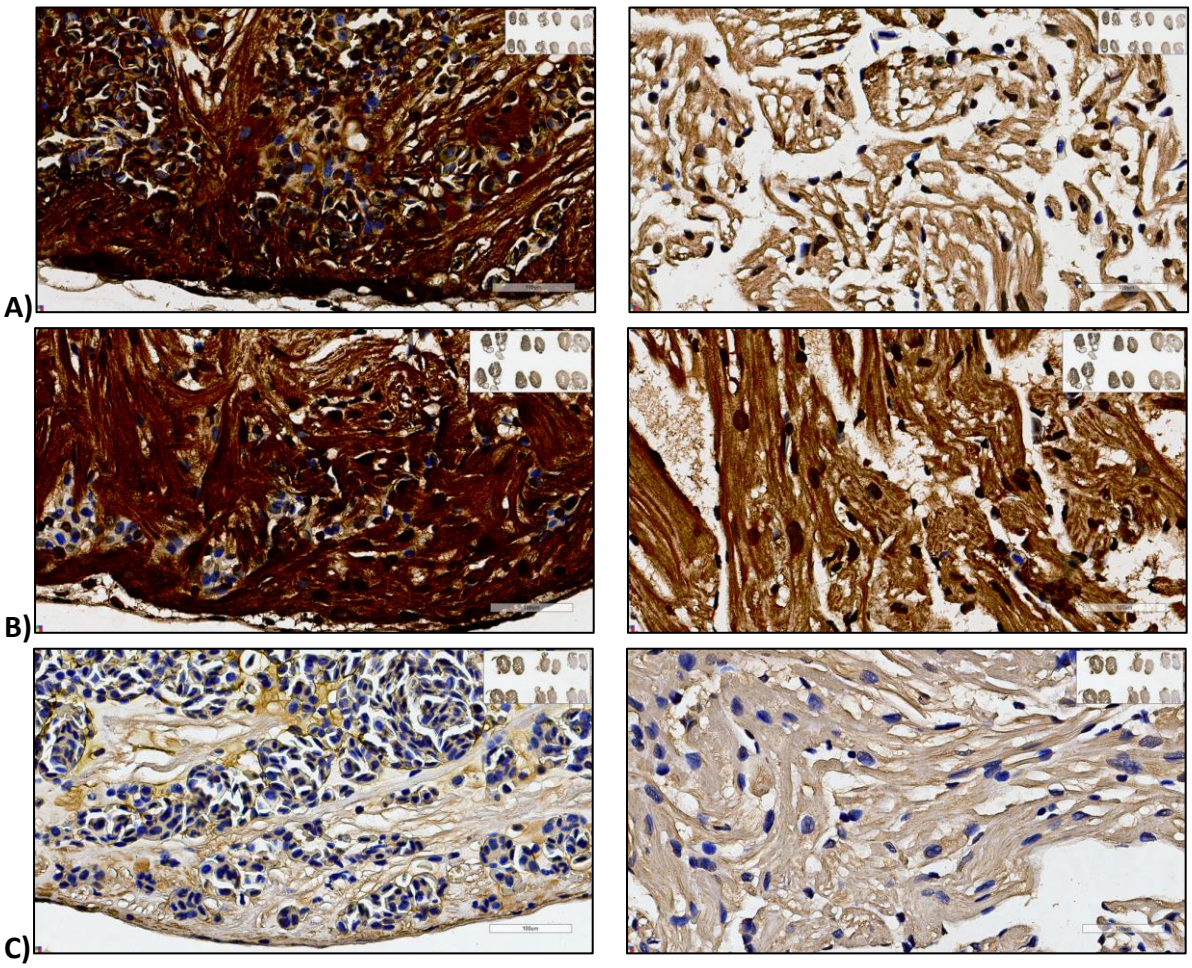

Figure 52: Non-Muscle Myosin Immunohistochemistry of Control and Treatment Groups 2 Days After Injury

All views are at 20X zoom with the left-hand views are from a field in the ischemic region while the right-hand views are from a field in the remote region. **A)** Control animal. **B)** Animal treated with medium-dose butorphanol. **C)** Animal treated with high-dose butorphanol. Not all views contain an instance of each histologic feature, each histologic feature not annotated. Scale bar included.

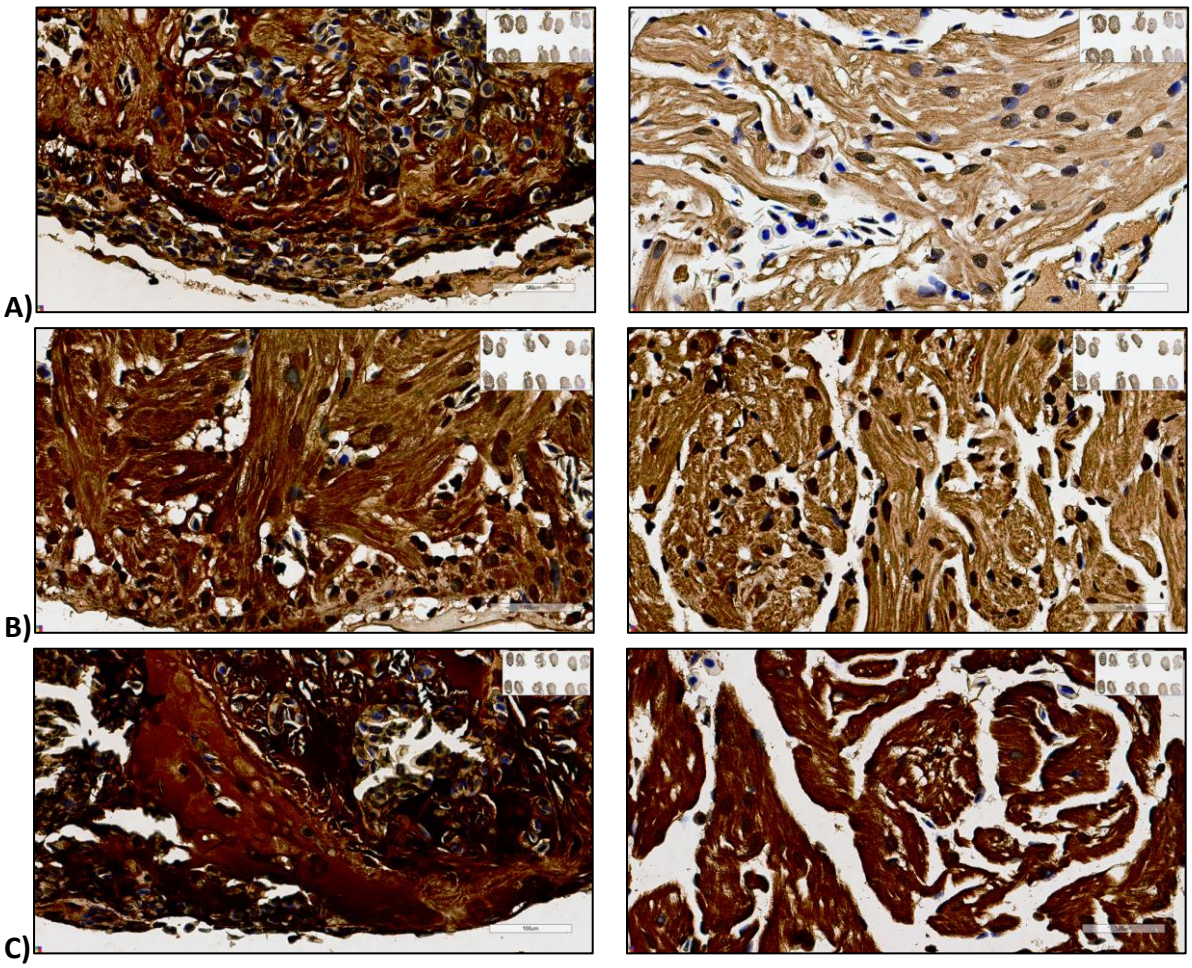

Figure 53: Non-Muscle Myosin Immunohistochemistry of Control and Treatment Groups 7 Days After Injury

All views are at 20X zoom with the left-hand views are from a field in the ischemic region while the right-hand views are from a field in the remote region. **A)** Control animal. **B)** Animal treated with medium-dose butorphanol. **C)** Animal treated with high-dose butorphanol. Not all views contain an instance of each histologic feature, each histologic feature not annotated. Scale bar included.

Quantitative Assessments of Pathology

Hyaline Change

Closer review of H&E stains shows a proteinaceous exudate (see blue asterisk in Figure 17) present in all injured hearts, which we have termed hyaline change. Using image analysis software Fiji (Schindelin et al., 2012) [a distribution of ImageJ (Schindelin et al., 2015; Schneider et al., 2012)] the amount of exudate in each sample was quantified using the Color Threshold

function (Image → Adjust → Color Threshold). Thresholding, also known as segmentation, separates pixels which fall into a designated range of values, based on the color space in use, from those pixels that do not satisfy the desired values. To process the H&E stains, the HSB (Hue, Saturation, and Brightness) color space was used with the "Default" thresholding algorithm. The thresholding values shown in Figure 54A were used to highlight areas containing the proteinaceous exudate. To systematically process the images, a sample map was created identifying ten fields within each area to sample. The sampling map is found in Figure 54B.

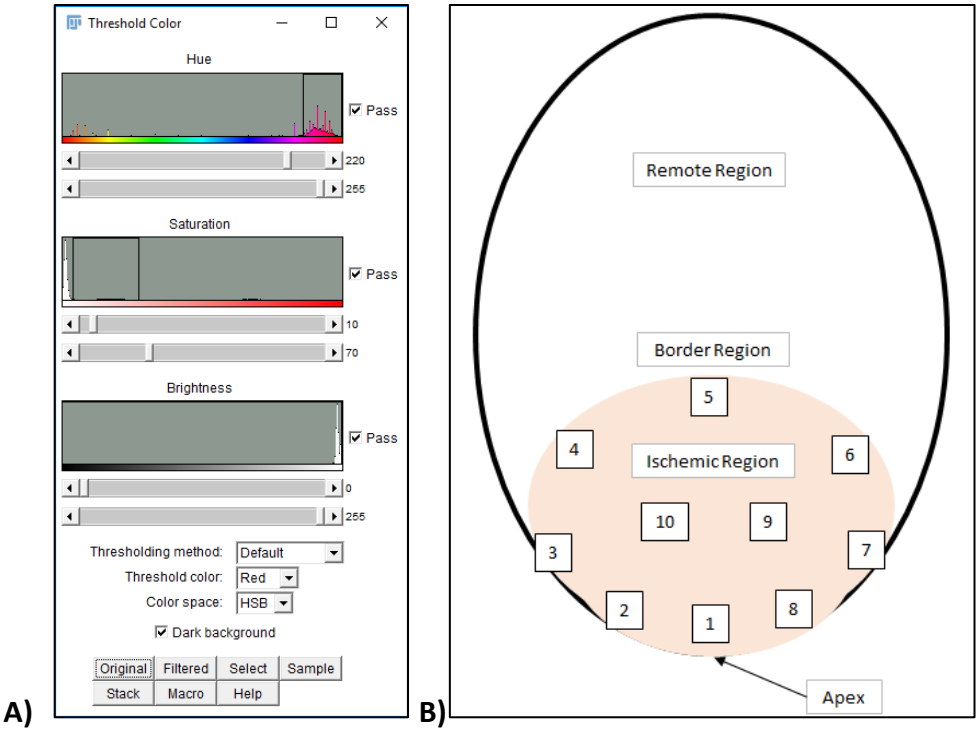

Figure 54: Image Analysis Settings & Sampling Map
A) The values shown in this dialog box were used to segment loaded image files in Fiji into areas correspond to the light-pink proteinaceous exudate present in H&E histology stains. **B)** The sampling map to process histologic sections for proteinaceous exudate/edema.

Examples of the thresholding algorithm highlighting the areas of proteinaceous exudate are shown in Figure 55. Once the areas are selected, the measure function in Fiji (Analyze → Measure) determines the number of pixels that were selected. The percent area covered by the

proteinaceous exudate is determined by dividing this measured area by the total number of pixels in each image (Image Resolution: 1913 x 1171 – See status bar of Fiji window in Figure 55).

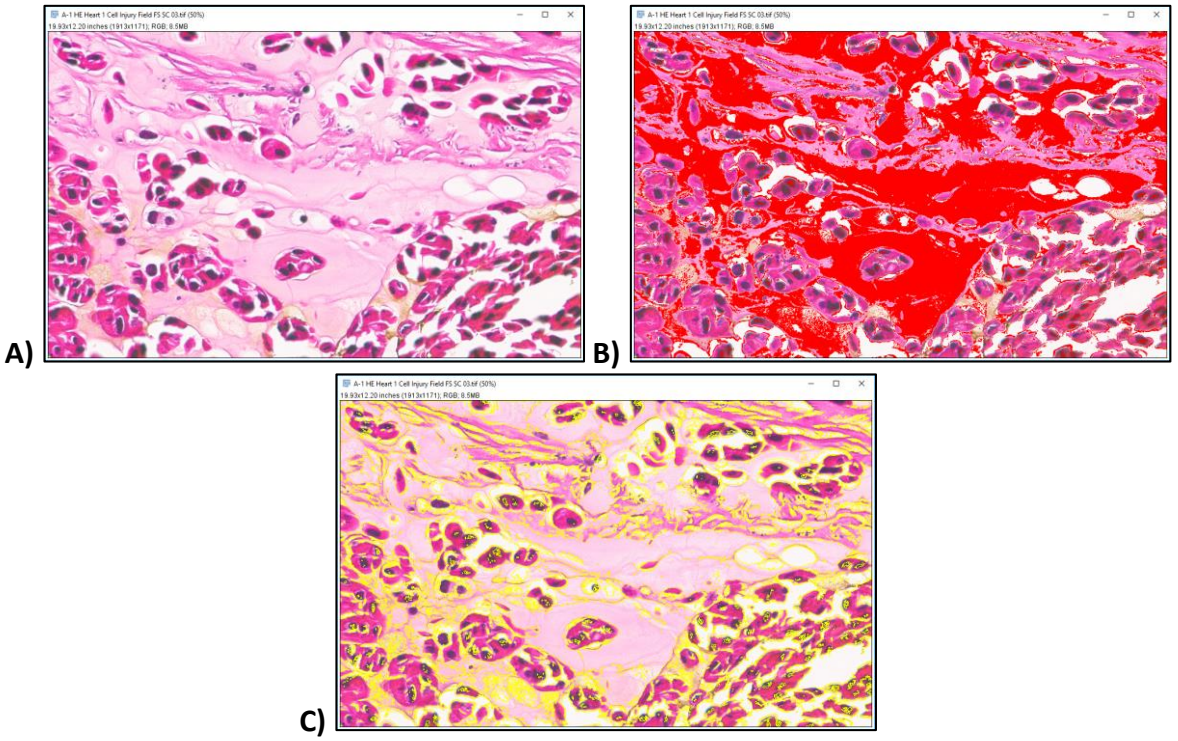

Figure 55: Examples of Histology Image Thresholding Using Fiji
A) Raw H&E image. **B)** H&E image after color thresholding using HSB values in text. **C)** Area selection ("Select" button in Threshold Color dialog box) for Measure function (Analyze → Measure) in Fiji.

For each heart sample, the amount of proteinaceous exudate coverage in the field of view was calculated for the ten sampling fields. In SPSS, each treatment group, consisting of three to four animals (n = 3 – 4) were compared to each other based on time of euthanasia: 12-hours, 48-hours, and 7-days post ischemia-reperfusion injury. Using univariate one-way ANOVA, the following are the between group p-values:

Table 6: Significance of ANOVA Testing for Proteinaceous Exudate Pathology

Group	12-hour Samples	48-hour Samples	7-day Samples
F Statistic	F(2,8) = 6.280	F(2,7) = 0.816	F(2,5) = 0.984
Significance	p = 0.023	p = 0.480	p = 0.984

Since the 12-hour samples means are statistically significant from each other, post-hoc multiple comparisons were performed and corrected using Tukey's Honest Significant Difference (HSD) test. The data show that the only significant difference is between the medium-dose and high-dose animals ($p = 0.020$). Since the test statistic that is of interest is the difference between control and treatment groups, it is concluded that there is no difference in proteinaceous content between control and treatment groups across all euthanasia time points. From this conclusion, all samples were collapsed across time to see if there is a difference between all control animals and all animals treated with medium-dose butorphanol and all animals treated with high-dose butorphanol.

After grouping all animals under the same treatment group (control: $n = 9$; medium dose: $n = 9$; high dose: $n = 11$), SPSS was again used to run a univariate one-way ANOVA. There was a statistically significant difference between the amount of exudate across all three groups, $F(2,26) = 3.430$, $p = 0.048$. Since the omnibus test suggests a statistical difference between the groups, post-hoc multiple comparisons were performed and corrected using Tukey's Honest Significant Difference (HSD) test. The data show that the only significant difference is between the medium-dose and high-dose animals ($p = 0.038$). Since the test statistic that is of interest is the difference between control and each of the treatment groups, it is concluded that there is no difference in proteinaceous content between control and treatment groups. A graph of the mean exudate area with error bars denoting the standard error the mean across all animals in the group is found in Figure 56.

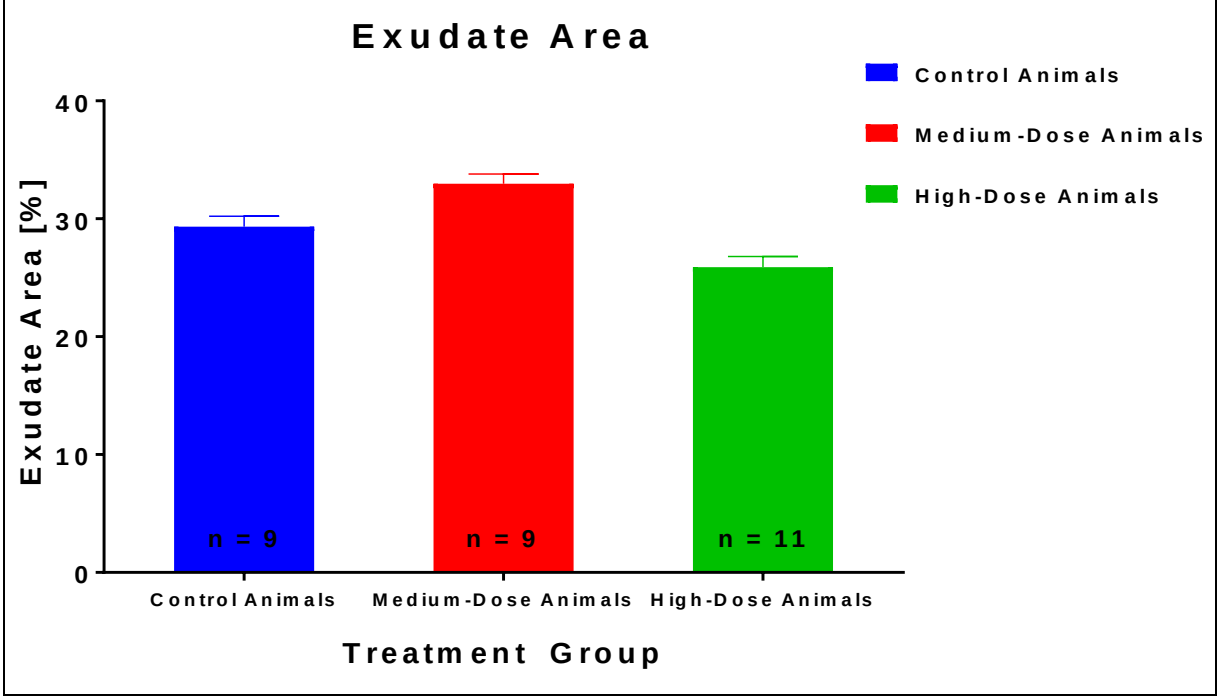

Figure 56: Coverage of Proteinaceous Exudate Area in H&E Histology Samples
The percentage of the field of view covered by the proteinaceous exudate. The error bars denote the standard error of the mean across all animals in the group.

Immunohistochemistry

Ordinal scoring rubrics for other clinically relevant pathology were developed and statistics evaluated by Kruskal-Wallis one-way ANOVA for unrelated samples and two-sample Kolmogorov-Smirnov testing for post-hoc analysis comparing treatment to control. In these non-parametric tests, low-ranked scores translate to histology features closer to features denoted by a score of zero (see Table 7). TUNEL testing is significant ($p < 0.001$) for more DNA breaks with high-dose butorphanol at twelve hours after injury compared to control. BrdU testing is significant ($p < 0.001$) for less cellular turnover with mid-dose butorphanol, but greater cellular turnover with high-dose butorphanol at forty-eight hours after injury compared to control.

Table 7: Histology Scoring Rubric in Experiment 4

Test	Score (Based on High-Power Field [40X])	
	Lowest	**Highest**
TUNEL	0: None	5: > 80% of strong nuclear staining in CM cells in 5+ fields.
BrdU	0: None	3: Few to moderate (multifocal) positive CMs ± endothelial cells, usually not in area damaged.
Heterophils	0: None	5: Diffuse infiltration of large numbers of heterophiles.
Lymphocytes	0: None	3: Numerous lymphocytic infiltrates.

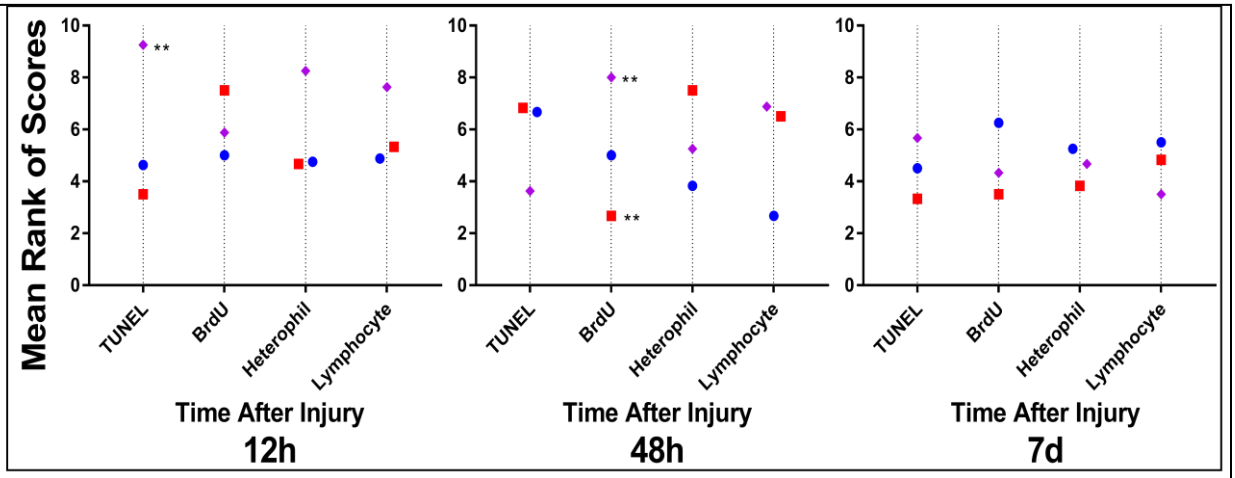

Figure 57: Results of Pathology Evaluations in GLAS Experiment 4
Pathology scoring results for four different pathologic features versus treatment and time.
Significance: * $p < 0.020$, ** $p < 0.001$.
Legend: ● Control; Butorphanol (■ Mid) and (◆ High)

Conclusion: Drugs and doses used did not demonstrate a consistent dose or time dependent effect on tissue pathology.

Study deviations: *None.*

Unanticipated findings: Cardiac muscle myosin and non-muscle myosin IIB IHC did not provide conclusive results.

Troubleshooting: Antibody optimization was performed at contracted third-party.

Future directions: Additional time points (chronic studies) should be used to determine long-term impact of significant findings associated with changes to tissue pathology. Also, additional dosages or drugs could be tested in the future.

Specific Aim 2

Surgical Outcomes

Prior to the start of experiments in Specific Aim 2, some animals from the University of Wisconsin (UW) experienced bouts of anorexia. Ectoparasites like *Ichthyobodo necator*, *Chilodonella uncinate*, and various species from the genus *Trichodina* were found from skin scrapings on multiple animals. Animals were treated with one, eight-hour baths of formalin solution (0.025 mL per 1L of 50% Holtfreter's solution) and a follow-up eight-hour bath at a higher strength (0.050 mL per 1L of 50% Holtfreter's solution). Any animals that did not recover to baseline feeding behavior were not used in the long-term follow-up studies of Specific Aim 2 – four of the animals from UW were not allowed to enter the study, resulting in twenty-six from UW and twenty-from newly-ordered animals from the University of Kentucky (UK).

In total, fifty operations (n = 50) were performed in this set of experiments. Animals were separated based on origin (UW and UK) with one animal per follow-up group undergoing a sham procedure and used as a naïve heart sample. Although experiments were design to have eight animals per origin and time point for heart collection, some clinical events during the experiments required changes to experimental groupings and animal husbandry. Although no surgical complications occurred, eleven animals from UW showed inappetence following induction of ischemia-reperfusion injury and were removed from the study. With the genetic lineage of the UW animals unknown, a group of animals were sacrificed fifteen days after surgery

to see if a robust healing response was observed. This helped prepare surgical and harvesting schedules for the animals arriving from UK that have more traceable genetic origins. With evidence of gross tissue injury after fifteen days, no adjustments to the euthanasia schedule were required. The endpoint of ninety days was maintained given published results of the complete rescue of the partial ventricular amputation of axolotl hearts (Cano-Martinez et al., 2010). The final experimental groups are as follows:

Table 8: Final Experimental Groupings for Chronic Ischemia-Reperfusion Studies

Animal Origin	Days of Follow-Up Before Euthanasia			
	15-Days	**30-Days**	**60-Days**	**90-Days**
University of Wisconsin	7 (1 as sham)	N/A	4 (1 as sham)	4 (1 as sham
University of Kentucky	N/A	8 (1 as sham)	8 (1 as sham)	8 (1 as sham)

Qualitative Assessments of Pathology

Simple Stains

Although the acute follow-up studies (one-half-day, two-days, and seven-days follow-up following ischemia-reperfusion injury) were performed in Specific Aim 1, they are included here to create a complete timeline of axolotl cardiac tissue response from twelve hours (one-half-day) to ninety-days following ischemia-reperfusion injury. Results reported in Specific Aim 1 are derived from animals all sourced from the University of Kentucky.

One-Half Day (Twelve Hours) Status-Post Ischemia Reperfusion Injury

Representative results of Mayer's hematoxylin/eosin (H&E) stains staining in the ischemic region of damaged hearts are shown in Figure 22 animals sacrificed twelve hours (one-half day) after ischemia-reperfusion injury. There is evidence of massive hemorrhage up to the very border of the heart wall (paralleling the appearance of the gross heart picture in Figure 15) and into

tissue spaces that are separate from spaces defined by cardiac sinuses and free areas between trabeculated myocardium that allow for RBC perfusion. Although some fibers are still organized like normal myocardium, they exhibit evidence of intracellular derangements. Evidence of progressive muscle fiber damage include wavy fibers (elongated and narrow) that are common in acute ischemia-reperfusion injuries (Robbins et al., 2010) to myocardium thinning and dissolution with these fibers lacking basophilic contents (no nucleic material remains) representing coagulative necrosis. There is wide coverage of hyaline change (light pink) that does not represent non-specific binding to the glass slide as there are areas within the ischemic zone that are free of the pink hyaline change. Finally, in addition to the dissolution of nuclear material denoting necrosis, pyknosis, karyorrhexis, and karyolysis of some cellular nuclei is evidence of apoptosis.

Results of Masson's trichrome stains of a naïve axolotl heart are shown in Figure 25. Representative results from Masson's trichrome staining in the ischemic region of damaged hearts are shown in Figure 26 for animals sacrificed twelve hours (one-half day) after ischemia-reperfusion injury. Comparing the naïve heart to the damaged heart show clear differentiation between damaged myocardium (deep purple) in region of ischemia-reperfusion injury versus healthy myocardium in remote/undamaged region (deep burgundy). Myocardium thinning and dissolution reflects the same results as H&E stains. In contrast to the organized, deep-blue staining of intact collagen at the heart-border wall in Figure 25, the damaged hearts exhibit hyaline change that stains like connective tissue but at a lower intensity (pale blue). Areas of light purple reflect the possibility of deep burgundy-staining myofibers with the pale blue hyaline change in the background.

Representative results from AFOG stains are shown in Figure 35 for animals sacrificed twelve hours (one-half day) after ischemia-reperfusion injury respectively. Although the samples have been overstained, the lack of bright-red staining communicates that fibrin is not present, but the glassy, pale-blue staining in-between myocardium support the notion that basement membrane proteins predominantly make up the hyaline change found in H&E staining. The wide-spread pale-blue staining is clearly absent in naïve hearts, shown in Figure 34. Supporting evidence of myocardium thinning and dissolution confirms what is seen in H&E and Masson's Trichrome stains.

Two Days Status-Post Ischemia-Reperfusion Injury

Representative results of H&E staining in the ischemic region of damaged hearts are shown in Figure 23 for animals sacrificed two days after ischemia-reperfusion injury. There is evidence of the ongoing presence of massive hemorrhage into the myocardial tissue space and up to the border of the heart wall (paralleling the appearance of the gross heart picture in Figure 58). Further myocardial-fiber thinning and dissolution continues with many fibers beginning to

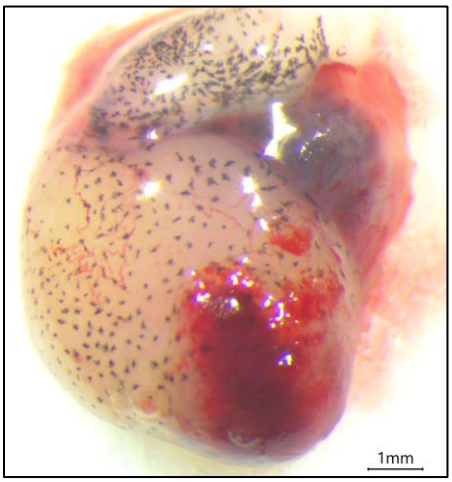

Figure 58: Heart from an Axolotl 2 Days Post Injury
Gross view of an axolotl heart 2 days post mechanical induction of ischemia-reperfusion injury. Hemorrhaging at the site of clamp application is evident after heart is rinsed with heparin lock solution and amphibian saline.

stain entirely light pink throughout, suggesting complete destruction of nucleic material. For myocardial fibers that are still partially intact, they are loosely organization with evidence of intracellular derangements and destruction of nuclear material, portending their commitment to cellular death pathways.

Representative results from Masson's trichrome staining in the ischemic region of damaged hearts are shown in Figure 27 for animals sacrificed two days after ischemia-reperfusion injury respectively. Damaged myocardium in ischemia-reperfusion injury continue to stain deep purple compared to the deep burgundy color of normal myofibers (see Figure 25). The damaged hearts continue to exhibit hyaline change that stains like connective tissue but at a lower intensity (pale blue).

Representative results from AFOG stains are shown in Figure 36 for animals sacrificed two days after ischemia-reperfusion injury. Although the samples have been overstained, the lack of bright red staining continues to support the evidence that fibrin is not present, but rather basement membrane proteins denoted by pale-blue staining predominantly make up the hyaline change. Supporting evidence of myocardium thinning and dissolution continues to confirm what is seen in H&E and Masson's Trichrome stains.

Seven Days Status-Post Ischemia-Reperfusion Injury

Representative results of H&E staining in the ischemic region of damaged hearts are shown in Figure 24 for animals sacrificed seven days after ischemia-reperfusion injury. The damage at seven days post ischemia-reperfusion injury parallels the histopathology two days following ischemia-reperfusion injury. There is continued evidence of ongoing hemorrhage into the myocardial tissue space and up to the border of the heart wall (paralleling the appearance of

the gross heart picture in Figure 16). Myocardial-fiber thinning and dissolution continues with many fibers continuing to stain entirely light pink throughout, suggesting complete destruction of nucleic material. For myocardial fibers that are still partially intact, they are loosely organization with evidence of intracellular derangements, destruction of nuclear material, or evidence of pyknosis, karyorrhexis, and karyolysis, portending their commitment to cellular death pathways.

Representative results from Masson's trichrome staining in the ischemic region of damaged hearts are shown in Figure 28 for animals sacrificed seven days after ischemia-reperfusion injury respectively. The damage at seven days post ischemia-reperfusion injury parallels the histopathology two days following ischemia-reperfusion injury. Damaged myocardium in ischemia-reperfusion injury continue to stain deep purple compared to the deep burgundy color of normal myofibers (see Figure 25). Interestingly, the myocardium fibers have mostly degraded in the high-dose animals (see Figure 28C). Without the burgundy color mixing, the damaged hearts exhibit hyaline change that stains like connective tissue but at a lower intensity (pale blue).

Representative results from AFOG stains are shown in Figure 37 for animals sacrificed seven days after ischemia-reperfusion injury respectively. The damage at seven days post ischemia-reperfusion injury parallels the histopathology two days following ischemia-reperfusion injury. Although the samples have been overstained, the continued lack of bright red staining continues to support the evidence that fibrin does not play a role in acute tissue regeneration in the axolotl, unlike the process that occurs in the zebrafish. In that animal model, fibrin is preset four to seven days following injury in the zebrafish (Chablais et al., 2011). In axolotls, instead of

fibrin, basement membrane proteins denoted by pale-blue staining predominantly make up the proteins that are present in the healing heart tissue. Supporting evidence of ongoing myocardium thinning and dissolution continues to confirm what is seen in H&E and Masson's Trichrome stains one-half and two days after ischemia-reperfusion injury.

Fifteen Days Status-Post Ischemia-Reperfusion Injury

Animals sacrificed fifteen days after ischemia reperfusion injury all originated from the University of Wisconsin (UW). All animals analyzed at fifteen days after ischemia-reperfusion injury are young-to-normal adults (about three years of age at euthanasia). Since the genetic lineage of these animals is not traceable to a known origin, these results are observational and reported for completeness since they are results from older animals and animals that are genetically heterogenous compared to the animal colony kept by the University of Kentucky (UK) Ambystoma Genetic Stock Center (AGSC). The AGSC raise axolotls for research purposes with funding from the Office of the Director at the National Institutes of Health (P40-OD019794).

Representative results of H&E staining in the ischemic region of damaged hearts are shown in Figure 60B for animals sacrificed fifteen days after ischemia-reperfusion injury. Although hemorrhage is evident in the gross picture of the heart (see Figure 60A) and is supported by large agglomerations of RBCs in the interior of the ischemic region, the hemorrhage no longer saturates areas near the heart border wall (see the 20X view in Figure 60B). Additionally, infiltration of white blood cells (see Figure 59: Blood Cells of Amphibians) has become more apparent by fifteen days after ischemia-reperfusion injury as seen in by the azurophils and basophils in the lower left corner and a neutrophil below the slide thumbnail in the upper right corner of the 40X H&E view (see Figure 60B). Furthermore, there is now a growing

thickness to the injured wall composed of connective tissue and disorganized myofibers (compare border wall of H&E stains to border wall of Masson's trichrome and AFOG stains in Figure 60). This thickening border is mostly acellular, with scatterings of infiltrating WBCs, possible myofibroblasts, and evidence of new myocardial cells indicated by elongated, oblong-shaped nuclei that stain light-blue.

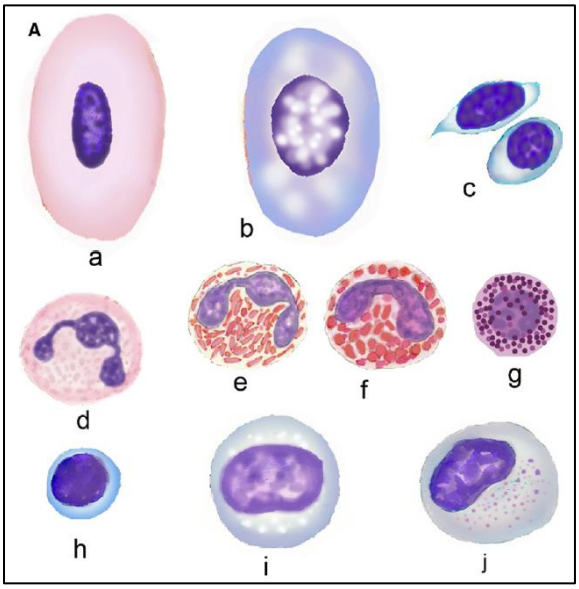

Figure 59: Blood Cells of Amphibians
A) Amphibian blood cells: (a.) Red blood cell (erythrocyte), (b.) polychromatic erythrocyte, (c.) thrombocytes, (d.) neutrophil, (e.) heterophil, (f.) eosinophil, (g.) basophil, (h.) small lymphocyte, (i.) monocyte, and (j.) azurophil. Reference: (Claver and Quaglia, 2009)z

Representative results of Masson's trichrome staining in the ischemic region of damaged hearts are shown in Figure 60C for animals sacrificed fifteen days after ischemia-reperfusion injury. The results of this stain confirm the presence of a nicely delineated tissue border that is not infiltrated by hemorrhaged blood. However, unlike the one-half-, two-, and seven-day samples stained with Masson's trichrome, the protein exudate stains pink instead of pale blue. The reason behind this change of protein staining is unknown. Based on Table 5, the tissues that stain red include muscle and fibrin. Per the results of AFOG staining in these animals (see below),

the pink protein is less likely to be fibrin. However, one cannot discount loose or disorganized nascent myofibrils agglomerations or secretions from myofibroblasts that may contribute to

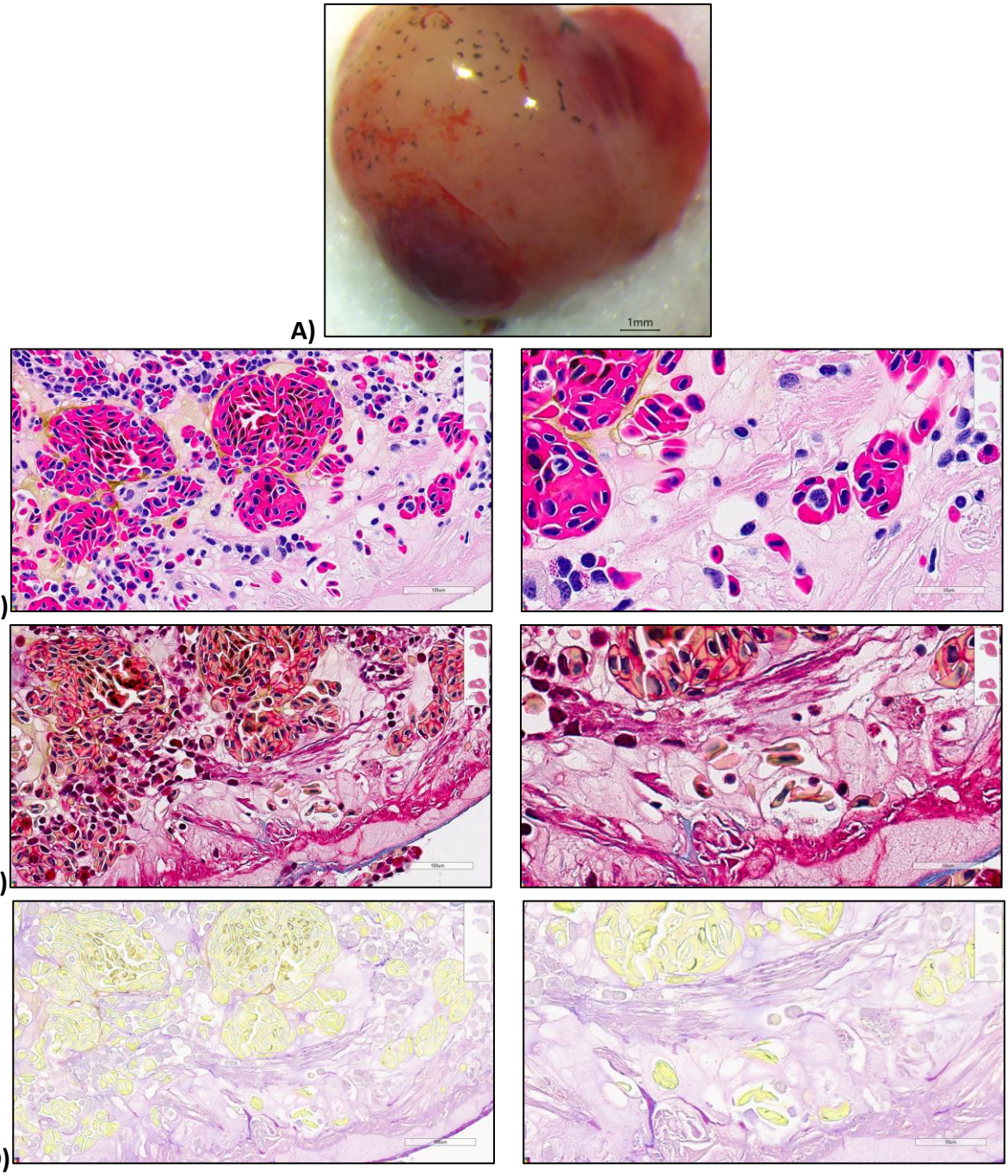

Figure 60: Representative Histologic Results of Axolotl Hearts Fifteen Days After Injury
All views on the left are at 20X zoom while views on the right are at 40X zoom. **A)** Gross view of the injured heart showing area of injury with gross hemorrhage evident. **B)** Hematoxylin and eosin stain. **C)** Masson's trichrome stain. **D)** Acid fuchsin orange G stain. Scale bar included.

these staining results.

Representative results of AFOG staining in the ischemic region of damaged hearts are shown in Figure 60D for animals sacrificed fifteen days after ischemia-reperfusion injury. The slides here show more typical AFOG staining with the RBCs appearing light yellow as expected (Mihatsch and Bremer, 1978). Myocardium in these stains appear light purple whereas healthy myocardium should appear light orange with damaged or injured myocardium appearing dark orange (Chablais et al., 2011). Basement membrane proteins under AFOG protocols should stain pale- or light-blue (Mihatsch and Bremer, 1978). When mixing primary colors, blue and orange (essentially a shade of red) can lead to a pale purple color, which may explain the pale purple staining seen here (Simonot and Hebert, 2014). Unfortunately, the pale purple staining of this region does not help identify the protein content of acellular material being deposited at the heart wall border.

Thirty Days Status-Post Ischemia-Reperfusion Injury

Animals sacrificed thirty days after ischemia reperfusion injury all originated from the UK Ambystoma Genetic Stock Center (AGSC) and are young-to-normal adults (about three years of age at euthanasia).

Representative results of H&E staining in the ischemic region of damaged hearts are shown in Figure 61B for animals sacrificed thirty days after ischemia-reperfusion injury. Large areas of hemorrhage continue to persist in areas of ischemic damage, but the amount of hemorrhaging appears to be decreasing. This may indicate a decrease in the volume of injured tissue space or a return of normal sinus architecture to allow perfusion of trabeculated myocardium. The return of normal sinus architecture is less likely since undamaged myocardium

in remote areas of the heart flush clear of RBCs. Therefore, the RBCs that remain in tissues damaged by ischemia-reperfusion injury likely are trapped in hemorrhagic spaces. The thickening border wall shows an increasing presence of various cell types, including infiltrating WBCs such as eosinophils and basophils, more nascent cardiomyocytes (cells with elongated and pale-purple nuclei), possible myofibroblasts (cells with ovoid and pale-purple nuclei), and likely endocardium (plump rod-like cells that stain deep purple). Although the tissue is beginning to show more uniform, pale eosinophilic staining, rather than the deep eosinophilic staining of damaged myofibers in the acute setting, the healing tissue is highly disorganized with haphazard layering of infiltrating cells, connective tissue and connective tissue matrix. The protein exudate contributing to hyaline change is no longer present in the same concentration as previously noted in the more acute injury setting.

Representative results of Masson's trichrome staining in the ischemic region of damaged hearts are shown in Figure 61C for animals sacrificed thirty days after ischemia-reperfusion injury. Few additional details are revealed with samples stained using this approach. There is some evidence of organized collagen in the heart border wall, but the single timepoint sample does not provide details if this is pre-existing or newly formed collagen. The disorganized tissue that is present at the apex is beginning to stain deep burgundy like undamaged myocardium in remote, healthy regions.

Representative results of AFOG staining in the ischemic region of damaged hearts are shown in Figure 61D for animals sacrificed thirty days after ischemia-reperfusion injury. Although H&E and Masson's trichrome staining show that myocardium in areas of ischemia-reperfusion injury stain more uniformly like undamaged, remote myocardium, the AFOG staining shows clear

differences between the disorganized myocardium in area of ischemia-reperfusion injury (stains light purple) compared to healthy remote myocardium (stains light orange with nice thin layer of

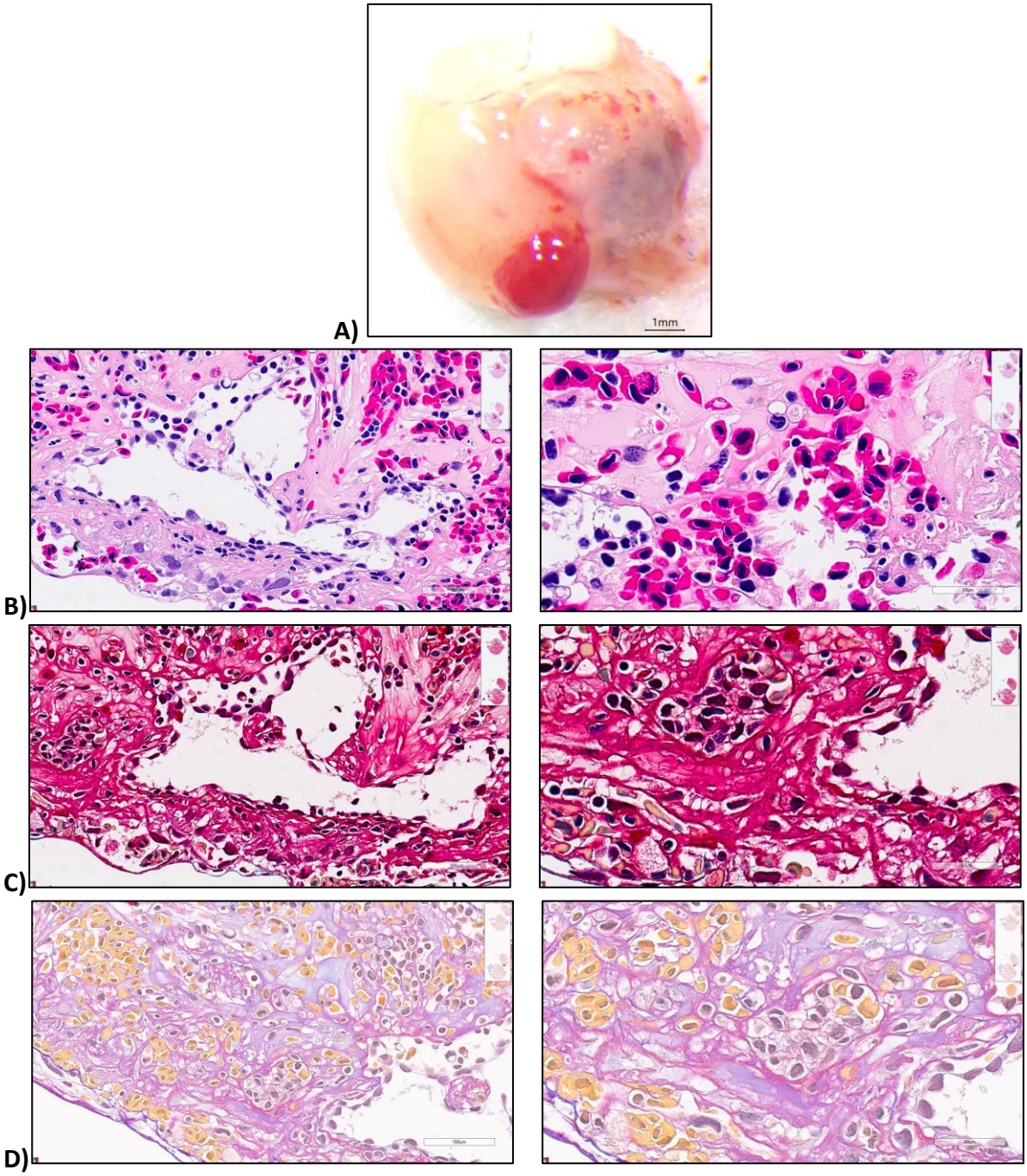

Figure 61: Representative Histologic Results of Axolotl Hearts Thirty Days After Injury
All views on the left are at 20X zoom while views on the right are at 40X zoom. **A)** Gross view of the injured heart showing area of injury with gross hemorrhage evident. **B)** Hematoxylin and eosin stain. **C)** Masson's trichrome stain. **D)** Acid fuchsin orange G stain. Scale bar included.

connective tissue surrounding fibers). Areas of proteinaceous exudate staining light blue indicating basement membrane proteins are still present in border regions between remote healthy tissue and the inured myocardium, but are beginning to regress at the heart border wall of regions of ischemia.

Sixty Days Status-Post Ischemia-Reperfusion Injury

Animals sacrificed sixty days after ischemia reperfusion injury include animals sourced from UW that are from two different age stratifications: older adults (about eight to ten years of age at euthanasia) and young-to-normal adults (about three to five years of age at euthanasia). Additionally, animals from UK Ambystoma Genetic Stock Center (AGSC) were used to compare to the heart regeneration results in the acute setting of Specific Aim 1. Animals from UK are young-adults (about three years of age at euthanasia).

Representative results of H&E staining in the ischemic region of damaged hearts are shown in Figure 62B (older adults, UW), Figure 63B (young-to-normal adults, UW), and Figure 64B (young adults, UK) for animals sacrificed sixty days after ischemia-reperfusion injury. Although all animals show evidence of new myocardium formation, when comparing the UW older-adults to the UW young-to-normal and UK young-adult animals, the much older UW animals do not show formation of myocardium. Instead, there continues to be disorganized formations of proteins with a brighter eosinophilic staining as compared to the younger animals that have areas of forming cardiomyocytes that stain very pale pink. The amount of hemorrhaging present near the heart border wall of the ischemic area are similar between the animals regardless of age and origin. The apical border continues to show increased cellularity with a mixture of infiltrating WBCs (such as basophils), possible myofibroblasts, and likely

endocardium. Additionally, the younger animals from UW and UK show nascent cardiomyocytes with the newly forming myocardium in areas of ischemia-reperfusion injury showing similar light-pink staining as healthy, remote myocardium. Although the regenerating tissue appears different in the apical region when comparing older vs. younger animals, the border regions show similar pathology regardless of age. Regenerating at a slower rate, the border areas all show highly cellular tissue, regardless of age and animal origin.

Representative results of Masson's trichrome staining in the ischemic region of damaged hearts are shown in Figure 62C (older adults, UW), Figure 63C (young-to-normal adults, UW), and Figure 64C (young adults, UK) for animals sacrificed sixty days after ischemia-reperfusion injury. Trichrome: At the apical border of the ischemia-reperfusion injury, the older adult animals from UW show ongoing presence of proteinaceous pockets whereas younger adult animals from UW and UK show remodeling of this same area with disorganized myofibers interspersed within fibrillar connective tissue that appears to be forming a supporting network.

Representative results of AFOG staining in the ischemic region of damaged hearts are shown in Figure 62D (older adults, UW), Figure 63D (young-to-normal adults, UW), and Figure 64D (young adults, UK) for animals sacrificed sixty days after ischemia-reperfusion injury. The apical region of older adult animals from UW shows light purple staining of highly disorganized structures that resemble myofibers in areas of ischemia-reperfusion injury. On the other hand, the myocardium of young-old animals is more organized and show light-orange (properly formed / undamaged myofibers.

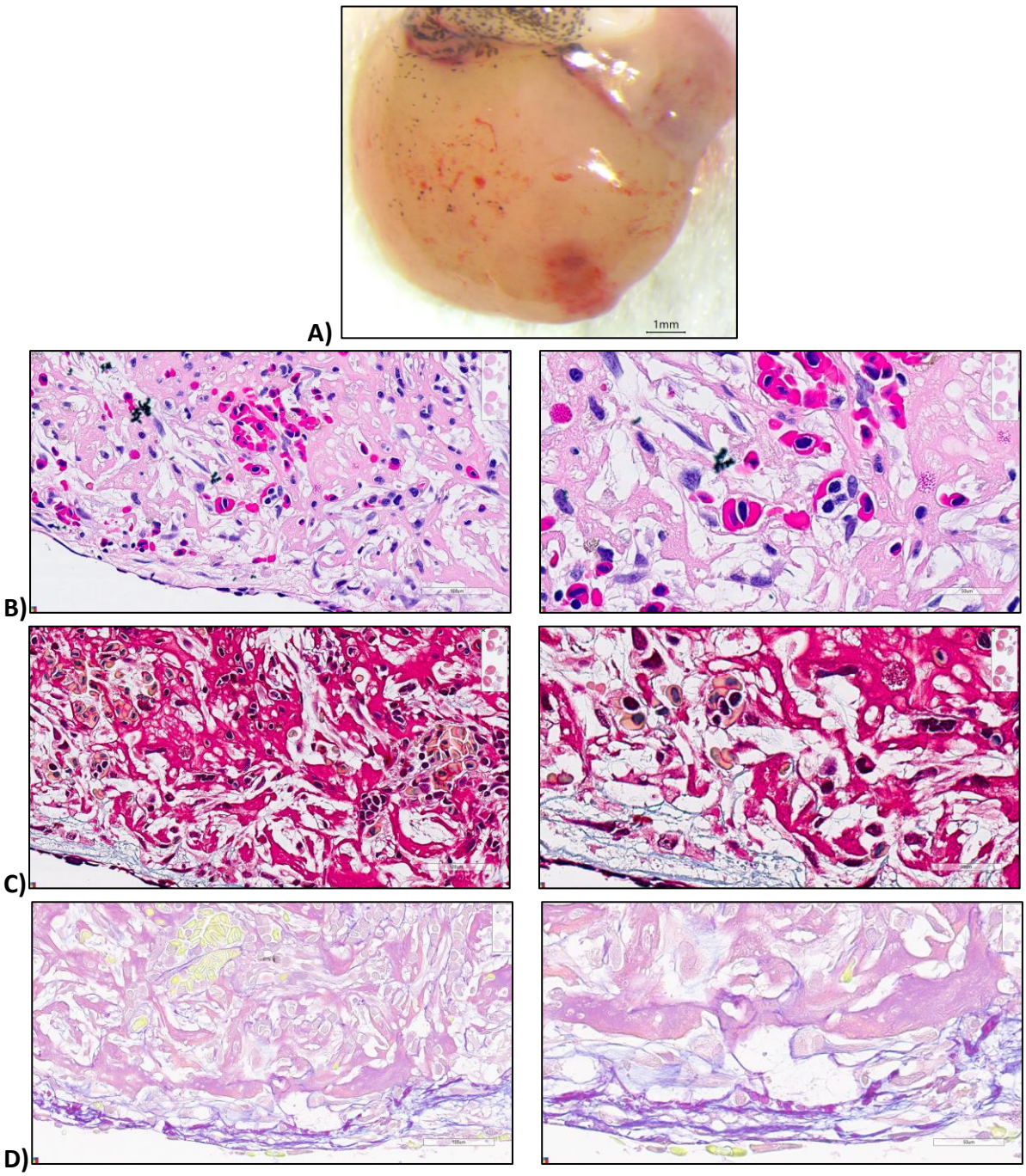

Figure 62: Representative Histologic Results of Older-Adult Axolotl (UW) Hearts Sixty Days After Injury

All views on the left are at 20X zoom while views on the right are at 40X zoom. **A)** Gross view of the injured heart showing area of injury with gross hemorrhage evident. **B)** Hematoxylin and eosin stain. **C)** Masson's trichrome stain. **D)** Acid fuchsin orange G stain. Scale bar included.

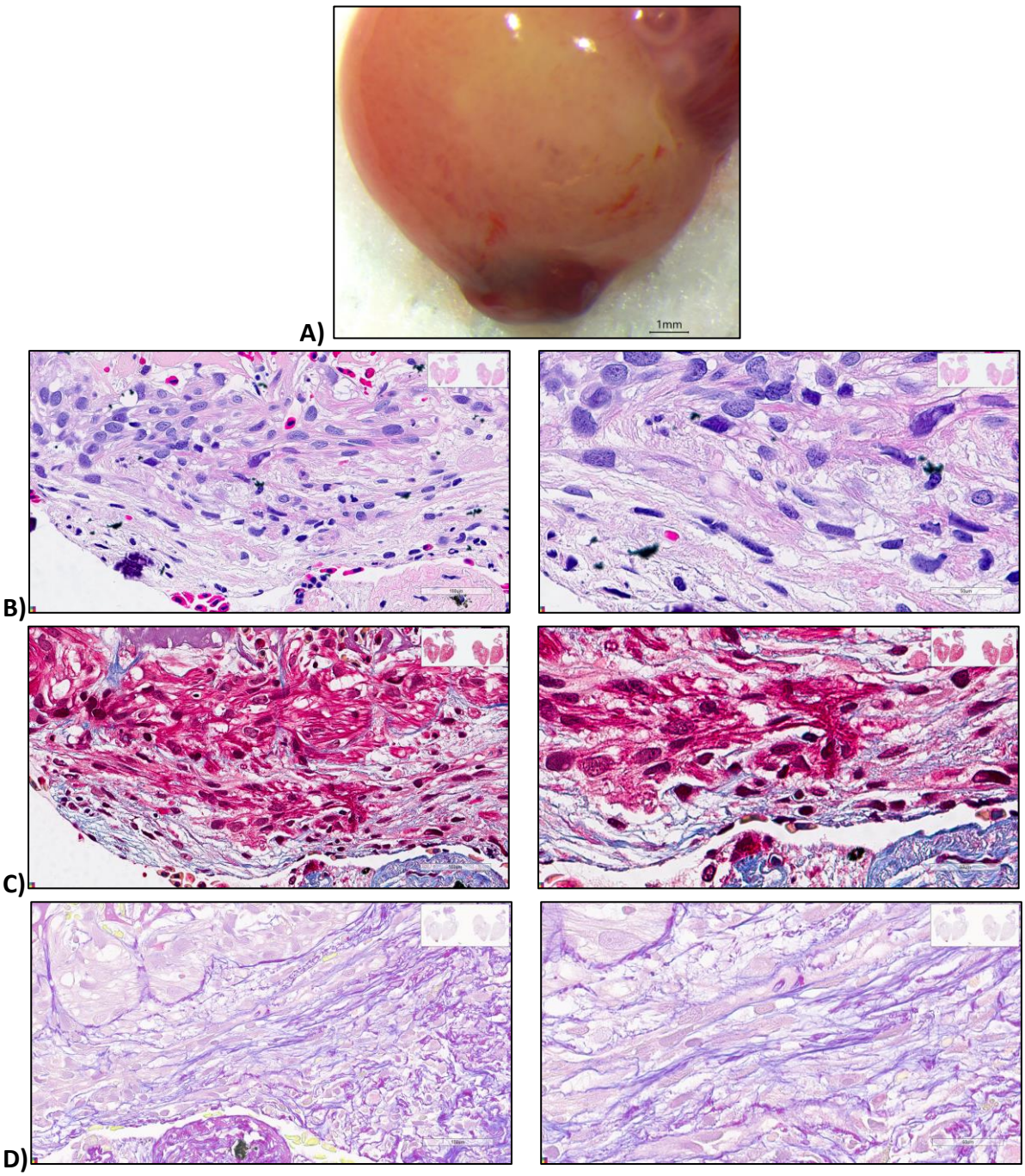

Figure 63: Representative Histologic Results of Adult Axolotl (UW) Hearts Sixty Days After Injury

All views on the left are at 20X zoom while views on the right are at 40X zoom. **A)** Gross view of the injured heart showing area of injury with gross hemorrhage evident. **B)** Hematoxylin and eosin stain. **C)** Masson's trichrome stain. **D)** Acid fuchsin orange G stain. Scale bar included.

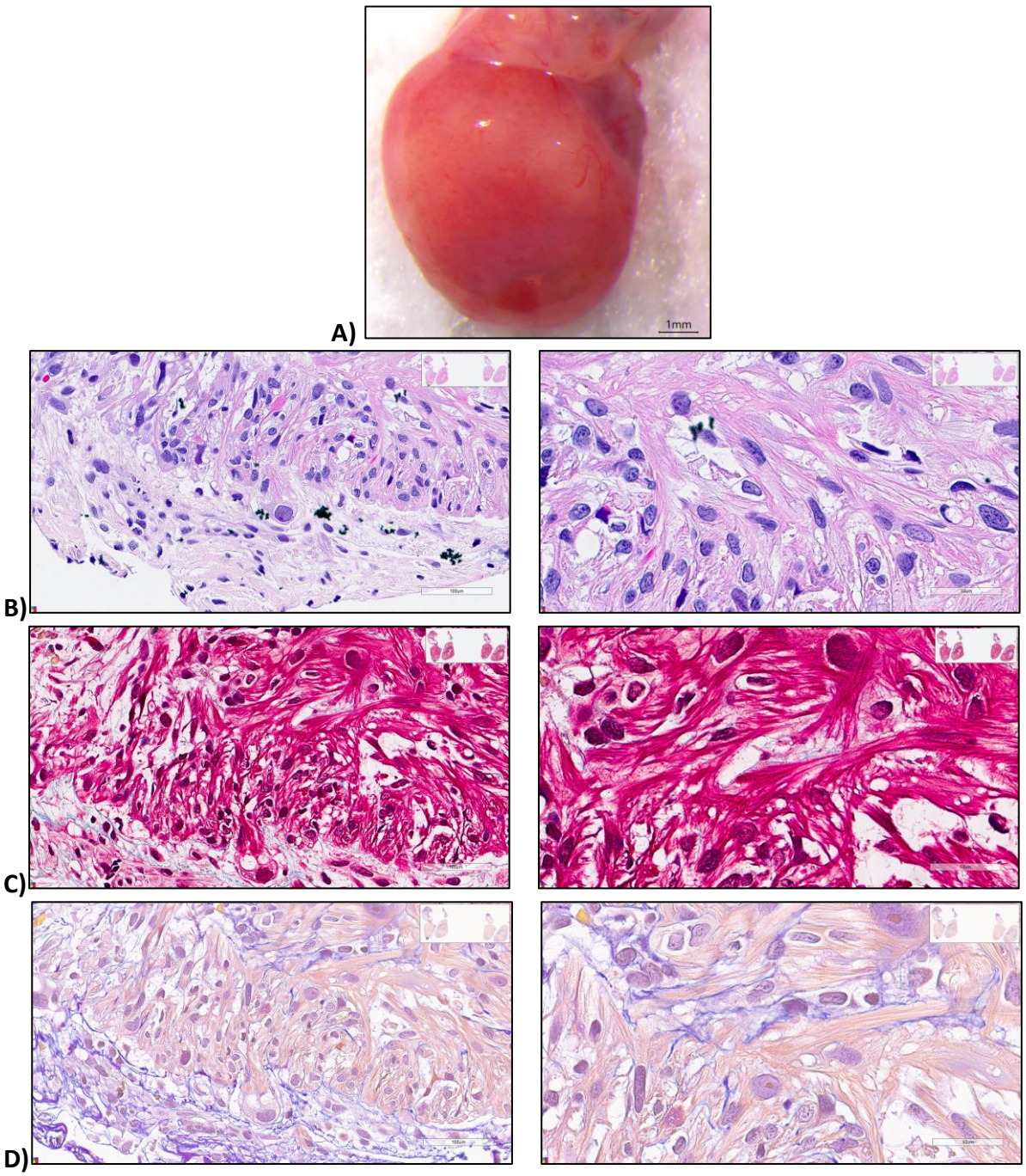

Figure 64: Representative Histologic Results of Adult Axolotl (UK) Hearts Sixty Days After Injury

All views on the left are at 20X zoom while views on the right are at 40X zoom. **A)** Gross view of the injured heart showing area of injury with gross hemorrhage evident. **B)** Hematoxylin and eosin stain. **C)** Masson's trichrome stain. **D)** Acid fuchsin orange G stain. Scale bar included.

Ninety Days Status-Post Ischemia-Reperfusion Injury

Animals sacrificed ninety days after ischemia reperfusion injury include animals sourced from UW that are from two different age stratifications: older adults (about eight to ten years of age at euthanasia) and young-to-normal adults (about three to five years of age at euthanasia). Additionally, animals from UK Ambystoma Genetic Stock Center (AGSC) were used to compare to the heart regeneration results in the acute setting of Specific Aim 1. Animals from UK are young-adults (about three years of age at euthanasia).

Representative results of H&E staining in the ischemic region of damaged hearts are shown in Figure 65B (older adults, UW), Figure 66B (young-to-normal adults, UW), and Figure 67B (young adults, UK) for animals sacrificed ninety days after ischemia-reperfusion injury. Although all animals show evidence of new myocardium formation, the animals from UW show myocardium that is more disorganized with evidence of ongoing hemorrhage. Although animals from UK have fewer RBCs entrapped in myocardial tissue spaces, hemorrhage is still present in border regions of most animals, with less blood present at the border region of younger animals from UW and UK. The apical heart border continues to show increased cellularity with a mixture of nascent and maturing myocardium and infiltrating WBCs such as basophils. Although myocardium is regenerating in all animals, the density and organization still does not match normal myocardium.

Representative results of Masson's trichrome staining in the ischemic region of damaged hearts are shown in Figure 65C (older adults, UW), Figure 66C (young-to-normal adults, UW), and Figure 67C (young adults, UK) for animals sacrificed ninety days after ischemia-reperfusion injury. The UW animals show a developing network of connective tissue fibers in the ischemia-

reperfusion injury at the apex whereas the UK animal shows a more organized connective tissue framework at the apical heart border with few fibers infiltrating the newly-forming myocardium. All animals show the presence of connective tissue deposits at the border between the area damaged by ischemia-reperfusion injury and remote healthy regions – in combination with the histology at the apical border, the UW animals show distribution of connective tissue fibers throughout the entire ischemia-reperfusion injury zone.

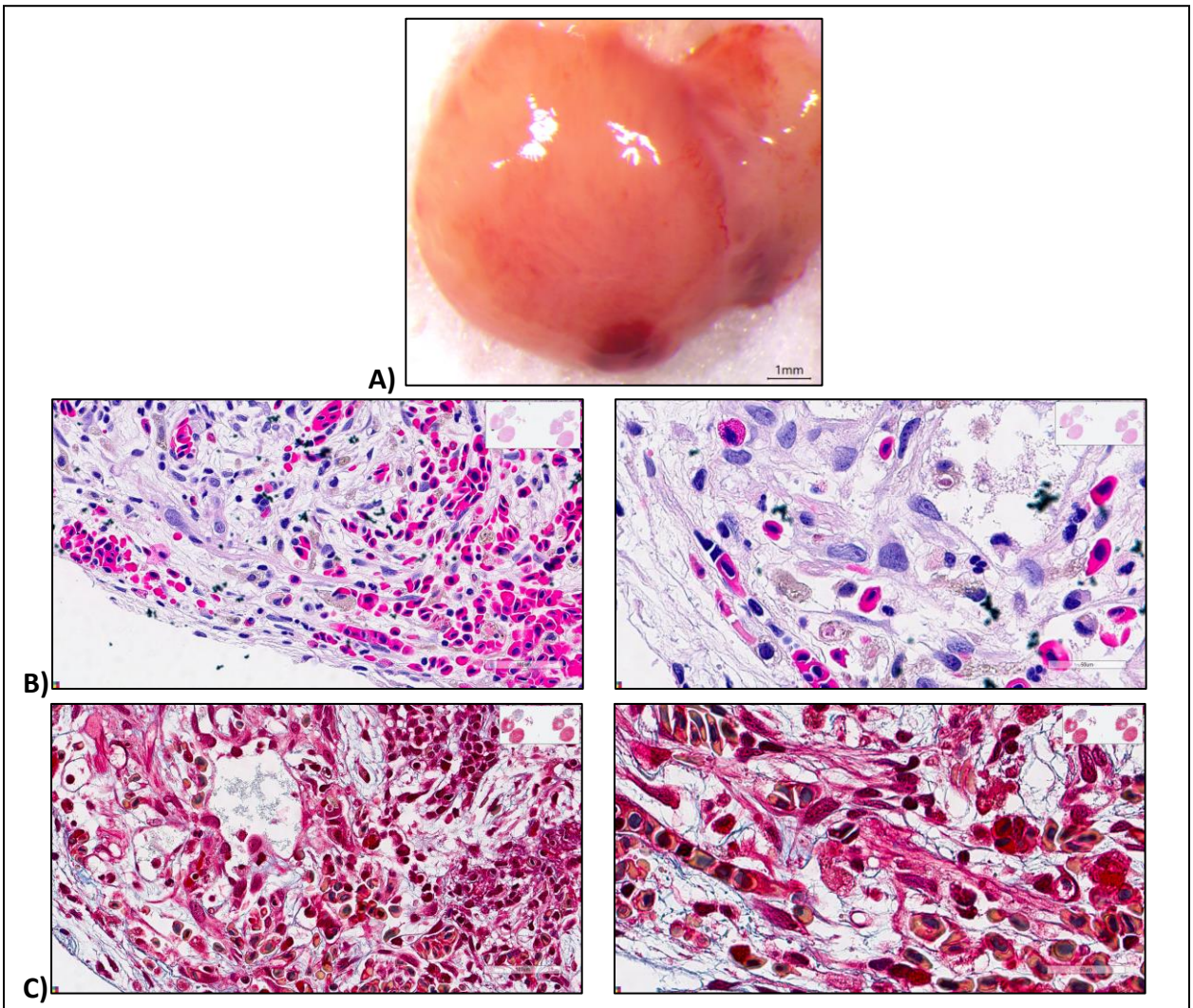

Figure 65: Representative Histologic Results of Older-Adult Axolotl (UW) Hearts Ninety Days After Injury

All views on the left are at 20X zoom while views on the right are at 40X zoom. **A)** Gross view of the injured heart showing area of injury with gross hemorrhage. **B)** Hematoxylin and eosin stain. **C)** Masson's trichrome stain. No AFOG results are available. Scale bar included.

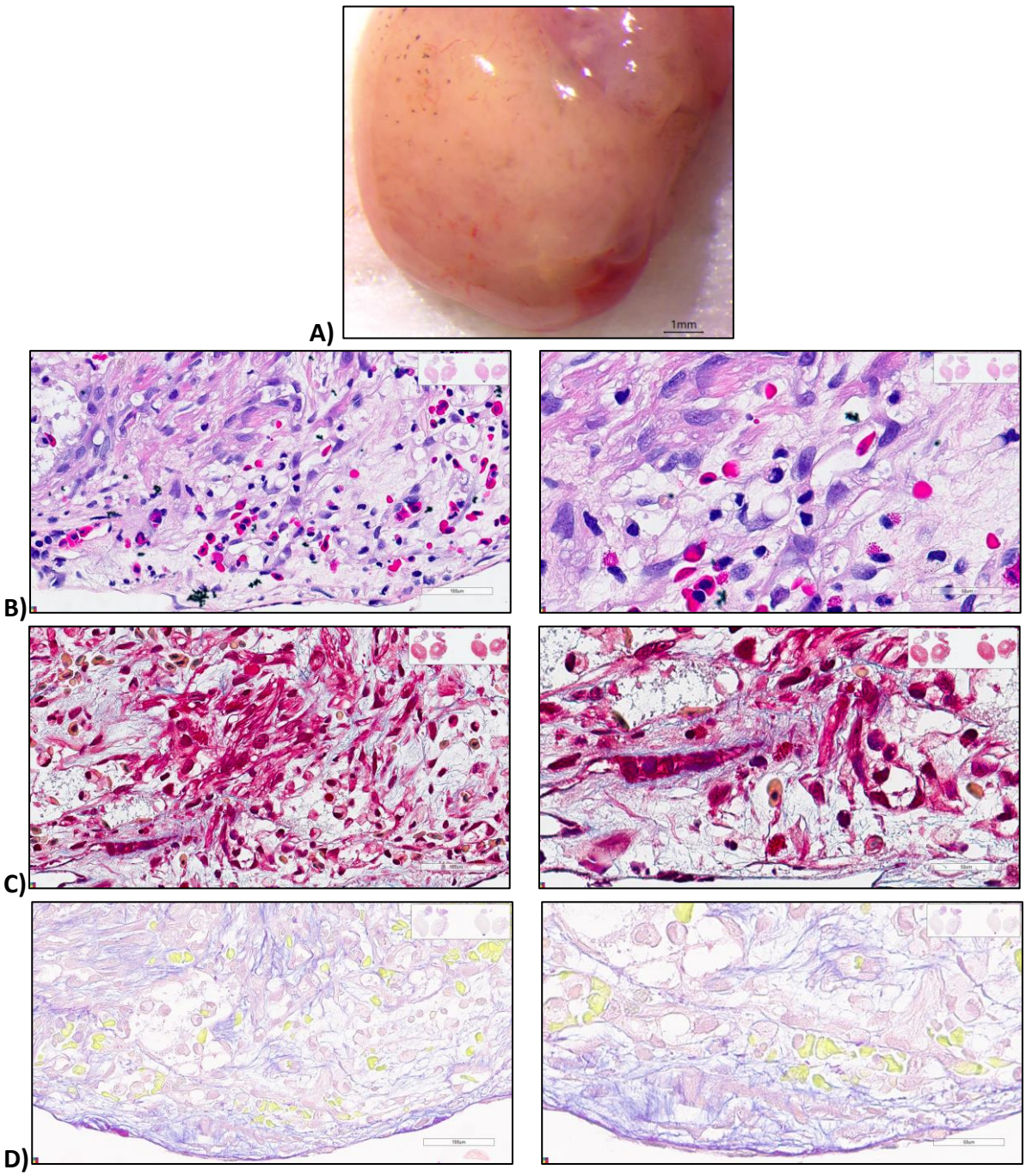

Figure 66: Representative Histologic Results of Adult Axolotl (UW) Hearts Ninety Days After Injury

All views on the left are at 20X zoom while views on the right are at 40X zoom. **A)** Gross view of the injured heart showing area of injury with gross hemorrhage evident. **B)** Hematoxylin and eosin stain. **C)** Masson's trichrome stain. **D)** Acid fuchsin orange G stain. Scale bar included.

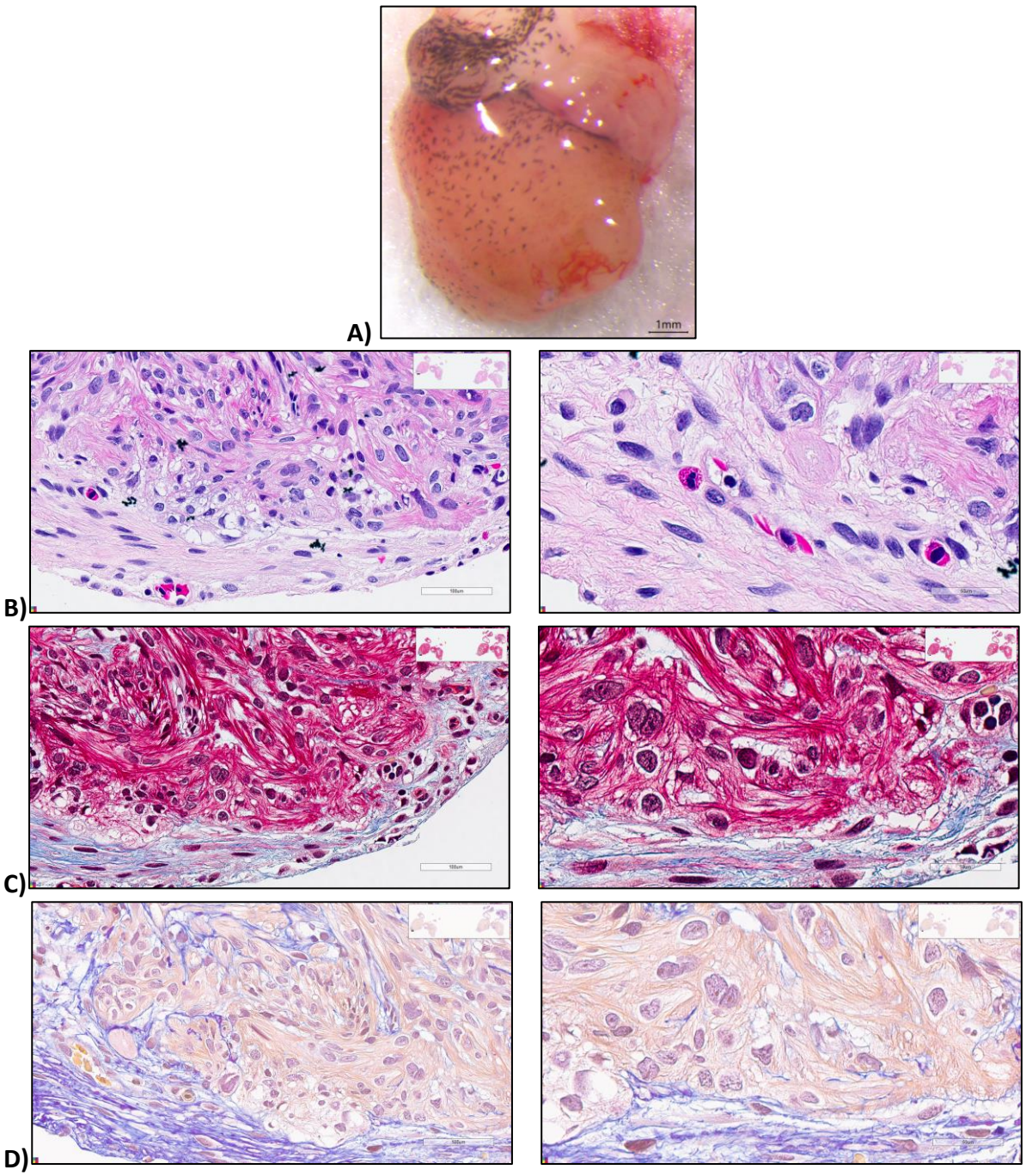

Figure 67: Representative Histologic Results of Adult Axolotl (UK) Hearts Ninety Days After Injury

All views on the left are at 20X zoom while views on the right are at 40X zoom. **A)** Gross view of the injured heart showing area of injury with gross hemorrhage evident. **B)** Hematoxylin and eosin stain. **C)** Masson's trichrome stain. **D)** Acid fuchsin orange G stain. Scale bar included.

Representative results of AFOG staining in the ischemic region of damaged hearts are shown in Figure 66D (young-to-normal adults, UW) and Figure 67D (young adults, UK) for animals sacrificed ninety days after ischemia-reperfusion injury. Results from the older adult from UW are not available. Myocardium of younger adult animals from UW is still less organized, but shows pale-orange staining (possible evidence of properly formed / undamaged myofibers) while one animal from the UK group shows very good remodeling (light-orange staining of myocardium) with increasing density and organization. To add further validity to the formation of new myocardium, AFOG staining of the apical portion of all UK animals that were followed for ninety days after surgery are shown in Figure 68. Given the light-orange staining, the seven animals that underwent the ischemia-reperfusion injury (see Figure 68 A-G) show the presence of newly forming myocardium. The single animal that underwent the sham procedure (all surgical steps performed, including exposing the heart in the pericardial cavity and suturing the pericardium closes, except mechanical clamping of the heart) is shown in Figure 68H. The myocardium of injured animals stain with the same intensity as the sham animal, while the sham animal exhibits no connective tissue infiltration within the parenchyma – the connective tissue in the sham heart is localized to the heart border wall.

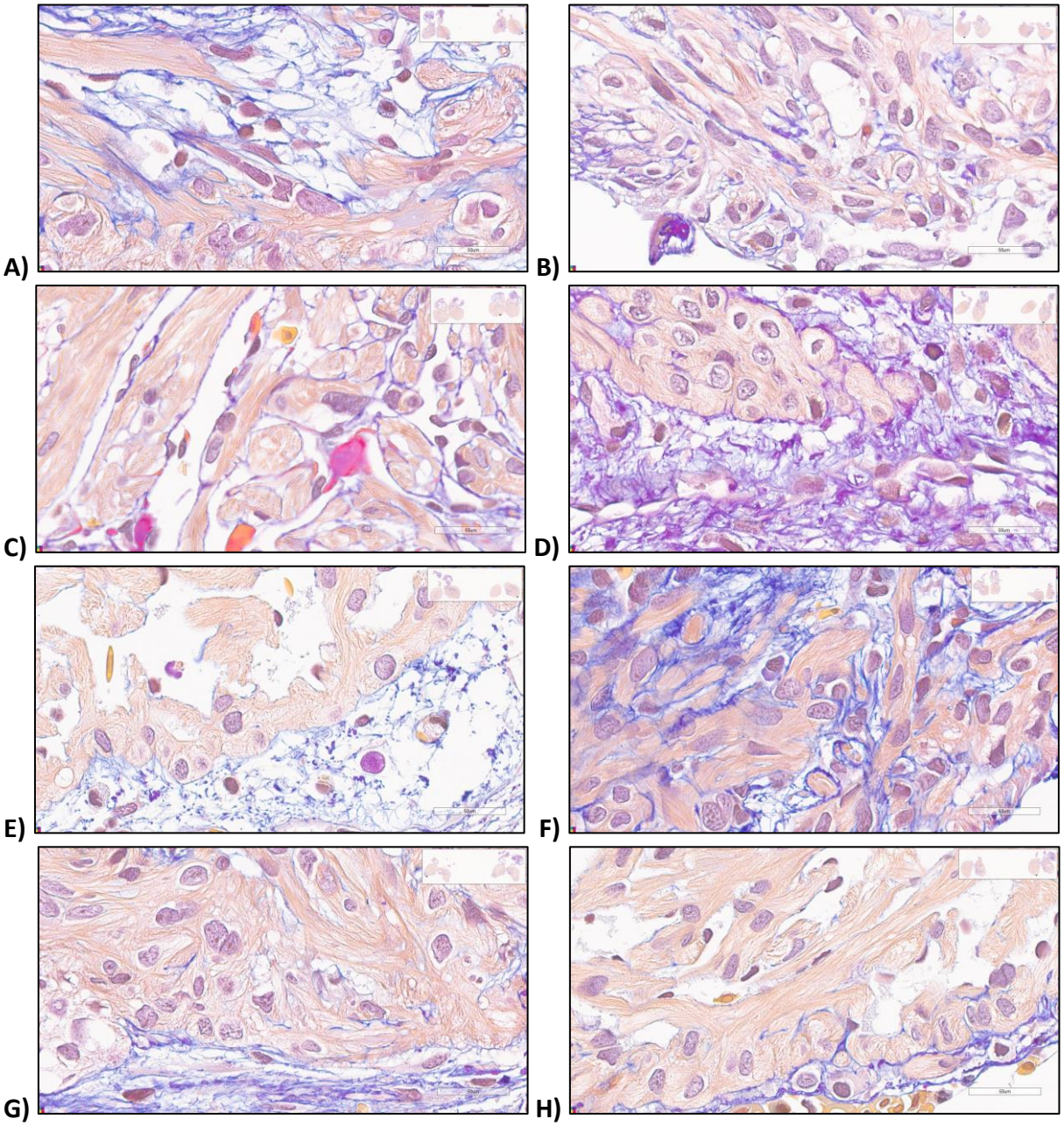

Figure 68: AFOG Staining at Heart Apex for all UK Animals Sacrificed Ninety Days After Ischemia-Reperfusion Surgery
A-G) Animals undergoing I/R procedure. **H)** Animal that underwent sham procedure.

Quantitative Assessments of Pathology

Based on the histology stains used in Specific Aim 1 and Specific Aim 2, features defined by the dyes were chosen for quantitative assessment. From H&E stains, hyaline change feature of interest; from Masson's Trichrome stains, connective tissue appearing as fibers is most likely

collagen and is a feature of interest; and from AFOG stains, fibrin is the unique feature protein that is differentiated by this stain and is the feature of interest. For cells, the lack of cross-reacting antibodies makes it difficult to identify certain cells like cardiomyocytes and lymphocytes that take on different appearances under stress (e.g. cardiomyocytes) or cannot be differentiated within a class on appearance alone (e.g. lymphocytes). However, granulocytes that stain with a unique appearance and with highly contrasting colors compared to surrounding tissue can easily be identified by their gross appearance. Thus, quantitative cell counts in this section focus on granulocytes and erythrocytes (also easily identifiable in normal and stressed tissues).

Data about hyaline exudate, studied in animals from UK in Specific Aim 1, can now be extended using results from animals sacrificed thirty, sixty, and ninety days after ischemia-reperfusion injury. Additionally, upon further review of chronic follow-up data, the amount of collagen and fibrin over time in the regenerating axolotl heart is of interest. The following data are computed using Fiji with similar histology field sampling schemes (ten fields per animal, see Figure 54B) as performed in Specific Aim 1. The color thresholding HSB values for H&E stains to identify areas of hyaline are shown in Figure 54A for injured tissues. Changes to the HSV values were required to highlight areas of hyaline in samples with very low background of hyaline or samples of naïve or sham animals. Without adjusting “hue” from 210 as used in Specific Aim 1 to 230, Fiji highlighted large areas of myocardium instead of hyaline. HSB thresholding values for collagen (Figure 69B) and fibrin (Figure 69C) were tested on known naïve and injured sections and were used in blinded sections without modifications based on appearance of tissue.

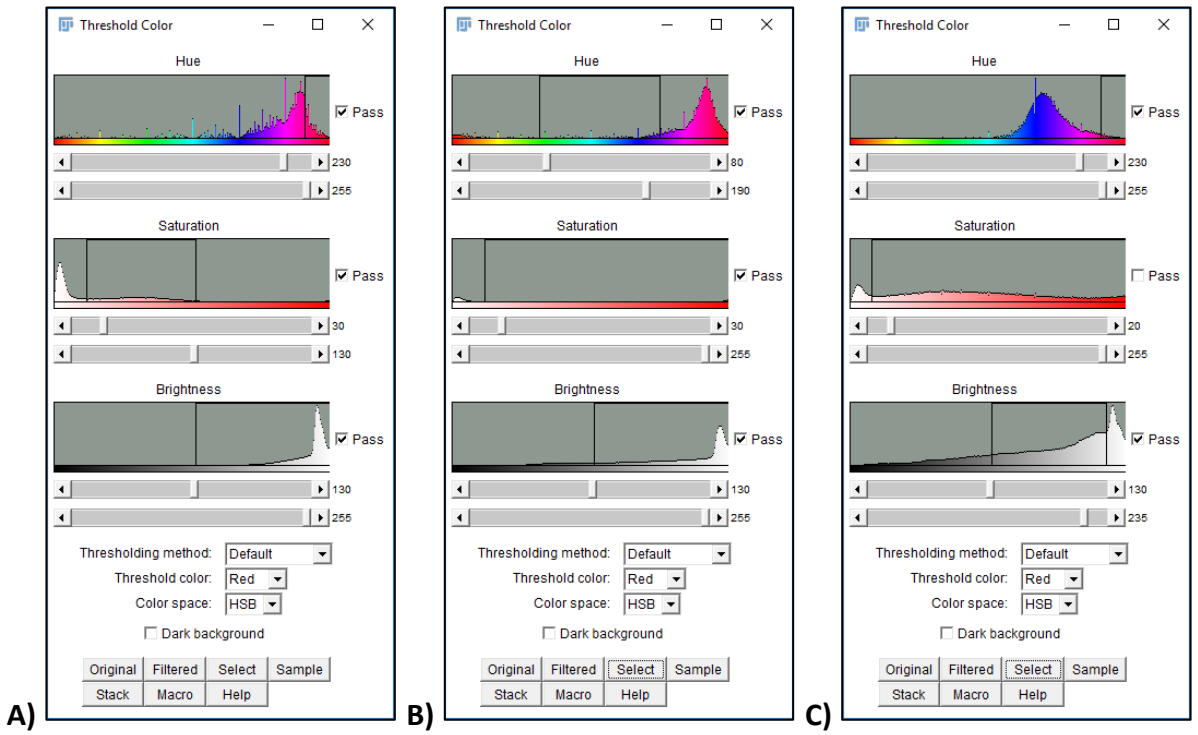

Figure 69: Image Analysis Settings for Low-Background Hyaline, Collagen, and Fibrin
The values shown here were used to threshold loaded image files in Fiji into: **A)** Areas corresponding to hyaline change in H&E histology stains of animals with low background of hyaline change or sham animals with no hyaline change present. **B)** Areas corresponding to light-green to light blue collagen in Masson's trichrome stain. **C)** Areas corresponding to bright-red areas of fibrin in AFOG stains.

Following the animal welfare experiments in Specific Aim 1, all animals in Specific Aim 2 were treated with butorphanol at 0.75 mg per liter of tank water (labeled as "high-dose" in Specific Aim 1). To compare animals from the same source (UK) that received the same animal husbandry and post-surgical care between the acute (Specific Aim 1) and chronic (Specific Aim 2) follow-up studies, only high-dose animals were used in the quantitative comparisons presented here, resulting in a sample size of four animals (n = 4) per group (only four animals per group, maximum, were used in Specific Aim 1). However, the ten inspected views for each heart used in the following results were chosen at random in the sampling field (i.e. mouse cursor was clicked in a thumbnail figure in the area defined in the sampling scheme without further

panning/localizing the field of view once the appropriate zoom was chosen) and the animal IDs were blinded (by friend of the author) to the user performing the analysis (the author). For red blood cell and granulocyte counts, each field was assessed by the author and cells were counted by hand. For granulocytes, eosinophilic and basophilic cells were grouped and counted, including neutrophil, heterophil, eosinophil, and basophils (see Figure 59)

The evolution of hyaline change, collagen formation, and fibrin over time is shown in Figure 70A, Figure 71A, and Figure 73A, respectively. The mean for each animal is depicted by the data point and the standard error of the mean from the ten fields used to determine the mean for each animal is denoted by the error bars. Error bars that are not visible are hidden by the data point (i.e. very small standard error of the mean). Results of threshold calculations for samples taken over time using one-way ANOVA (GraphPad Prism, Version 7.04) with follow-up multiple comparison tests compared to control and corrected by Dunnett's test are shown in

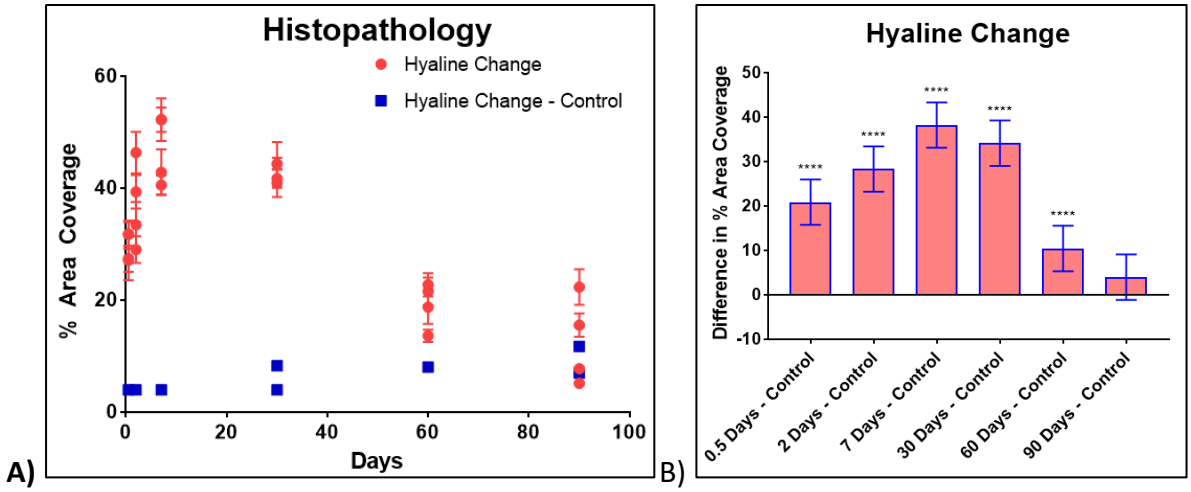

Figure 70: Evolution of Hyaline Change Over Time Following Ischemia-Reperfusion Injury **A)** Means for each individual animal are depicted by a data point – error bars are standard error of the mean for each individual animal (calculated from ten separate measurements). **B)** One-way ANOVA results comparing sample to control groups. p-values: * < 0.05, ** < 0.01, *** < 0.001, **** < 0.0001

Figure 70B, Figure 71B, and Figure 73B for hyaline change, collagen formation, and fibrin respectively.

The quantitative results of hyaline change agree with the qualitative observations. At all points except at ninety days after ischemia-reperfusion injury, the amount of hyaline change present is significantly different than control. After ninety days of repair and regeneration, the amount of hyaline has regressed and is no longer different than control, supported by the fact that new myocardium (see Figure 68) is present in greater quantities in the previously-damaged area of ischemia-reperfusion injury.

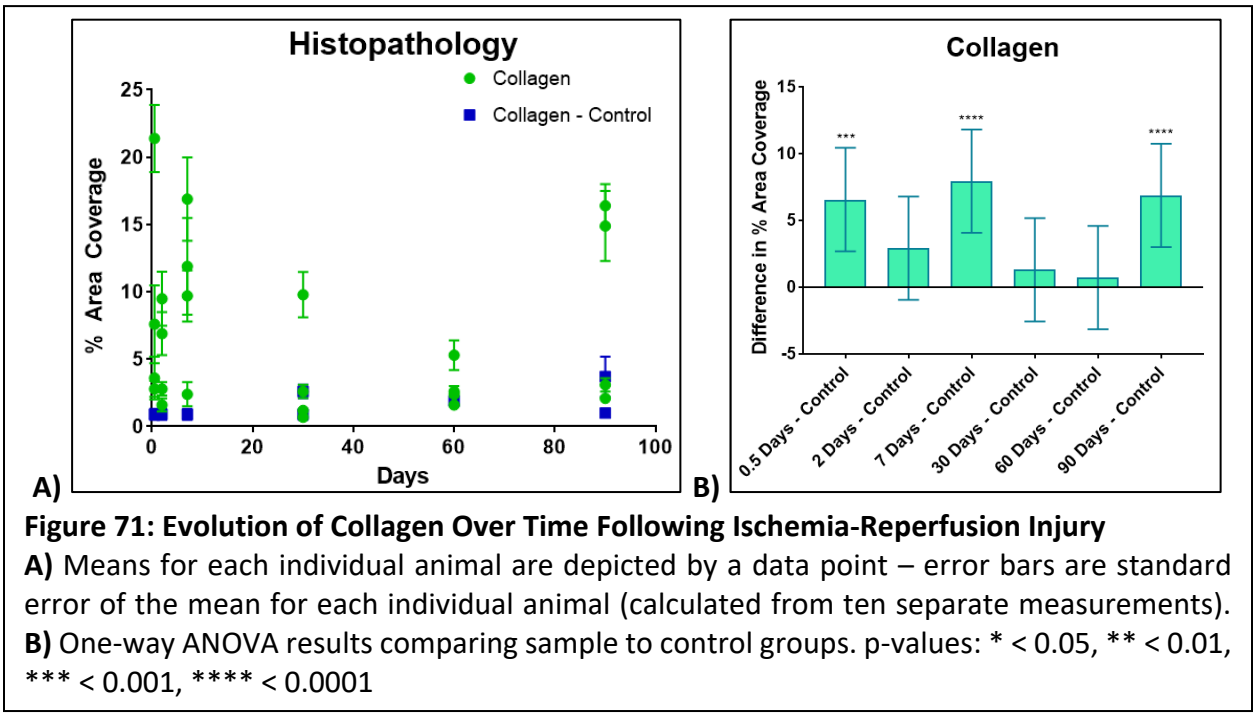

Figure 71: Evolution of Collagen Over Time Following Ischemia-Reperfusion Injury
A) Means for each individual animal are depicted by a data point – error bars are standard error of the mean for each individual animal (calculated from ten separate measurements). **B)** One-way ANOVA results comparing sample to control groups. p-values: * < 0.05, ** < 0.01, *** < 0.001, **** < 0.0001

Based on the results of Figure 71B and Figure 73B, there are no clears trend of the evolution of collagen and fibrin deposition or formation over time in healing axolotl cardiac tissue after ischemia-reperfusion injury. The results do not support the qualitative observations - collagen deposition or formation is not supported by picrosirius, Masson's trichrome, or AFOG staining and no fibrin is evident as shown in the representative slides of injured axolotl cardiac

tissue. Additional validation of pixel HSB values to known control samples is warranted to extend any quantitative claims about collagen and fibrin behavior over time in the regenerating axolotl heart after ischemia-reperfusion injury.

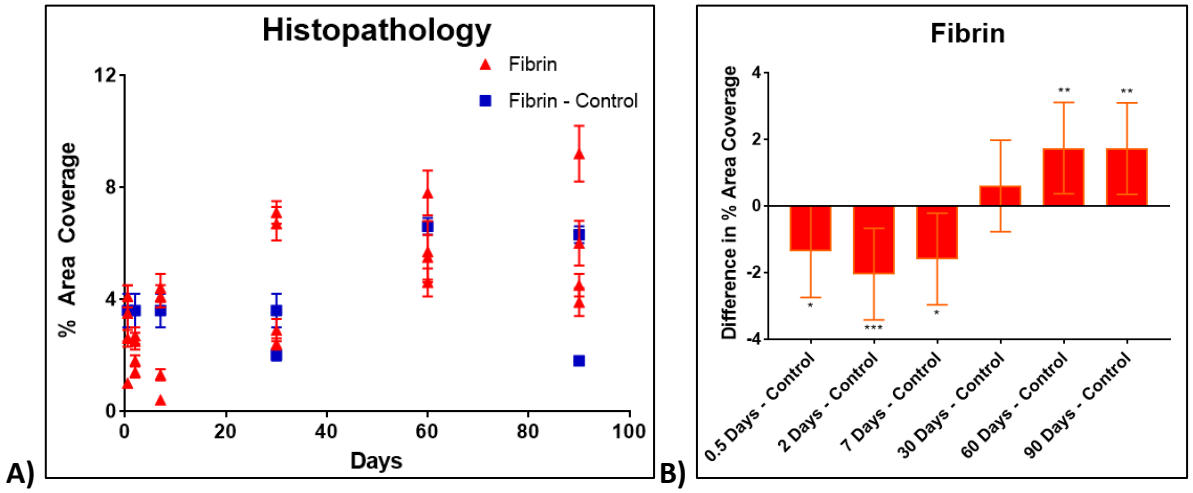

Figure 73: Evolution of Fibrin Over Time Following Ischemia-Reperfusion Injury
A) Means for each individual animal are depicted by a data point – error bars are standard error of the mean for each individual animal (calculated from ten separate measurements). **B)** One-way ANOVA results comparing sample to control groups. p-values: * < 0.05, ** < 0.01, *** < 0.001, **** < 0.0001

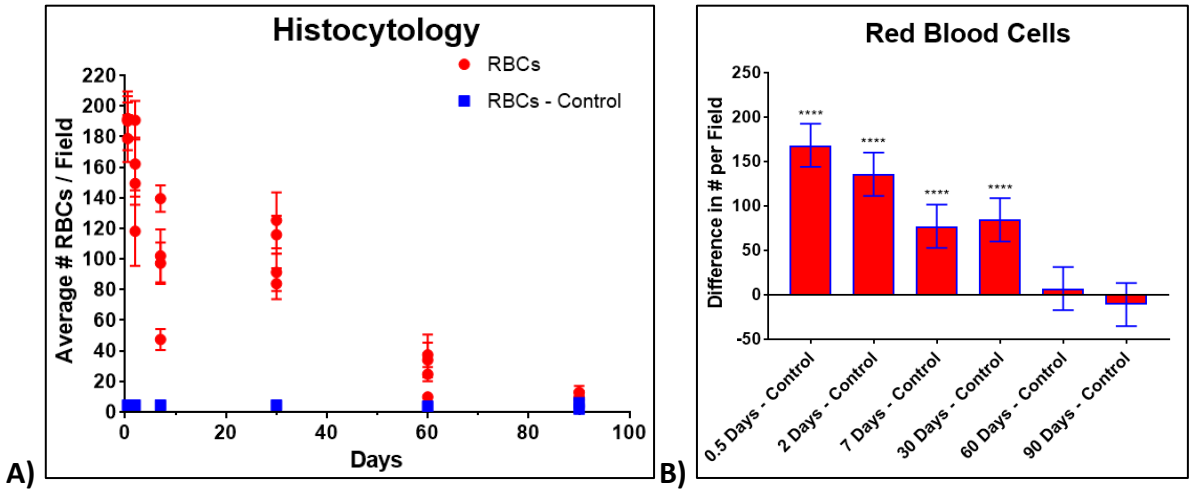

Figure 72: Presence of RBCs Over Time Following Ischemia-Reperfusion Injury
A) Means for each individual animal are depicted by a data point – error bars are standard error of the mean for each individual animal (calculated from ten separate measurements). **B)** One-way ANOVA results comparing sample to control groups. p-values: * < 0.05, ** < 0.01, *** < 0.001, **** < 0.0001

The results of manually counting erythrocytes and granulocytes are shown in Figure 72 and Figure 74, respectively. The one-way ANOVA results comparing the amounts of RBCs at specific time points after ischemia-reperfusion injury to control confirm the observations noted in the qualitative assessments – massive hemorrhaging evident on gross heart observation and histologically into areas of injured myocardium are observable in animals through thirty days of follow-up. For animals sacrificed sixty- to ninety-days after ischemia-reperfusion injury, very few RBCs remain in and around the regenerating tissue. With respect to granulocytes, their presence is statistically different compared to control animals at all points after ischemia-reperfusion injury except for one-half day after the procedure. Although no granulocytes are evident one-half day after surgery, other acute-phase inflammatory lymphocytes are present.

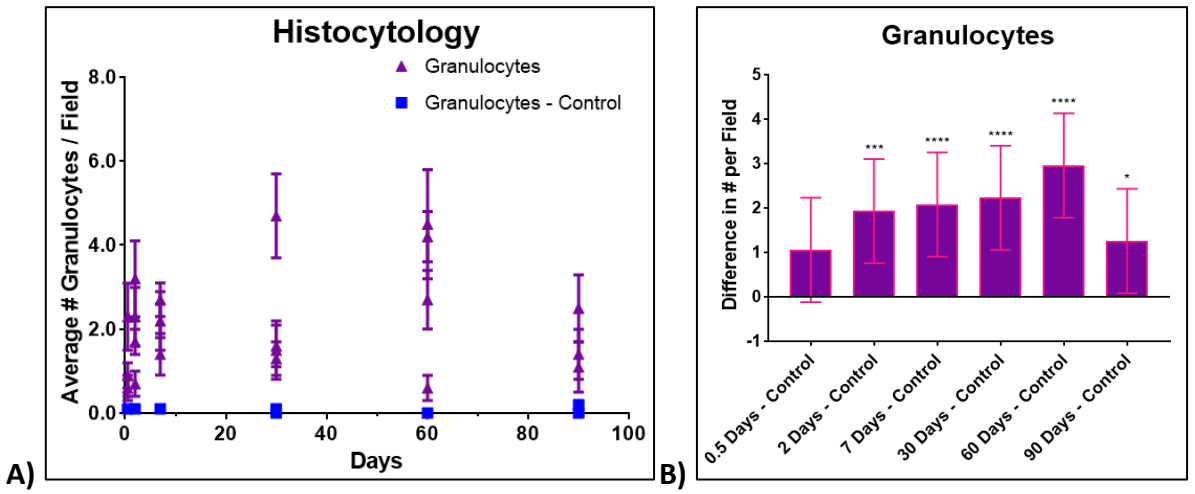

Figure 74: Presence of Granulocytes Over Time Following Ischemia-Reperfusion Injury
A) Means for each individual animal are depicted by a data point – error bars are standard error of the mean for each individual animal (calculated from ten separate measurements). **B)** One-way ANOVA results comparing sample to control groups. p-values: * < 0.05, ** < 0.01, *** < 0.001, **** < 0.0001

Overall Spatiotemporal Histology Trend

The results presented here provide evidence that the adult axolotl can regenerate a cardiac ischemia-reperfusion injury. Unlike the results of the partial ventricular amputation study

in axolotls (Cano-Martinez et al., 2010), complete regeneration has not been achieved by ninety days of follow-up. After ninety days following an ischemia-reperfusion injury to the axolotl heart, new myocardium is forming, but it is less organized with connective tissue infiltrating around the nascent myofibers. The delay in healing a more serious tissue injury parallels studies in zebrafish: apical resection studies completely heal in about sixty days whereas cryoinjury studies take about one-hundred thirty days to perfectly remodel in the zebrafish (Choi and Poss, 2012). The expectation here is that complete axolotl heart regeneration will take greater than ninety days to return cardiac tissue injured by an ischemia-reperfusion event to its pre-injury state.

Heart Function Over Time Following Ischemia-Reperfusion Injury

For each follow-up scan (e.g. twenty-eight-day scan), an animal was appropriately anesthetized and scanned immediately when a light- to deep-plane of anesthesia was achieved. The linear ultrasound transducer was placed directly on the animal's skin and oriented using two landmarks (one-way valve leading to bulbus cordis outflow tract and attachment of ligamentum mesocardium to dorsal surface of pericardial cavity). Once properly oriented, a five-hundred frame capture was executed in the MATLAB® script. The transducer was then moved away from the animal's skin and repositioned for additional scans. Three to five scans were performed and recorded per animal on each scheduled day for follow-up imaging.

After extracting all five-hundred image files from each output video, each frame was viewed to find the extents of systole and diastole for one heartbeat. Once a set of frames were identified, another cardiac cycle three to four seconds away (about one hundred frames between individual FAC calculations) was viewed to evaluate a different heartbeat. A total of three separate heartbeats were evaluated per video and anywhere from three to five trials were

assessed per animal per scheduled scan day. Many of the calculated FAC values were in close agreement (e.g. less than 10% absolute difference between minimum and maximum values calculated). However, if one of three FAC calculations is more than ten percent different from the other two calculated values (i.e. because of slight animal movement or transducer position drift), additional sets of sequential systolic and diastolic images of a continuous heartbeat were evaluated and replaced any outlying values. To calculate the FAC values reported here, all long-term animals with fifty-six to ninety days of follow-up scans were used (n = 8 to 16 animals, see Figure 70). For the data on the twenty-eight-day scan follow-up, the Verasonics ultrasound machine was in use by another PI, so only eight (n = 8) animals were scanned for that data set.

A publication using cryoinjury to injure axolotl hearts and a production Vevo 2100 ultrasound machine (FUJIFILM/VisualSonics Inc., Canada) designed for small animal ultrasound to measure the fractional area change (FAC) in axolotl hearts report similar results. At baseline, Godwin et al. report a baseline FAC of about 45%, with an upper limit 95% confidence interval level around 50% (the lower 95% confidence interval limit is not provided), with a drop in FAC to about 28% (with an upper limit 95% confidence interval of about 32%) fourteen days after cryoinjury. At forty-five days of follow-up, injured hearts returned to baseline function (Godwin et al., 2017b). Results of fractional area change over time in this study over time are shown in Figure 75. Comparing the raw FAC values in Figure 75C to the figures from Godwin et al., the approach used in this study, an in-house image-analysis algorithm including manually defining the regions of interest (axolotl hearts in diastole and systole) produces results that agree with the values determined using the commercial system with built-in LV-trace algorithm. Control animals in this study had baseline FAC of 40.08% (35.62% - 44.54% for 95% confidence interval)

and FAC at fourteen days after injury of 30.05% (33.41% - 26.69% for 95% confidence interval), values consistent with Godwin et al.

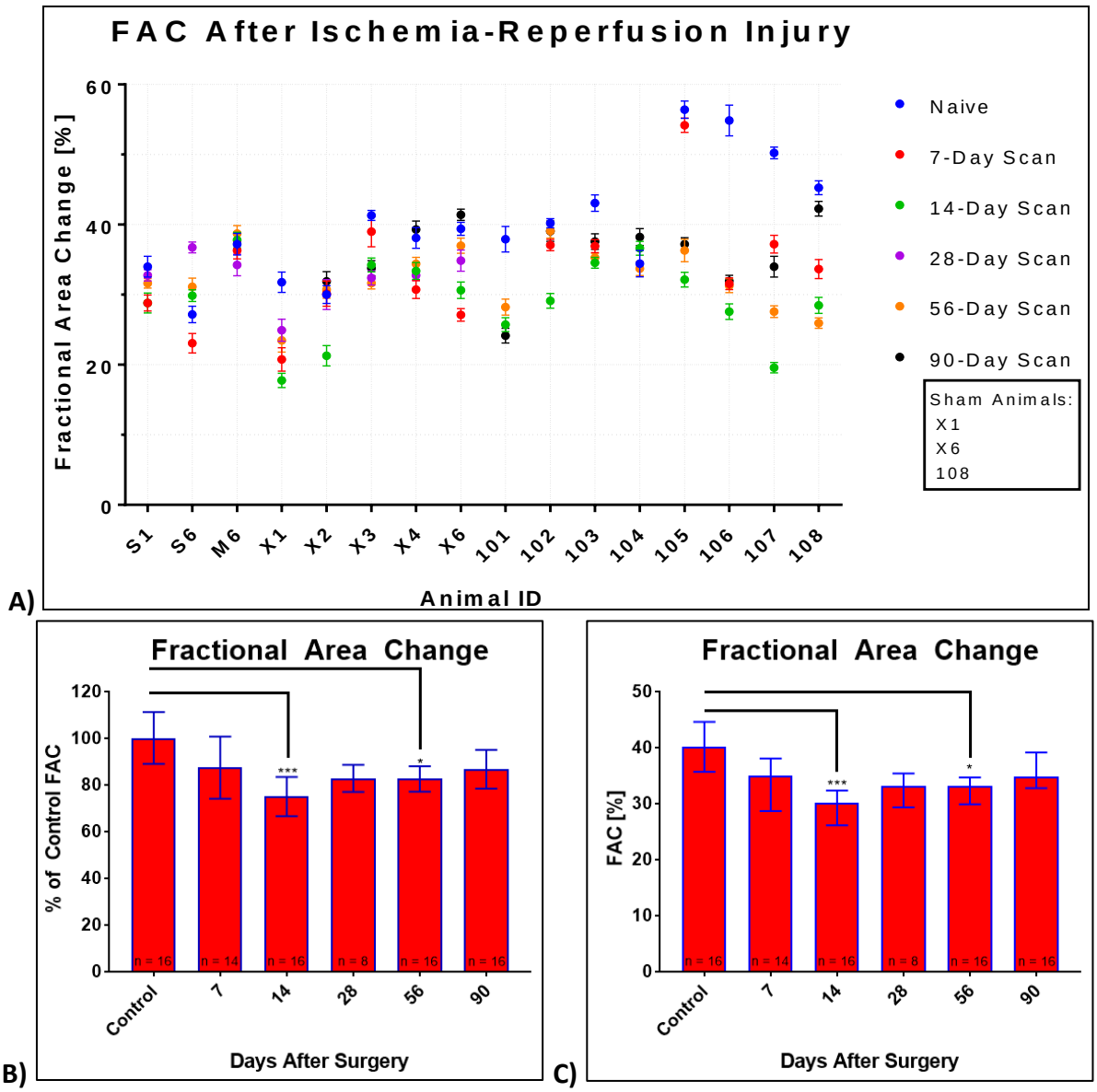

Figure 75: Fractional Area Change Over Time Following Ischemia-Reperfusion Injury
A) Means for each individual animal are depicted by a data point – error bars are standard error of the mean for each individual animal. **B)** One-way ANOVA results comparing sample to control groups. p-values: * < 0.05, ** < 0.01, *** < 0.001, **** < 0.0001

Considering only the animals in this study, when comparing the ischemia-reperfusion results to controls, there is a statistically significant difference between animals at fourteen and fifty-six days of follow-up after ischemia-reperfusion injury, matching the acute drop in function

noted by Godwin et al. Although the mean at twenty-eight days after injury (33.16%; 30.82% - 35.49% for 95% confidence interval) is close to the mean at fifty-six days after injury (33.06%, 30.88% - 35.24% for 95% confidence interval), the smaller amount of data (ultrasound machine was not available) does not allow for significance to be calculated. Supporting the tenet that ischemia-reperfusion injury is a more serious cardiac injury modality, cardiac function does not return to baseline until ninety days after surgery with a mean of 34.72% (31.38% - 38.05% for 95% confidence interval). According to Godwin et al., the axolotl heart injured by cryoinjury returns to baseline function after forty-five days following surgery.

CHAPTER 7: DISCUSSION

Specific Aim 1

Development of Ischemia-Reperfusion Model in the Axolotl

After being subjected to various types of injuries of differing severity, published experiments studying non-mammalian vertebrates have shown that hearts of animals of various developmental stages can fully regenerate and rescue cardiac function through epimorphic or epimorphic-like repair processes (Choi and Poss, 2012; Roy and Gatien, 2008). However, as outlined the section "Cardiac Injury Models", the molecular signaling pathways involved in cryoinjury, conditional genetic ablation, or apical resection do not recapitulate the events in an ischemia-reperfusion event. Therefore, the cardiac regeneration field still does not have direct evidence that an adult vertebrate animal can regenerate a cardiac ischemia-reperfusion injury.

Lacking coronary arteries and while having a trabeculated ventricle, inducing an ischemia-reperfusion injury must take an entirely different approach than a coronary artery ligation. After searching for the correct tool that can induce a mechanically-induced injury in the murine and axolotl heart, the work here has shown that the pathophysiology following a myocardial infarction in the mouse is recapitulated using mechanical compression of the mouse heart, and can be replicated in the axolotl heart. The only difference between the two model systems is the time to induce sufficient ischemia to ensure irreversible cardiac muscle injury. In mammals, twenty to thirty minutes is sufficient to induce transmural (ST-elevation myocardial infarction, or STEMI) cardiac damage. In the axolotl, it was found that one-hundred and twenty minutes of induced ischemia is sufficient to repeatably produce an ischemia-reperfusion injury. In short, one

of the main outcomes of Specific Aim 1 is the development of a method to induce a heart attack in axolotls.

Ensuring Axolotl Welfare when Using Ischemia-Reperfusion Model

Previous studies in frogs (*Rana pipiens and Xenopus laevis)* have described mechanical (manual von Frey [vF] aesthesiometers), thermal (light energy), and chemical (acetic acid test [AAT]) methods to assess pain and analgesic efficacy in a quantitative manner (Willenbring and Stevens, 1996), which require modifications to produce repeatable results in axolotls. The work presented here evaluated vF and AAT quantitative assessments to determine the repeatability and reproducibility of the two quantitative tests and determine which is a better tool to use to quantify pain in the axolotl.

While there are several demonstrated differences in pain responses between frogs, newts, and salamanders, it has been shown that A- and C-nociceptive fibers are present in most vertebrate animals, including amphibians (Coble et al., 2011; Hamamoto and Simone, 2003; Sneddon, 2014). Although axolotls are classified in a different family and order from newts and frogs respectively, it is expected that pain receptors are likely conserved within the class. However, nociceptor fiber distribution and number may vary (Sneddon, 2014). Spinothalamic projections (via a brainstem-thalamus tract) conveying cutaneous sensory information to the thalamus are not well understood in amphibians, but are known to exist (Northcutt, 1984; Stevens, 2004). Additionally, thalamocortical projections that convey sensory signals to the telencephalon are poorly organized and only contain scant numbers of fibers in amphibians (Stevens, 2004). The neuroanatomy of frogs (Vesselkin et al., 1971) suggests the transmission of noxious stimuli (nociception) and the processing of the sensory information (pain) is poorly

represented in amphibians and that most central nervous system (CNS) pathways are related to spinal (does not ascend to brain) and long-loop (does ascend to brain) reflexes to the brain stem and thalamus (Koeller, 2009). Nevertheless, the presence of sensory projections to the brains of amphibians suggests these animals perceive pain and that appropriate analgesics should be used whenever performing experiments that can cause pain.

Comparing AAT versus vF as quantitative tools to assess pain in amphibians, the present findings are in direct contrast to the reproducibility and repeatability of these same methods when used in frogs. Willenbring and Stevens (Willenbring and Stevens, 1996) found vF had less individual variation than AAT when assessing pain thresholds in *Rana pipiens*. This difference in measurement variation may be due to species differences and/or dissimilarities in experimental methods. With respect to species differences, there may be dissimilar distributions of cutaneous mechanoreceptors of the lateral line system in each animal or variations of sensory-discriminative pathways between frogs and axolotls. The experimental setups used also differ between the frog study and the experiments presented here. At least two days before testing, the frogs in the Willenbring and Stevens study were transferred from their home environment to individual plastic cages with 2 cm of water covering the cage bottom (reduced to 0.5 cm on the day of test), clearly leaving the frog's hindlimb exposed for probing and testing. In contrast, to minimize extraneous non-noxious stimuli or environmental cues that might prime a response like restraining the animal or allowing the animals to see the test devices, the aesthesiometers probed the animals or acetic acid was placed on them while the axolotls were in a quiescent and restful state in their home or test cage, submerged in 6 – 8 cm of water with their dorsal surface briefly exposed only for testing. Additionally, to prevent a coached response, probes or pipettes

were brought towards the animal from the caudal body aspect, preventing the animal from seeing the device's approach. Although using these precautions, unlike results in frogs (Willenbring and Stevens, 1996), the vF shows more measurement variation compared to the AAT.

Multiple factors contribute to the difficulty in translating the vF to the axolotl. Although care is taken such that the flexible fiber is placed perpendicular to the site of evaluation before the force is applied, the shape of the animal (curved body lateral to dorsal fin) and the presence of its natural mucous coating sometimes make it difficult to consistently apply the evaluator perpendicular to the animal's skin. Conversely, using an adjustable-volume pipettor, a small-caliber pipette tip, and a very small volume of acetic acid allows for the more precise application of this noxious stimulus. Furthermore, after a simple solution (i.e. cage tilting) was developed to keep the animal predominantly submerged while only exposing the dorsal surface just for the few seconds to apply the acetic acid, it was found that the AAT is an easier test to perform. Although noxious stimuli like the acetic acid test are transmitted along unmyelinated C fibers and thinly myelinated Aδ fibers while non-noxious stimuli like mechanical sensation activate rapidly conducting Aβ-like fibers (Willenbring and Stevens, 1996), which can account for variation between species, the human factors necessary to perform the tests and experimental setups must not be ignored when assessing a measurement tool's usefulness. The results of the two different quantitative approaches to measure pain in axolotls show that an adapted AAT is more repeatable and reproducible in causing a noxious stimulus in this model animal versus the non-noxious stimuli using the manual vF fibers.

After adopting the acetic acid test to work in axolotls, mixed partial opioid-receptor agonist-antagonist antinociceptives were tested to determine if they provide antinociception in these animals. Although studies caution the application of doses across unrelated species in the same class (e.g. Amphibia) (Farkas and Monaghan, 2015), without guidance on doses and route of application, buprenorphine (intracoelomic injection) and butorphanol (immersion) were used in the same doses and routes as published in the eastern red-spotted newt (Koeller, 2009). Using the doses in newts (buprenorphine: 50 mg/kg injection; butorphanol: 5 mg/L home cage water) versus control animals, no significant difference exists in response to acetic acid testing. Two animals in the buprenorphine arm also showed signs of adverse effects (constipation – no feces detected for two weeks after treatment) and had to be euthanized, removing buprenorphine from further use in this study. Although TUNEL staining is strong near the rectum, suggesting greater DNA damage, H&E results do not indicate any pathology in this area. However, the TUNEL staining results could be due to increased GI epithelial turnover. The only clear clinical observation is that the fecal output was reduced. This finding could be caused by the primary effect of opioids causing reduced GI motility or a local reaction to the intracoelomic injection of this buprenorphine formulation and concentration.Increasing the butorphanol dose by 50% to 0.75 mg/L of home cage water also did not show any significant differences in response to acetic acid testing versus control animals. Although these results suggest that butorphanol, using this route of administration and tested doses, does not provide antinociceptive effects for somatic pain, testing moved forward to see if butorphanol played a role in suppressing visceral pain, by comparing the response to noxious somatic stimuli after invasive cardiac surgery.

Following the application of a novel model of cardiac ischemia-reperfusion injury, axolotls were again subjected to the acetic acid test. Examining the results of the three treatment arms (mid-dose butorphanol, high-dose butorphanol, and control) no significant difference exists in response to acetic acid testing. Although this suggests that the doses of butorphanol did not have any effect on reducing stress, pain, or pain-induced stress, no adverse effects were seen in 37 animals that were treated with mid-dose (n = 19) and high-dose butorphanol (n = 18). Additional dose-response experiments are warranted to explore the required dosing for antinociception in axolotls. To determine if opioid use in studies for regeneration in axolotls do not confound tissue response, additional histology studies were completed.

After noxious stimulus testing, heart samples were collected to determine if butorphanol affects tissue regeneration through the modulation of immune function or direct cardioprotection through μ-opioid receptor stimulation. Samples were evaluated in a blinded manner by a veterinary pathologist (BHR) with training and experience in evaluating amphibian tissue histology and pathology. After performing a first-pass view of all samples, creating a scoring rubric, and then reassessing all samples against the scoring rubric, four features stood out as meaningful pathologic features for comparison: cellular proliferation scored by BrdU uptake, cellular death scored by TUNEL staining, and extent of inflammation scored by leukocyte (lymphocyte and heterophil) infiltration. Examining the results of the three treatment arms (mid-dose butorphanol, high-dose butorphanol, and control) no significant difference exists when evaluating the four histopathologic features, suggesting the doses of butorphanol administered to the animals do not have a dose-dependent or time-based (within 7-days) effect on tissue response after injury.

In summary, the work in this Specific Aim provides guidelines for future studies of tissue regeneration in the axolotl, and specifically, when combined with the model development in this Specific Aim, studies of cardiac tissue regeneration. By evaluating methods to assess pain, studying the use of opioids as antinociceptives, and applying these results to invasive surgical procedure in axolotls, investigators now have additional tools in their toolkit to ensure animal welfare while minimizing factors that can confound tissue responses after injury.

Specific Aim 2

Cardiac Regeneration After Ischemia-Reperfusion Injury

As previously mentioned, the cardiac regeneration field still does not have direct evidence that an adult vertebrate animal can use epimorphic or epimorphic-like processes to heal the heart after ischemia-reperfusion injury. Other cardiac injury surrogates have been used, all with differing severity and molecular signaling pathways that mediate injury, and shown to result in complete regeneration of the injured heart. However, these surrogates do not recapitulate an ischemia-reperfusion injury. Therefore, until now, the cardiac regeneration field has not been provided direct evidence that an adult vertebrate animal can regenerate a cardiac ischemia-reperfusion injury.

The evidence presented in this body of work is, to the author's knowledge, the first evidence that an adult vertebrate animal, the axolotl, can regenerate its heart after sustaining an ischemia-reperfusion event using a methodology (mechanically-induced ischemia) that produces the same pathophysiology of a myocardial infarction in mammals (i.e. coronary artery ligation). Histologic sections with qualitative and quantitative assessments, show a unique spatiotemporal evolution of the regenerating heart in the axolotl, creating just as many questions as answers to

how the axolotl mediates regeneration. Heart function is also seen to return as the reduction in fractional area change fourteen days following injury slowly returns to baseline by ninety days after injury. The interesting histology results require development of further immunohistochemical tools or next-generation sequencing and omics to help identify the constituents that may be involved in regenerating the axolotl heart. For now, the conclusion by Roy and Gatien from 2008 still hold (emphasis theirs): "One of the most frequent answers provided by experts in the field of epimorphic regeneration working on urodele amphibians during the question period following their presentations is: *unfortunately the answer to that question is unknown since no-one has yet looked at that pathway or tested that hypothesis*." Given the results of this body of work, hypotheses can be formed to drive future research directions.

Conclusions

Diseases of the heart, especially Ischemic heart disease, are the number one cause of death in the US and worldwide (Murphy et al., 2017; Organization, 2017; Xu et al., 2016). In adult patients that survive acute ischemic events, especially life-threatening conditions in the acute coronary syndrome spectrum, any areas of cardiac muscle that die from ischemia are repaired by connective tissue deposition (Robbins et al., 2010) rather than replacement with new cardiomyocytes. Because of severe sequelae that results from the replacement of functional cardiac muscle by inert, but structural connective tissue, most therapy for patients that survive to have chronic ischemic heart disease are treated mostly with supportive-care measures to reduce the oxygen needed by the heart, reduce the chance of deadly arrhythmias, prevent further arteriosclerosis development, and avoiding the formation of mural thromboses in the

heart that can lead to additional cardiovascular events (Lilly, 2011). With the only treatment option to return normal heart function only met by heart transplant, many researchers in the field have turned to stem cells and cell-based therapy as an approach to remodel hearts damaged by ischemia-reperfusion injuries.

With almost two decades of research using stem cells in human patients, the multiple clinical trials have had mixed results, from no significant change to slight improvements to left ventricle function (Nguyen et al., 2016). Cell-based therapy has not been the panacea many were hoping for, giving the field of cardiac regeneration the opportunity to pivot to new directions. While research on cell-based therapies on diseases of the heart continue, exploring other pathways of achieving heart remodeling after ischemia-reperfusion must be pursued. The motivation of this body of work was to study if an adult vertebrate animal known to heal injuries through epimorphic regeneration can rescue a heart damaged by an ischemia-reperfusion injury. From the question, the following hypothesis is formed:

> The axolotl, an animal capable of healing damaged organs and limbs throughout its lifespan through the process of epimorphic regeneration, can regenerate a cardiac ischemia-reperfusion injury as an adult.

Providing evidence to retain or reject this hypothesis provides two important answers to the field of regenerative medicine in cardiology: 1) “Is there something fundamental about the ischemia-reperfusion injury that prevents damaged cardiac tissue from being repaired by replacing dead tissue with new, healthy myocardium?”, and 2) “If a vertebrate animal can rescue myocardium damaged by an ischemia-reperfusion injury, how does it mediate this response?”.

Spatiotemporal histopathology results of the healing axolotl heart following ischemia-reperfusion injury provides evidence that adult vertebrate animals can regenerate damaged cardiac tissue without therapeutic interventions. However, complete regeneration of this serious injury requires more time than other injury modalities like apical resection, ventricular amputation, cardiac genetic ablation, or cryoinjury. To the author's knowledge, this is the first evidence of cardiac tissue regeneration in an adult vertebrate animal that is achieved without any therapeutic interventions. The evidence presented here concludes that there is nothing unique about an ischemia-reperfusion event in cardiac tissue – it can be repaired with new, healthy myocardium. However, due to limitations of antibodies that cross-react with axolotl proteins, the exact mechanism or mechanisms behind the regeneration of injured myocardium still needs to be elucidated. In place of a known mechanism, three working hypotheses on how cardiac tissue regeneration is mediated in the axolotl are informed from qualitative and quantitative data presented in this body of work.

Mechanisms of Regeneration: Hypotheses

With the evidence presented in this body of work, the following hypotheses are presented to outline additional opportunities for further study:

- The cardiac regeneration process differs from processes observed in zebrafish. Of note, instead of fibrin playing a role in the spatiotemporal regeneration in zebrafish, unknown eosinophilic protein(s) are present in the regenerating axolotl heart for thirty to sixty days following ischemia-reperfusion injury, possibly mediating repair.

- Nucleated RBCs are abundantly present in the wound area about thirty to sixty days post injury. These nucleated RBCs do not look like normal, smoothly shaped RBCs in naïve hearts. The jagged appearance may possibly indicate activated or stressed RBCs that may be more metabolically active, secreting small molecules or other paracrine signals and playing a proactive role in mediating tissue repair.
- Structural changes such as wavy fibers, contraction bands/coagulative necrosis, and hyaline change may distribute loading throughout the heart, stabilizing the injury, maintaining cardiac output, and mediating repair. Biomechanical unloading has been seen to play a role in reverse remodeling in human patients with heart failure – long-standing left ventricular assist device (LVAD) use has been shown to assist in reversing adverse remodeling in heart failure patients (Ambardekar and Buttrick, 2011)

Beyond creating a model of ischemia-reperfusion injury in the axolotl, the results presented here provide a platform to study proteins or other small molecules, paracrine signaling mechanisms, and biomechanical forces that play a role in axolotl heart regeneration after an ischemia-reperfusion event that can be translated to other animal models, first to rodents, then to pigs, and ultimately to human patients. The evidence of heart regeneration in an adult vertebrate animal following an ischemia-reperfusion event provides additional opportunities to tease out cardiomyocyte biology and can even bolster the current understandings of cell-base therapy approaches to make them more effective.

Future Research Directions

Ninety days following apical resection in the axolotl, the heart was completely regenerated after injury (Cano-Martinez et al., 2010). After developing a reproducible method to induce a true ischemia-reperfusion injury in the axolotl, cardiac tissue regeneration is evident ninety days after injury, but the regenerating myocardium is not fully organized and is infiltrated by connective tissue. Interestingly, unknown eosinophilic proteins in the hyaline change spectrum and red blood cells persist in the regenerating tissue structures, possibly mediating repair. Future studies should follow cardiac function through cardiac ultrasound, gross tissue inspection, and light-microscopy with histological staining, immunohistochemistry and electron microscopy for longer periods of time after injury. Some cryoinjury studies in zebrafish report complete regeneration one-hundred thirty days post injury (Gonzalez-Rosa et al., 2011) while a cautery injury model in the giant danio (*Danio aequipinnatus*) returned to non-injured morphology after one-hundred eighty days post injury (Lafontant et al., 2012). These results should guide future long-term studies post ischemia-reperfusion injury in the axolotl.

As the knowledge base develops from Specific Aims 1 and 2, the regions of the regenerating cardiac tissue should be carefully sampled and studied through RNA-sequencing approaches to elucidate the signaling mechanisms involved in axolotl cardiac regeneration following an ischemic injury. These activities should then be followed-up with proteomic analysis to determine what proteins eventually form and play a role in mediating cardiac repair in the axolotl following an ischemia-reperfusion injury in the heart. Additionally, antibodies that cross-react with axolotl proteins must be developed to help identify proteins that are not differentiated by simple histology staining.

APPENDIX A: PILOT STUDIES AND SUPPLEMENTARY INFORMATION

Quantitative Pain Assessments

Although bacteria can sense life threatening mechanical forces, is not until the evolution of the basic nervous system of the phyla Cnidaria and Ctenophora that we can find evidence of nociceptors. From these simple aquatic phyla, nociceptors have evolved throughout the animal kingdom to diversify into different classes in vertebrates that can detect multiple types of stimuli (Smith and Lewin, 2009). Noxious thermal, mechanical, and chemical stimuli testing in amphibians, and the increased latency to respond after the administration of morphine (Willenbring and Stevens, 1996) suggests that, as in mammals, an endogenous opioid system is present. From this evidence, and further characterization of cutaneous nociceptors, amphibians sense noxious thermal, mechanical, and chemical stimuli through Aδ-nociceptors and polymodal C-fiber nociceptors, the same signaling pathways as those found in mammals. Various quantitative testing methods have been developed to measure pain in laboratory animals. Two approaches used in previous amphibian testing (Willenbring and Stevens, 1996) were piloted for use in axolotls for this study.

Mechanical Stimulation with von Frey (vF) Filaments:

For these tests, axolotls are kept in their home polypropylene rat cage. Using manual von Frey [vF] aesthesiometers (Touch Test Sensory Evaluator, Stoelting, Wood Dale, IL), increasing force is applied at the site of evaluation (lateral to dorsal fin, in line with forelimb) until nociceptive behavior is observed at which point the applied force is recorded. Care is taken such that the flexible fiber is placed perpendicular to the site of evaluation before the force is applied. Additionally, the manual aesthesiometers are brought in from a caudal direction preventing the animal from visually detect the approaching stimulus.

The probes are supplied in force increments that are not linear. The following data (Evaluator marking and Force) in Supplementary Table 1 describe the manual vF probes used in this study:

Supplementary Table 1: Characteristics of von Frey Evaluators

Evaluator Marking	1.65	2.36	2.44	2.83	3.22	3.61	3.84	4.08
Force (Grams)	0.008	0.02	0.04	0.07	0.16	0.4	0.6	1
Evaluator Code	0	1	2	3	4	5	6	7
Evaluator Marking	4.17	4.31	4.56	4.74	4.93	5.07	5.18	
Force (Grams)	1.4	2	4	6	8	10	15	
Evaluator Code	8	9	10	11	12	13	14	

To make appropriate comparisons about the repeatability of von Frey aesthesiometers, the evaluators were mapped to an ordinal scale that includes 0. The smallest gauge filament (0.008 g of force) was defined as the scale's zero point as it would bend when touching the water surface due to surface tension (e.g. cohesive forces between liquid molecules at the liquid-air interface). The evaluator codes listed were used in the statistical analysis of data.

Chemical Stimulation with Acetic Acid Test (AAT):

For these tests, axolotls are placed in a smaller polypropylene mouse cage with enough 50% Holtfreter's solution to cover half of its body, leaving the dorsal surface above the waterline. The AAT is performed according to previously published reports in frogs(Willenbring and Stevens, 1996). Glacial acetic acid is serially diluted to produce 15 dilutions evenly spaced on a logarithmic scale. Testing starts with a negative control, a single drop (20 µL) of 50% Holtfreter's solution, to ensure the animal does not respond simply due to the mechanical stimulation of the water droplet. Testing proceeds by placing a single drop (20 µL) of the weakest concentration acetic acid lateral to dorsal fin, in line with hindlimb. The animal will be observed for a repeatable behavioral response (wiping, turning, escape behavior). If a response is not observed within 5 seconds, the area is rinsed using 50% Holtfreter's solution. Testing on the opposite side using the next highest concentration will occur. The testing continues, alternating sides, until the nociceptive threshold is reached which is the lowest concentration to produce a response. Once a response is observed, a subsequent test is performed with the next highest concentration on the alternate side. If the alternate side shows a positive response, the previous dose is recorded as the threshold. If no response is recorded on this alternate side, testing continues as described above. This approach ensures that the lowest dose is captured since there may be differences between the left and right sides of the animal. In between tests, the polypropylene mouse cage

is tilted to one side using a wedge to increase the perceived level of water by the animal, allowing the animal to be fully submerged, reducing the stress of being partially exposed during the AAT.

To make appropriate comparisons about the repeatability of the acetic acid test, the logarithmic concentrations were mapped to an ordinal scale that includes 0. The weakest concentration of diluted acetic acid (0.03 M) was defined as the scale's zero point as its use did not produce any response during pilot testing, controlling for mechanical stimuli (i.e. presence of liquid drop) with a negative control of 50% Holtfreter's solution. The following concentration/vial codes were used in the statistical analysis of data:

Supplementary Table 2: Serial Dilutions of Acetic Acid

Molarity	0.03	0.05	0.08	0.12	0.17	0.26	0.39	0.59
Vial Code	0	1	2	3	4	5	6	7
Molarity	0.88	1.32	1.98	2.96	4.44	6.67	10.00	15.00
Vial Code	8	9	10	11	12	13	14	15

Behavioral Assessments

Colloquially, nociception and pain are used interchangeably. Semantically, they are different as nociception deals with the detection and processing of a noxious stimuli while pain is the manifestation of this sensory processing. Specifically, nociception can be defined as "the neural process of encoding and processing noxious stimuli" while pain is described as a "complex constellation of unpleasant sensory, emotional and cognitive experiences provoked by real or perceived tissue damage and manifested by certain autonomic, psychological, and behavioral reactions" (Dubin and Patapoutian, 2010). To explore the efficacy of antinociceptives with interrupting the neural processing of noxious stimuli, it is important to observe behavioral reactions to qualitatively describe pain.

Feeding

At least one week of food consumption will be measured to establish a baseline intake. Also, feeding behavior (latency to feed) will be measured using a highly palatable treat, such as black worms. A few black worms (3-5) are placed in front of the animal in clear sight. Animals are

given up to 5 minutes to feed. A positive response is if the animal feeds on the worms, rather than simply snapping in the general direction of the worms.

Cageside Assessments

The animals will be assessed cageside by blinded operators at least twice daily at predetermined time points. One blinded operator consistently performs the cageside assessment methods to ensure repeatability of testing. Assessment methods will include observing body posture and physical responses after gently tapping on cage; squirting 3-5 mL of water from a syringe at the base of the head with an inline jet squirting from a caudal-to-rostral direction, a transverse jet aimed at the forelimb aimed at the dorsal fin, and a transverse jet aimed at the hindlimb at the dorsal fin; gently touching the animal at the mid-body and tail; and response to the placement of a novel object near the animal. The animals will be scored using a Likert-style system (0-3; no response, minor response, nominal response, and major response) developed from observations during pilot studies. The scoring rubric is found in Supplementary Table 3.

Supplementary Table 3: Likert Scores for Behavioral Testing

RESPONSE KEY				
TEST	**SCORE**			
	0	**1**	**2**	**3**
Tapping	No response	Bubbles	Limb movement	Gross movement
Water Jet	No response	Bubbles	Limb movement	Gross movement
Touching	No response	Any movement	Move away	Escape
Novel Object	No response	Bubbles	Limb movement	Gross movement

Pathology Scoring Rubrics

Histopathology was evaluated by an outside veterinary pathologist (Dr. Barry H. Rickman, BHR). BHR assessed all samples under blinded conditions and created ordinal scoring rubrics for clinically relevant pathology. After gaining familiarity with the samples, a Likert-style ordinal scale was created to describe the histologic features under review. Only immunohistochemistry slides

identifying TUNEL and BrdU and simple stains identifying heterophils, and lymphocytes were evaluated. The following tables contain the descriptions of the scoring rubric for each evaluation. Cardiomyocytes are abbreviated as CMs, high-power field is HPF.

Supplementary Table 4: Histology Scoring Rubric for TUNEL Immunohistochemistry

Score	Description
0	All fields negative.
1	Rare cells stain positive, dusting of nuclei, <5% of cells.
2	Few foci of few positive CMs, 5-25% of cells in ≥1 field.
3	25-50% with moderate nuclear staining in CMs in ≥1 field.
4	50-80% of cells with moderate nuclear staining in CMs in ≥2 fields
5	Over 80% of strong nuclear staining in CMs in ≥5 fields.

Supplementary Table 5: Histology Scoring Rubric for BrdU Immunohistochemistry

Score	Description
0	All fields negative.
1	Rare CMs or endothelial cells with positive nuclei, usually in undamaged area.
2	Few scattered positive CM ± endothelial cells, usually in undamaged area.
3	Multifocal, few to moderate positive CMs ± endothelial cells, usually in undamaged area.

Supplementary Table 6: Histology Scoring Rubric for Heterophils from H&E Staining

Score	Description
0	All fields negative.
1	Rare heterophils at the site of damage and hemorrhage, 1-2 per 40X HPF.
2	Few heterophils at site of necrosis and degeneration, 3-8 per HPF, 1 or more fields.
3	Moderate numbers of heterophils at the site of damage, 9-15 per HPF.
4	Large multifocal to coalescing numbers of heterophils at the site of damage, too many to count, > 17 per HPF.
5	Diffuse infiltration of large numbers of heterophiles.

Supplementary Table 7: Histology Scoring Rubric for Lymphocytes from H&E Staining

Score	Description
0	All fields negative.
1	Few scattered lymphocytes.
2	Moderate lymphocytic infiltrates.
3	Numerous lymphocytic infiltrates.

Preliminary Drug Studies

Past studies on opioid receptors in amphibians have described the subcutaneous (SC), intracoelomic (IC), intraspinal (IS), and intracerbroventricular (ICV) administration of opioids in these animals (Stevens, 1996, 2004; Stevens et al., 1994; Stevens and Rothe, 1997). With the parenteral delivery of analgesia, no external confounds to the pharmacodynamics or pharmacokinetics are expected. However, for the transcutaneous delivery of butorphanol, its behavior in the axolotl water used in our WSU DLAR husbandry of axolotls is unknown. The water used in all WSU DLAR axolotl husbandry is tap water treated using Kordon® water conditioner NovAqua® Plus™ and ammonia detoxifier AmQuel® Plus™ (http://www.kordon.com/kordon/products) with the addition of various salts to make 50% Holtfreter's solution. The only study identified in a publication search that used a transcutaneous method of butorphanol delivery in newts (Koeller, 2009) used aged tap water. Aged tap water is tap water that sits in an open container to allow chlorine to evaporate, allow dissolved gases to come out of solution (since tap water is usually delivered cold and under pressure), and allow water to equilibrate in temperature. Since the husbandry of axolotls here at WSU uses chemically conditioned water, characterizing how the axolotl water interacts with butorphanol is necessary to properly compare the efficacy of butorphanol against the efficacy of buprenorphine.

Butorphanol Degradation

The combination of axolotl water and butorphanol is a mixture of multiple chemicals and compounds. High-performance liquid chromatography (HPLC) was chosen as an appropriate method to separate, identify, and quantify the various components in the solution mixture. Various test runs were performed to choose the best parameters to elute the butorphanol (Torbugesic®, 10 mg/mL) in a timely manner. Also, to provide a reference signal that can

normalize the various runs with respect to differences in injected volume, buprenorphine (Buprenex®, 0.3 mg/mL) was used as an internal reference standard. Using guidelines from published studies that utilized HPLC to identify opioids in blood, plasma and urine (Boulton et al., 2002; Dams et al., 2002), various conditions were run on a 1260 Infinity Quaternary LC System (Agilent Technologies, Cat. No. 1260 Infinity Quaternary LC System). Following this parameter study, all the subsequent HPLC experiments used the following settings: Diode Array Detector Wavelength = 240 nm; Mobile Phase = 25% HPLC-grade water and 75% HPLC-grade acetonitrile; System Flowrate = 1.0 mL/min. To reduce the height of the internal reference standard peak, the supplied buprenorphine was diluted to 0.1 mg/mL using distilled water. Using these settings, butorphanol eluted from the column after around 2 minutes; buprenorphine was detected after about 15 minutes. A graph of characteristic elution curves is shown in Supplementary Figure 1. All experiments were run using the Agilent Technologies 1260 Quaternary LC System.

From the butorphanol study in newts (Koeller, 2009), the target dose is 0.5 mg of butorphanol per liter of axolotl water (or $0.5x10^{-3}$ mg/mL of axolotl water). Calibration standards were made that spanned a range from $1.0x10^{-4}$ – $1.0x10^{-3}$ mg/mL, bracketing the target dose. Each calibration standard was run at least three times to determine a calibration curve for future analytical studies. Combining all the elution curves from the final runs for each calibration concentration shows no significant trend between the various samples (see Supplementary Figure 1). Using the analytic reports from the Agilent Technologies 1260 Quaternary LC System, the percentage of area under each butorphanol curve, as compared to the entire area under the curve (AUC) for the total run, were graphed to check if any significant trends were apparent. For each identified peak, the area under each peak's curve signifies the quantity of the specific compound that is separated, eluted and detected by the diode array detector. The calibration solutions were mixed in a 1:1 ratio with the internal reference standard (buprenorphine, 0.1 mg/mL) with 50 µL of the sample injected into the HPLC apparatus. The intent was to determine a relationship between the calibration concentrations of butorphanol and the constant concentration of internal standard; any variations in volume injected would be compensated by taking the area percent that is due to butorphanol.

Considering the computed standard deviations for each proportion of area due to the elution of butorphanol, Supplementary Figure 2 does not reveal any clear trend in butorphanol concentration. Using SPSS (IBM Corporation©, Version 22) to run an ANOVA and correcting for multiple comparisons (Bonferroni method) confirmed that there are significant differences between comparisons of certain areas under the curve of the different calibration solutions, but there is no significant difference between all comparisons. Therefore, a distinct trend is not clear to enable the calculation of a calibration curve. A plot of the means from the ANOVA calculation is shown in Supplementary Figure 3. From these results, the HPLC runs are more qualitative than quantitative; a butorphanol concentration cannot be determined given elution data from an unknown sample. Thus, data from butorphanol samples run through the HPLC will at best be a "go/ no-go" assessment for the presence or absence of the analgesia in the axolotl water.

Moving forward, the next step was to determine if the axolotl water causes the degradation of butorphanol. The dosing frequency (Koeller, 2009) was a single bolus of 0.5 mg of butorphanol per liter of tank water for the 72-hour recovery period. In the WSU IACUC protocol (A 02-02-14) covering the animal studies, a daily water change was approved. Therefore, samples of "aging" butorphanol were analyzed at multiple time points during the first 24 hours to determine if additional "maintenance" doses of butorphanol would need to be added before a scheduled cage and water change strictly due to the background degradation of butorphanol. To compare to the previously published study, a reduced sampling interval of the butorphanol sample was used between 24-72 hours of aging.

Characteristic curves for the aging, degradation samples are shown in Supplementary Figure 4. Inspecting these curves shows that the shape of the butorphanol peak (~ 2 min) does not appreciably change from the 0-hour sample to the 73-hour sample. Graphing the percent AUC over all the time points also shows a mean value without an apparent trend over time (see Supplementary Figure 5). Running an ANOVA also show that there are no significant differences between the samples when correcting for multiple comparisons. From this data, we can conclude that butorphanol does not degrade when exposed to the chemicals used to treat tap water for use with amphibians, nor does it have any undue interaction with the salts in the axolotl water (50% Holtfreter's solution) that make it suitable for the physiology of axolotls.

Butorphanol Metabolism

Unlike the daily dosing of buprenorphine in the published study on newts (Koeller, 2009), butorphanol was administered only at the start of the 72-hour period in the recovery tank. The data do not show if this butorphanol dosing frequency maintained adequate levels of drug in the water; it can only be inferred that butorphanol was present after 72 hours from the results of the paper's behavioral assay showing differences between the animals in the treated group and the untreated control group. Still, even if metabolism kinetics of butorphanol in the newts were provided in the study, it is not expected to be directly applicable to axolotls(Farkas and Monaghan, 2015). Thus, a small study (n = 4) of the metabolism of butorphanol in axolotls was executed at the proposed initial dose (0.5 mg per liter of tank water) to determine if additional butorphanol must be administered during the 24-hour period between cage and axolotl water changes to compensate for axolotl metabolism of the drug.

The axolotls used in this drug metabolism study ranged in weight from 80-130g. This required the use of large, static mouse cage bottoms to house the animals with enough room for them to fit in either cage dimension without having to curl their body. Additionally, polycarbonate tunnels (designed for mouse enrichment) are included in WSU axolotl husbandry. With the large static mouse cage, it was determined that 5 liters of water is sufficient to fully submerge the polycarbonate tunnels.

To prepare for the metabolism study, clean large mouse cages were filled with 5 liters of fresh axolotl water using a 1000 mL beaker (measurement lines are ±5%). Subsequently, 2.5 mg of butorphanol was added to each cage (0.25 mL of as-supplied Torbugesic®). The contents in the cage were slightly agitated to mix the drug solution. Before placing the animal back into the cage, using a syringe and 18g needle, a 0-hour sample was taken by withdrawing ~1 mL from the center of the cage at a point halfway into the water. Each sample was combined, mixed thoroughly by pipetting and shaking, and then run through the HPLC. Over the next 48 hours, multiple samples (7, 24, and 46 hours) were removed from each animal in the same manner in the same position. These later samples were not combined – each individual axolotl's sample was run through the HPLC at the different sampling time points. Characteristic elution curves for the 0-hour sample are shown in Supplementary Figure 6. As this experimental condition replicated the target-dose

sample used during the characterization of the HPLC system, this figure closely mirrors Supplementary Figure 1. Characteristic elution curves for 7-hour, 24-hour, and 46-hour samples are shown in Supplementary Figure 7, Supplementary Figure 8, and Supplementary Figure 9 respectively. The elution curves for the 7-hour samples show little difference to the baseline 0-hour sample. The data at this timepoint suggests little to no change in the butorphanol has occurred. Looking at the 24-hour elution curves, we start to see additional peaks after the butorphanol peak, around the 3-minute and 4-minute time points. Although the appearance of these new, smaller peaks suggest that new compounds are appearing in the axolotls' water, possibly degradation products of the butorphanol, a strong butorphanol peak at the 2-minute time point is still present. Finally, in the 46-hour elution curves, we see the development of strong peaks at the 3-minute and 4-minute time points along with the appearance of smaller peaks in the 5 to 10-minute window. Like the 24-hour elution curves, even with the growth of the 3-minute and 4-minute time point peaks and the evolution of new smaller peaks, there is still a strong presence of the butorphanol peak at the 2- minute time point. The data suggests that butorphanol is still present in the axolotls' water even after 46 hours of metabolism. However, since the experiments to characterize a calibration curve were unsuccessful, the values of the various peaks obtained during this metabolism test give no indication of the butorphanol concentration in the axolotl water. This data reveal that the axolotls do not completely metabolize butorphanol over a 48-hour period, eliminating the need to re-dose the animals before a water change is required (water is changed every day during the analgesia study). To reveal if the initial dose of butorphanol provides a high enough plasma level for therapeutic levels of pain relief, executing the surgery protocol is required.

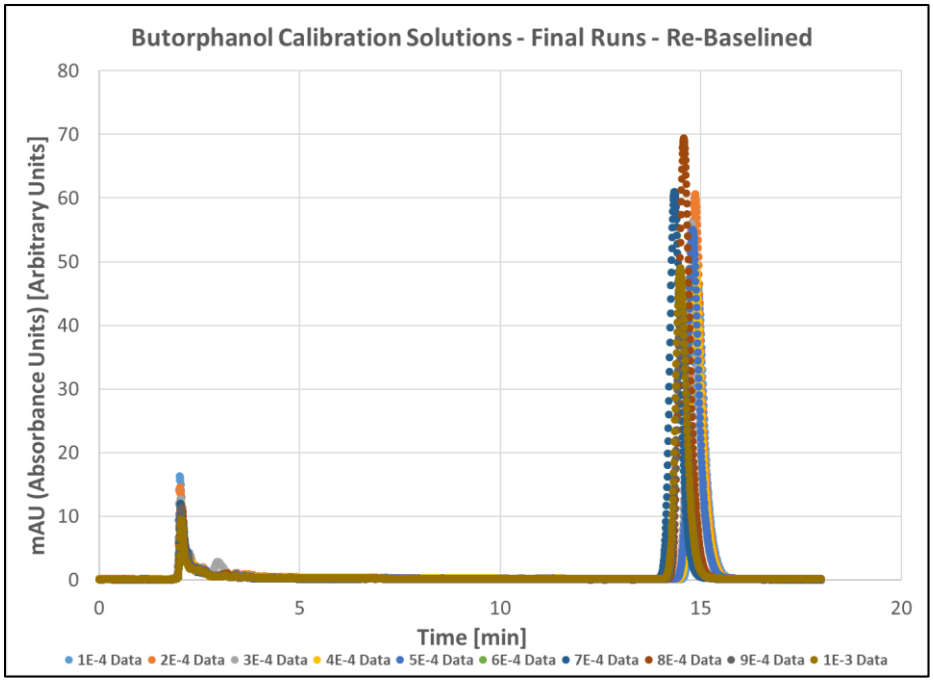

Supplementary Figure 1: Characteristic elution curves of butorphanol (~2 minutes) and buprenorphine (~15 minutes) in axolotl water using various calibration solutions for butorphanol.

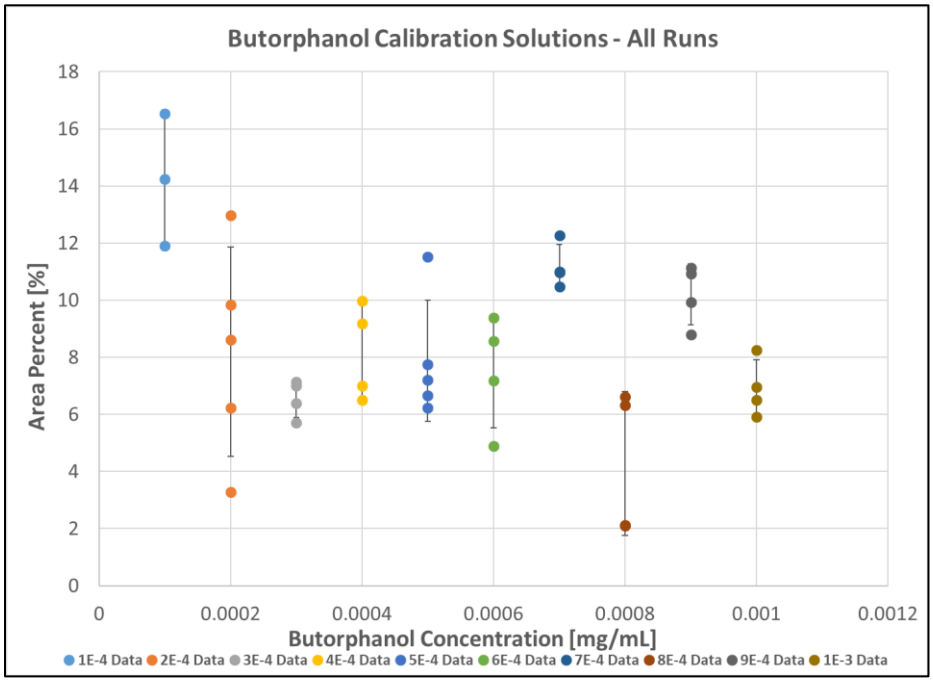

Supplementary Figure 2: Area percent of the identified peak for various butorphanol calibration solutions.

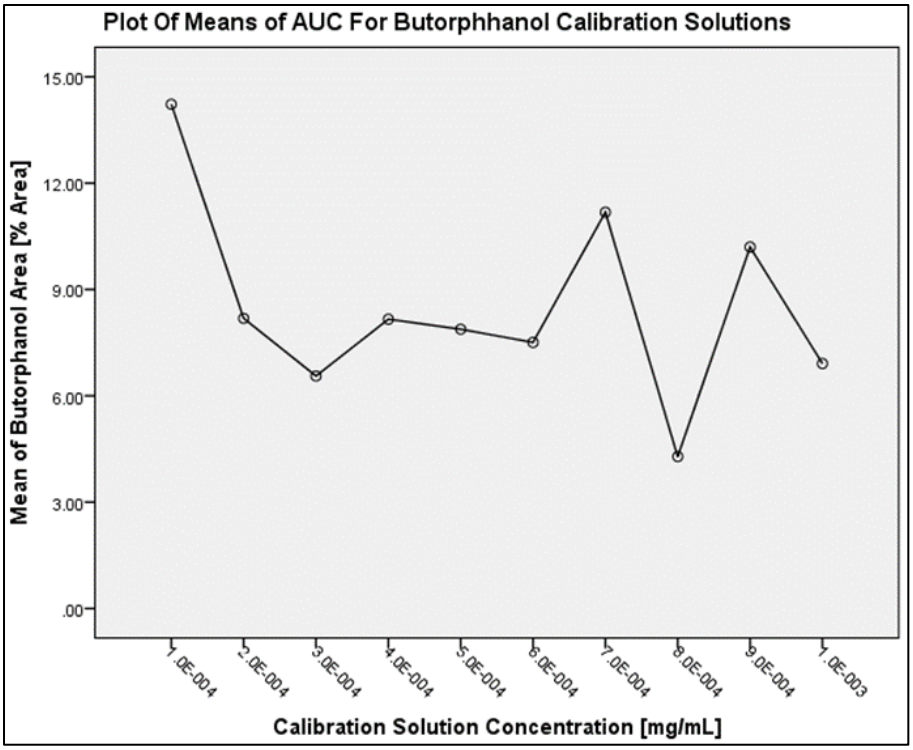

Supplementary Figure 3: Plot of the means of the AUC for each butorphanol calibration solution. No clear calibration curve can be determined from this data.

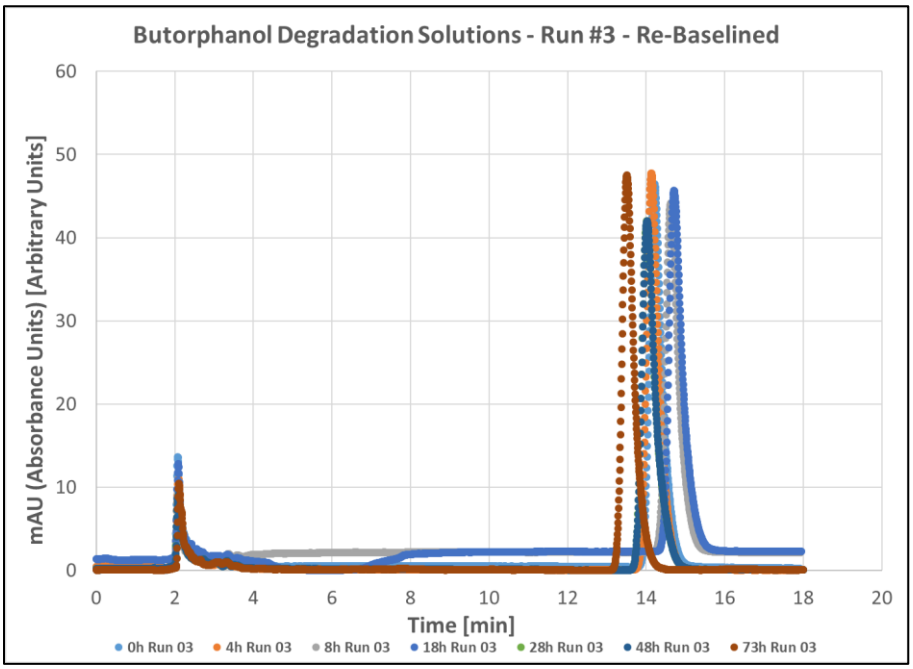

Supplementary Figure 4: Characteristic elution curves of butorphanol and buprenorphine in axolotl water using a solution of target-dose butorphanol aged before running the HPLC characterization. The curves have been shifted to a zero baseline.

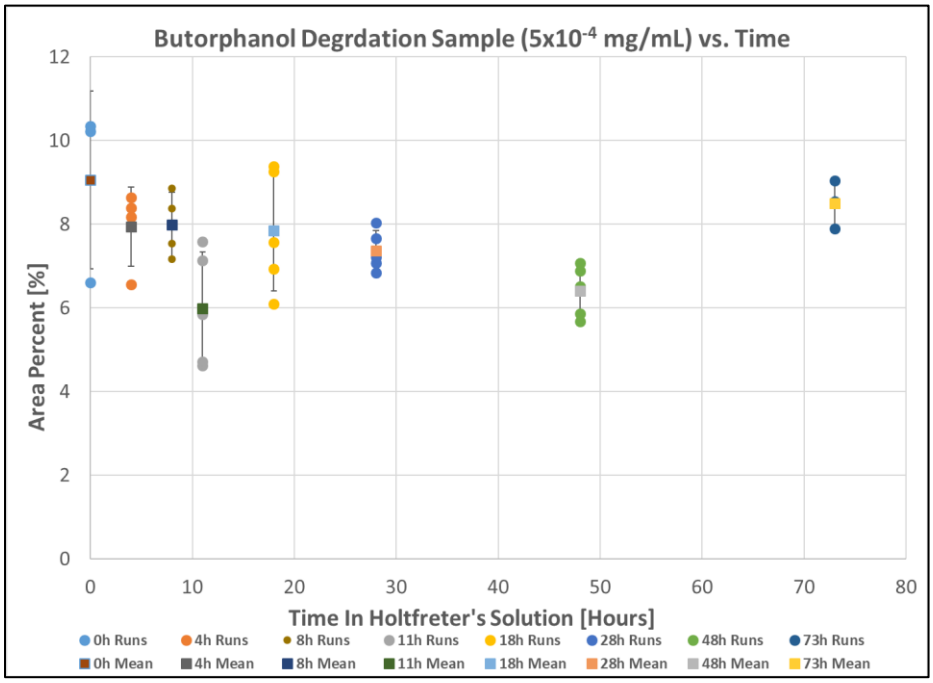

Supplementary Figure 5: Area percent of the identified peak for various time points for the butorphanol degradation sample.

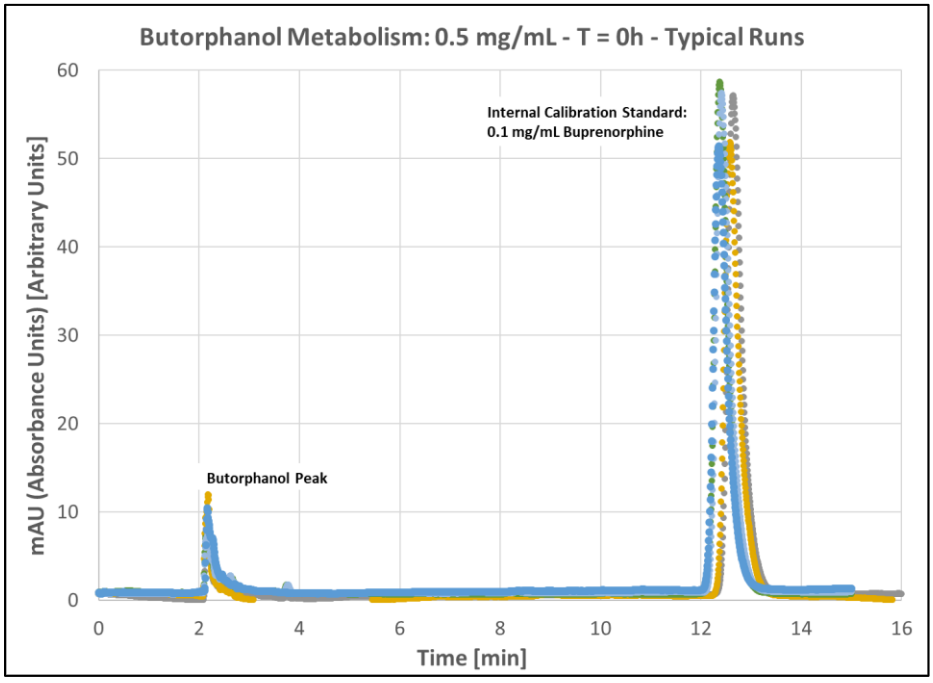

Supplementary Figure 6: HPLC results of 0-hour samples in the axolotl butorphanol metabolism study.

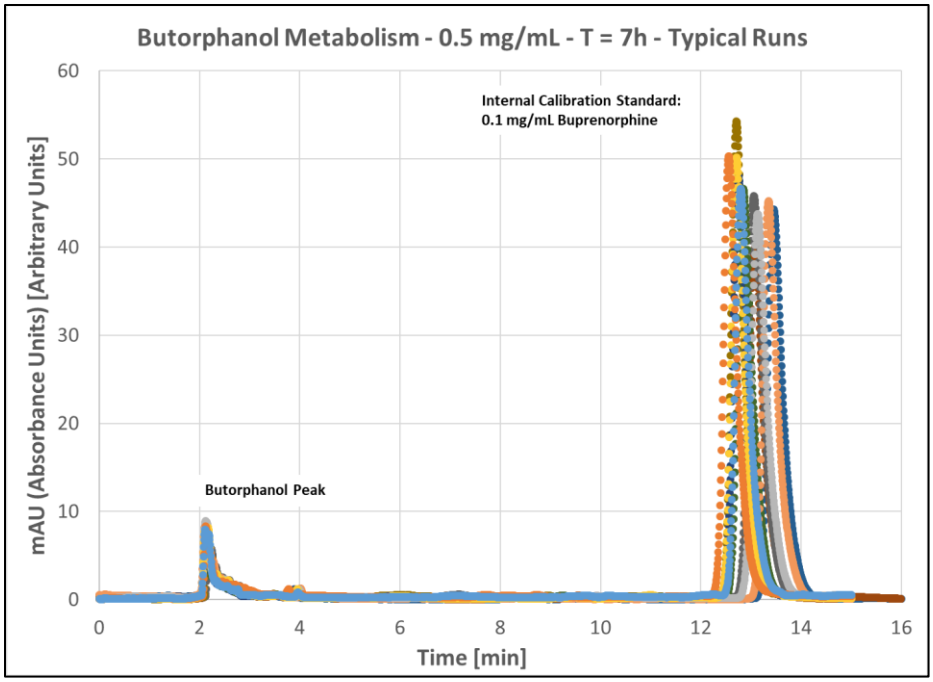

Supplementary Figure 7: HPLC results of 7-hour samples in the axolotl butorphanol metabolism study.

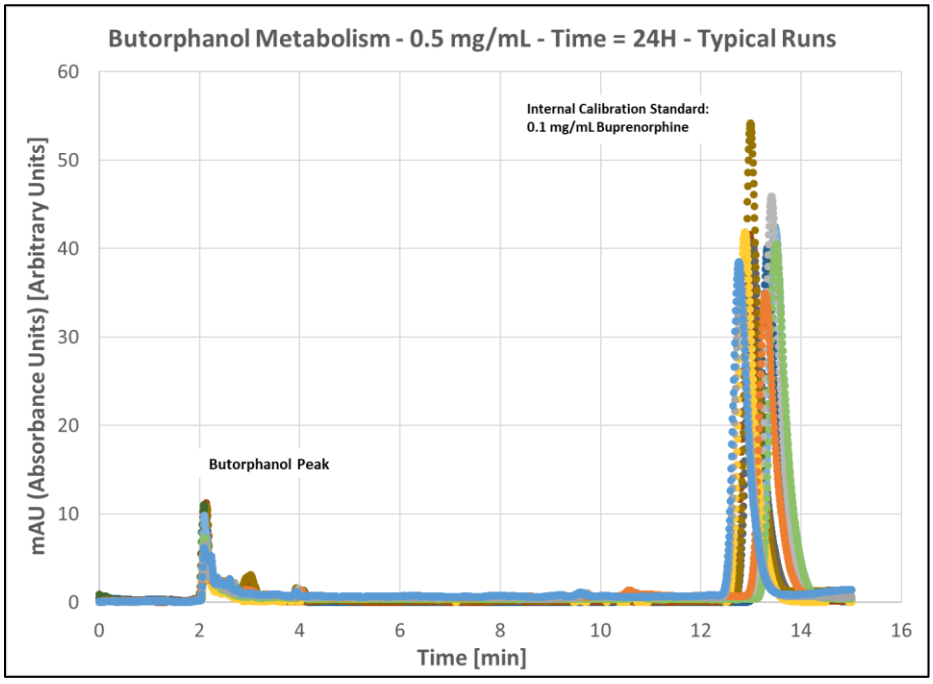

Supplementary Figure 8: HPLC results of 24-hour samples in the axolotl butorphanol metabolism study.

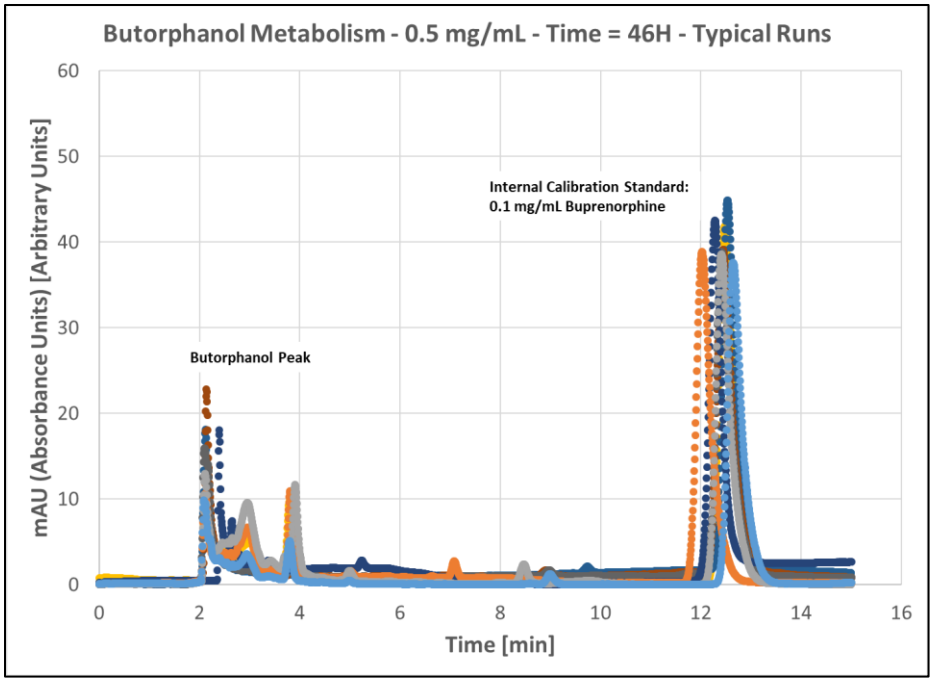

Supplementary Figure 9: HPLC results of 46-hour samples in the axolotl butorphanol metabolism study.

MATLAB® Code for Image Post-Processing and Fractional Area Change Calculations

Verasonics provides template codes to end users as a programming example. The base script with file name SetUpL22_14vFlashAngles.m from Verasonics, last updated 12/07/2015 for SW 3.0, was used a baseline script file to operate the L22 linear transducer. The only modification was to enable the ongoing storage of 500 frames in a frame buffer and enable a Control Panel button to capture the current frames in the buffer and output to an audio-video interleave file.

Although no post-processing of the incoming receive signal is performed, there are controls on the MATLAB® front panel that allow for refinement of the ultrasound waves that are emitted by the crystals and detected by the transducer. Supplementary Figure 10 shows the settings used when scanning and recording heart motion.

The Image Processing Toolbox suite add-on is required to access additional MATLAB® functions to process image data that were used to process ultrasound images in this work. Image contrast adjustment functions were piloted and options were identified to the author's preference since all analysis will be done by the author.

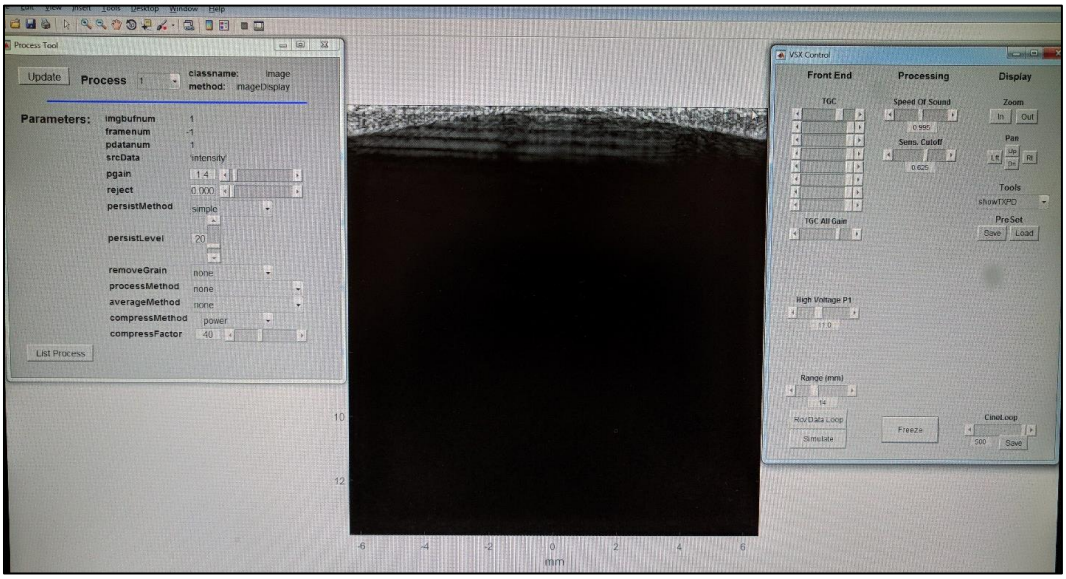

Supplementary Figure 10: VSX Control and Process Tool Settings in MATLAB®
Settings to run Verasonics Vantage 128 system to collect echocardiography data on axolotls.

The final function call to enhance a grey scale image has the form:

Filtered_Image = adapthisteq(Raw_Image,'distribution','exponential','NumTiles',[16 16])

Final MATLAB® Code

Note: To use in MATLAB®, replace | in code with curly brackets (||=} and (| = {). This was done to prevent EndNote X7 from creating errors in Word.

```
% This script is written to calculate Fractional Area Change (FAC) of heart
% function. Regions of interest (ROI) are manually defined by the user and
% MATLAB does the FAC calculations.
% Jay Llaniguez (jllanigu@med.wayne.edu)

clearvars; clc; % Clear variables and command window

%% Choose image for systole and define path and filename.
[FileNameSys,PathNameSys,FilterIndexSys] = uigetfile(...
                    |'*.jpg;*.tif;*.png;*.gif','All Image Files';...
                    '*.*','All Files'||,...
                    'Select Image for Systole');
%% Choose image for diastole and define path and filename.
[FileNameDia,PathNameDia,FilterIndexDia] = uigetfile(...
```

```
                |'*.jpg;*.tif;*.png;*.gif','All Image Files';...
                '*.*','All Files'||,...
                'Select Image for Diastole');
%% Read images into workspace as variables.
FilePathSys = strcat(PathNameSys,FileNameSys); %Systole image.
FilePathDia = strcat(PathNameDia,FileNameDia); %Diastole image.
SysFormatSpec = "Systole File Read Is: %s \n";
DiaFormatSpec = "Diastole File Read Is: %s \n";
SysFileRead = sprintf(SysFormatSpec,FilePathSys);
DiaFileRead = sprintf(DiaFormatSpec,FilePathDia);
fprintf(SysFormatSpec,FilePathSys);
fprintf(DiaFormatSpec,FilePathDia);
I_Sys = imread(FilePathSys); %Reads in RGB (Truecolor) file.
I_Dia = imread(FilePathDia); %Reads in RGB (Truecolor) file.
% An RGB image, sometimes referred to as a truecolor image, is stored as an
% m-by-n-by-3 data array that defines red, green, and blue color components
% for each individual pixel.
% Need to convert to Black & White (Grayscale) to perform following
% calculations.
BW_Sys = rgb2gray(I_Sys);
BW_Dia = rgb2gray(I_Dia);
% Apply contrast filters.
Filtered_Sys = adapthisteq(BW_Sys,'distribution','exponential','NumTiles',[16 16]);
Filtered_Dia = adapthisteq(BW_Dia,'distribution','exponential','NumTiles',[16 16]);
%% Turn off image resize warnings.
% Turn off this warning "Warning: Image is too big to fit on screen; displaying at 50% "
% To set the warning state, you must first know the message identifier for the one warning you
want to enable.
% Query the last warning to acquire the identifier.  For example:
% warnStruct = warning('query', 'last');
% messageID = warnStruct.identifier
% messageID = Images:initSize:adjustingMag
warning('off', 'Images:initSize:adjustingMag');
%% Manually define Regions of Interest (ROI).
ROI_Sys = roipoly(Filtered_Sys);
ROI_Dia = roipoly(Filtered_Dia);
close(intersect(findall(0,'type','figure'),1)) %Close last roipoly window.
%% Calculate Fractional Area Change Using Two Methods
% bwarea
BW_Sys = bwarea(ROI_Sys); %# of pixels in systolic binary image (BI) mask.
BW_Dia = bwarea(ROI_Dia); %# of pixels in diastolic binary image (BI) mask.
FAC_BW = (BW_Dia - BW_Sys) / BW_Dia * 100; %FAC using bwarea.
formatSpec_BI = 'Fractional Area Change using bwarea is %4.2f%% \n';
fprintf(formatSpec_BI,FAC_BW)
```

```
% regionprop
% Calculate area and perimeter in systolic binary image (BI) mask.
RP_Sys = regionprops(ROI_Sys,'Area','Perimeter');
% Calculate area and perimeter in diastolic binary image (BI) mask.
RP_Dia = regionprops(ROI_Dia,'Area','Perimeter');
FAC_RP = (RP_Dia.Area-RP_Sys.Area)/(RP_Dia.Area)*100; %FAC using regionprop.
formatSpec_RP = 'Fractional Area Change using regionprop is %4.2f%% \n';
fprintf(formatSpec_RP,FAC_RP)
% Extra Calculations - Fractional Perimter Change using regionprop.
FPC_RP = (RP_Dia.Perimeter-RP_Sys.Perimeter)/(RP_Dia.Perimeter)*100;
%% Write image files to disk.
prompt = |'Enter Axolotl ID:','Enter Video Number:','Enter Systolic Frame Number:','Enter
Diastolic Frame Number:','Trial'||;
dlg_title = 'Input';
num_lines = 1;
answer = inputdlg(prompt,dlg_title,num_lines); % Cell array of inputs.
% Build names of output files.
Filtered_Sys_Out = strcat(PathNameSys,answer|1||,'_','Video',answer(Galvez et
al.),'_','Systole','_',answer|3||,'.png');
Filtered_Dia_Out = strcat(PathNameSys,answer|1||,'_','Video',answer(Galvez et
al.),'_','Diastole','_',answer|4||,'.png');
ROI_Sys_Out = strcat(PathNameSys,answer|1||,'_','Video',answer(Galvez et
al.),'_','Systole','_',answer|3||,'_','ROI','.png');
ROI_Dia_Out = strcat(PathNameSys,answer|1||,'_','Video',answer(Galvez et
al.),'_','Diastole','_',answer|4||,'_','ROI','.png');
% Write out individual files.
imwrite(Filtered_Sys,Filtered_Sys_Out);
imwrite(Filtered_Dia,Filtered_Dia_Out);
imwrite(ROI_Sys,ROI_Sys_Out);
imwrite(ROI_Dia,ROI_Dia_Out);
% Save workspace variables.
Variables_Out = strcat(PathNameSys,answer|1||,'_','Trial','_',answer|5||);
save(Variables_Out); % Creates MATLAB® formatted binary file (MAT-file).
%% Plot filtered images.
figure; imshow(Filtered_Sys); title(['Filtered Systolic Image Of Axolotl: ',num2str(answer|1||),';
Trial: ',num2str(answer|5||),'; Video: ',num2str(answer(Galvez et al.)),'; Frame:
',num2str(answer|3||)]);
figure; imshow(Filtered_Dia); title(['Filtered Distolic Image Of Axolotl: ',num2str(answer|1||),';
Trial: ',num2str(answer|5||),'; Video: ',num2str(answer(Galvez et al.)),'; Frame:
',num2str(answer|4||)]);
```

APPENDIX B: IACUC & DLAR DOCUMENTATION – ANIMAL PROCEDURES

The development of a novel, mechanical approach to induce ischemia in both mammalian and amphibian animal models is central to this plan of work. Paramount to comparing the tissue response to ischemia between the two animals is the use of an identical injury model that uses a consistent method to induce ischemia, leading to cellular necrosis, and subsequently producing an area of infarcted tissue. Performing the commonly used ligation of the left anterior descending (LAD) artery to induce ischemia in mammals leads to a consistent and reproducible volume of myocardium at risk (Salto-Tellez et al., 2004; Wang et al., 2006). However, lacking coronary arteries (Reese et al., 2002), performing a coronary artery ligation in amphibians is not an option. Other models to induce cardiac tissue damage such as cryoinjury (van den Bos et al., 2005) or diphtheria-toxin-receptor conditional ablation (Akazawa et al., 2004) do not recapitulate the pathophysiologic processes in ischemia-induced cardiac tissue necrosis. Therefore, the concept of mechanically clamping the apex of the heart to prevent perfusion of cardiac tissue can be applied in both animals and produces the environment (inadequate blood flow to the beating ventricular myocardium) for the desired pathophysiology (ischemia-induced cellular necrosis) and tissue pathology (myocardial infarction).

Justification of Use

Axolotl (Ambystoma mexicanum) – The zebrafish (*Danio rerio*) has been extensively studied as a model for cardiac regeneration (Jopling et al., 2010; Poss, 2007; Poss et al., 2002; Raya et al., 2004; Zhang et al., 2013) due to its many advantages in modeling human disease (Chico et al., 2008; Dooley and Zon, 2000; Kari et al., 2007). However, the zebrafish heart is much more primitive than mammalian hearts: zebrafish have two-chambered hearts that currently lack any evidence of secondary heart field derivatives (Lieschke and Currie, 2007). With their three-chambered hearts, amphibians also exhibit physiological traits in common with all vertebrates including mammals (Burggren and Warburton, 2007). Compared to zebrafish, the closer developmental ancestry of amphibians to mammals suggest they are more suitable models for modeling mammalian and human diseases (Burggren and Warburton, 2007; Voss et al., 2011); despite differences with higher mammals, epicardial development in the axolotl is similar to the general pattern described for higher vertebrates (Fransen and Lemanski, 1990). Additionally,

they also have been recently evaluated as models for cardiac regeneration (Cano-Martinez et al., 2010; Roy and Gatien, 2008).

Observations of the axolotl's ability to regenerate have historically been attributed to the neotenic development of axolotls (Roy and Gatien, 2008). The ability to robustly regenerate during juvenile stages of development is corroborated by observations that animals of the *Xenopus* genus lose the ability to regenerate when they begin to metamorphose into an adult (Whited et al., 2012)]. The overall goal of this proposal is to move towards a more mechanistic explanation to elaborate the differences between non-mammalian vertebrates and higher mammals. Studies have detailed robust myocardium regeneration in higher mammals, albeit only in very young animals (Haubner et al., 2012; Porrello et al., 2011; Rumyantsev, 1977). More importantly, these studies confirm the genetic programs for cardiac repair exist within mammalian DNA, but are somehow quickly suppressed. Determining the presiding molecular and cellular mechanisms in the axolotl heart and expressing them in mammalian cardiomyocytes will help elucidate the mechanisms behind the repressed ability to remodel the damaged adult mammalian heart with native cardiac cells (Xin et al., 2013).

To elucidate the processes that prevent cardiac regeneration in humans, we must use an animal model with a known, robust response in repairing cardiac tissue after injury. The axolotl has been chosen based on its well-documented repair and regeneration capabilities that are not duplicated in commonly used laboratory animal models (Cano-Martinez et al., 2010; Roy and Gatien, 2008). Also, using a less sentient, non-mammalian species for survival-surgery procedures is desired over similar studies performed on higher mammals.

Studies outlined in the axolotl cannot be replaced by non-animal models. There are currently no established axolotl cell lines available for purchase and the full axolotl genome is almost completely sequenced, but not fully characterized, preventing researchers from performing *in vitro* experiments or using mathematical or computer models. The sample size of 6 animals per matched group (each animal will serve as its own matched groups, 10 separate days for sampling) was determined by assuming an $\alpha = 0.05$ and a $\beta = 0.05$ in sample size calculations while estimating a large effect size ($\sigma = 0.25$ for laboratory-bred animals) (Drăghici, 2012) in the differential expression of ligands, receptors, transcription factors, signaling proteins

and cell cycle regulators. The choice of a large effect size is based on the benchmarks for success in axolotl survival surgery. Since our protocol for inducing a myocardial infarction relies on a visible functional change of cardiac tissue (damaged tissue must be quiescent or contracting irregularly and at a much lower rate than remote regions of the heart), the intracellular and extracellular milieu of the damaged heart should be significantly different than remote regions of the heart. Also, since the axolotls are being purchased from a laboratory-bred colony, the genes should be quite homogenous leading to a lower standard deviation in measurements across animals.

Mouse (*Mus musculus*) – For comparisons to a higher mammal, the mouse has been chosen due to the wide use of this animal in cardiovascular disease research (Battey et al., 1999). Protocols detailing cardiac procedures for inducing cardiac injury such as MI are widely published (Azhar et al., 1999; Bernal et al., 2009; Michael et al., 1995; Tarnavski et al., 2004; Yang et al., 2002; Yue et al., 2013). Additionally, the availability of robust technologies for the mechanistic study of cellular gene expression and gene regulation (Field, 1993; Lewandoski, 2001; Yamamoto et al., 2001) make the mouse a particularly well-suited model for studying cellular pathways and molecular mechanisms. Well-characterized models of molecular-genetic systems can be used to validate the results of this research proposal *in vitro* with primary cell cultures of cardiomyocytes. The future application of Specific Aims 1 and 2 is to generate transgenic mice that express cardiac-specific, drug-inducible genes that confer increased myocardial regenerative capacity. In these conditionally drug-induced transgenic animals, the efficacy of reawakening myocardial regeneration will be assessed in a model of MI compared to control animals (non-induced transgenes and syngeneic wild-type animals).

Veterinary Care

Animals will be housed in Association of Assessment and Accreditation for Laboratory Animal Care- (AAALAC) accredited vivariums located in facilities supervised by the Animal Facilities Core/Department of Laboratory Research. These facilities are overseen by licensed veterinarians, supervised by Wayne State University's (WSU) Attending Veterinarian (AV), as required by the Animal Welfare Act Regulations. Daily feeding, care and monitoring are performed by DLAR personnel as defined by protocols that are being developed by the PI and the

AV. Newly ordered axolotls will be isolated from current animals and allowed to acclimate to their new surroundings for 7-10 days before any procedures are initiated. This is to reduce stress on the new animals and prevent the transmission of any organisms or contaminants from the supplier.

Procedures to Minimize Discomfort, Stress, Pain and/or Injury

Axolotls and mice will be visually inspected daily for signs of discomfort, stress, pain and injury. Since axolotls are an uncommonly used laboratory animal, specific protocols will be developed with the AV to ensure DLAR personnel are vigilant to their needs. Any animals that show signs of prolonged discomfort or pain shall be removed from the study and treated as needed; if measures become futile, animals shall be euthanized. All survival surgical procedures will be performed under anesthesia (0.1% tricaine methanesulfonate baths for axolotls, intraperitoneal pentobarbital [70-80 mg/kg] injections or isoflurane [1-3% in oxygen] for mice).

Method of Euthanasia

Axolotls requiring euthanasia will first be brought to a surgical plane of anesthesia by placing the animal into a bath of 0.1% tricaine methanesulfonate. Once anesthesia has been induced, the animal can be euthanized by placing it into a bath of 0.5-1.0% tricaine methanesulfonate for at least 60 minutes. For assurance of death, the axolotl will be decapitated and the brain and spinal cord pithed. This method is taken directly from the 2013 edition of American Veterinary Medical Association (AVMA) Guidelines for the Euthanasia of Animals.

Mice requiring euthanasia will be subject to an environment of increasing carbon dioxide concentration until breathing has stopped. For assurance of death, a cervical dislocation will be performed after breathing has stopped for at least one minute in the hypoxic environment. This method is taken directly from the 2013 edition of AVMA Guidelines for the Euthanasia of Animals.

Proposed Use of Animals

The following section provides detail on the use of animals in this plan of work. This is the full approved version of WSU IACUC Protocol A 02-02-14 incorporating all amendments through February 2017. This was moved to eProtocol 16-12-173 once the protocol expired in February 2017.

WAYNE STATE UNIVERSITY

APPLICATION TO USE VERTEBRATE ANIMALS FOR RESEARCH OR TEACHING

2015

Animal Welfare Assurance # A3310-01

INSTRUCTIONS:

1. Check deadline dates for submission.
2. Verify that this is the most recent version of the Protocol Application (see footer).
3. Submit the Protocol Application and the associated grant(s) (if applicable) with an Animal Hazardous Agents Form *via email* to IACUC@Wayne.edu. The subject line of the email should read: "NEW PROTOCOL (PI Name)"
4. You will be contacted by the IACUC Office regarding the *pre-review* of your application.
5. After you have *finalized the application through the pre-review process*, you will be instructed to deliver the following to the IACUC Office:
   a. The SIGNED ORIGINAL application
   b. ONE copy of the grant(s)/proposal(s) (if applicable)

For IACUC Office Use Only – Leave Blank
IACUC NUMBER: A 02-02-14
Veterinary Reviewer: Brossia-Root
Primary Reviewer:
Secondary Reviewer:
REVISED:

INSTITUTIONAL ANIMAL CARE AND USE COMMITTEE
87 E. Canfield, Second Floor
Phone Number: (313) 577-1629
Protocol submission: IACUC@Wayne.edu

I. – ADMINISTRATIVE DATA

1. Principal Investigator for Protocol (PI on Grant Proposal)**:**

Name and Degree: Jeremy T. Llaniguez, B.S, M.S.	University Title: MD/PhD Candidate	WSU Access ID (e.g. aa1234): Et9286
Primary Department/Division: Biomedical Engineering	Office Address: 6135 Woodward Ave, Room 1420	Office Phone: 313.577.1360
E-Mail Address: jllanigu@med.wayne.edu	Laboratory Phone: 313.577.1304	Emergency Phone: 310.880.9946 (Mobile)

2. Title of Project: (This should match the title on the grant proposal)
"Elucidating Cardiac Repair Mechanisms in Animals with Robust Regeneration to Enhance Cardiac Repair in Humans"

3. Title of Master Protocol or Core/Program/Consortium Project: (Include name of PI listed on face page of grant):
N/A

4. Co-Investigator or Faculty Advisor:

	Not Applicable
	Co-Investigator
X	**Faculty Advisor** (if the PI is not a faculty member)

	The Co-Investigator will be responsible for ALL animal work

Name and Degree: Dr. Juri Gelovani, MD/PhD	University Title: Chair, Biomedical Engineering	WSU Access ID (e.g. aa1234): fg0846
Primary Department/Division: College of Engineering/Biomedical Engineering	Office Address: 6135 Woodward Ave, Room 1417	Office Phone: 313.577.1346
E-Mail Address: juri.gelovani@wayne.edu	Laboratory Phone: 313.577.1304	Emergency Phone: 713.632.4969 (mobile)

5. Research Personnel: List all persons (other than the PI/Co-I) who will work with animals on this project. Indicate which individuals should be listed as Emergency Contacts. Emergency Contacts need to be able to authorize treatment or euthanasia in the event that the PI/Co-I CANNOT BE REACHED.
IMPORTANT: Review the IACUC Training Requirements**.** All laboratory personnel must complete the appropriate training, some of which must be finished ***before*** this protocol can be submitted.

Name/Degree/Title	WSU Access ID:	Office/Lab Phone	Home/Cell Phone	E-mail Address	Emergency Contact (Y/N)
Stephen DiCarlo, PhD, Professor	ae8278	313.577.1557	N/A	sdicarlo@med.wayne.edu	N
Heidi Lujan, PhD, Assistant Professor of Research	ae8936	313.577.1557	N/A	hlujan@med.wayne.edu	N
Tara Cotroneo, DVM, Director, Veterinary Technical Services	et1135	313.577.1156	N/A	tara.cotroneo@wayne.edu	N
Gerald Hish, DVM, Director, Veterinary Surgical Services	fz2469	313.577.1405	N/A	fz2469@med.wayne.edu	N
Charles Chung, PhD, Assistant Professor	fx6780	313.577.1540	N/A	cchung@med.wayne.edu	N
Morgan Szczepaniak	fp3474	313.577.8303	N/A	morgan.szczepaniak@wayne.edu	N

[X] This research will/may involve students/visitors (not listed above). Checking this box affirms that you will comply with the Supervised Student or Visitor Training Policy.

6. Primary Contact for IACUC Correspondence (choose one):

[X] **Principal Investigator**
[ ] **Co-Investigator**
[ ] **Research Staff Member (from question #5), specify:** **N/A**

[ ] **Other (list below):**

Name/Degree/Title	Office/Lab Phone	Home/Cell Phone	E-mail Address
N/A	N/A	N/A	N/A

7. Source of Funding:

[ ] **Internal (specify):**

[ ] **Subcontract (specify):**
[X] **External (specify):**

[ ] Submitted (notification pending):
[ ] Just In Time (funding anticipated)
[X] Awarded: AALAS GLAS Standard Grant

8. If this protocol is being submitted with a GRANT/PROPOSAL/CONTRACT, are all the procedures described in this protocol?
NOTE: Federal agencies require that all procedures using animals described in the grant/proposal must be approved by the IACUC. If this is an initial submission of a multi-year grant beyond the three year protocol period, all the work and number of animals must be included in this protocol application.
[ ] **Not Applicable**

[ ] **Yes**
[X] **No**

If no, list any animal experiments in the associated document(s) that are NOT described in this protocol, and explain their exclusion in the box below. This may include work that has already been completed, work that will not be conducted (the granting agency must already be aware of the exclusion), or work that will be performed by collaborators at other institutions.

This protocol is a pilot study for surgical techniques and procedures to ensure the success of a novel cardiac ischemia model. This protocol does not cover the exact studies outlined in the accompanying F30 NIH grant; it will be used to ensure the surgical approaches we use will result in the highest animal survival rates once the full protocol is executed. Thus, an amendment to this protocol will be filed (after the pilot study is complete and before actual experiments begin) detailing the use of multiple animals (n=6) per experimental group (a group consisting of a cohort of animals euthanized at a certain time point after surgery) to achieve statistical significance will be submitted once the exact surgical procedures have been ascertained using the pilot study outlined in this protocol. Additionally, the accompanying grant also describes testing the findings of Specific Aim 1 (which uses the novel cardiac ischemia model) with primary cell culture studies (Specific Aim 2). The creation of the primary cell cultures using neonatal cardiac muscle cells has also been excluded from this surgical pilot study protocol; it shall be included in the protocol amendment that shall encompass all tests of the accompanying grant.

9. Has this protocol (or a very similar protocol) been submitted to the IACUC under an alternate funding source?

[X] **No**
[ ] **Yes: STOP – file an amendment to add/change the funding source and modify animal number or procedures if necessary.**

10. Type of Project: (Check all appropriate boxes below)

[X] **New Protocol**

[ ] **Continuation of Expiring Protocol** **Replacing Protocol:** **A** [ ][ ] - [ ][ ] - [ ][ ]

a. Provide a brief summary of the work completed under the expiring protocol. *It may be helpful to include the number of animals that were used/bred related to how many were approved in the expiring protocol; DLAR can provide you with a report, call 577-1107.*

b. Describe any unexpected adverse events that resulted in increased pain, distress or death rates to animals that were not described in the original protocol. Include how these were managed and what steps were taken to prevent recurrence (if applicable). *Please make sure that any additional adverse effects, expected mortality, pain category changes, humane endpoints, etc. have been incorporated into this application.*

c. Do you have animals currently in-house that will be transferred to this renewal protocol upon approval?
[ ] **No**
[ ] **Yes (Please include them in Q18 Transfer of Animals table)**

[X] **Research**
[ ] **Teaching**
[ ] **Other (Please List):**

[ ] This includes research that involves the *use of facilities* at **John D. Dingell VAMC, Detroit, MI (station number 553)**
Add "**(VAMC)**" to the end of your project title.
Please note that VA research cannot be initiated until after R&D Committee approval.

II. – QUALIFICATIONS/EXPERIENCE OF PRINCIPAL INVESTIGATOR AND RESEARCH PERSONNEL

11. Previous Experience and Responsibilities for this Protocol: Identify the responsibilities of each individual (include the PI and all research personnel), his/her experience with the procedures and the animal species, and who will train personnel on the procedures for work specific to ***this protocol***.

			Years of Experience			
Name	Species	Specific Role in Project*	**With this species**	**With these procedures**	**With survival surgery** (if applicable)	Who will train the individual?**
Dr. Juri Gelovani	Axolotl	Faculty advisor; will not perform procedures on animals.	0	0	0	N/A
	Mice		20	20	20	N/A – Trained & Experienced
Jeremy (Jay) Llaniguez	Axolotl	Care, handling, pre-treatments, anesthesia, surgery (survival & non-survival), monitoring, post-procedural care, euthanasia, and behavioral assessment.	0	0	0	DLAR External Labs***
	Mice		<1	<1	0	DLAR
Dr. Stephen DiCarlo	Mouse	Training/advice on surgical procedures.	>30	>30	>30	N/A – Trained & Experienced
Dr. Heidi Lujan	Mouse	Training/advice on surgical procedures, perform intubations, assist with thoracotomies.	>20	>20	>20	N/A – Trained & Experienced
Dr. Tara Cotroneo	Axolotl	Care, handling, pre-treatment, monitoring, post-procedural care, behavioral assessment and euthanasia.	N	<1	<1	N/A
Dr. Gerald Hish	Axolotl		N	<1	<1	N/A
Morgan Szczepaniak	Axolotl	Care, handling, pre-treatment, monitoring, post-procedural care, and pain/behavioral assessments.	N	<1	<1	N/A
Charles Chung	Axolotl	Echocardiography of animals, training of other personnel on protocol.	N	<1	<1	N/A

*Examples include: care, handling, pre-treatments, **oral gavage**, anesthesia, **surgery** (***indicate*** whether it is **survival** or **non-survival)**, monitoring, post-procedural care, euthanasia in the stated species.

**Training can be listed as "N/A – Trained and Experienced" (this question only applies to the procedures described in this protocol)

***Axolotl training from an external lab will be through the University of Kentucky's Ambystoma Genetic Stock Center.

12. Are there any non-routine measures, such as special vaccines or additional health screening techniques that would potentially benefit staff (e.g. research, husbandry, veterinary) that participate in or support this project? Routine measures included in the Occupational Health and Safety Program (vaccination for tetanus, rabies, and hepatitis B, and TB screening) need not be mentioned here.

[X] **No**
[ ] **Yes (describe them below):**

III. – PURPOSE AND POTENTIAL VALUE OF STUDY

13. **In non-technical, everyday language that a senior high school student would understand, BRIEFLY state the research or development question to be addressed in this protocol. Also, explain the potential value of this study and the ways the proposed animal use might benefit human or animal health, the advancement of knowledge, education and training, or the good of society.**
A scientific abstract from a grant or funding proposal is not acceptable. Do not describe experiments or procedures, or use abbreviations. The information provided in this section could be used for possible press release. Please limit the response to one-half page.

The leading cause of death in the US and worldwide result from cardiovascular diseases such as myocardial infarction (heart attack), that due to the lack of cardiac tissue repair or regeneration often leads to death. In contrast to humans and other mammals, lower vertebrate species such as the axolotl (an aquatic salamander) and zebrafish can regenerate severed or injured limbs and other organs including the heart. The major innovation of this project is to use systems biology (the study of interactions between individual biological components and/or pathways) and comparative transcriptome analysis (the characterization of messenger RNA to understand which areas of DNA are important) approaches to understand the differences in gene expression responsible for higher regenerative capacity of cardiomyocytes (heart muscle cells) in lower vertebrates that is lost or suppressed in mammals and humans. The ultimate application of this knowledge will be to modify cells (e.g. cardiomyocytes or stem cells) to enhance myocardial regeneration for therapy of myocardial infarction.

IV. – ANIMAL USE JUSTIFICATION

The US Animal Welfare Act (AWA) and USDA Policy #12 regulations require principal investigators to consider alternatives to procedures that may cause more than momentary or slight pain or distress to animals, and provide a written narrative of the methods used and sources consulted to determine the availability of alternatives, including **refinements**, **reductions**, and **replacements** (the 3Rs).

Examples of Refinement: The use of most appropriate anesthetics and analgesics, the use of remote telemetry to increase the quality and quantity of data gathered, and humane endpoints.

Examples of Reduction: The use of shared control groups, preliminary screening in non-animal systems, innovative statistical packages or a consultation with a statistician.

Examples of Replacement: Alternatives such as tissue culture models, or computer-based simulations. Alternative animal models lower on the phylogenetic scale (i.e. using a mouse model in lieu of a non-human primate model).

14. **Consideration of Alternatives and the Prevention of Unnecessary Duplication.** Complete items below. Keep copies of computer database search results in your files to demonstrate your compliance with the law if regulatory authorities or the IACUC should choose to audit your project.

The USDA webpage **Literature Searching and Databases** contains links to excellent resources that can help you better understand the requirements and organize your search for alternatives.

WSU Medical School – contact Shiffman Medical Library via askmed@wayne.edu or 313-577-1094
WSU General Libraries – visit ASK-A-LIBRARIAN; subject specialists are available.

a. **Investigators must consider less painful or less stressful alternatives to procedures, and provide assurance that proposed research does not unnecessarily duplicate previous work.** You should perform one or more database searches to meet these

mandates unless compelling justifications can be made without doing so. Complete the table below for each database search you conduct to answer the questions below.

The literature search must **not be older than 3 months** at time of submission of this protocol application.

Name of the database(s)	Date search was performed	Period (years) covered by each search	Key words and/or search strategy used	Indicate below for which alternative mandate each search was conducted by placing an "X" in the proper column			
				Computer models or *in vitro* techniques	Use of less-sentient species	Use of less stressful model or methods, or fewer animals	Lack of unnecessary duplication
Google Scholar PubMed Web of Science Scopus	22/DEC/13	1990-2013	Axolotl Sal Site	X (Computer models)			
Google Scholar PubMed Web of Science Scopus	22/DEC/13	1990-2013	Axolotl Culture Cardiomyocyte	X (*In vitro* techniques)			
Google Scholar PubMed Web of Science Scopus	22/DEC/13	1990-2013	Axolotl Cell Line	X (*In vitro* techniques)			
ATCC (www.atcc.org)	22/DEC/13	N/A	Axolotl	X (*In vitro* techniques)			
Google Scholar PubMed Web of Science Scopus	14/FEB/14	1990-2014	Computer Models Cardiac Axolotl Study	X (Computer models)			
Google Scholar PubMed Web of Science Scopus	14/FEB/14	1990-2014	Models Cardiac Axolotl Study		X		
Google Scholar PubMed Web of Science Scopus	14/FEB/14	1990-2014	Myocardial Infarction Axolotl			X	X
Google Scholar PubMed Web of Science Scopus	14/FEB/14	1990-2014	Cryoinjury Myocardial Infarction Axolotl			X	X
Google Scholar PubMed Web of Science Scopus	14/FEB/14	1990-2014	Murine Cardiac Regeneration Computer Model	X (Computer models)			
Google Scholar PubMed Web of Science Scopus	14/FEB/14	1990-2014	Murine Cardiac Regeneration in vitro	X (*In vitro* techniques)			
ATCC (www.atcc.org)	14/FEB/14	1990-2014	Murine	X (*In vitro* techniques)			
Google Scholar PubMed Web of Science Scopus	14/FEB/14	1990-2014	Cardiac Regeneration Model Organisms		X		
Google Scholar	14/FEB/14	1990-2014	Mechanical			X	X

PubMed Web of Science Scopus			Clamp Myocardial Infarction Murine				
Google Scholar PubMed Web of Science Scopus	14/FEB/14	1990-2014	Cryoinjury Myocardial Infarction Murine			X	X

b. Could any of the animal procedures described in this protocol be replaced by non-animal models, such as mathematical models, computer simulations, or *in vitro* biological systems? Indicate below if such replacement is or is not possible, and ***provide a narrative*** as on how you came to your conclusion.

Initial studies outlined in the axolotl cannot be replaced by non-animal models. A search using Google Scholar and PubMed (Search 3) show there are currently no established axolotl cell lines available for purchase to conduct *in vitro* experiments. This is corroborated by the lack of axolotl cell lines (Search 4) from a commercial laboratory (American Type Culture Collection [ATCC]). Additionally, the full axolotl genome has not been completely sequenced and characterized, preventing researchers to rely solely on computational models (Search 1). We plan on using the axolotl based on its well-documented repair and regeneration capabilities that are not duplicated in commonly used laboratory animal models [1-14]. Also, per question 14c below, the use of a less sentient, non-mammalian species (such as the axolotl) for survival-surgery procedures is desired over similar studies performed on higher mammals.
For comparisons of findings in the axolotl to a higher mammal, the mouse has been chosen due to the wide use of this animal in cardiovascular disease research. Protocols detailing cardiac procedures for inducing cardiac injury such as myocardial infarctions are widely published [15-27]. Additionally, the availability of robust technologies for the mechanistic study of cellular gene expression and gene regulation make the mouse a particularly well-suited model for studying cellular pathways and molecular mechanisms [28-31]. Gene transduction systems can be used to validate the results of this research proposal in vitro with primary cell cultures of cardiomyocytes.

c. Could a smaller, less sentient mammalian species or a non-mammalian species (e.g. fish, invertebrates) substitute for the mammals in any of the experiments planned? Indicate below if such substitution is or is not possible and ***provide a narrative*** on how you came to your conclusion.

Smaller, less sentient, non-mammalian species will be used as the starting animal model to determine gene expression in cardiac tissue after cardiac injury. Since we are comparing the differences in cardiac regeneration between lower vertebrates and mammals, comparisons with a mammalian species (*Mus musculus* in our protocol) is paramount to the success of the research proposal. Thus, as the ultimate goal of the research is to verify if regeneration mechanisms in mammals can be reawakened using mechanisms found in other lower vertebrates, a non-mammalian model cannot be used. The findings must be validated in a mammalian system.

i. Describe the *BIOLOGICAL* characteristics that make each *species, strain* and *sex* selected the most appropriate for this project. If you will use transgenic, knockout or knockin animals, describe the unique feature(s) of each. Cost is not an acceptable consideration.

Axolotl (*Ambystoma mexicanum*) – This species is being chosen for its ability to repair and regenerate damaged tissues due to experimentally induced injury [8,11] or natural trauma [9]. Multiple laboratories are working on completing the genomic sequence and characterizing the next-generation sequencing reads for this species, making the axolotl attractive to performing genomic/transcriptomics studies in the field of regeneration. Additionally, they are larger than newts, making them easier to manually handle and perform survival cardiac surgery compared to their smaller-sized cousins. Males and females will be used in the experiments to reduce confounding. The wild-type, laboratory bred animals available from the Ambystoma Genetic Stock Center (AGSC) located in the Department of Biology at the University of Kentucky (Lexington, KY) will be sufficient for our experiments. No specific transgenic axolotl strain is required for the proposed procedures.
Mice (*Mus musculus*) – The strain of choice for cardiac injury procedures in mice will be wild type C57BL/6J mice, to be acquired as outlined in Question 17. Both male and female mice will be used to reduce confounding. As stated before, this strain is widely used in cardiovascular research and in genomic studies. Additionally, the mouse has been chosen for comparison testing as recent studies have been published concerning the transient regeneration of the

neonatal mouse heart, including one study that provided information on transcriptome data (RNA-Seq) of the transient regeneration evinced by neonatal mice. Results in this research proposal can be compared to these published studies.

d. Could a different animal model or different animal procedure that involves (1) less distress, pain, or suffering, or (2) fewer animals substitute for any proposed animal model or animal procedure planned? Indicate below if such replacement is or is not possible, and ***provide a narrative*** on how you came to your conclusion:

The overall project course described in question 13 will use less sentient, non-mammalian species that are known to express the desired tissue repair and regeneration characteristics to drive more focused experiments in mammalian *in vitro* models. This will reduce distress, pain and suffering when validating the results in the mammalian cellular system. However, to ascertain the differences between the lower vertebrates and mammalian models, we still must use mammalian species when performing survival surgery procedures to compare the tissue response between the two animals.

In the cardiac anatomy of the axolotl [1], cardiac arteries are not present to provide a blood supply to the exterior portions of the heart. Unlike mammals that have coronary vasculature (e.g. right coronary artery [RCA], left anterior descending [LAD] artery and/or left circumflex [LCX|| artery), inducing a myocardial infarction (MI) by coronary artery ligation or occlusion to produce an environment of ischemia (for studies in mice see [15-21,23-27]) is not possible in axolotls (salamanders in general); past studies in myocardial regeneration in axolotls have used resection models [8,11] that do not replicate the tissue injury in ischemia. In order to compare the differences in cardiac-tissue response and regeneration after ischemia between lower vertebrates and mammals, a common model of inducing ischemia in both animals is required.

Although there is building evidence of the utility of cryoinjury for studying mammalian cardiac scarring and regeneration responses (due to the similarity in evolving tissue histology during tissue repair and scarring) [25], the mechanism of cellular damage due to cryoinjury [32] do not engage the same response mechanisms of apoptosis due to ischemia [33,34]. In summary, cell death due to cryoinjury is immediate, a consequence of the rapid rate of tissue freezing using liquid nitrogen (LN_2). Specifically, in cryoinjury, ice crystal formation first occurs in the extracellular matrix, creating a hyperosmotic extracellular environment (solution-effect injury) that draws water away from cells. As a result, cells shrink damaging cell membranes and intracellular constituents. With further cooling, ice crystals soon form within cells, disrupting organelles, protein trafficking and physically shearing cell membranes. This rapid and mechanically-based disruption of normal cell physiology does not allow the cell to respond to the insult by transcribing new mRNA and translating new proteins that can help it survive the injury.

On the other hand, the cellular-response to damage from ischemia is not mediated by immediate cell death. For irreversible injury to occur, cardiac cells must be subject to ischemia for greater than 20 minutes [33,34]. During this time, the cells are able to respond to the insult by upregulating and/or downregulating genes that regulate apoptosis and cell function [33,35]. Additionally, late-phase responses to ischemia play a role in cell survival [36].

With coronary artery ligation/occlusion not possible in both animals and with cryoinjury a non-ideal approach to study the change in tissue responses due to ischemia, a novel method of inducing ischemia (mechanically occluding tissue) is being explored. We are also looking to use the same regions of tissue (apical portions) between the two animals, instead of achieving ischemia in axolotls using mechanical clamping and an established model of ischemia in mice like LAD ligation since it has been noted that different regions of the heart respond differently to ischemia (apical vs. ventricular vs. atrial cardiac tissue) [37].

Mechanically clamping a portion of tissue has inherent variability in the resulting infarct size. However, this pilot protocol will develop procedures and time points for mechanical clamping to induce ischemia in a minimum volume (e.g. a 30-minute clamping time results in a minimum volume of ischemic tissue from the apex to a point 2mm deep from that landmark). Therefore, although the border regions may vary in distance from the apical landmark, defining a minimum volume will allow us to sample tissue in the full protocol that excludes tissues of variable ischemic exposure.

e. Does the proposed research unnecessarily duplicate previous work? Indicate below if the proposed work unnecessarily duplicates previous work and ***provide a narrative*** on how you came to your conclusion:

The proposed research does not unnecessarily duplicate previous work. Unlike past studies in the axolotl (and urodeles in general), most experiments have examined the repair and regeneration of limbs of the appendicular skeleton. Most

studies have focused on these areas of the axolotl and urodeles due to the ease of tissue sampling and animal handling. Studies that have focused on the regeneration and repair of the heart have not used the same approach that we propose – combining immunohistochemistry, cellular mitogenic response and cellular morphology to identify robustly regenerating axolotl cardiac tissue for next-generation sequencing studies. Past studies have relied on observational studies of regeneration, rather than the mechanisms that regulate and control its expression.
Many reviews in the field of regenerative biology and medicine have called for greater understanding of the molecular pathways that drive cardiac regeneration to help serve as the platform for understanding outcomes of prior pre-clinical and clinical human studies of cardiovascular diseases and to drive future experiments in understanding cardiac tissue repair. Some investigators have attempted stem-cell therapies in human patients using data from murine studies; however, due to the lack of standardized protocols of stem cell isolation/cultivation and/or stem cell administration and dosing schedules, the results of these clinical trials have been mixed. We would like to elucidate the exact spatiotemporal gene expression cascade in animals with robust cardiac tissue regeneration in order to understand what proteins, signaling molecules and receptors play a role and when they are needed in order to reawaken cardiac tissue regeneration in mammals.

15. Indicate the METHOD used to determine the group size of animals needed for this study.

Note: The *Guide* states that whenever possible, the number of animals requested should be justified statistically. A power analysis is strongly encouraged to justify group sizes when appropriate. Please provide this information.

a. [ ] Group sizes determined statistically. State what statistical analysis was performed and give the power function. The variance may be estimated from similar previously published studies. Software such as that available at www.poweranalysis.com or www.statistics.com may be helpful.

N/A

b. [ ] Group sizes based on quantity of harvested cells or amount of tissue required. Elaborate. (Note: A statement such as "The study requires 50 experiments" is not sufficient.)

N/A

c. [X] Pilot study or preliminary project, group variances unknown at present. ***Minimal number of animals should be requested***. You must provide justification for the number of animals you are requesting. State the basis for your request.

This protocol is piloting a novel model of inducing cardiac ischemia. Through this study, we will be honing techniques to increase the post-operation survivability of the animals and to determine the overall rate of mortality due to complications from ischemia/reperfusion. A total of 5 of each animal species will be needed to practice techniques, while 10 will be used to determine the feasibility of the mechanical clamping method to induce ischemia, determine the minimum clamping time to ensure a minimum volume of ischemic tissue and to calculate the post-operative mortality rate. The total number of animals required for the pilot study is 15.

d. [ ] Other – Elaborate and justify criteria used to determine group size.

N/A

V. – ANIMAL SUBJECTS (NUMBER, HOUSING AND CARE)

Please review the detailed Explanation of USDA Reporting Codes.

Brief examples:
Category B: Animals being bred but not used for experimental purposes.
Category C: Experimental animals that will experience no pain or distress.
Category D: Experimental animals where anesthetic or analgesic agents are used to avoid pain or distress.
Category E: Experimental animals where anesthetic or analgesic agents cannot be used to avoid pain or distress.

NUMBER OF ANIMALS - If this is an **initial submission of a multi-year grant** beyond the three year protocol period, **all the work and number of animals** must be included in this protocol application. For all other submissions, list the total number of animals to be used over the **3 YEAR PERIOD of this protocol** (or for the life of the project if less than 3 years)

16. Indicate how the total number of animals needed for this study was reached for each USDA category (group size X groups in each experiment X number of experiments). Provide the number and type of experimental and control groups in each experiment, the number of experiments planned, and the number of animals in each group. Include all animals in each USDA category, including those that will be needed for training and those that will be culled.
The number and category of animals in this section must match the animal tables below (17, 18, 19).

DO NOT cut and paste your experimental aims from your grant proposal.

Details of each procedure are to be described in the appropriate questions (33, 34 and/or 35), **NOT** here.

Surgical Technique Study:
This group will be used to test intubation equipment and surgical tools for thoracotomy.
Axolotl (*Ambystoma mexicanum*) – Group Size (n=1) X Groups / Experiment (g = 1) X Number of Experiments = 1 X 1 X 5 = 5
Mice (*Mus musculus*) – Group Size (n=1) X Groups / Experiment (g = 1) X Number of Experiments = 1 X 1 X 5 = 5

Ischemia Model Pilot Study:
This group will be used to validate the mechanical clamping methodology of inducing ischemia in the animal models.
Axolotl (*Ambystoma mexicanum*) – Group Size (n=1) X Groups / Experiment (g = 1) X Number of Experiments = 1 X 1 X 14 = 10
Mice (*Mus musculus*) – Group Size (n=1) X Groups / Experiment (g = 1) X Number of Experiments = 1 X 1 X 10 = 10

Analgesia Sub-Study:
This sub-study will be used to identify the optimal analgesia dosing and determine, whether, and to what degree, opioid analgesics affect tissue healing and regeneration in a surgical model in axolotls.
Experiment 1: 6 axolotls/group x 2 groups = 12 axolotls
Experiment 2: 6 axolotls/group x 6 drug/dose groups (Re-use 12 animals from Experiment 1 + 24 additional animals)
Experiment 3: 6 axolotls/group x 3 groups (Re-use 12 animals from the low dose groups in Experiment 1 + 6 additional axolotls for no the analgesic group)
Experiment 4: 6 axolotls/group x 3 groups x 3 sample endpoints (12h, 2d and 7d) = 54 animals
Total Animals = (12 + 24 + 6 + 54) x 10% (unexpected attrition) = 106

Ischemia Study:
Axolotl (*Ambystoma mexicanum*) – Group Size (n=6) X Sample Endpoints (s = 5) = 6 X 5 = 30
The 5 group endpoints are: 12h, 2d, 7d, 30d, and 90d.
To account for 10% unexpected losses (i.e. sudden cardiac death): Total = 30 + (0.10 * 30) = 33 animals

If applicable, the results from the 12h, 2d, and 7d endpoints from the Analgesia Sub-Study can be used to reduce the total number of animals that need to be used.

Mice that have been identified for euthanasia can be transferred from other PIs/Protocols/DLAR VTS (using source transfer) to be used in acute surgical practice procedures. Also, retired breeders can be ordered as outlined in Question 17 to be used in acute surgical practice procedures.

17. Animals to be PURCHASED from an approved vendor:
☐ **Not Applicable**

SPECIES, STRAIN, SEX, AGE/WEIGHT *State nomenclature of genetically engineered (GE) or mutant rodents*	NUMBER OF ANIMALS TO BE USED UNDER USDA CATEGORY				SOURCE Vendor (include stock/catalog number for transgenics)	HOUSING LOCATION Building
	B	**C**	**D**	**E**		

Axolotl (*Ambystoma mexicanum*) Phenotype: Wild-type / Mutation: None Sex: Male & Female Age: Juvenile (8-10m) or older	0	0	107	14*	Ambystoma Genetic Stock Center (Lexington, KY). No stock number; use phenotype description.	Gordon Scott Hall Building IBIO Building
Mice (*Mus musculus*) Strain: C57BL/6J Sex: Male & Female Age: Adults (3-5 m)	0	0	19	9*	The Jackson Laboratory Harlan, Taconic	Gordon Scott Hall Building IBIO Building
Mice (*Mus musculus*) Strain: C57BL/6J Sex: Male & Female Age: Retired Breeders	0	0	15	0	The Jackson Laboratory Harlan, Taconic	Gordon Scott Hall Building IBIO Building

18. Animals to be TRANSFERRED FROM an expiring WSU protocol and/or SHIPPED FROM another institution.

[X] **Not Applicable**

SPECIES, STRAIN, SEX, AGE/WEIGHT *State nomenclature of GE or mutant rodents*	NUMBER OF ANIMALS TO BE USED UNDER USDA CATEGORY				SOURCE IACUC protocol number (or PI & Institution)	WSU HOUSING LOCATION Building
	B	**C**	**D**	**E**		
Mice (*Mus musculus*), C57BL/6J, Sex: Male, Age: Adults (3-5 m)	0	0	1	1	WSU IACUC Protocol: A 06-13-13, A 08-04-14	Elliman DLAR

[ ] I will contact DLAR Hospital (577-1343) regarding shipping arrangements and quarantine requirements.

If animals are shipped/transferred TO OTHER INSTITUTIONS, the request must be submitted prior to shipment as an **amendment to the protocol and DLAR must be contacted for shipping arrangements.*

19. OFFSPRING/FETUSES/EMBRYOS OBTAINED FROM ARRIVING PREGNANT DAMS OR FROM IN-HOUSE BREEDING: Accurate records of the number of animals produced and their ultimate disposition are required

[ ] **Not Applicable**

SPECIES, STRAIN and SEX *State nomenclature of GE or mutant rodents*	NUMBER OF ANIMALS TO BE USED UNDER USDA CATEGORY				HOUSING LOCATION Building
	B	**C**	**D**	**E**	
N/A	N/A	N/A	N/A	N/A	N/A

***All animals bred in-house must be included in this table, including any excess or unsuitable animals that may not be used for experiments.** If this protocol involves complicated breeding you may want to submit a flowchart with your application to more clearly explain the animal numbers listed in the tables above; examples can be found on the IACUC website under Helpful Links.*

20. USDA CATEGORY E: Identify the condition that places the animals in Category E and provide scientific justification for withholding alleviation of pain/distress. Describe any non-pharmaceutical methods that will be used to minimize pain and distress.

NOTE: If animals may die as a result of experimental procedures (e.g., infectious disease or oncology studies), or because an endpoint is used that allows the animals to experience significant pain or distress, justify why an alternate endpoint (e.g., weight loss, clinical signs, tumor size) cannot be used prior to death or pain or distress.

[ ] **Not Applicable**

The proposed surgical procedures (induced myocardial ischemia using a mechanical clamping method) can lead to all of the standard sequelae of myocardial remodeling after myocardial infarction (MI). Sudden death due to rupture of the ventricular free wall and/or deadly arrhythmias are common complications in mammals post-MI. One of the first studies describing the LAD ligation/reperfusion model in mice reported a 23-38% mortality rate in their various subgroups [15]. Although we will monitor the animals frequently during the postoperative recovery period, there may be animals that die without intervention. Thus, since we are proposing a new

methodology to induce cardiac ischemia, we will use a worst-case mortality rate of 40%; the projected rate of 4/10 mice may expire due to sudden death from complications of MI.
In order to show any difference in reducing pain, a groups of animals (n=6) in the antinociceptive pilot study must not receive any treatment to reduce pain and suffering. This is necessary in order to create a clinical baseline of behavior secondary to nociception in order to ascertain if the experimental treatments have any clinical antinociceptive effect in the treated animals.

21. Breeding: Will animals be bred in-house?

[X] **NO**

[ ] **YES***

**All animals bred in-house must be listed in the "offspring table" (#19), including any excess or unsuitable animals that will not be used for experiments*

a. Review the Rodent Breeding and Weaning Policy and complete the table below.

- [ ] Pair mating
- [ ] Trio mating
- [ ] Other (describe below):
- [ ] Breeders replaced after 6 months
- [ ] Breeders replaced after 12 months
- [ ] Other (describe below):
- [ ] Pups weaned at 21 days
- [ ] Other (describe below):

N/A

22. Rodent Identification Method (e.g. ear punch, tattoo, ear notch) See Rodent Identification for guidance.

[ ] **None**

[X] List: Ear Tag, Ear Punch (If not already sterilized, It is recommended to clean and/or disinfect any ear tags or punches, if at all possible, before applying or using.)

Axolotl Identification Method (e.g. ear punch, tattoo, ear notch).

[ ] **None**

[X] List: Electronic Identification Transponders [38]. BMDS DAS-7008 Reader and IMI-1000 Transponders, PharmaSeq WA-4000 Reader and IJ-2010 p-Chips, or other equivalent systems. If housed singly, axolotls can be identified by cage or cage card markings.

23. Will Transgenic, Knockout and Knockin animals be used?

[X] **NO**

[ ] **YES** (review the Genetically-Modified Animals Guideline)

a. Describe any special care or monitoring that the animals will require, or need for special breeding systems.

- [ ] No special care required
- [ ] Special care required (describe below)

N/A

b. For ***each*** strain: what is the inserted or knocked-out gene (avoid abbreviations; for an inserted gene, indicate the source species, wild-type or mutant; if mutant, indicate how) ***and*** what is the function of the wild-type gene product?

N/A

c. Will these modifications to the genome cause an increased risk for the animal to shed intentionally introduced infectious agents, biological toxins, hazardous chemical agents, radioisotopes or create other hazards for the animal handlers and research staff?

☐ **NO**

☐ **YES** Explain the hazard the animal will present to staff handling the animals and provide safety precautions required to be observed in housing and handling these animals in the space below.

N/A

d. Are two or more different strains of transgenic animals being bred?

☐ **NO**

☐ **YES**

i. Which strains are being bred?

N/A

ii. What is the expected biological characteristic(s) or outcome of the novel strain(s)?

N/A

iii. Will the novel strain(s) pose any additional risks to staff? If yes, please explain.

N/A

24. Housing Outside DLAR Facilities: Will animals need to be maintained outside the DLAR facilities for more than 12 hours?

☒ **NO**

☐ **YES** (Review Overnight and Long-Term Housing of Animals in Investigator Laboratories)

☐ Short Term (>12 Hours but ≤7 Days)
☐ Long Term (>7 Days)

Building:
Room:

☐ DLAR will provide all husbandry and oversight.*
☐ DLAR and PI will share the responsibilities for husbandry and oversight.*
☐ PI will be responsible for all husbandry and oversight. Provisions for care and housing, animal monitoring and environmental monitoring will meet or exceed standard DLAR SOPs.*

*All outside housing requests require a Husbandry Agreement between the DLAR and PI. A signed agreement must be submitted prior to protocol approval.

a. How long will the animals be maintained outside the DLAR facilities?

N/A

b. Justify why is it necessary to house animals outside of the regular DLAR animal facilities.

N/A

c. If DLAR will not provide all the husbandry and oversight, identify the person(s) who will provide the care of the animals while they are outside of the DLAR facilities.

N/A

25. Caging Requirements

X Standard housing (appropriate for species, including sterile for immunocompromised animals)
X Special housing needs required (e.g. suspended wire mesh flooring, non-standard size) Requires justification, describe below:

The axolotls (*Ambystoma mexicanum*) require special aquatic housing (Holtfreter's solution and regular changes). Standard operating procedures will be filed with DLAR personnel. See SOP No. 02.19.01.

26. Social Housing: The *Guide* states: "Single housing of social species should be the exception and justified based on experimental requirements or veterinary-related concerns about animal well-being."

X Standard social housing
X Singly housed (justify below and include duration of time animal will be singly housed):

Axolotl (*Ambystoma mexicanum*) – It is preferred to house adult axolotls individually, especially adult males. If necessary, groups of two or three adult females (in containers having enough 50% Holtfreter's solution per animal to cover their gills and heads without the animals having to actively submerge their bodies) can be housed in appropriately sized containers. Adolescent and juvenile axolotls MUST be housed singly as they may nip at the limbs of their neighbors.
Mice (*Mus musculus*) – Standard social housing.

27. Environmental Enrichment: The *Guide* states: "The primary aim of environmental enrichment is to enhance animal well-being by providing animals with sensory and motor stimulation, through structures and resources that facilitate the expression of species-typical behaviors and promote psychological well-being through physical exercise, manipulative activities, and cognitive challenges according to species-specific characteristics"

X Species-specific enrichment will be provided (see Environmental Enrichment and Behavioral and Social Management of Research Animals Policy/Guideline)
X Enrichment will either not be provided or will vary from the IACUC Policy (justify below)

Axolotls shall be housed in plastic tubs/mouse polys without sand/pebbles or other small additions/decorations for enrichment. These can be ingested and cause GI complications Axolotls are known to be sedentary, especially in the low-temperature of the 50% Holtfreter's solution and small container sizes used in research laboratories. Mouse tunnels/houses (PVC/plastic or equivalent) that are large enough for the axolotl to fit shall be added into the plastic tub/mouse poly for environment enrichment. Tunnels can be removed during periods of video recording and behavioral assessment.

VI. – PROCEDURE DETAILS

28. Location(s) use and detail.

a. List the location(s) where the procedures will be performed.

In DLAR facilities
X Building: Gordon Scott Hall Building, IBIO Building

Axolotl and mouse survival surgery and terminal procedures will be performed in the procedure rooms of the DLAR facilities in Scott Hall's or IBIO's basement.

In Research Lab(s)

[X] Building(s): Gordon Scott Hall Building, IBIO Building
Room(s): 3323 (Scott Hall), 6213 (Scott Hall) 1310 (IBIO)

Axolotl and mouse survival surgery and terminal procedures will be performed in the Sponsor's or Advisor's laboratories in the Gordon Scott Hall Building, Room 3323/6213 or IBIO Building, Room 1310.

b. Will animals be transported between buildings for procedures?

[ ] NO
[X] **YES***

***A Transportation of Animals Attachment must be submitted with this protocol to transport animals between buildings.

c. Will photographs and/or videos of animals be taken in an animal holding facility (i.e. DLAR)? Review the Security Policy/Guideline.

[ ] NO
[X] **YES,** list building and room number(s) and describe:

Gordon Scott Hall and/or IBIO DLAR Facility – Pictures of axolotls used to practice surgery will be taken to help catalog and annotate procedures in appropriate laboratory notebook(s).

29. List all procedures to be performed on animals: (Check boxes that apply)

[X] **USE OF ANESTHETIC, ANALGESIC, OR TRANQUILIZING AGENTS (animals will be in USDA Category D)**

[X] **SURGERY**
- [X] Non-survival
- [ ] Survival minor
- [X] Survival **major**
- [ ] Multiple survival
- [ ] **Multiple major** survival

[X] **ADMINISTRATION OF STUDY DRUGS, HORMONES, CHEMICALS, OR CYTOTOXIC SUBSTANCES**[1]
- [ ] Oral Gavage
- [ ] Addition to food or water supply
- [X] Acute Injections (*other than anesthetic agents*)
- [ ] Chronic Injections (*other than anesthetic agents*)
- [X] Other(s)
  List: 5-Bromo-2'-Deoxyuridine (BrdU)

[ ] **PROLONGED RESTRAINT**

[ ] **ANTIBODY PRODUCTION**
- [ ] Monoclonal
- [ ] Polyclonal

[ ] **HOUSING OUTSIDE OF DLAR ANIMAL FACILITIES**[2]
- [ ] Short-Term (>12 Hours but ≤7 Days)
- [ ] Long-Term (>7 Days)

[ ] **INOCULATION WITH CELLS, TISSUES, OR BODY FLUIDS**
- [ ] Tumor Induction
- [ ] Tumor Transplantation
- [ ] Acute Injections (*other than anesthetic agents*)
- [ ] Chronic Injections (*other than anesthetic agents*)

[ ] **BLOOD COLLECTION***
**for procedures other than antibody production*

[X] **FOOD AND/OR WATER REGULATION (RESTRICTION)**

[ ] **BREEDING OF ANIMALS**
- [ ] Genotyping of Rodents

[X] **OTHER PROCEDURES NOT LISTED**
- [X] Tissue Harvesting
- [ ] Behavioral Testing
- [ ] Bone Marrow Transplantation
- [ ] Nutrition Trials
- [ ] Neurological Impairment
- [ ] Trauma (bone, brain, spinal cord, etc.)
  List:
- [X] Imaging / Scans (CAT, MRI, MRS, PET, etc.)
  List: Echocardiography
- [ ] Other(s)
  List:

[1] Review the Administration of Substances: Maximum Volumes and Other Recommendations SOP.
[2] A Husbandry Agreement between the DLAR and PI is required.

30. State the period of time animals will be allowed to acclimate following arrival at WSU and prior to the initiation of experimental or breeding procedures (Review the Acclimation of Animals Guideline).

Axolotl (*Ambystoma mexicanum*) – 5-7 days for acclimation.
Mice (*Mus musculus*) – 2 days for acclimation.

31. Schedule of procedures for experimental groups: State or list in chronological order all procedures for each experimental group, their frequency, and time points over the course of the experiment. Details of each procedure are to be described in the appropriate questions (31, 32 and/or 33), NOT here. A diagram or chart may be helpful to explain complex designs.

Establishment of surgical best practices and ischemia model development in axolotls:
Day -5 to -7: Axolotls arrive in facility
Day -1: Axolotls begin fast. Perform baseline echocardiography.
Day 0: Axolotls are micro-chipped (if available) and undergo survival surgery
Day 0-2: Postoperative monitoring 4x daily for axolotls remaining in cohort
Days 1, 3, 5*, 7*, 9*, 11*, 13*, 15*, 17*, 19*: One axolotl in cohort is euthanized each day to harvest heart for histology studies.
*If animals die due to sudden death (see Question 20 for details), these sampling days may not apply.
Per Question 16, the schedule of procedures pertains to 10 total animals to develop the ischemia model. One animal (group size = 1) per day (total experimental days = 10) will be euthanized per the schedule above, to give a total of 10 axolotls for this portion of the pilot study.
Optional: Perform echocardiography as needed to assess cardiovascular function prior to harvesting heart for downstream studies.

Establishment of surgical best practices and ischemia model development in mice:
Day -2: Mice arrive in facility
Day -1: Perform baseline echocardiography.
Day 0: Mice are ear tagged and undergo survival surgery
Day 0-2: Postoperative monitoring 4x daily for mice remaining in cohort
Days 1, 3, 5*, 7*, 9*, 11*, 13*, 15*, 17*, 19*: One mouse in cohort is euthanized each day to harvest heart for histology studies.
*If animals die due to sudden death (see Question 20 for details), these sampling days may not apply.
Per Question 16, the schedule of procedures pertains to 10 total animals to develop the ischemia model. One animal (group size = 1) per day (total experimental days = 10) will be euthanized per the schedule above, to give a total of 10 mice for this portion of the pilot study.
Optional: Perform echocardiography as needed to assess cardiovascular function prior to harvesting heart for downstream studies.

Determination of optimal analgesia dosing in a surgical model in axolotls:
Days -5 to -7: Axolotls arrive in facility
Day 0: Axolotls are micro-chipped (if available) and are assessed for baseline pain response using qualitative and quantitative measures.
Days 1-2+: Experiment 1 – Validate quantitative methods using naïve animals. In this experiment, cage-side assessments [von Frey (vF) testing or acetic acid testing (AAT)] will be performed to establish a baseline pain response. Tests are repeated at least twice per day for a least two consecutive days.
Days 3-8+: Experiment 2 – Using validated quantitative methods, determine optimized analgesic doses. In this experiment, evaluate the effects of different doses of butorphanol and buprenorphine on quantitative and behavioral parameters (see [39]). Six animals will be assigned to each analgesic group, buprenorphine or butorphanol (low [L], medium [M], or high [H] dosage).

Table 1: Study schedule for each dose (L, M, and H) in Experiment 2.

	Baseline	Analgesia	Assessments			Analgesia	Assessments				
Test	-24h	0h	1h	6h	12h	24h	25h	31h	36h	48h	120h
Quantitative test (vF or AAT)	✓		✓	✓	✓	✓	✓	✓		✓	✓

Cageside	✓		✓	✓			✓	✓			
Video	✓ (x2)*		✓		✓	✓			✓	✓	✓
Feeding	✓			✓				✓			

*Two measures in 24 hours

Buprenorphine Doses: L = 25 mg/kg, M = 50 mg/kg, H = 75 mg/kg
Butorphanol Doses: L = 0.25 mg/L, M = 0.50 mg/L, H = 0.75 mg/L

Notes:

- Medium (M) dose listed above is based on published newt study [39].
- When animals are used in more than one experiment, they will be provided a minimum of 1-week washout between treatments and must return to baseline behavior.
- If an analgesia dose does not provide coverage for a full 24 hours, with the guidance of the veterinarians, consider re-dosing the analgesia every 6-12h over each 24-hour period before moving to a higher base dose.
- If adverse effects (e.g. GI motility issues) are evident, continue testing at a lower dose if statistical analyses show there is a significant difference (clinically or statistically) in nociceptive threshold between the treated and untreated groups.
- If adverse effects (e.g. GI motility issues) are evident, consider diluting the dose of analgesia using an appropriate vehicle. Dilute to a maximum volume of 25 mL/kg [40].

Interim Results: Adverse GI motility effects observed in one of the testing groups. Will continue testing as described above.

Days 9-19+: Experiment 3 – Evaluate optimal analgesic dose in a surgical model in axolotls. Three surgical groups of animals (6 per group, receiving either butorphanol, buprenorphine, no analgesic) will undergo mechanical induction of cardiac ischemia. Using data from Experiment 2, animals will receive optimized analgesic doses. The same evaluation criteria and schedule (behavioral and quantitative methods) that were used in Experiment 2 will be used in Experiment 3, however the 0-hour time point will be designated as the point of recovery from anesthesia. Axolotls begin fast 1 day before survival surgery; perform baseline echocardiography at this point as well.
Days 20-27+: Experiment 4 – Compare the histologic differences in healing response after mechanically inducing ischemia in an axolotl heart, with and without the administration of opioid analgesia. Three surgical experimental groups (buprenorphine, butorphanol, and no analgesia) of naïve axolotls will undergo mechanical induction of cardiac ischemia using the same doses utilized in Experiment 3. Axolotls begin fast 1 day before survival surgery; perform baseline echocardiography at this point as well. Each experimental group will consist of 18 animals; 6 will be humanely euthanized at each of three post-operative time points (12 hr, 2 days, 7 days). These time points were selected based upon observations from pilot studies we have performed examining cardiac histology in axolotls following mechanical ischemic injury. Following euthanasia, cardiac tissue will be collected for histologic processing and analysis. Quantitative and behavioral assessments will be performed as described in Table 2 for each group as allowed until the time of euthanasia.
Optional: Perform echocardiography as needed to assess cardiovascular function prior to harvesting heart for downstream studies.

32. NON-SURGICAL PROCEDURES

a. Tumor growth in rodents

[X] **Not Applicable**
[ ] SOP for Monitoring Tumor Growth in Rodents will be followed.
[ ] SOP will not be followed. Describe variance from SOP and justify below.

N/A

b. Prolonged Restraint (does not include brief restraint for the purpose of performing routine clinical or experimental procedures). The *Guide* states that "Prolonged restraint, including chairing of nonhuman primates, should be avoided unless it is essential for achieving research objectives and is specifically approved by the IACUC." Prolonged restraint must be justified with appropriate oversight to ensure it is minimally distressing. Describe any sedation, acclimation or training to be used.

[X] **Not Applicable**

☐ Describe and justify below. (Review the Prolonged Physical Restraint Policy)

N/A

c. Food/Water Regulation (Restriction) The *Guide* definition: "The regulation process may entail *scheduled* access to food or fluid sources, so an animal consumes as much as desired at regular intervals, or *restriction*, in which the total volume of food or fluid consumed is strictly monitored and controlled." Describe the method for assessing the health and wellbeing of animals. Amount of food and/or water earned during testing and amount freely given must be recorded and assessed to assure proper nutrition.

☐ **Not Applicable**
☒ Describe and justify below. (Review the Food/Water Restriction or Regulation Policy/Guideline)

Prior to axolotl survival surgery, a 24-hour fast is necessary [40-42] in order to reduce the coelom volume to allow space for moving internal organs during surgery. Since axolotls only eat every other day, it should not be stressful to go up to 24 hours without food. Due to their metabolic rate and surface area to volume ratio, a fast is not recommended prior to mice survival surgery [22,24].

d. Rodent tail biopsy

☒ **Not Applicable**
☐ Policy/SOP for Rodent Tail Biopsy will be followed.
☐ SOP will not be followed. Describe variance from SOP and justify below.

N/A

e. Rodent toe clipping

☒ **Not Applicable**
☐ Policy/SOP for Rodent Toe Clipping will be followed; justification is required, include below.
☐ SOP will not be followed. Describe variance from SOP and justify below.

N/A

f. Blood collection

☒ **Not Applicable**

List the site, method of collection (include the needle gauge), frequency, and volume needed at each time point:

N/A

☐ SOP for Blood Collection: Maximum Volumes and Fluid Replacement will be followed.
☐ Blood collection will exceed guidelines. Justify below.
☐ Blood collection takes place at the time of euthanasia (e.g. cardiac puncture)

N/A

g. Use of Non-Pharmaceutical Grade Compounds – Identify any non-pharmaceutical grade (neither human nor veterinary) drugs, biologics or reagents that will be administered to animals. Provide scientific justification for their use and describe methods that will be used to ensure appropriate preparation and administration. Please review the Use of Non-Pharmaceutical Grade Drugs Policy.

☐ **Not Applicable**

Pentobarbital (commercial preparation Nembutal®) is now considered logistically unavailable by the NIH Office of Laboratory Animal Welfare (OLAW). Per the IACUC Policy "Use of Non-Pharmaceutical Grad Drugs", the use of compounded pentobarbital for anesthesia is considered acceptable. For this protocol, compounded pentobarbital will be purchased from specialty pharmacies currently selling to other PIs at WSU.
5-Bromo-2'-deoxyuridine (i.e. BrdU / Br-dU / BUdR / 5-BrdU / 5-Bromodeoxyuridine, CAS 59-14-3) is a commonly used complex biologic that is used to study cellular division and proliferation in research environments. Since it is incorporated into DNA, it is considered a mutagen and carcinogen. An Animal Hazardous Agent Form shall be prepared for DLAR staff and a Laboratory Specific Standard Operating Procedure shall be created for laboratory staff using information from the BrdU MSDS. This will ensure the safe handling, preparation, and administration of the compound.

33. DESCRIBE ALL NON-SURGICAL PROCEDURES: Summarize in a narrative what procedures will be done with each species. Include only those experiments where animals are directly involved. When animals are used as donors of organs, tissues, or cells, only describe how the organs, tissues or cells will be obtained. Do not describe what will be done with those organs, tissues or cells once they have been removed from the animal.

☐ **NOT APPLICABLE**

a. Describe every procedure.

Axolotl (*Ambystoma mexicanum*)

Operators must always wear powder-free latex or nitrile gloves when handling axolotls. For the purposes of this protocol, no axolotls are planned to be bred for colony stabilization. All animals will be purchased from the Ambystoma Genetic Stock Center (AGSC) located in the Department of Biology at the University of Kentucky (Lexington, KY).
Identification procedures for the axolotl will follow best practices as described in [38]. Due to their robust regeneration capability, any method involving toe clipping, limb punching or limb notching is impractical. Additionally, as axolotls continually slough off their skin, tattoos quickly disappear. The best choice is the use of a subcutaneous transponder, a.k.a microchip. Systems from BMDS (DAS-7008 Reader and IMI-1000 Transponders), PharmaSeq (WA-4000 Reader and IJ-2010 p-Chips) or other equivalent systems. The preferred site is a subcutaneous placement, parallel to the tail fin, 2.5 – 3.0 centimeters posterior to the head. For consistency, tags will be placed over the right shoulder area as shown in Figure 1.
The procedures described in [38] use an ice bath as an anesthetic to reduce pain and suffering of the animals. To further prevent additional pain to the animal, the transponders will be inserted while the axolotls are under anesthesia, prior to starting the cardiac survival surgery.
Detailed Procedures:

1. Ensure the axolotl is at the appropriate depth of anesthesia.
2. Take a sterile, disposable needle/transponder assembly from the package and inject transponder as shown in Figure 1. Dispose of used needle/transponder assembly in appropriate container.
3. Briefly massage the injection site with gloved finger to help approximate the skin edges.
4. Dab injection site with dry gauze to remove excess moisture.
5. Place topical tissue adhesive (GLUture, Abbott Laboratories, cat. no. 32046 or equivalent) on injection site.

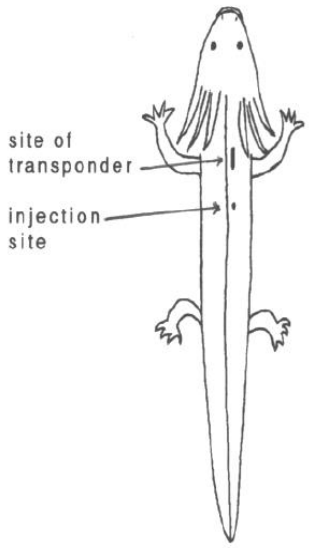

Figure 1: Injection Site and Resulting Location of Microchip Transponder

Analgesic Sub-Study

1. Two antinociceptives will be compared, with doses established in newts [39] as a starting point. The sample size of n = 6 animals per group was determined by assuming an $\alpha = 0.05$ and a $\beta = 0.05$ in sample size calculations while estimating a large effect size ($\sigma = 0.25$ for laboratory-bred animals and assuming there will be clear behavioral differences in animals with and without antinociceptives [43]). The treatment and control groups are listed below:
   a. Surgery (Mechanically Induced Ischemia) + Buprenorphine
   b. Surgery (Mechanically Induced Ischemia) + Butorphanol
   c. Surgery (Mechanically Induced Ischemia) + No Antinociceptive
   d. Anesthesia + Buprenorphine – If little to no differences are seen in the surgery arms, animals that are treated with anesthesia and buprenorphine alone can be used to establish another control arm for comparison.
   e. Anesthesia + Butorphanol – If little to no differences are seen in the surgery arms, animals that are treated with anesthesia and butorphanol alone can be used to establish another control arm for comparison.
   f. Optional: Anesthesia Alone – If little to no differences are seen in the surgery arms, animals that are treated with anesthesia alone can be used to establish another control arm for comparison.
   g. Optional: Complete Control – Each animal can be observed before any procedures are performed or pharmacological agents are administered, serving as its own control. Completely naïve (throughout the study) animals can be used as optional controls.
   h. Buprenorphine shall be administered as an intracoelomic (IC) injection; administer up to 1h prior to surgery.
      1.h.1. The best point of intracoelomic administration is just in front of a hind leg, approximately parallel to the body and about midway between the dorsal and ventral surfaces: that is, dorsal to the bladder and ventral to the kidneys and caudal enough to prevent injecting into the liver or spleen.

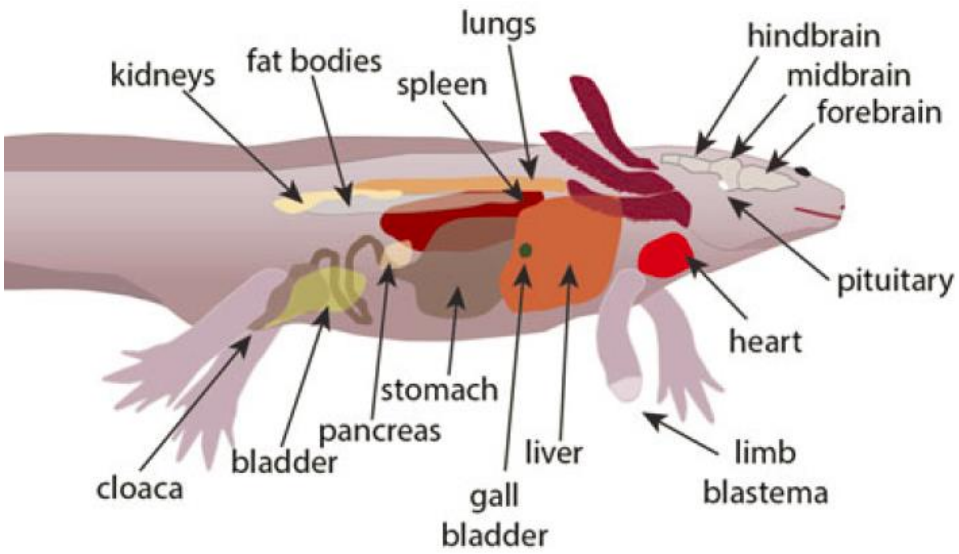

Figure 2: Diagram of major axolotl organs

1.h.2. To facilitate the IC injection into the animal, the axolotls can be placed into a state of anesthesia induction or even into a light plane of anesthesia before injecting buprenorphine.

Induction	Light Anesthesia	Deep (Surgical) Anesthesia
• Decreased gular movement • Diminished withdrawal reflex	• Loss of righting reflex • Absence of abdominal respirations	• No withdrawal reflex (toe pinch) • Gular movements cease

i. Butorphanol shall be administered directly into the 50% Holtfreter's solution of the animal's cage up to 1h prior to surgery.

2. Buprenorphine (Penro Specialty Compounding, Colchester, VT) shall be administered at one of three doses (low=25 mg/kg, medium=50 mg/kg, high=75 mg/kg) as an intracoelomic (IC) injection every 24-hours for 48 hours. Butorphanol (MWI Veterinary Supply, Boise, ID) shall be administered at one of three concentrations (low=0.25 mg/L, medium=0.50 mg/L, high=0.75 mg/L) directly into the 50% Holtfreter's solution of the animal's cage every 24-hours for 48 hours. The medium dose is based upon a published dose [39] that was effective in newts and the low and high doses are 50% lower or higher, respectively.
3. When animals are used in more than one experiment, they will be provided a minimum of 1 week washout between treatments and must return to baseline behavior.
   a. If an analgesia dose does not provide coverage for a full 24 hours, with the guidance of the veterinarians, consider re-dosing the analgesia every 6-12h over each 24-hour period before moving to a higher base dose.

Behavioral Parameters For Analgesic Assay

1. Changes in behavior will be monitored to assess the efficacy of the antinociceptives. The following behaviors shall be monitored:
   a. Feeding: At least one week of feeding behavior should be collected to establish a baseline food intake. Individual variability has been observed during the husbandry of the first cohort of axolotls. Thus, not only will animal feeding behavior be compared to a control, it shall be compared to the animal's own pre-experiment intake baseline. Food intake will be quantitatively assessed at each feeding post-surgery for changes between each group. The axolotls will be offered food daily post-surgery to assess feeding behavior. The animals will be weighed 3 times a week at cage change to assess changes.
   b. Cageside Assessments: The animals will be assessed at least twice daily cageside. This assessment will determine if there are behavioral changes based on analgesic administration post-surgery. This will continue for up to 48 hours after surgery. Assessment methods may include observing body posture, spontaneous movement, responses after gently tapping on cage, squirting 3-5 mL of water from a syringe into the water surface to assess response to water disruption, touching the animal, or placing a novel object into the cage and assessing movement away from the object.

1.b.1. One or more of the following techniques may be used (depending on response). These techniques may be implemented prior to surgery to determine which will be the most effective at eliciting a response.

1.b.1.1. Movement after Tapping on Cage: Twice daily cageside observations for 3 days prior to procedures can be recorded to establish a self-control baseline. The cageside observer shall gently tap on the cage a few times and record any responses.

1.b.1.2. Movement after Creating Gross Water Movement: Twice daily cageside observations for 3 days prior to procedures can be recorded to establish a self-control baseline. Gross water movement stimulates axolotls' mechanoreceptive neuromasts that run along the sides of their bodies. Creating gross water movement by injecting 3-5 mL of fresh 50% Holtfreter's solution nearby an animal (e.g. using a serological pipette) should stimulate the neuromasts, eliciting a response.

1.b.1.3. Movement When Touched: Twice daily cageside observations for 3 days prior to procedures can be recorded to establish a self-control baseline. The cageside observer shall gently touch the back or tail of each animal and record any responses.

1.b.1.4. Movement in response to novel object: A novel object will be placed in the cage and the animals escape behavior monitored.

c. Animals may be videotaped for intervals of time throughout the recovery period to assess spontaneous movement and behavioral signs of stress/pain. The videos will be maintained by the laboratory and only individuals involved in the project will have access.

1.c.1. Body Posture/Stance and Spontaneous Movement: At least one hour of video can be collected or twice daily cageside observations for 3 days prior to procedures can be recorded to establish a self-control baseline. Behavior such as tail curling, gill position, any abnormal signs of posture, spurts of movement, and any flipping/rolling around their body axes should be noted.

d. Optional: Stimulation With Von Frey Filaments: This is a non-noxious method to elicit a response to a controlled application of force. Von Frey fibers may be used to assess pain response at the incision site and a site distant to the incision. This is a novel model and it is not clear whether this species will demonstrate a response to the fibers. The Von Frey fibers of various sizes shall be applied once daily starting the day of surgery and continuing for 48 hours post-surgery. A baseline assessment would be performed prior to the surgical procedure. Each filament will be pressed to the point of bending at the site of evaluation starting with the lowest gauge filament. The filaments are increased in size until a response is elicited. At that point the experiment is stopped and the gauge recorded. Von Frey fibers have been successfully used to assess nociception in frogs.

1.d.1. Mild restraint of the axolotl shall be required in order to stimulate the ventrally-located wound region. Axolotls shall be placed into a colander or mesh-like holder to gain access to their ventral side. Once the animal has calmed down and become acclimated to its new environment, the Von Frey filament shall be inserted through the mesh and used to stroke the wound area. The animal can be kept moist my spritzing with 50% Holtfreter's solution.

1.d.2. If the animal does not respond to the Von Frey filament AND does not show signs of stress, testing can continue to the next force increment as long as the animal is kept moist. The animal should be returned to its cage if it shows continued signs of stress or is in danger of becoming desiccated.

e. Acetic acid test: Axolotls will be placed in a polypropylene mouse cage with enough 50% Holtfreter's solution to cover half of its body, leaving the dorsal surface above the waterline. The AAT is performed according to previously published reports in frogs. Glacial acetic acid is serially diluted to produce 10 dilutions evenly spaced on a logarithmic scale. Testing is performed by placing a single drop of the weakest concentration acetic acid on the same location described above for the vF Fibers. The animal will be observed for a repeatable behavioral response (wiping, turning, escape behavior). If a response is not observed within 5 seconds the area is rinsed using 50% Holtfreter's solution. Testing on the opposite side using the next highest concentration will occur. The testing continues until the nociceptive threshold is reached which is the highest concentration to produce a response. If no response is observed with the highest concentration the nociceptive threshold will be designated at at 10, consistent with the highest concentration of acetic acid.

Immunohistochemistry and Standard Tissue Staining Techniques:

For standard fixation of tissues, animals shall be euthanized as allowed per procedures in "Question 37. Euthanasia Methods". After euthanasia, tissues will be sampled as needed and fixed per protocols defined by our laboratory.

For perfusion fixation of tissues, the animals will be properly anesthetized and the perfusion fixation protocol shall be followed per "Question 35. Surgical Procedures in Non-Rodents."

Fixatives:

10% Normal Buffered Formaldehyde

1. Use as supplied by manufacturer (Thermo Fisher Scientific, Waltham, MA or equivalent).
2. To make in lab:
   a. Add 50 mL of 37% formaldehyde to 450 mL of dH_20.
   b. Add 3.25 gm Sodium Phosphate, Dibasic (Na_2HPO_4).
   c. Add 2 gm Sodium Phosphate, Monobasic (NaH_2PO_4).
   d. Mix well to dissolve salts and store at room temperature.

8% Paraformaldehyde Stock

1. Use as supplied by manufacturer (Thermo Fisher Scientific, Waltham, MA or equivalent).
2. To make in lab:
   a. Add 40g paraformaldehyde to 500 mL of dH_2O.
   b. Heat the solution to 60-65°C while stirring (do not exceed 65°C; this will affect the performance of the fixative).
   c. To clear the solution, reduce heat and slowly add 2-3 mL of 1.0 M NaOH with a dropper.
   d. Filter and store at 4°C for up to 1 month.

4% Paraformaldehyde Fixative

1. Add equal parts 8% paraformaldehyde stock to 0.2 M sodium phosphate buffer
2. Note: this fix is best prepared fresh, no more than 72 hours before use.

RNAlater® Fixative

1. Use as supplied by manufacturer (Ambion, Austin, TX).
2. Store at room temperature.

Buffers:

Note: Autoclave buffers if they are to be used during survival surgeries. Non-sterile buffers can be used in terminal procedures.

Dilution Buffer for Paraformaldehyder

0.2 M Sodium Phosphate Buffer, pH 7.7

1. For the sodium phosphate monobasic stock, add 27.8 g $NaH_2PO_4 \cdot H2O$ (sodium phosphate monobasic monohydrate) to 1L dH_2O.
2. For the sodium phosphate dibasic stock, add 28.4 g Na_2HPO_4 (anhydrous sodium phosphate dibasic) to 1L dH_2O.
3. Add 895 mL of the monobasic stock to 105 mL of the dibasic stock to make 0.2 M sodium phosphate buffer.
4. Check and adjust pH to 7.7±0.1 as necessary with HCl or NaOH.
5. Autoclave (if necessary) and store at 4°C

Flushing Buffers

1X Phosphate Buffered Saline with Heparin and Lidocaine, (~280-315 mOsm/kg)

1. Combine 8 g NaCl, 0.2 g KCl, 1.44 g Na_2HPO_4 and 0.24 g KH_2PO_4 with 930 mL dH_2O.
2. Add 60 mL of Heparin flush solution (100 USP units/mL).
3. Add 5 g of lidocaine hydrochloride (CAS 137-58-6 or 6108-05-0, Thermo Fisher Scientific, Waltham, MA or equivalent.
4. Adjust pH to 7.7±0.1 with HCl and/or NaOH; add dH_20 to 1 L.
5. Autoclave (if necessary) and store at 4°C.

Amphibian Ringers Solution with Heparin and Lidocaine, (~200-250 mOsm/kg)

1. Combine 6.6 g NaCl, 0.15 g KCl, 0.15 g $CaCl_2$, and 0.2 g $NaHCO_3$ to 930 mL dH_2O.
2. Add 60 mL of Heparin flush solution (100 USP units/mL).

3. Add 5 g of lidocaine hydrochloride (CAS 137-58-6 or 6108-05-0, Thermo Fisher Scientific, Waltham, MA or equivalent.
4. Adjust pH to 7.7±0.1 with HCl and/or NaOH; add dH_20 to bring volume to 1 L.
5. Autoclave (if necessary) and store at 4°C.
6. Sterile solution is good for up to 3 months; non-sterile solution can be stored for up to 1 week.

Perfusion Device Setup:

1. The static pressure of the perfusate determines the speed of perfusion. The static pressure of the solutions must be high enough to displace blood, but not much higher than the maximum, natural arterial pressure of the ambulatory animal.
2. The systolic blood pressure of *Salamandra salamandra*, closely related to the axolotl, is 22 mmHg [44]. To provide an equivalent static pressure, the top of the fluid level of the perfusates should be about 25-30 cm above the level of the animal's heart.
3. Control the perfusate flowrate using a clamp; the source of the perfusate can be controlled using a three-way valve. See Figure 3 for an example.

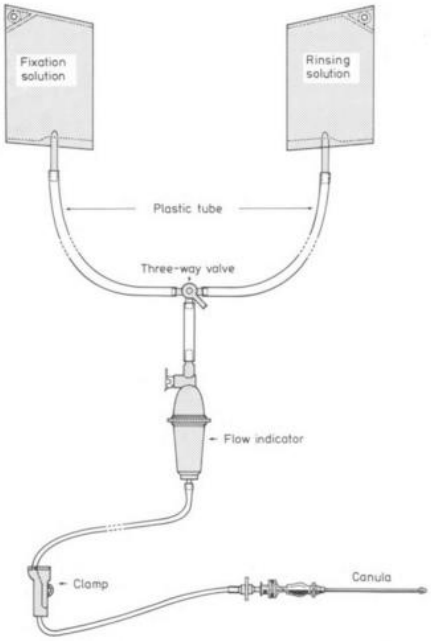

Figure 3: General setup for perfusion fixation.

Echocardiography to Assess Cardiovascular Function:

1. Begin with a 24-hour fast [40-42] to avoid emesis during anesthesia
2. Induce an appropriate plane of anesthesia. Place the axolotl in a water bath with 0.1% tricaine methanesulfonate (MS-222); depth of surgical plane of anesthesia is determined by the loss of righting reflex, no spontaneous movements and no reflex to pain.
3. Transfer the axolotl to a pan of 0.05% tricaine methanesulfonate (maintenance dose) solution in a dorsal-recumbent position. Enough solution shall be placed in the pan to adequately cover the gills.
   a. Option: Cover the animal with Kimwipe™ laboratory tissues or gauze that have been moistened with 50% Holtfreter's solution. Tease away the tissues to expose the area to be examined with the echocardiography transducer or probe.
   b. Regularly monitor the depth of anesthesia by testing the pain reflex; additional anesthesia can be achieved by placing the animal in a bath of maintenance dose MS-222 solution or squirting 3-5 mL of additional maintenance dose MS-222 directly to the gills and the moistened Kimwipes™ laboratory tissues or gauze that cover the animal.
4. Take heart images using an appropriate echocardiography with the appropriate transducer or probe. Machines capable of using very high frequency probes (>30 MHz) can be used if available. Clean the end of the ultrasound probe/transducer with isopropyl alcohol or Sporicidin (or equivalent) disinfectant wipes and rinse with distilled water before performing a scan. Since axolotl skin is naturally moist and covered by a coat of mucus, the ultrasound probe/transducer can be placed directly onto the skin of the axolotl.

5. Obtain echocardiograms. If possible on axolotls, attach EKG needle leads in order to allow for electrocardiogram gating.
   a. Explore heart structures and acquire images as needed.
6. Flush any area on the axolotl that was contacted by the ultrasound probe/transducer with 50% Holtfreter's solution. Return the axolotl to a cage of fresh 50% Holtfreter's solution for recovery. Clean the end of the ultrasound probe/transducer with isopropyl alcohol or Sporicidin (or equivalent) disinfectant wipes. Rinse the ultrasound probe/transducer with distilled water before performing a subsequent scan.

Mice (*Mus musculus*)

For the purposes of this protocol, no mice are planned to be bred for colony stabilization or transgenic mouse development. All mice will be purchased from the Jackson Laboratory (Bar Harbor, ME). For the identification of mice, the procedures for animal identification in the IACUC SOP – Rodent Identification, listed in Question 22, shall be followed. No deviations from the SOP are planned.

Immunohistochemistry and Standard Tissue Staining Techniques:

For standard fixation of tissues, animals shall be euthanized as allowed per procedures in "Question 37. Euthanasia Methods". After euthanasia, tissues will be sampled as needed and fixed per protocols defined by our laboratory.

For perfusion fixation of tissues, the animals will be properly anesthetized and the perfusion fixation protocol shall be followed per "Question 34. Surgical Procedures in Rodents."

Fixatives:

The same fixatives outlined for axolotls can be used in mice:
10% Normal Buffered Formaldehyde
8% Paraformaldehyde Stock
4% Paraformaldehyde Fixative
RNAlater® Fixative

Buffers:

Note: Autoclave buffers if they are to be used during survival surgeries. Non-sterile buffers can be used in terminal procedures.
Except as listed below, the same buffers outlined for axolotls can be used in mice.

Dilution Buffer for Paraformaldehyder
0.2 M Sodium Phosphate Buffer, pH 7.4
1. Prepare basic buffer as listed for axolotls.
2. Check and adjust pH to 7.4±0.1 as necessary with HCl or NaOH.
3. Autoclave (if necessary) and store at 4°C

Flushing Buffers
1X Phosphate Buffered Saline with Heparin and Lidocaine, (~280-315 mOsm/kg)
1. Combine 8 g NaCl, 0.2 g KCl, 1.44 g Na_2HPO_4 and 0.24 g KH_2PO_4 with 930 mL dH_2O.
2. Add 60 mL of Heparin flush solution (100 USP units/mL).
3. Add 5 g of lidocaine hydrochloride (CAS 137-58-6 or 6108-05-0, Thermo Fisher Scientific, Waltham, MA) or equivalent.
4. Adjust pH to 7.4±0.1 with HCl and/or NaOH; add dH_20 to 1 L.
5. Autoclave (if necessary) and store at 4°C.

Amphibian Ringers Solution with Heparin and Lidocaine, (~200-250 mOsm/kg)
Do not use in mice.

Perfusion Device Setup:

1. The static pressure of the perfusate determines the speed of perfusion. The static pressure of the solutions must be high enough to displace blood, but not much higher than the maximum, natural arterial pressure of the ambulatory animal.
2. The average systolic blood pressure of C57BL/6J mice is 120±2 mmHg [45]. To provide an equivalent static pressure, the top of the fluid level of the perfusates should be about 140-160 cm above the level of the animal's heart.
3. Control the perfusate flowrate using a clamp; the source of the perfusate can be controlled using a three-way valve. See Figure 3 for an example.

Echocardiography to Assess Cardiovascular Function:

1. 1. If necessary, induce an appropriate plane of anesthesia. Conscious echocardiograms can be performed if appropriately trained (i.e. a user has a WSU DLAR VTS certification card for aseptic axolotl surgery) or under the guidance of a trained user (as defined).
   a. Pentobarbital sodium (Target Dose = 70-80 mg/kg; Acceptable Dose Range = 60-90 mg/kg) shall be injected intraperitoneally. Use 10-20% of the initial dose for maintenance.
   b. If an inhaled anesthetic is to be used, anesthetize the mouse with isoflurane (3-4% induction, 1-3 % maintenance) in 100% oxygen.
2. Using an animal hair clipper or an appropriate depilatory lotion, remove the hair on the animal's chest.
3. Using appropriate methods (e.g. electric warming pad, phase-change heat pad, far infrared heating, or equivalent), maintain the mouse core temperature at approximately 37°C.
4. Place warmed (37°C) echocardiography gel onto the shaved chest of the animal and take heart images using an appropriate echocardiography machine. Machines capable of using very high frequency probes (>30 MHz) can be used if available.
5. Obtain echocardiograms. Attach EKG needle leads if needed in order to allow for electrocardiogram gating.
   a. Place the transducer or probe along the long-axis of the left ventricle (LV) and direct it to the right side of the mouse's neck (see Figure 4A). This helps visualize two-dimensional (2-D) LV long-axis. Acquire images as needed.
   b. Rotate the transducer or probe clockwise by 90° to visualize the LV 2-D short axis (see Figure 4B). Acquire images as needed.
   c. Additional exploration of heart structures can be performed as the operator's discretion. Acquire images as needed.
6. After all images have been acquired, remove any residual echocardiography gel and return the mouse to a heated cage for recovery.

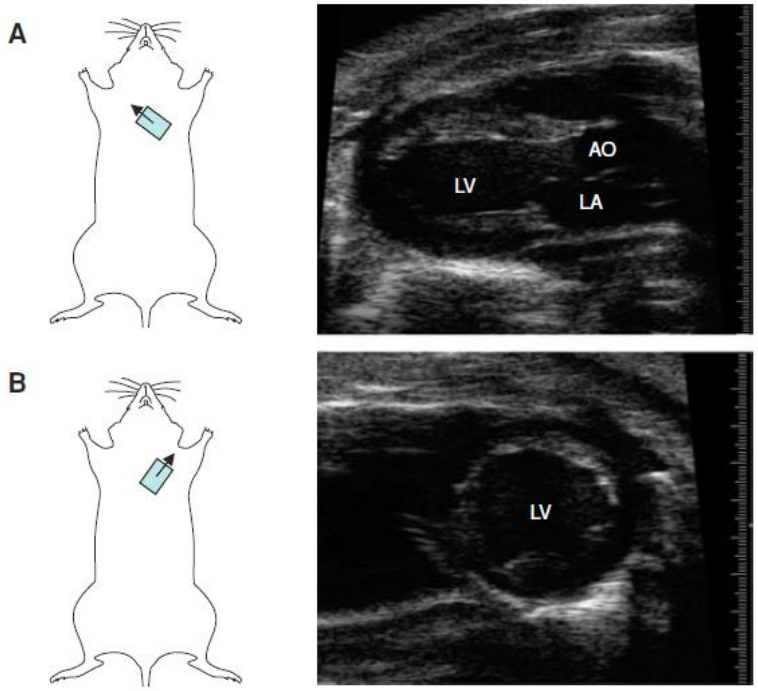

Figure 4: Probe placement for basic echocardiography views.

b. How will the animals be monitored for adverse effects? Describe any likely effects.

The PI shall visit the animals every day to fill out a post-operation monitoring form until the microchip transponder insertion site is healed.
Axolotls and mice will be visually inspected daily for signs of discomfort, stress, pain and injury. Since axolotls are an uncommonly used laboratory animal, specific standard operating procedures (SOPs) will be developed (see DLAR SOP Axolotl Care, SOP No. 02.19.01) with the AV to ensure DLAR personnel are vigilant to their needs. Synopses for signs of distress are listed in Question 36. Any animals that show signs of prolonged discomfort or pain shall be removed from the study and treated as needed; if measures become futile, animals shall be euthanized.

c. Fill out the following anesthesia and/or analgesia table for every procedure.

☐ **Not Applicable**

Sedation, anesthesia, muscle relaxation and analgesia

Species/Procedure	Sedative/Anesthetic	Dosage/Route/ Frequency	Analgesic	Dosage/Route/ Frequency
Axolotl / Animal Identification	Tricaine Methanesulfonate (MS-222)	0.1% / Transcutaneous & Branchial / As needed (PRN)	Buprenorphine	Target = 50 mg/kg (Published Range = 0.2 – 75 mg/kg) / Intracoelomic / Before injection of transponder.
Axolotl / Echocardiography	Tricaine Methanesulfonate (MS-222)	0.1% / Transcutaneous & Branchial / As needed (PRN)	N/A	N/A
Mouse / Echocardiography	Pentobarbital sodium	60-90 mg/kg intraperitoneally. Use	N/A	N/A

	Or isoflurane	10-20% of the initial dose for maintenance. (3-4% induction, 1-3 % maintenance) in 100% oxygen		

Indicate what parameters will be used to determine the need for additional doses of anesthesia and/or analgesia.

Anesthesia: If the axolotl continues to thrash around and shows signs of obvious pain (reflex withdrawal from analgesia needle insertion), the axolotl should be placed back in the MS-222 bath.
Mouse: If responds to toe pinch.
Analgesia: Although no analgesia was listed in [38], buprenorphine will be given as described in the table [46].

d. Post-Anesthetic Care of Rodents.

- [X] **Not Applicable**; anesthesia is not used; the animal is not a rodent; the procedure is non-survival
- [X] SOP for Post Operative/ Post Anesthetic Care of Rodents will be followed
- [ ] SOP will not be followed. Describe variance from SOP and justify below.

N/A

e. Post-Anesthetic Care of Non-Rodents.

- [ ] **Not Applicable**; anesthesia is not used; the animal is a rodent; the procedure is non-survival

1. Describe supportive care and monitoring provided during immediate anesthetic recovery period (from cessation of anesthesia until sternal recumbency is regained) and intermediate recovery period (from sternal recumbency until the animal is able to walk).

Axolotl (*Ambystoma mexicanum*) – The following are detailed procedures for post-anesthetic care of non-rodents after microchip insertion.

Immediate Recovery Period
The period from cessation of anesthesia or completion of surgery until animal achieves normal ambulation and can eat, drink, and groom.
1. At the end of microchip implantation cardiac surgery will ensue. Please follow procedures for Immediate Recovery Period in Post-Operative Care in the Surgical Procedures in Non-Rodents (see Question 35e).

Long Term Recovery Period
The period when normal activity resumes until the incision is healed.
At the end of microchip implantation cardiac surgery will ensue. Please follow procedures for Long Term Recovery Period in Post-Operative Care in the Surgical Procedures in Non-Rodents (see Question 35e).

34. SURGICAL PROCEDURES in RODENTS:

- [ ] **NOT APPLICABLE**

a. Classification

- [X] Non-survival surgery (animals do not recover from anesthetic for any period of time)
- [ ] Minor survival surgery
- [X] **Major** survival surgery
- [ ] **Multiple survival surgeries -** Review the Multiple Survival Surgeries Policy and provide justification below.

N/A

b. Surgeon(s)

Provide the names of the person(s) who will perform ***survival*** surgery (must also be listed in Q11).

☐ **Not Applicable**; only non-survival surgery will be performed.

Jeremy (Jay) Tolentino Llaniguez

c. General Surgical Requirements

☒ Principles of Rodent Anesthesia and Surgery SOP will be followed.

☐ SOP will not be followed. Describe variance from SOP and justify below.

N/A

d. Specific Surgical Details

Give a detailed overview of the surgical procedures to be performed, the size and anatomical location of incisions, the anticipated time to perform each, methods of closure, time of suture removal, and the time frames of their performance in relation to the overall protocol and also in relation to each other (if more than one procedure is performed on the same animal). Clearly indicate the time of planned euthanasia following the surgery.

Mice (*Mus musculus*):

Survival Surgery - Mechanically Induced Ischemia:

1. Pentobarbital sodium (Target Dose = 70-80 mg/kg; Acceptable Dose Range = 60-90 mg/kg) is an ideal anesthetic providing an adequate depth of anesthesia for 30-40 minutes. The anesthetic shall be injected intraperitoneally with a short 27-gauge ½-inch needle. While withdrawing needle, it is recommended to pinch the skin at the site of injection in order to prevent any pentobarbital from adhering to the needle and being removed from the site of injection.
   a. **Optional:** Dilute to a concentration of 5 mg/mL using sterile water or sterile saline. The diluted drug should be prepared in a small vial (e.g. sterile empty injection vial) just prior to injection into the animal. Invert the vial a few times and draw the diluted drug from the bottom of the vial (drug is more dense than water).
   b. If an inhaled anesthetic is to be used, anesthetize the mouse with isoflurane (3-4% induction, 1-3 % maintenance) in 100% oxygen.
2. After administering an injectable anesthetic, allow the animal to sit undisturbed in an empty cage as the anesthetic takes effect; agitating the animal can affect its metabolism and stress levels, affecting the quality of the surgical procedure. Regularly monitor the depth of anesthesia by testing the pain reflex (toe-pinch); the lack of the pain reflex signals a medium-deep plane of anesthesia.
   a. A top-up dose of injectable anesthesia (~10-20% of the initial dose) should be administered if the proper depth of anesthesia is not reached after 10 minutes.
3. Once the mouse is at the appropriate plan of anesthesia, administer buprenorphine-SR (sustained release) (1.0 mg/kg). The analgesic shall be injected subcutaneously. Optional: Buprenorphine-SR can be administered 24-48 hours prior to any surgical procedures.
   a. If buprenorphine-SR is not available, administer 0.05 mg/kg of Buprenex (buprenorphine hydrochloride) as a prophylactic analgesic by subcutaneous injection.
4. Using an animal hair clipper with a size 40 clipper blade (Harvard Apparatus, catalog no. 525204 or equivalent), remove hair on the animal's chest at the surgical site. It is advisable to ~~{~~perform this portion of the protocol in an area of the laboratory away from the surgical suite~~}~~, but depending upon the anesthesia used, maintaining aseptic areas as best as possible shall be followed, such as using clearly defined, but separate areas on the same table and/or placing sterile pads/coverings over areas defined for surgery AFTER the animal has been shaved.
5. Masking tape and a simple platform or a commercially available small animal surgical tray (Harvard Apparatus catalog no. 722590) can be used to secure the animal in the proper position for intubation and surgery. Care should be taken to avoid excessive tension and/or stretching of the limbs while positioning and fixing the mouse's limbs; joints can be traumatized or breathing may be impaired.

6. A supplemental heat source will be used (e.g. electric warming pad, phase-change heat pad, far infrared heating, or equivalent) to maintain normal mouse body temperature. Ensure sterile and aseptic techniques are observed when external equipment is incorporated into the procedure. Care should be taken to avoid overheating or burning the animal.
7. Intubation for ventilation will be used in survival surgery procedures in mice whenever a thoracotomy is performed. Commercially available intubation systems are available from Harvard Apparatus (Catalog no. ST1 72-9085) or Hallowell EMC (Catalog no. 000A3747). A safe and effective method that exposes the animals to minimal stress shall be developed and used by the surgeon as part of this pilot protocol.
8. Artificial ventilation using a mouse ventilator 687 series (Harvard Apparatus, catalog no. 550001) or equivalent should be used with ventilation rates and tidal volumes as provided by company formulas or per recommendations in [22]. For the Harvard Apparatus 687 series mouse ventilator, the formulas are:

$$V_t = 0.0062 \times Mb^{1.01}$$

$$\text{Ventilation Rate (Breaths/min)} = 53.5 \times Mb^{-0.26}$$

Where V_t is tidal volume, and

Mb is animal mass in kg.

9. Sterile, non-medicated ophthalmic ointment should be applied to the eyes to prevent corneal drying [20].
10. Surgical site preparation uses three cycles of alternating scrubbing with chlorhexidine solution (0.75%) and 70% alcohol; the solutions should be warmed to 37°C to prevent hypothermia.
11. Subcutaneous, parenteral administration of warmed, sterile fluids (1-2 mL / 100g) body weight) will be administered as mice are vulnerable to fluid loss given their body volume to surface area ratio.
12. The mouse should be positioned for survival cardiac surgery in the right lateral position as described in [24].
13. Before an incision is made, a local anesthetic (0.1 mL of a 50%/50% mixture of lidocaine [0.5 mg/kg] and bupivicaine [1.5 mg/kg]) shall be injected subcutaneously in the area surrounding the incision.
14. The landmark for the incision is the left armpit. Using scissors, an oblique (~8-mm) incision is made (~2 mm) away from the left sterna border toward the left armpit (~1-2 mm below it). Both layers of thoracic muscles can either be cut or bluntly dissected, taking caution to avoid the superficial thoracic vein. The ribs and inflating lung should now be visible through the thin and semitransparent chest wall.
    a. If any arteries are accidentally transected while opening the chest, quickly cauterize them as needed to prevent increased morbidity/mortality secondary to hemorrhaging.
15. The chest cavity is opened with microsurgical scissors or hemostats by a small incision (~5-10 mm in length) at the level of the fourth or fifth intercostal space.
    a. The chest retractor is inserted and opened gently to spread the wound ~8-10 mm in width. The heart and lung can now be visualized. The time from incision to visualizing the heart and lung should be ≤ 10 minutes.
16. Grasping the pericardium with curved and straight forceps, gently separate the covering and fold over the arms of the retractor if possible. This maneuver pushes the lung slightly upwards, providing a clearer view of the apex of the heart.
17. The apex of the ventricle (Figure 5) will be mechanically clamped for at least 30 minutes [33,34] with microsurgical clips, vascular occlusion clamps or hemostats (e.g. Satinsky-type clamps) to reduce the blood flow to the region to ensure irreversible cellular damage [33,34], inducing myocardial injury by ischemia.
    a. While the apical portion of the heart is clamped, the ribcage should be reapproximated, overlying muscles and skin should be returned to their normal position and the incision can be covered by sterile gauze socked in warmed (37°C) sterile saline.
    b. Ischemia can be verified by the blanching of the clamped cardiac tissue.
    c. Irreversible damage can be verified after clamp removal if observations of muscle activity at the apical portion of the ventricle are quiescent or contracting irregularly and at a much lower rate than remote regions of the heart.

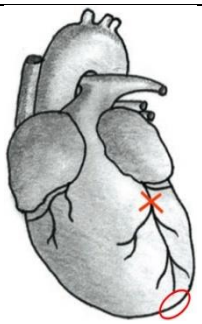

Figure 5: Red circle denotes site of mechanical clamping to simulate the same injury as ligating the LAD at the red X[22].

18. The cardiac cavity can be rinsed with 3-5 mL of sterile Lactated Ringer's solution or sterile saline to flush the cavity, compress the lungs and remove any air in the pleural cavity.
19. The chest cavity is closed by bringing together the 4th and 5th ribs with two 6-0 nylon (non-absorbable) sutures (with gentle pressure applied to the chest wall to reduce the volume of free air).
    a. Immediately before tightening the second suture, the lungs will be reinflated by blocking the ventilator outflow for no more than 3 respiratory cycles. The Lactated Ringer's or saline solution (if used) will ensure there is no air upon chest closure; the excess solution will be reabsorbed gradually by the surrounding tissue.
20. The muscles are closed with 4-0 absorbable sutures while the skin is closed with 3-0 or 4-0 nylon (monofilament, non-absorbable) sutures. Interrupted suture patterns should be used on the skin to prevent wound dehiscence. Rodent skin has the propensity to invert; everting suture patterns (horizontal mattress, simple interrupted, etc.) should be used. Time from clamp removal to chest closure should be ≤ 10 minutes.

Immediate Recovery Period: Any variance from the SOP – Post Operative / Post Anesthetic Care of Rodents is denoted in *underlined italics.*

The period from cessation of anesthesia or completion of surgery until animal achieves normal ambulation and can eat, drink, and groom.

1. *Immediately after closing the animal, a 0.5 mL bolus of 37°C sterile saline will be given.*
2. Animals are carefully observed every 5 minutes; anesthetized animals are never left unattended.
3. *Mice shall be placed on a warm platform under continued ventilation (100% oxygen) in a designated recovery area to allow recovery from surgery.*
4. *After the mouse resumes a normal breathing pattern, it can be extubated. To prevent respiratory distress, the mouse should breathe oxygen for another 5-10 minutes before returning to a cage.*
5. The animal is placed in a clean dry cage without bedding, as it may be ingested or inhaled during recovery. The cage should be placed on a supplemental heating source (e.g. electric warming pad, phase-change heat pad, far infrared heating, or equivalent) to prevent hypothermia. One should carefully monitor and regulate the anesthetized animals' core temperature because hyperthermia can easily occur and cause permanent damage and even death. To prevent possible injury to the anesthetized animal, recovering animals should be singly housed. If recovering animals are group housed, more frequent monitoring must be done.
6. Additional eye lubricant shall be instilled at this time.
7. Rate and depth of respiration is visually monitored, temperature is taken or palpate extremities to check animal's temperature. Color of mucous membranes, ears and tail are monitored to confirm normal tissue perfusion. Reflexes (i.e. pedal, palpebral and eye position) are monitored to assess recovery from anesthesia.
8. Animals should be turned every 10 minutes to improve respirations and decrease recovery time.
9. For surgical procedures longer than 30 minutes and/or where fluid loss due to hemorrhage or evaporation is anticipated, fluid support will be provided.
10. The analgesic regime will be followed as indicated in the approved protocol. Unless justification to the contrary is provided, all animals will receive at least 24 hours of analgesia following any surgical procedure.
11. The procedure performed will be noted on the animal's cage card.
12. If no complications arise, animal is monitored and care provided as described above every 30 to 60 minutes until the patient regains normal ambulation.

13. Once animal has normal ambulation, and is able to eat and drink normally, it will be returned to normal housing (in a cage with bedding) to the DLAR housing facility. Food will be provided on the cage floor. Additional supportive care will be provided by the research team unless DLAR staff is directed to assume this responsibility.

Long Term Recovery Period

The period when normal activity resumes until the incision is healed.

1. Research staff will check on the animal early the following day and at least four times (4X) daily for the first two days after surgery. Research staff will ensure that the animal is eating, drinking, eliminating, and ambulating normally. Also, body weight should be obtained daily for the first four days after surgery [or until the animal is sacrificed], then every other day thereafter until the animal is sacrificed for heart tissue harvesting).
2. *DietGel® 76A (Clear H_2O, Portland, ME) or equivalent can be administered for supportive care (nutrition and hydration).*
3. *Daily assessments of the wounds for any complications shall occur until the animal is euthanized (mice are to be kept until 19 days post-surgery, see Question 31). Suture removal shall be 10-14 days post-surgery.*
   a. The incision site is checked for clear or purulent discharge, redness, swelling, pain, suture removal by the animal, or incision breakdown.
4. Signs of surgical complication such as infection or pain will prompt a consultation with a DLAR veterinarian.
5. Any abnormalities (i.e. dehydration, lethargy and inappetence) will warrant supportive care, consultation with a DLAR veterinarian, and continued frequent monitoring and care; detailed records will be kept. Continued weight loss, dehydration and lethargy are not acceptable and may require early euthanasia.
6. Monitoring will continue daily until incision is healed and sutures are removed.

Heart Harvesting Procedure

1. For nuclei labeling index studies, each animal shall be injected with BrdU [30 mg/kg] three hours prior to collecting the heart.
2. Since this is a terminal procedure, portions of the full survival surgery procedure (Question 34c, Survival Surgery - Mechanically Induced Ischemia, Steps 1-19) can be omitted.
   a. To open the thorax of the animal, follow Question 34c, Survival Surgery - Mechanically Induced Ischemia, Steps 1-4, 13-15.
3. Hearts shall be cut in half and immediately flash frozen using LN_2 and/or placed in chilled (2-8°C) Allprotect Tissue Reagent (Qiagen, Cat. No. 76405) to stabilize DNA, RNA and protein.
   a. If sample staining does not follow immediate tissue harvesting, the samples may be frozen and stored in -80°C.
4. To study the histological evolution of heart repair after mechanically induced ischemia, one half of each sampled heart shall be sectioned for immunohistochemistry studies; the other heart shall be stored in Allprotect Tissue Reagent and frozen. The apex of the heart shall be included in each section as a reference point of the origin of ischemia.
5. Within each tissue sample, the goal is to identify, under microscopy, areas of necrotic, perinecrotic and penumbral tissue to elaborate the spatial relationships of tissue response to mechanically-induced ischemia. This will help identify the proliferating zone in relation to areas of necrosis (e.g. tissue 2 mm away from the apex) in each heart.
6. Cellular proliferation activity in the penumbra will be indexed by staining with antibodies specific for BrdU. Across the tissue samples, the goal is to identify how these zones of heart tissue evolve in response to an MI.

Perfusion Fixation In Mice

Terminal procedure to fix and stabilize heart tissue for downstream processing.

1. Terminal procedures will take place in Scott Hall DLAR facility, Advisor's Laboratory (Scott Hall 6213), IBio DLAR facility or Sponsor's Laboratory (IBio 1310).
2. Prepare fixative(s) and perfusion buffer(s) as required; see Question 33. "Describe All Non-Surgical Procedures".
3. Set up the perfusion device as stated in Question 33. "Describe All Non-Surgical Procedures".
4. Induce anesthesia. Administer pentobarbital sodium (Target Dose = 70-80 mg/kg; Acceptable Dose Range = 60-90 mg/kg).
   a. Optional: Dilute to a concentration of 5 mg/mL using sterile water or sterile saline. The diluted drug should be prepared in a small vial (e.g. sterile empty injection vial) just prior to injection into the animal. Invert the vial a few times and draw the diluted drug from the bottom of the vial (drug is more dense than water).

5. After administering an injectable anesthetic, allow the animal to sit undisturbed in an empty cage as the anesthetic takes effect. Regularly monitor the depth of anesthesia by testing the pain reflex (toe-pinch); the lack of the pain reflex signals a medium-deep plane of anesthesia.
   a. A top-up dose of injectable anesthesia (~10-20% of the initial dose) should be administered if the proper depth of anesthesia is not reached after 10 minutes.
6. Once the mouse is at the appropriate plan of anesthesia, use an animal hair to remove hair on the animal's chest at the surgical site.
7. Secure the animal in a dorsal-recumbent position for intubation. Intubate as outlined in the procedures describing survival surgery.
8. Place the animal in a large enough pan to collect any and all blood and perfusate that is drained.
9. With the animal in a dorsal-recumbent position, open the chest cavity by making a lateral incision through the skin and abdominal wall just below the rib cage.
10. Make an incision across the entire diaphragm to expose the thoracic cavity.
11. Make cuts along the midline of the rib cage on each side, allowing the surgeon to lift the entire rib cage away from the chest cavity. Carefully trim any fascia connecting the rib cage away from the heart.
12. After attaching an appropriate needle (25-30 Ga.) to the end of the perfusion device, insert the needle into the left ventricle and into the ascending aorta. Make sure the tip does not reach the aortic arch.
13. Using appropriate hemostats, clamp the needle where it enters the heart and around the needle tip in the ascending aorta in order to secure the heart in place.
14. In order to allow for the drainage of blood from the animal, make a small incision into the right atrium. Make sure not to damage the descending aorta.
15. Flush the mouse with about 40-50 mL of flushing buffer, adjusting the clamp to allow for a flowrate of 2-4 mL/min.
16. Switch to the appropriate fixative, taking care to avoid introducing air bubbles into the system. Flush the mouse with the fixative for 20-30 minutes at a flowrate of 1-2 mL/min.
17. Harvest the heart and place in a container of the same fixative used in the terminal perfusion procedure. Ensure the heart is fully immersed in the fixative.
18. Complete the euthanization of the animal per Question 37. "Euthanasia Methods".

e. Fill out the following anesthesia table for every surgical procedure considered.

Pre/Intra-operative analgesia, anesthesia, sedation, and muscle relaxation

Species/Procedure	Initial Regimen	Dosage/Route/ Frequency	Maintenance Regimen**	Dosage/Route / Frequency
Mice / Survival Cardiac Surgery & Terminal Perfusion	Pentobarbital sodium	70-80 mg/kg / Intraperitoneal (IP) / Start of surgery only.	~10-20% of initial regimen.	As needed (PRN).
Mice / Survival Cardiac Surgery	Buprenorphine-SR (Sustained Release)	1.0 mg/kg / Subcutaneous / Up to 24-48h prior to surgery	N/A	N/A
Mice / Survival Cardiac Surgery	Buprenex (Buprenorphine chloride)	0.05 mg/kg / Subcutaneous / Onset of surgery	N/A	N/A
Mice / Survival Cardiac Surgery	50%/50% mixture of lidocaine [0.5 mg/kg] and bupivicaine [1.5 mg/kg]	0.1 mL / Subcutaneous / Prior to incision only.	N/A	N/A

**Indicate what parameters will be used to determine the need for additional doses of anesthesia.

Regularly monitor (every 5-7 minutes) the depth of anesthesia by testing the pain reflex (toe-pinch); a top-up dose of anesthesia (~10-20% of the initial dose) should be administered as needed. The lack of the pain reflex signals a medium-deep plane of anesthesia.

f. Post-Operative Surgical Details

	Not Applicable; the surgery is non-survival
X	SOP for Post Operative/ Post Anesthetic Care of Rodents will be followed
	SOP will not be followed. Describe variance from SOP and justify below.

N/A

Post-operative sedation and analgesia

Species/Procedure	Sedative	Dosage/Route/ Frequency	Analgesic	Dosage/Route/ Frequency
Mice / Post-operative follow up	N/A	N/A	Buprenorphine-SR (Sustained Release)	1.0 mg/kg / Subcutaneous / Every 72h (q72h) PRN (Applicable to mice that are sacrificed after 72h.)
Mice / Post-operative follow up	N/A	N/A	Buprenex (Buprenorphine chloride)	0.05mg/kg SQ 8-12h S/P surgery for at least 24h, then q8-12h PRN

**Indicate what parameters will be used to determine the need for additional doses of analgesia.

If mice show continued sign of stress (lack of grooming behavior or a dull hair coat, decreased activity and/or a hunched posture) additional doses of analgesia shall be administered.

g. How will the animals be monitored for adverse effects? Describe any potential effects.

Because myocardial infarction surgeries may cause significant mortality, mice will be monitored often (4X daily) for the first few days. Lethargy, inactivity, non-responsive or reluctance to move with gentle stimulation, increased respiratory rate or effort and/or lateral recumbency are signs we will watch for and euthanize following this surgery. Research staff will check on the animal per the SOP for Post Operative/Post Anesthetic Care of Rodents. Also, body weight should be obtained daily for the first four days after surgery [or until the animal is sacrificed], then every other day thereafter until the animal is sacrificed for heart tissue harvesting).

35. SURGICAL PROCEDURE in NON-RODENTS:

	NOT APPLICABLE

a. Classification

X	Non-survival surgery (animals do not recover from anesthetic for any period of time)
	Minor survival surgery
X	**Major** survival surgery
	Multiple survival surgeries - Review the Multiple Survival Surgeries Policy and provide justification below.

N/A

b. Surgeon(s)

Provide the names of the person(s) who will perform ***survival*** surgery (must also be listed in Q11).

	Not Applicable; only non-survival surgery will be performed.

Jeremy (Jay) Tolentino Llaniguez

c. Surgical Details

Give a detailed overview of the surgical procedures to be performed, the size and anatomical location of incisions, the anticipated time to perform each, and the time frames of their performance in relation to the overall protocol and also in relation to each other (if more than one procedure is performed on the same animal). Clearly indicate the time of planned euthanasia following the surgery.

Axolotl (*Ambystoma mexicanum*) – Operators must always wear powder-free latex or nitrile gloves when handling axolotls.

Survival Surgery - Mechanically Induced Ischemia:

1. The general surgical procedure for induced myocardial ischemia in axolotls will begin with a minimum 24-hour fast [40-42] of the animal(s) to avoid emesis during anesthesia induction and to reduce stomach volume to provide room for organ movement during surgery.
2. Anesthesia will be induced by placing the animal(s) in a water bath with 0.1% tricaine methanesulfonate (MS-222); depth of surgical plane of anesthesia is determined by the loss of righting reflex, no spontaneous movements and no reflex to pain.
3. Insert the microchip transponder as outlined in Question 33a. Animals can also be identified and tracked if singly housed.
4. A single dose of enrofloxacin/Baytril® (Dosage: 5 mg/kg, Recommended: Dilute stock Baytril® solution from 22.7 mg/mL to a 5 mg/mL concentration) will be administered pre-operatively as amphibian procedures are considered "clean-contaminated" at best. Inject the antibiotic intracoelomically just in front of a hind leg, approximately parallel to the body and about midway between the dorsal and ventral surfaces: that is, dorsal to the bladder and ventral to the kidneys and caudal enough to prevent injecting into the liver or spleen. See Figure 2 for details.
    a. To dilute the enrofloxacin, it is suggested to use one of the following formulations suited for amphibian patients: (1) one part of saline (0.9% NaCl) mixed with two parts of 5% dextrose, or (2) seven parts of saline mixed with one part of sterile water.
    b. To facilitate the IC injection into the animal, the axolotls can be placed into a state of anesthesia induction or even into a light plane of anesthesia before injecting.
    c. For animals receiving buprenorphine, administer both the analgesic and antibiotic at the same time to reduce stress upon the animal.
5. The animal(s) will then be transferred to a pan with 50% Holtfreter's solution (1.75 g NaCl, 0.050 g $CaCl_2$, 0.025 g KCl, and 0.100 g $NaHCO_3$ per liter of dechlorinated water) [40] in a dorsal-recumbent position. Enough solution shall be placed in the pan to adequately cover the gills.
    a. Another option is to cover the animal with Kimwipe™ laboratory tissues or gauze that have been moistened with 50% Holtfreter's solution. Tease away the tissues to expose the surgical area while keeping the rest of the animal covered. Regularly monitor the depth of anesthesia by testing the pain reflex; additional anesthesia can be achieved by placing the animal in a bath of maintenance dose MS-222 solution or 3-5 mL of additional maintenance dose MS-222 can be applied directly to the gills and the moistened Kimwipes™ laboratory tissues or gauze that cover the animal until the pain reflex subsides.
6. The ventral surface of the thorax will be disinfected by placing sterile gauze soaked in chlorhexidine solution (0.75%) or benzalkonium solution (2 mg/L) for 5-10 minutes at the intended site of incision; do not rub the gauze on the animal's skin. It is important to maintain the mucus layer covering the animal's skin.
7. Before proceeding with the incision, remove the gauze containing chlorhexidine and gently wash the area with sterile normal saline (0.9% NaCl) over another bucket or sink, placing the animal back in the pan with 50% Holtfreter's solution once finished**.** If Kimwipes™ are used, simply irrigate the chest area that is left exposed with sterile normal saline (0.9% NaCl).
8. With the animal in a dorsal-recumbent position, a **~**10mm paramedian ventral thorax-area incision will be made with a #15 blade (amphibian integument is thin, but very tough [41]) on the animal's right or left side to prevent damaging the ventricular muscle and midline abdominal vein.
9. Microsurgical scissors will be used to expose the cardiac cavity; the pectoral girdle and muscles will be retracted with micro hemostats, sutures or rib separator.
10. The apex of the ventricle will be mechanically clamped for at least 30 minutes with microsurgical clips, vascular occlusion clamps or hemostats (e.g. Satinsky-type clamps) to reduce the blood flow to the region to ensure irreversible cellular damage [33,34], inducing myocardial injury by ischemia. Ischemia can be verified by the blanching of the clamped cardiac tissue.
    a. Irreversible damage can be verified after clamp removal by observations of the muscle activity at apical portion of the ventricle are quiescent or contracting irregularly and at a much lower rate than remote regions of the heart.

11. The cardiac cavity can be rinsed with 3-5 mL of sterile Lactated Ringer's or amphibian fluid solution (as mentioned above) to flush the cavity before the pericardium is approximated using non-absorbable, monofilament sutures.
12. The skin will then be closed using an everting suture pattern (to prevent keratin cysts [40,41]) with non-absorbable, monofilament sutures; 3-0 or 4-0 suture is generally adequate.

Axolotl (*Ambystoma mexicanum*) – The following are detailed procedures for post-anesthetic care of non-rodents.

Immediate Recovery Period

The period from cessation of anesthesia or completion of surgery until animal achieves normal ambulation and can eat and drink.

13. After closing the incision, administer subcutaneous or intracoelomic postoperative fluids. Two easily formulated solutions for use in amphibian patients are (1) one part of saline (0.9% NaCl) mixed with two parts of 5% dextrose, and (2) seven parts of saline mixed with one part of sterile water. An appropriate dose of either solution is 25 mL/kg of body weight [40].
14. The animal(s) will be placed into a fresh bath of 50% Holtfreter's solution to allow full recovery from anesthesia.
    a. Once placed in a cage with fresh 50% Holtfreter's solution, the administration of antinociceptives shall be followed per the dosing described in the Long Term Recovery Period.
        14.a.1. For animals in the buprenorphine arm, no further action is required.
        14.a.2. For animals in the butorphanol arm, butorphanol shall be added to the cage water.
15. The analgesic regime will be followed as described in below. Unless justification to the contrary is provided, all animals will receive at least 24 hours of analgesia following any surgical procedure.
16. The procedure performed will be noted on the animal's cage card.
17. If no complications arise, animal is monitored and care provided as described above every 30 to 60 minutes.
18. Once animal has normal ambulation, it will be returned to normal housing (original aquatic container) to the DLAR housing facility. Food will be provided following feeding protocol. Additional supportive care will be provided by the research team unless DLAR staff is directed to assume this responsibility.

Long Term Recovery Period

The period when normal activity resumes until the incision is healed.

19. Research staff will check on the animal early the following day and at least daily thereafter. Research staff will ensure that the animal is eating, drinking, eliminating, and ambulating normally. Also, body weight should be obtained daily for the first four days after surgery [or until the animal is sacrificed], then every other day thereafter until the animal is sacrificed for heart tissue harvesting).
20. For 3-5 days following surgery (as applicable by experimental design of sampling procedures), the animals shall be given daily injections of enrofloxacin/Baytril® (Dosage: 5 mg/kg, Recommended: Dilute stock Baytril® solution from 22.7 mg/mL to a 5 mg/mL concentration) intracoelomically [46].
    a. To dilute the enrofloxacin, it is suggested to use one of the following formulations suited for amphibian patients: (1) one part of saline (0.9% NaCl) mixed with two parts of 5% dextrose, or (2) seven parts of saline mixed with one part of sterile water.
    b. To facilitate the IC injection into the animal, the axolotls can be placed into a state of anesthesia induction or even into a light plane of anesthesia before injecting.
    c. For animals receiving buprenorphine, administer both the analgesic and antibiotic at the same time to reduce stress upon the animal.
21. The analgesic regime in the long term recovery period is:
    a. Buprenorphine shall be given q24h for 48h. To treat the animals as similarly as possible, animals receiving buprenorphine shall have their cage water changed every day, at the time of administering the analgesic.
    b. Butorphanol shall be administered in the axolotl's cage water for 48h. In order to keep the levels of dissolved antinociceptives consistent, cage water shall be changed every day with a fresh bolus of Butorphanol added.
        21.b.1. Depending upon the rate of metabolism of butorphanol, as determined in the Anesthesia + Butorphanol arm, additional butorphanol MAY be added to the axolotl's environment to maintain steady levels of the drug before a fresh cage change occurs.
22. Food shall be offered starting on postoperative day 1 (surgical procedure is deemed day 0).
23. Daily assessments of the wounds for any complications should occur up to suture removal (7-10 days) and for a few days afterwards.

24. The incision site is checked for clear or purulent discharge, redness, swelling, pain, suture removal by the animal, or incision breakdown.
25. Sutures shall be removed under anesthesia (0.1% tricaine methanesulfonate/MS-222) [40-42,47].

Heart Harvesting Procedure

1. For nuclei labeling index studies, each animal shall be injected with BrdU (250 mg/kg [11,48]) through the intracoelomic route at least three hours prior to collecting the heart.
    a. BrdU is soluble in water up to 10 mg/mL without the use of heat. To dissolve the BrdU, it is suggested to use one of the following formulations suited for amphibian patients: (1) one part of saline (0.9% NaCl) mixed with two parts of 5% dextrose, or (2) seven parts of saline mixed with one part of sterile water.
        1.a.1. A typical axolotl weighs about 100 g (0.1 kg). At a BrdU concentration of 10 mg/mL, a 100 g axolotl will require a BrdU injection volume of 2.5 mL to achieve a 250 mg/kg BrdU dose.
    b. If staining results are not sufficient, BrdU [250 mg/kg] can be injected every 24 hours for up to 7 days prior to heart harvesting (as allowed by sampling timeline) [48].
2. Since this is a terminal procedure, portions of the full survival surgery procedure (Question 35c, Survival Surgery - Mechanically Induced Ischemia, Steps 1-12) can be omitted.
    a. To open the thorax of the animal, follow Question 35c, Survival Surgery - Mechanically Induced Ischemia, Steps 8-9.
3. Hearts shall be cut in half and immediately flash frozen using LN_2 and/or placed in chilled (2-8°C) Allprotect Tissue Reagent (Qiagen, Cat. No. 76405) to stabilize DNA, RNA and protein.
    a. If sample staining does not follow immediate tissue harvesting, the samples may be frozen and stored in -80°C.
4. To study the histological evolution of heart repair after mechanically induced ischemia, one half of each sampled heart shall be sectioned for immunohistochemistry studies; the other heart shall be stored in Allprotect Tissue Reagent and frozen. The apex of the heart shall be included in each section as a reference point of the origin of ischemia.
5. Within each tissue sample, the goal is to identify, under microscopy, areas of necrotic, perinecrotic and penumbral tissue to elaborate the spatial relationships of tissue response to mechanically-induced ischemia. This will help identify the proliferating zone in relation to areas of necrosis (e.g. tissue 2 mm away from the apex) in each heart.
6. Cellular proliferation activity in the penumbra will be indexed by staining with antibodies specific for BrdU. Across the tissue samples, the goal is to identify how these zones of heart tissue evolve in response to an MI.

Perfusion Fixation In Axolotls:

Terminal procedure to fix and stabilize heart tissue for downstream processing.

1. Terminal procedures will take place in IBio DLAR Facility or Sponsor's Laboratory (IBio 1310).
2. Any general surgical procedure should begin with a minimum 24-hour fast [40-42] of the animal(s) to avoid emesis during anesthesia induction and to reduce stomach volume to provide room for organ movement during surgery.
3. Prepare fixative(s) and perfusion buffer(s) as required; see Question 33. “Describe All Non-Surgical Procedures”.
4. Set up the perfusion device as stated in Question 33. “Describe All Non-Surgical Procedures”.
5. Anesthesia will be induced by placing the animal(s) in a water bath with 0.1% tricaine methanesulfonate (MS-222); depth of surgical plane of anesthesia is determined by the loss of righting reflex, no spontaneous movements and no reflex to pain.
6. Place the animal in a large enough pan to collect any and all blood and perfusate that is drained.
7. With the animal in a dorsal-recumbent position, a ~10mm paramedian ventral thorax-area incision will be made with a #15 blade (amphibian integument is thin, but very tough [41]) on the animal's right or left side to prevent damaging the ventricular muscle and midline abdominal vein.
    a. If the animal has already had a prior surgery, re-open the prior incision using microsurgical scissors.
8. Microsurgical scissors will be used to expose the cardiac cavity; the pectoral girdle and muscles will be retracted with micro hemostats, sutures or rib separator.
9. Carefully grasp the pericardium and cut open with microsurgical scissors.
    a. If the animal has already had a prior surgery, re-open the prior incision using microsurgical scissors.
10. Using fine forceps, raise the bulbus cordis and truncus arteriosus and pull a fine suture or thread (4-0 to 6-0 is suggested) behind the structure. Create a loosely fitting loop around the truncus arteriosus in preparation for holding an injection needle in place.

11. After attaching an appropriate needle (25-30 Ga.) to the end of the perfusion device, insert the needle starting from the proximal end of the bulbus cordis. Before tightening the thread around the bulbus cordis to hold the needle in place, ensure the injection needle is not inserted too far into the truncus arteriosus. Inserting the needle too far to the distal edge of the truncus will prevent the flow of perfusate into all of the exiting arteries.
12. In order to allow for the drainage of blood from the animal, make a small incision into the sinus venosus (dorsal side of the heart). See Figure 6.
13. Flush the axolotl with about 40-50 mL of flushing buffer, adjusting the clamp to allow for a flowrate of 2-4 mL/min.
14. Switch to the appropriate fixative, taking care to avoid introducing air bubbles into the system. Flush the axolotl with the fixative for 20-30 minutes at a flowrate of 1-2 mL/min.
15. Harvest the heart and place in a container of the same fixative used in the terminal perfusion procedure. Ensure the heart is fully immersed in the fixative.
16. Complete the euthanization of the animal per Question 37. "Euthanasia Methods".

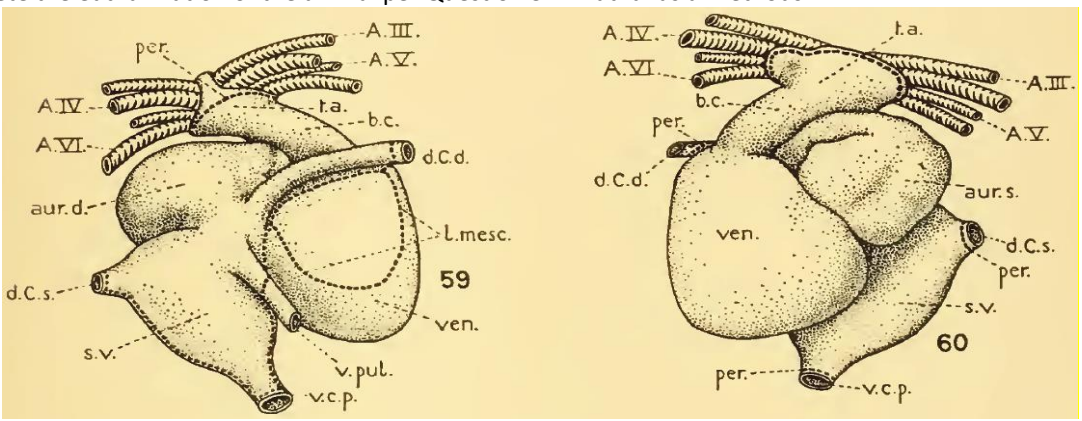

Figure 6: Anatomy of the axolotl heart. b.c. = Bulbus Cordis, t.a. = Truncus Arteriousus, s.v. = Sinus Venosus, ven. = Ventricle, A.III. = Carotid Arch, A.IV. = Systemic Arch, A.V. = "Third" Arch, A.VI = Pulmonary Arch

d. Pre-operative procedures

1. Describe any research procedures (e.g. conditioning, manipulations, study drug treatments, catheter placement, etc.) to be performed before initiating surgery: **[ ] None** (acclimation only)

1. The first dose of enrofloxacin (5 mg/kg) will be administered intracoelomically pre-operatively as amphibian procedures are considered "clean-contaminated" at best.
2. Depending upon the experimental group, antinociceptives shall be administered as such:
   a. A dose of buprenorphine shall be given pre-operatively as an intracoelomic (IC) injection at least 1h prior to surgery.
   b. Butorphanol shall be administered directly into the 50% Holtfreter's solution of the animal's cage at least 1h prior to surgery.

2. Describe any withholding of food or water prior to surgery and the time span: **[ ] None**

The general surgical procedure for induced myocardial ischemia in axolotls will begin with a minimum 24-hour fast [40-42] of the animal(s) to avoid emesis during anesthesia induction and to reduce stomach volume to provide room for organ movement during surgery.

3. Fill the following table for every surgical procedure considered. Specify any pre-operative sedative or pre-emptive analgesic to be administered. **[ ] None**

Pre-operative sedation and analgesia				
Species/Procedure	Sedative	Dosage/Route/ Frequency	Analgesic	Dosage/Route/ Frequency

Axolotl / Survival Cardiac Surgery	Tricaine Methanesulfonate (MS-222)	0.1% / Transcutaneous & Branchial / As needed (PRN)	Buprenorphine Or: Butorphanol	Target = 50 mg/kg (Published Range = 0.2 – 75 mg/kg) / Intracoelomic / One dose at least 1h prior to surgery Target = 0.5 mg/L 50% Holtfreter's solution / Transcutaneous & Branchial / One dose at least 1h prior to surgery
Axolotl / Terminal perfusion	Tricaine Methanesulfonate (MS-222)	0.1% / Transcutaneous & Branchial / As needed (PRN)	N/A	N/A

e. Surgical anesthesia induction and intra-operative procedures

1. List each surgery and the initial and maintenance anesthetic protocol.

Intra-operative anesthesia, sedation, muscle relaxation and analgesia

Species / Procedure	Initial Regimen	Dosage/Route/ Frequency	Maintenance Regimen	Dosage/Route/ Frequency
Axolotl / Survival Cardiac Surgery and Terminal perfusion	Tricaine Methanesulfonate (MS-222)	0.1% / Transcutaneous & Branchial / As needed (PRN)	Tricaine Methanesulfonate	0.05% [40] / Transcutaneous & Branchial / As needed (PRN)

2. Describe any supportive care given to the anesthetized animal.

Skin of axolotls shall be continually moistened throughout surgical procedure. This can be achieved by performing the surgery in a tray filled with enough 50% Holtfreter's solution (see Question 35.d.4) to keep the gills submerged or by wrapping the axolotl in moistened Kimwipes™ and ensuring they stay well-saturated with 50% Holtfreter's solution.

3. Describe the methods and time frames by which surgical anesthesia, analgesia, physiologic parameters (e.g. vital signs) and over all well-being of the animal will be monitored. Indicate what parameters will be used to determine the need for additional doses of anesthesia. Describe what type of written intra-operative record will be kept.

Monitoring Physiologic Parameters

1. The depth of surgical plane of anesthesia will be continuously monitored (every 5-7 minutes) by observing for the loss of righting reflex, ensuring no spontaneous movements and no reflex to pain.
2. The appropriate plane of anesthesia is characterized by branchial and gular respiratory movements of 8 – 10 respirations/ [49].
   a. Additional anesthesia can be achieved by placing the animal in a bath of maintenance dose MS-222 solution or 3-5 mL of additional maintenance dose MS-222 can be applied directly to the gills and the moistened Kimwipes™ laboratory tissues or gauze that cover the animal until the pain reflex subsides.

Written intra-operative records shall note the following:

1. Time of incision.
2. Time of chest cavity exposure using retractors.
3. Time of application of mechanical clamp.
4. Time of removal of mechanical clamp.
5. Time to close chest cavity.
6. Time to close animal.

Any additional notes, observations or recommendations.

4. Describe how the surgical site(s) will be prepared prior to surgery.

1. The animal(s) will be transferred to a pan with 50% Holtfreter's solution (1.75 g NaCl, 0.050 g $CaCl_2$, 0.025 g KCl, and 0.100 g $NaHCO_3$ per liter of dechlorinated water) [40] in a dorsal-recumbent position. Enough solution shall be placed in the pan to adequately cover the gills.
    a. Another option is to cover the animal with Kimwipe™ laboratory tissues or gauze that have been moistened with 50% Holtfreter's solution. Tease away the tissues to expose the surgical area while keeping the rest of the animal covered. Regularly monitor the depth of anesthesia by testing the pain reflex; additional anesthesia can be achieved by placing the animal in a bath of maintenance dose MS-222 solution or by squirting 3-5 mL of maintenance dose MS-222 solution, applying the 3-5 mL directly on the axolotl's gills and the covering Kimwipe™ laboratory tissues or gauze, until the pain reflex subsides.
2. The ventral surface of the thorax will be disinfected by placing sterile gauze soaked in chlorhexidine solution (0.75%) or benzalkonium solution (2 mg/L) for 5-10 minutes at the intended site of incision. It is important not to rub the gauze at the surgical site. Maintaining the mucus layer over the skin will speed healing and improve outcomes. The sterilization procedure simply sterilizes the mucus layer and underlying skin.
3. Before proceeding with the incision, remove the gauze containing chlorhexidine and gently wash the area with sterile normal saline (0.9% NaCl) over the sink or another bucket or tray. This procedure should not be repeated 3X like in the mouse since axolotl skin is sensitive to chemicals [40].

5. Describe the sterile techniques used for surgery. Describe the use of surgeon's clothing, drapes, and instruments. If sterile clothing, equipment, drapes, and instruments are used, describe how they are initially sterilized, and how they are kept sterile if used for more than one animal.

1. The surgeon(s) shall wear at minimum a clean scrub shirt, gown or lab coat; since axolotl surgeries are at best clean-contaminated, a cap and mask are optional but advised. The surgeon(s) shall wash their hands and puts on sterile gloves.
2. Kimwipe™ laboratory tissues or gauze soaked in 50% Holtfreter's solution shall be used to cover the rest of the axolotl's main body mass, or the animal shall be immersed in 50% Holtfreter's solution.
3. Instruments are sterilized prior to surgery via steam autoclave.
    a. Instruments are wiped clean of debris then tips are re-sterilized with a glass bead sterilizer between animals.
    b. Instruments are re-sterilized by autoclave after each group of six (6) axolotls.
    c. An aseptic surface on which to place instruments during surgery will be provided.

f. Post-operative care

☐ **Not Applicable**; the surgery is non-survival

1. Describe the expected condition of the animal following full recovery from surgical anesthesia. If any physical or functional abnormalities are described, indicate their expected effect on the animal and their anticipated duration. Describe potential post-operative complications that might arise, and how they will be dealt with. Do not include highly unlikely complications.

1. After recovering from anesthesia and surgery, the axolotl should show purposed and organized limb movements. Branchial and gular respiratory movements should return and increase in frequency from what is used to determine depth of anesthesia (> 8 – 10 respirations / minute).
    a. If the animal is not showing recovery from anesthesia, additional time in an oxygenated water bath is recommended until normal limb movements and breathing patterns return.
2. If the wound is slow to heal, additional administration of antibiotics is recommended. Also, the water temperature should be reduced by refrigerating the animals (while they are in their plastic tubs/mouse polys) at 5-7°C (41-45°F) to speed the healing process [50].

2. Provide a plan for post-operative monitoring and supportive care covering the period from end of surgery until the next morning. Indicate what type of written post-operative monitoring and care records will be kept. Describe what clinical signs will be used to determine if adequate analgesia is being provided. In the table below, indicate what analgesic agents will be used during this time.

Immediate Recovery Period

The period from cessation of anesthesia or completion of surgery until animal achieves normal ambulation and can eat and drink.

1. After closing the incision, administer subcutaneous or intracoelomic postoperative fluids. Two easily formulated solutions for use in amphibian patients are (1) one part of saline (0.9% NaCl) mixed with two parts of 5% dextrose, and (2) seven parts of saline mixed with one part of sterile water. An appropriate dose of either solution is 25 mL/kg of body weight [40]. Fluids should be at room temperature or cooler.
2. At the end of surgery, irrigation with fresh, de-chlorinated water or 50% Holtfreter's solution will be performed until reflex movement is returned.
3. After uncoordinated limb movements and branchial/gular respiratory movements return, the animal(s) will be placed into a fresh bath of 50% Holtfreter's solution to allow full recovery from anesthesia.
4. The analgesic regime will be followed as indicated in the approved protocol. Unless justification to the contrary is provided, all animals will receive at least 24 hours of analgesia following any surgical procedure.
5. The procedure performed will be noted on the animal's cage card.
6. If no complications arise, animal is monitored and care provided as described above every 30 to 60 minutes.
7. Check on the transponder injection site to ensure the wound is still appropriately covered by wound glue.

Once animal has normal ambulation, it will be returned to normal housing (original aquatic container) to the DLAR housing facility. Food will be provided following feeding protocol. Additional supportive care will be provided by the research team unless DLAR staff is directed to assume this responsibility.

Post-operative sedation and analgesia (short-term – *from surgery until the following morning*)

Species/Procedure	Sedative	Dosage/Route/ Frequency	Analgesic	Dosage/Route/ Frequency
Axolotl / Post-operative follow up	N/A	N/A	Buprenorphine Or: Butorphanol	Target = 50 mg/kg (Published Range = 0.2 – 75 mg/kg) / Intracoelomic / q24h for 48h. Target = 0.5 mg/L 50% Holtfreter's solution / Transcutaneous & Branchial / Continuous for 48h

3. Provide a plan for post-operative monitoring and supportive care for the period from morning after surgery and for the next 9 days. Describe what clinical signs will be used to determine if adequate analgesia is being provided. In the table below, indicate what analgesic agents will be used during this time.

Long Term Recovery Period

The period when normal activity returns while the incision completely heals.

1. Research staff will check on the animal early the following day and at least 4X daily thereafter for postoperative days 1 & 2.
   a. Research staff will ensure that the animal is eating, drinking, eliminating, and ambulating normally. Also, body weight should be obtained on a frequent basis (daily for the first four days after surgery [or until the animal is sacrificed], then every other day thereafter until the animal is sacrificed for heart tissue harvesting).
2. Food shall be offered starting on postoperative day 1 (cardiac surgery is day 0).
3. For 3-5 days following surgery (as applicable by experimental design of sampling procedures), the animals shall be given daily injections of enrofloxacin/Baytril® (Dosage: 5 mg/kg, Recommended: Dilute stock Baytril® solution from 22.7 mg/mL to a 5 mg/mL concentration) intracoelomically [46].
4. Daily assessments of the wounds for any complications should occur up to suture removal (7-10 days) and for a few days afterwards. Additionally, check on the transponder injection site to ensure the wound covered by cyanoacrylate is healing properly.
5. The incision site is checked for clear or purulent discharge, redness, swelling, pain, suture removal by the animal, or incision breakdown.
6. Sutures shall be removed under anesthesia (0.1% tricaine methanesulfonate/MS-222) [40-42].

[ ] None

Post-operative sedation and analgesia (long-term)				
Species/Procedure	Sedative	Dosage/Route /Frequency	Analgesic	Dosage/Route/ Frequency
Axolotl / Post-operative follow up	N/A	N/A	Buprenorphine Or: Butorphanol	Target = 50 mg/kg (Published Range = 0.2 – 75 mg/kg) / Intracoelomic / q24h for 48h. Target = 0.5 mg/L 50% Holtfreter's solution / Transcutaneous & Branchial / Continuous for 48h

4. Who (individual or group of people) will be responsible for post-operative care during regular working hours? Who will provide care, if necessary, after regular work hours (including weekends and holidays)?

Post-operative care during regular working hours: DLAR staff and PI.
Post-operative care after regular working hours: PI.

g. How will the animals be monitored for adverse effects? Describe any potential effects.

Research staff will check on the animal per the axolotl care and husbandry SOP that will be developed by PI and Attending Veterinarian (AV). Please see that protocol (SOP No. 02.19.01) ways to monitor adverse effects and any potential effects. In short, DLAR staff will check on the animal at least daily. Research staff will ensure that the animal is eating, drinking, eliminating, and ambulating normally. For any abnormal signs or behavior, the PI and/or AV shall be contacted for guidance on next steps.

VII. – EUTHANASIA AND ASSURANCE OF DEATH

36. STATE the SPECIFIC CRITERIA for the euthanasia of abnormal or moribund animals (assume someone may have to euthanize animals IN YOUR ABSENCE). Review the Defining Humane Endpoints Guideline.

[ ] **Not Applicable** (e.g. animals are used for tissue harvesting only and will not undergo any procedures prior to death)

[X] Weight loss of 20% or more

[X] Other conditions (examples may include, but are not limited to: a clinical condition that does not respond to treatment, such as an infected surgical site; any condition that a veterinarian deems severe enough to warrant euthanizing the animal). ***Please describe below:***

*Assessing Weight Loss: Consider euthanasia if animal's weight loss is >20%.
1. Each animal shall be weighed immediately prior to surgery.
2. Each animal shall be weighed every day following surgery for the first 4 days.
3. After the first 4 days post-surgery, animals can be weighed every other day until their hearts are sampled per the sampling schedule. Please see Question 31 for heart sampling schedule.

**Axolotl (*Ambystoma mexicanum*) – The following criteria can stage severity of illness in axolotls.
1. First signs of illness are:
   a. Loss of appetite;
   b. Deterioration of the gills; and/or
   c. Weight loss (you may see some anemia) of 20% or more.

   Health assessments shall be performed and isolation of the animal in cooler, antibiotic-laced baths (or housing in standard 50% Holtfreter's solution with administration of antibiotics by IP) is recommended if first signs of illness are detected.
2. More severely ill axolotls may be jaundiced and have small open skin sores.
3. Very ill animals may develop ascites or severe edema.
4. If animals do not respond to antibiotics and therapeutic baths, consider euthanasia.

**Mice (*Mus musculus*) – The following criteria from the Defining Humane Endpoints IACUC Guideline shall be used to define humane endpoints for euthanasia in mice.

1. Weight loss (rapid or chronic; meeting or exceeding 20% body weight of age matched controls).
2. Clinical conditions (rough hair coat, hunched posture, lethargy or recumbency, inactivity, non-responsive or reluctance to move with gentle stimulation, labored breathing/respiratory distress) unresponsive to treatment.
3. Significant self-induced trauma.

Any condition which interferes with the ability to eat/drink or ambulate.

37. EUTHANASIA METHODS:

PHS Policy on Humane Care and Use of Laboratory Animals requires the IACUC to use the recommendations of the *AVMA Guidelines for the Euthanasia of Animals: 2013 Edition*; please refer to it when necessary. If anesthetic overdose or CO_2 narcosis is used, a secondary procedure such as bilateral pneumothorax, severing the aorta, or removal of a critical organ must be used to assure that the animal will not recover.

Species	Method of Euthanasia*	Dosage(s) (mg/kg)	Route	Method to Assure Death
Axolotl (*Ambystoma mexicanum*)	3-stage euthanasia protocol: 1. Anesthesia 2. Euthansia 3. Removal of heart or decapitation and Pithing First induce surgical plane of anesthesia [0.1% MS-222] Tricaine methanesulfonate baths [MS-222].	1 g/L followed by 5-10 g/L water baths.	Branchial / Transcutaneous	Removal of heart or decapitation followed by pithing.
Axolotl (*Ambystoma mexicanum*)	Perfusion with fixative under anesthesia First induce surgical plane of anesthesia [0.1% MS-222] Tricaine methanesulfonate baths [MS-222].	1 g/L followed by 5-10 g/L water baths.	Branchial / Transcutaneous	Removal of heart or decapitation followed by pithing.
Mouse (*Mus musculus*)	Pentobarbital sodium	140-210 mg/kg	IP	Removal of heart, cervical dislocation or bilateral pneumothorax.
Mouse (*Mus musculus*)	Carbon dioxide (CO_2)	Displace 10-30% of cage volume/min	Inhalation	Removal of heart, cervical dislocation or bilateral pneumothorax
Mouse (*Mus musculus*)	Induce anesthesia as outlined in Question 34.c.1. and continue with Heart Harvesting Procedure in Question 34.c.	Pentobarbital sodium (Target Dose = 70-80 mg/kg; Acceptable Dose Range = 60-90 mg/kg) Isoflurane (3-4% induction, 1-3 %	Pentobarbital Sodium: IP Isoflurane: Inhaled	Removal of heart, cervical dislocation or bilateral pneumothorax.

		maintenance) in 100% oxygen		

***If the method is not consistent with the *AVMA Guidelines for the Euthanasia of Animals: 2013 Edition*, please provide scientific justification for the use of the method below.**

N/A – Methods are taken from *AVMA Guidelines for the Euthanasia of Animals: 2013 Edition*, pgs. 48-50 and 76-78.

a. Euthanasia of mouse and rat fetuses and neonates (Note: This question should not be marked as "Not Applicable" if breeding of animals will occur in house.)

- [X] **Not Applicable**
- [ ] The Euthanasia of Mouse and Rat Fetuses and Neonates Guideline will be followed.
- [ ] The Guideline will not be followed. Describe variance and justify below.

N/A

b. Rodent Decapitation (if used as the **primary** method of euthanasia)**:**

- [X] **Not Applicable**
- [ ] Decapitation by guillotine; the Use of Guillotines Policy will be followed.

Provide scientific justification below:

N/A

c. Cervical Dislocation (if used as the **primary** method of euthanasia):

- [X] **Not Applicable**
- [ ] Animals will be anesthetized prior to cervical dislocation.
- [ ] Animals will NOT be anesthetized.

Provide scientific justification below:

N/A

38. If animals will not be euthanized, state their final disposition:

- [X] **Not Applicable**

N/A

ATTENTION:

Please submit an ***Animal Hazardous Agents Form*** with this application as an attachment ***regardless of whether or not this protocol has any identified hazards***. The Office of Environmental Health and Safety (OEHS) is required to review and sign-off on every protocol prior to approval.

VIII. – CONFLICT OF INTEREST DISCLOSURE

Endorsements and Financial Conflict of Interest Disclosure:
Objectivity in research is a key component of any research project. One method for maintaining objectivity is to have **all** individuals involved in research design, development, or data evaluation/analysis disclose any potential and/or real financial conflict of interest. This includes all personnel listed on the protocol.

Note that you are being asked about all financial interests related to your responsibilities at WSU or its affiliates, not just the financial interests that may be related the funded project.

Examples of relevant relationships for potential conflict of interest include but are not limited to:

1. Receiving past, current, or expecting future income in the form of salary, stock or stock options/warranties, equity, dividends, royalties, profit sharing, capital gain, forbearance or forgiveness of a loan, interest in real or personal property, or involvement in a legal partnership with the sponsor;
2. Receiving past, current, or expecting future income in the form of consulting fees, honoraria, gifts, gifts to the University, or payments resulting from seminars, lectures, or teaching engagements, or service on a non-federal advisory committee or review panel;
3. Serving in a corporate or for-profit leadership position, such as executive officer, board member, fundraising officer, agent, member of a scientific advisory board, member of a scientific review committee, or member of a data safety monitoring committee, regardless of compensation;
4. Inventor on a patent or copyright involving technology/processes/products licensed or expected to be licensed to the sponsor.

IX. – CERTIFICATION BY PRINCIPAL INVESTIGATOR

As principal investigator I certify the following:

1. My staff and I will comply with all standards for animal care and investigation established in the *Guide for the Care and Use of Laboratory Animals* (the *Guide*, NRC 2011) and the Federal Animal Welfare Act, and will follow all policies established by the University to assure that these standards are met.
2. I assume responsibility for the work described here.
3. All individuals working with the animals on this protocol are qualified by virtue of training or experience to perform proper handling, experimental, and restraint techniques required for the species to be used.
4. I recognize my responsibility to identify occupational health hazards related to this protocol including identifying hazards, providing the necessary training for those involved, and supplying the appropriate protective clothing and equipment to minimize the risks.
5. I acknowledge my responsibility to file the appropriate paperwork (e.g. an annual inventory to the State of Michigan) if I use controlled substances.
6. This research does not represent unnecessary duplication of previous experiments.
7. I realize that failure to adhere to policies related to animal care and use may result in suspension or revocation of permission to perform animal research in Wayne State University facilities.

- For additional requirements and expectations please see the Principal Investigator Responsibilities.

_____ _____

Signature of Principal Investigator
(must be original; no copies, image files, etc.)

Date

Do you, your spouse or domestic partner, or any of your dependent children have a potential conflict of interest with the sponsor of this project? Either YES or NO must be marked by hand at the time of the signature.

☐ NO

☐ **YES***

*A "Financial Conflict of Interest Detailed Disclosure Form" must be filed with the Financial Conflict of Interest Committee annually or when changes occur. Find the form and more information on the Conflict of Interest Website.

X. – CERTIFICATION BY CO-INVESTIGATOR OR FACULTY ADVISOR

As the Co-Investigator or Faculty Advisor I certify the following:

I have read this protocol, understand my role in the project, and will comply with all standards for animal care and investigation established in the *Guide for the Care and Use of Laboratory Animals* (the *Guide*, NRC 2011) and the Federal Animal Welfare Act, and will follow all policies established by the University to assure that these standards are met.

Signature of Co-Investigator or Faculty Advisor
(must be original; no copies, image files, etc.)

Date

Name (Type/Print)

University Title (Type/Print)

Do you, your spouse or domestic partner, or any of your dependent children have a potential conflict of interest with the sponsor of this project? Either YES or NO must be marked by hand at the time of the signature.

☐ NO

☐ **YES***

*A "Financial Conflict of Interest Detailed Disclosure Form" must be filed with the Financial Conflict of Interest Committee annually or when changes occur. Find the form and more information on the Conflict of Interest Website.

XI. – DEPARTMENT CHAIRPERSON, DIRECTOR, OR DEAN'S ASSURANCE

I endorse the certifications made by the Principal Investigator and assure the University that the procedures outlined above have been or will be reviewed for scientific or educational merit by an internal or external review panel prior to initiating the project.

Signature of Chairperson
(must be original; no copies, image files, etc.)

Date

Name (Type/Print)

University Title (Type/Print)

Do you, your spouse or domestic partner, or any of your dependent children have a potential conflict of interest with the sponsor of this project? Either YES or NO must be marked by hand at the time of the signature.

☐ NO

☐ **YES***

*A “Financial Conflict of Interest Detailed Disclosure Form” must be filed with the Financial Conflict of Interest Committee annually or when changes occur. Find the form and more information on the Conflict of Interest Website.

XII. – RESEARCH PERSONNEL

All laboratory personnel listed in Question #5 must sign (original signatures; no copies, image files, etc.) below and disclose any potential conflict of interest with this project.

***If there is a potential conflict of interest, then a "Financial Conflict of Interest Detailed Disclosure Form" must be filed with the Financial Conflict of Interest Committee annually or when changes occur. Find the form and more information on the Conflict of Interest Website.** Either YES or NO must be marked by hand at the time of the signature.

NAME:	**TITLE:**
Do you, your spouse or domestic partner, or any of your dependent children have a potential conflict of interest with the sponsor of this project?	☐ NO ☐ **YES***
I have read this protocol, understand my role in the project, and will comply with all standards for animal care and investigation established in the *Guide for the Care and Use of Laboratory Animals* (the *Guide*, NRC 2011) and the Federal Animal Welfare Act, and will follow all policies established by the University to assure that these standards are met.	
Signature:	Date:

NAME:	**TITLE:**
Do you, your spouse or domestic partner, or any of your dependent children have a potential conflict of interest with the sponsor of this project?	☐ NO ☐ **YES***
I have read this protocol, understand my role in the project, and will comply with all standards for animal care and investigation established in the *Guide for the Care and Use of Laboratory Animals* (the *Guide*, NRC 2011) and the Federal Animal Welfare Act, and will follow all policies established by the University to assure that these standards are met.	
Signature:	Date:

NAME:	**TITLE:**
Do you, your spouse or domestic partner, or any of your dependent children have a potential conflict of interest with the sponsor of this project?	☐ NO ☐ **YES***
I have read this protocol, understand my role in the project, and will comply with all standards for animal care and investigation established in the *Guide for the Care and Use of Laboratory Animals* (the *Guide*, NRC 2011) and the Federal Animal Welfare Act, and will follow all policies established by the University to assure that these standards are met.	
Signature:	Date:

NAME:	**TITLE:**
Do you, your spouse or domestic partner, or any of your dependent children have a potential conflict of interest with the sponsor of this project?	☐ NO ☐ **YES***
I have read this protocol, understand my role in the project, and will comply with all standards for animal care and investigation established in the *Guide for the Care and Use of Laboratory Animals* (the *Guide*, NRC 2011) and the Federal Animal Welfare Act, and will follow all policies established by the University to assure that these standards are met.	

Signature:	Date:

XIII. – BIBLIOGRAPHY & REFERENCES CITED

1. **Francis ETB**, *The anatomy of the salamander*. 1934, Oxford,: The Clarendon Press. xxxi, 381 p., 381 l.
2. **Rose SM.** Epidermal dedifferentiation during blastema formation in regenerating limbs of Triturus viridescens. *J Exp Zool*. 108(3): 337-361, 1948.
3. **Rose SM and Rose, FC.** Tumor agent transformations in Amphibia. *Cancer Res*. 12(1): 1-12, 1952.
4. **Neff AW, Dent, AE, and Armstrong, JB.** Heart development and regeneration in urodeles. *Int J Dev Biol*. 40(4): 719-725, 1996.
5. **Zajdel RW, Zhu, Y, Fransen, ME, and Lemanski, LF.** A method for the isolation and culture of embryonic cardiomyocytes from Mexican axolotl. *Int J Dev Biol*. 40(4): 907-908, 1996.
6. **Brockes JP.** Amphibian limb regeneration: rebuilding a complex structure. *Science*. 276(5309): 81-87, 1997.
7. **Smith JJ, Putta, S, Walker, JA, Kump, DK, Samuels, AK, Monaghan, JR, Weisrock, DW, Staben, C, and Voss, SR.** Sal-Site: integrating new and existing ambystomatid salamander research and informational resources. *BMC Genomics*. 6: 181, 2005.
8. **Vargas-Gonzalez A, Prado-Zayago, E, Leon-Olea, M, Guarner-Lans, V, and Cano-Martinez, A.** [Myocardial regeneration in Ambystoma mexicanum after surgical injury]. *Arch Cardiol Mex*. 75 Suppl 3: S3-21-29, 2005.
9. **Roy S and Gatien, S.** Regeneration in axolotls: a model to aim for! *Exp Gerontol*. 43(11): 968-973, 2008.
10. **Voss SR, Epperlein, HH, and Tanaka, EM.** Ambystoma mexicanum, the axolotl: a versatile amphibian model for regeneration, development, and evolution studies. *Cold Spring Harb Protoc*. 2009(8): pdb emo128, 2009.
11. **Cano-Martinez A, Vargas-Gonzalez, A, Guarner-Lans, V, Prado-Zayago, E, Leon-Oleda, M, and Nieto-Lima, B.** Functional and structural regeneration in the axolotl heart (Ambystoma mexicanum) after partial ventricular amputation. *Arch Cardiol Mex*. 80(2): 79-86, 2010.
12. **Singh BN, Koyano-Nakagawa, N, Garry, JP, and Weaver, CV.** Heart of newt: a recipe for regeneration. *J Cardiovasc Transl Res*. 3(4): 397-409, 2010.
13. **Whited JL and Tabin, CJ.** Regeneration review reprise. *J Biol*. 9(2): 15, 2010.
14. **Simon HG.** Salamanders and fish can regenerate lost structures--why can't we? *BMC Biol*. 10: 15, 2012.
15. **Michael LH, Entman, ML, Hartley, CJ, Youker, KA, Zhu, J, Hall, SR, Hawkins, HK, Berens, K, and Ballantyne, CM.** Myocardial ischemia and reperfusion: a murine model. *Am J Physiol*. 269(6 Pt 2): H2147-2154, 1995.
16. **Azhar G, Gao, W, Liu, L, and Wei, JY.** Ischemia-reperfusion in the adult mouse heart influence of age. *Exp Gerontol*. 34(5): 699-714, 1999.
17. **Jackson KA, Majka, SM, Wang, H, Pocius, J, Hartley, CJ, Majesky, MW, Entman, ML, Michael, LH, Hirschi, KK, and Goodell, MA.** Regeneration of ischemic cardiac muscle and vascular endothelium by adult stem cells. *J Clin Invest*. 107(11): 1395-1402, 2001.
18. **Orlic D, Kajstura, J, Chimenti, S, Jakoniuk, I, Anderson, SM, Li, B, Pickel, J, McKay, R, Nadal-Ginard, B, Bodine, DM, Leri, A, and Anversa, P.** Bone marrow cells regenerate infarcted myocardium. *Nature*. 410(6829): 701-705, 2001.
19. **Bayat H, Swaney, JS, Ander, AN, Dalton, N, Kennedy, BP, Hammond, HK, and Roth, DM.** Progressive heart failure after myocardial infarction in mice. *Basic Res Cardiol*. 97(3): 206-213, 2002.
20. **Yang F, Liu, YH, Yang, XP, Xu, J, Kapke, A, and Carretero, OA.** Myocardial infarction and cardiac remodelling in mice. *Experimental Physiology*. 87(5): 547-555, 2002.
21. **Murry CE, Soonpaa, MH, Reinecke, H, Nakajima, H, Nakajima, HO, Rubart, M, Pasumarthi, KB, Virag, JI, Bartelmez, SH, Poppa, V, Bradford, G, Dowell, JD, Williams, DA, and Field, LJ.** Haematopoietic stem cells do not transdifferentiate into cardiac myocytes in myocardial infarcts. *Nature*. 428(6983): 664-668, 2004.
22. **Tarnavski O, McMullen, JR, Schinke, M, Nie, Q, Kong, S, and Izumo, S.** Mouse cardiac surgery: comprehensive techniques for the generation of mouse models of human diseases and their application for genomic studies. *Physiol Genomics*. 16(3): 349-360, 2004.

23. **Klocke R, Tian, W, Kuhlmann, MT, and Nikol, S.** Surgical animal models of heart failure related to coronary heart disease. *Cardiovasc Res*. 74(1): 29-38, 2007.
24. **Bernal J, Baldwin, M, Gleason, T, Kuhlman, S, Moore, G, and Talcott, M.** Guidelines for rodent survival surgery. *J Invest Surg*. 22(6): 445-451, 2009.
25. **Strungs EG, Ongstad, EL, O'Quinn, MP, Palatinus, JA, Jourdan, LJ, and Gourdie, RG.** Cryoinjury models of the adult and neonatal mouse heart for studies of scarring and regeneration. *Methods Mol Biol*. 1037: 343-353, 2013.
26. **Xin M, Olson, EN, and Bassel-Duby, R.** Mending broken hearts: cardiac development as a basis for adult heart regeneration and repair. *Nat Rev Mol Cell Biol*. 14(8): 529-541, 2013.
27. **Yue X, Yu, H, Lin, X, Liu, K, Wang, X, Zhou, F, Zhao, J, and Zou, B.** Investigation into the optimal surgical conditions for coronary artery ligation for establishing a myocardial infarction model in mice. *Exp Ther Med*. 6(2): 341-346, 2013.
28. **Field LJ.** Transgenic mice in cardiovascular research. *Annu Rev Physiol*. 55: 97-114, 1993.
29. **Battey J, Jordan, E, Cox, D, and Dove, W.** An action plan for mouse genomics. *Nat Genet*. 21(1): 73-75, 1999.
30. **Lewandoski M.** Conditional control of gene expression in the mouse. *Nat Rev Genet*. 2(10): 743-755, 2001.
31. **Yamamoto A, Hen, R, and Dauer, WT.** The ons and offs of inducible transgenic technology: a review. *Neurobiol Dis*. 8(6): 923-932, 2001.
32. **Gage AA and Baust, J.** Mechanisms of tissue injury in cryosurgery. *Cryobiology*. 37(3): 171-186, 1998.
33. **Robbins SL, Kumar, V, and Cotran, RS**, *Robbins and Cotran pathologic basis of disease*. 8th ed. 2010, Philadelphia, PA: Saunders/Elsevier. xiv, 1450 p.
34. **Sattar HA**, *Fundamentals of Pathology*. 2011: Pathoma, LLC.
35. **Haunstetter A and Izumo, S.** Apoptosis: basic mechanisms and implications for cardiovascular disease. *Circ Res*. 82(11): 1111-1129, 1998.
36. **Bolli R.** The late phase of preconditioning. *Circ Res*. 87(11): 972-983, 2000.
37. **Rumyantsev PP.** Interrelations of the proliferation and differentiation processes during cardiact myogenesis and regeneration. *Int Rev Cytol*. 51: 186-273, 1977.
38. **Borland S.** New identification system makes 'axolotl life' easier. *Axolotl Newsletter*. 21: 28-28, 1992.
39. **Koeller CA.** Comparison of buprenorphine and butorphanol analgesia in the eastern red-spotted newt (Notophthalmus viridescens). *J Am Assoc Lab Anim Sci*. 48(2): 171-175, 2009.
40. **Gentz EJ.** Medicine and surgery of amphibians. *ILAR J*. 48(3): 255-259, 2007.
41. **Wright KM.** Surgery of amphibians. *Vet Clin North Am Exot Anim Pract*. 3(3): 753-758, viii, 2000.
42. **Wright KM and Whitaker, BR**, *Amphibian medicine and captive husbandry*. Original ed. 2001, Malabar, Fla.: Krieger Pub. Co. xxv, 499 p.
43. **Drăghici S**, *Statistics and data analysis for microarrays using R and Bioconductor*. Chapman & Hall/CRC mathematical and computational biology. 2012, Boca Raton, FL: CRC Press. xlviii, 1042 p.
44. **Shelton G and Jones, DR.** A comparative study of central blood pressures in five amphibians. *J Exp Biol*. 49(3): 631-643, 1968.
45. **Mattson DL.** Comparison of arterial blood pressure in different strains of mice. *Am J Hypertens*. 14(5 Pt 1): 405-408, 2001.
46. **Carpenter JW and Marion, CJ**, *Exotic animal formulary*. 4th ed. 2013, St. Louis, Mo.: Elsevier. xvii, 724 p.
47. **Menger B, Vogt, PM, Jacobsen, ID, Allmeling, C, Kuhbier, JW, Mutschmann, F, and Reimers, K.** Resection of a large intra-abdominal tumor in the Mexican axolotl: a case report. *Vet Surg*. 39(2): 232-233, 2010.
48. **Flink IL.** Cell cycle reentry of ventricular and atrial cardiomyocytes and cells within the epicardium following amputation of the ventricular apex in the axolotl, Amblystoma mexicanum: confocal microscopic immunofluorescent image analysis of bromodeoxyuridine-labeled nuclei. *Anat Embryol (Berl)*. 205(3): 235-244, 2002.
49. **McMillan MW and Leece, EA.** Immersion and branchial/transcutaneous irrigation anaesthesia with alfaxalone in a Mexican axolotl. *Vet Anaesth Analg*. 38(6): 619-623, 2011.
50. **Borland S.** Practical axolotl. *Axolotl Newsletter*. 28: 17-21, 2000.

APPENDIX C: GLAS Grant Submission

This checklist is intended to help you organize the information needed for this application and track the sections completed. Please insert a checkmark by clicking each box on the pertinent list to indicate sections and actions completed on the application.

Standard Grant Checklist
Section A. General Information ☐Research study title ☐Funds requested ☐Documentation of approval by institutional committee(s), or equivalent ☐Status of business/financial interest ☐Status of alternative/supplemental funding ☐Did you submit a prior application? ☐ Is this application a resubmission and have you addressed issues raised in the prior review? ☐Have you received a previous award? ☐Section B. Contact Information Principal investigator, co-investigator(s) Principal investigator's AALAS membership number Institutional representatives Signatures of principal investigator and authorized institutional official Section C. Abstract and Hypothesis Abstract: 250 word maximum Hypothesis: 250 word maximum Section D. Proposal: 6 page maximum Appendix included, if applicable Preliminary Work Statement of Work Anticipated Outcome(s) Anticipated Pitfall(s) Section E. Facilities and Equipment: 1 page maximum Section F. Budget Section G. Supporting Information References cited in the proposal: 1 page maximum Biographical sketches of all investigators: 2 page maximum per person Disclosures: 1 page maximum Other support sources: 1 page maximum

glas Grants for Laboratory Animal Science

Grants for Laboratory Animal Science Application Form

Submit your application for a **Standard** GLAS application as a Microsoft Word document and in a single file containing all application sections.

- Please do not convert the Word file to another file format or adjust the document margins (1 inch all around) or the page size (8.5 x 11 inches).
- Keep the text single-spaced, black, and in a Times New Roman font of 12 point or larger.
- You may delete the application instructions in each section to save space.
- Please observe the formatting requirements (see above instructions) and the page limits for each section; **applications that exceed these limits will be disqualified.**
- When completed, upload your application document (in docx format) to the GLAS Submittable website. Instructions for online submission of applications are at: https://www.aalas.org/glas
- **Do not email this document to AALAS as your GLAS application**; emailed applications will **NOT** be accepted for review.
- Signatures (page 5) may be sent as electronic signatures or images within the Word document, or you may submit (upload) the signed signature page as a separate PDF file.

Section A. General Information for a Standard GLAS Application

1. Research Study Title: Efficacy of buprenorphine and butorphanol in relieving pain in a surgical model in axolotls.

2. Funds Requested (USD): $31,788

3. Please indicate which documents will be submitted with your application. This will not affect the review process; however, grant awardees must submit these documents before funds can be disbursed.

   IACUC Approval ☐ IBC Approval ☐ IRB Approval
   Other (please describe)_____

4. Please indicate whether the principal investigator (PI) or a co-investigator (Co-I) has a business or financial interest in the proposed project.

   ☒ No.
   Yes. Please disclose the business or financial interests in Section G.

5. Please indicate whether the proposed study, or one similar, has been or will be submitted to other funding agencies.

☒ No.
☐ Yes. Please list these funding agencies and provide more details in Section G.

6. Is your institution willing to fund the balance of your project, if not all of your budget can be funded?

   No.
   Yes.

7. Have you previously **applied** for a GLAS award?

   No.
   Yes. What was the year/s you applied?_____

8. Is this application a resubmission?

   No.
   Yes. What was the last year of its submission?_____

   Please indicate how issues raised in review are addressed in this resubmission.
   1 page maximum

9. Have you previously **received** a GLAS award?

   No.
   Yes. In what year/s did you receive a GLAS award?_____

Section B. Contact Information

1. Principal Investigator:
   Name: Tara Cotroneo
   Degree(s)/Credentials: DVM, DACLAM
   AALAS Membership Number:
   Title: Senior Clinical Veterinarian / Director, Veterinary Technical Services
   Institution: Wayne State University (WSU)
   Department: Research Support – Division of Laboratory Animal Resources (DLAR)
   Building and room number: Eugene Applebaum College of Pharmacy and Health Sciences – DLAR
   Street Address: 259 Mack Avenue, Suite 5116
   City: Detroit
   State or Province: Michigan
   Country: USA
   Zip or Postal Code: 48202
   Email: tara.cotroneo@wayne.edu

Phone: 313-577-1405
FAX: 313-577-5890 (DLAR Business Office)
Employment status (please check one):
☒ Employee
Contractor

2. Co-Investigators:
(To add additional co-investigators, copy the following fields and insert them in the space below.)
Name: Gerald Hish
Degree(s)/Credentials: DVM, DACLAM
Title: Senior Surgical Service Veterinarian / Director, Veterinary Surgical Services
Institution: Wayne State University (WSU)
Department: Research Support – Division of Laboratory Animal Resources (DLAR)
Building and room number: Eugene Applebaum College of Pharmacy and Health Sciences – DLAR
Street Address: 259 Mack Avenue, Suite 5116
City: Detroit
State or Province: Michigan
Country: USA
Zip or Postal Code: 48202
Email: gerryh@wayne.edu
Phone: 313-577-1236
FAX: 313-577-5890 (DLAR Business Office)

Name: Jeremy (Jay) T. Llaniguez
Degree(s)/Credentials: BS/MS
Title: Graduate Research Assistant, MD/PhD Candidate
Institution: Wayne State University (WSU)
Department: Biomedical Engineering (BME), School of Medicine (SOM)
Building and room number: WSU/IBIO: Bio & Systems Engineering, Room 1420
Street Address: 6135 Woodward Avenue
City: Detroit
State or Province: Michigan
Country: USA
Zip or Postal Code: 48202
Email: jllanigu@med.wayne.edu
Phone: 313-577-1360
FAX: 313-577-8333 (BME Business Office)

3. Institutional Grants Management Official:

Name: Danetta Smith
Title: Grants Contract Officer III
Institution: Wayne State University (WSU)
Department: Division of Research – Sponsored Program Administration (SPA)
Building and room number: Maccabees Building, Suite 13001
Street Address: 5057 Woodward Avenue
City: Detroit
State or Province: MI
Country: USA
Zip or Postal Code: 48202
Email: af6258@wayne.edu
Phone: 313-577-2892
FAX: 313-577-5055

4. Financial Officer (to whom the check will be mailed):
Name: Marlene Erno
Title: Senior Director, Research Support Services
Institution: Wayne State University
Department: Division of Research – Sponsored Program Administration (SPA)
Building and room number: Maccabees Building, Suite 13001
Street Address: 5057 Woodward Avenue
City: Detroit
State or Province: MI
Country: USA
Zip or Postal Code: 48202
Email: merno@wayne.edu
Phone: 313-577-6594
FAX: 313-577-5055

We, the undersigned, certify that the statements herein are true and complete to the best of our knowledge and agree to conform to the policies and rules governing this award. We agree to maintain records of grant expenditures for a period of 5 years, with the right of AALAS to audit same.

The results generated by research must be published in a scientific journal, a public meeting presentation, or a published patent or patent application to satisfy the requirements of placing the research results in the public domain; and each entity or individual has the right to file and maintain patent applications and patents based on the research and results, and is not required to dedicate the patent rights to the public.

Signature of Principal Investigator: _____

Date: _____

Signature of Authorized Institutional Official: _____

Date: _____

Section C. Abstract and Hypothesis/Goals

Abstract

Axolotls, capable of robust, life-long epimorphic regeneration, can recover from virtually any non-fatal injury. Although observed to regenerate almost all body parts and internal organs, the signaling mechanisms and pathways mediating these abilities are not yet completely elucidated, allowing researchers to undertake these challenges and translate them to human medicine. To perform these studies, axolotls must undergo surgical manipulation. Although a significant body of knowledge on pain control exists in newts and frogs, caution is advised when applying doses and schedules to axolotls that diverged from the closest common ancestor 145 and 260-million years ago, respectively. Thus, guidance on analgesics in axolotls for animal welfare is lacking. In addition to animal welfare concerns, pain-induced stress is known to affect overall health and wound healing in animal and human patients. Therefore, we hypothesize that published doses of newt analgesia are not appropriate to control pain in axolotls. Furthermore, inappropriate pain control could show differences in tissue response during regeneration. The first aim of this study is to determine an effective opioid dose that will provide analgesia in axolotls. The second aim of our study is to determine whether the healing response in axolotls is affected by opioids administered at analgesic doses. The results will have a significant impact in establishing pain control in axolotls, ultimately guiding future studies that use this novel animal in regenerative medicine research.

Hypothesis/Goals

Recent studies comparing newt and axolotl forelimb regeneration have shown that proposed cellular mechanisms underlying the repair of skeletal muscle following limb amputation follow different pathways in the two amphibians[14]. The significant diversity in achieving epimorphic regeneration, even in these two related urodeles, suggests enough differences exist that simply translating protocols from newts to axolotls is ill-advised[4]. With clear differences in physiology, we hypothesize that simply using published doses from a newt study may show statistically different changes in nociception, but may not be optimized to show clinically significant pain control in axolotls. Furthermore, we believe that analgesic use will result in histologic differences in tissue regeneration after injury when compared to animals that don't receive analgesics.

Section D. Proposal

☒ Appendix included.

Preliminary Work: Past studies on opioid receptors in amphibians have described the subcutaneous (SC), intracoelomic (IC), intraspinal (IS), and intracerebroventricular (ICV) administration of opioids in these animals[9,16,17]. With the parenteral delivery of antinociceptives, no external confounds to the pharmacodynamics or pharmacokinetics are expected. However, for the transcutaneous delivery of butorphanol, its behavior in treated water appropriate for axolotl care is unknown. Commonly, tap water is treated using Kordon® NovAqua® Plus™ water conditioner and ammonia detoxifier AmQuel® Plus™ with the addition of various salts to make 50% Holtfreter's solution. The only study identified in a publication search that used a transcutaneous method of butorphanol delivery in newts[9] used aged tap water (tap water that is allowed to sit in an open container to allow chlorine and other dissolved gases to dissipate). Since the husbandry of axolotls uses chemically conditioned water with additional buffering salts, characterizing how axolotl water interacts with butorphanol is necessary in order to properly compare the efficacy of transcutaneous butorphanol against the efficacy of parenteral buprenorphine.

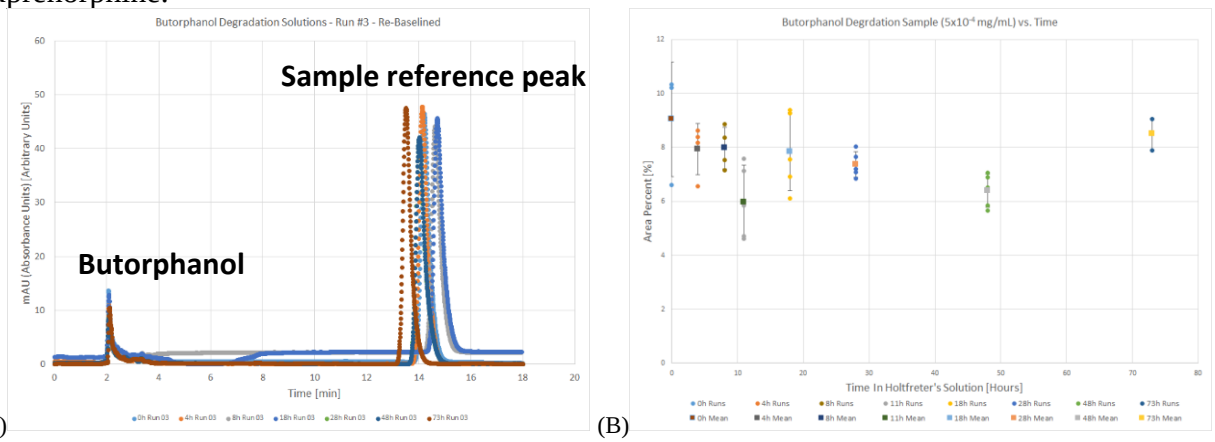

(A) (B)

Figure 1 (A) Characteristic elution curves of butorphanol (~2 min) in axolotl water using a solution of target-dose butorphanol aged before running the HPLC characterization. The curves have been shifted to a zero baseline. (B) Area under curve (AUC) for identified peak at various time points for the butorphanol degradation sample.

The dosing frequency from the newt study[9] was a single bolus of 0.5 mg/L (tank water) of butorphanol for the 72-hour recovery period. In our approved animal protocol governing axolotl procedures at Wayne State University (WSU), a daily water change is specified. Therefore, samples of "aging" butorphanol water were analyzed at multiple time points during the first 24 hours to determine if there was any background degradation of butorphanol that would require additional "maintenance" doses prior to the daily cage change. Characteristic HPLC elution curves for the aging, degradation samples are shown in Figure 1A. Inspecting these curves shows that the shape of the butorphanol peak (~2 min) does not appreciably change over a 72 hour period, well beyond the 24 hour maximum interval between cage changes. Graphing the percent AUC (total compound detected) over all the time points also shows a mean value without an apparent declining trend over time (see Figure 1B). Running an ANOVA also shows that there are no significant differences between the samples when correcting for multiple comparisons. From this data, we can conclude butorphanol does not degrade when exposed to the chemicals used to treat tap water for

use with amphibians, nor does it have any undue interaction with the salts in the axolotl water (50% Holtfreter's solution).

Using this information, studies on pain response were carried out with small numbers of animals. Manual von Frey [vF] aesthesiometers (Touch Test Sensory Evaluator, Stoelting, Wood Dale, IL) were used on the dorsal surface of the animal, lateral to the dorsal fin, generally in line with the forelimb. To ascertain if the animals' pain response shows hysteresis, the process of probing the animals with the evaluators was repeated in reverse, starting with an evaluator at a higher indicated force, and then progressively using evaluators that deliver less force until the animals no longer showed a response. A final sweep applying evaluators with increasing force was performed until the animal again showed a positive response. The three sweeps of evaluators (increasing force, decreasing force, increasing force) were considered one sensory test. Baseline responses were performed after the animals had at least 48-hours to acclimate to the WSU facility. Butorphanol (0.5 mg/L) was administered to five animals at the published doses[9], and one animal was treated using butorphanol after a surgical procedure on the heart. *Table* shows the newt doses seem to blunt the response on some animals (IDs 1, 2, and 11) but produced hyperalgesia in others (IDs 12 and 15). While the results of this limited pilot do show some inconsistencies, subjective assessment of the responses of four of the animals (1,2,5, and 11) suggests that vF aesthesiometry may be useful in evaluating analgesic efficacy in axolotls. This work also demonstrates the technical feasibility of adapting vF fibers to this aquatic species and additional evaluation with a larger number of animals will help bolster our confidence in the statistical value of our results. In addition, unlike the fixed force delivered by the manual evaluators, use of an electronic vF aesthesiometer will allow force to be applied along a continuous scale allowing for more rapid, precise measurements. We believe that this will improve the quality of the collected data and have incorporated it as part of the proposed statement of work.

Animal ID	Baseline	Butorphanol Treatment	Surgery With Analgesia
1	0.020	0.580	N/A
2	0.400	1.400	N/A
5	0.020	N/A	0.115
11	0.500	1.000	N/A
12	0.600	0.070	N/A
15	0.400	0.040	N/A

Table 1: Median force (in grams) eliciting a positive "pain" response in individual axolotl.

Statement of Work: While developing surgical procedures to induce a myocardial infarction in axolotls, guidance on analgesics in amphibians for appropriate animal welfare was lacking. Federally funded animal research must adhere to the Public Health Service Policy on Humane Care and Use of Laboratory Animals, which states that "procedures that may cause more than momentary or slight pain or distress to animals will be performed with appropriate sedation, analgesia, or anesthesia" unless the procedure is justified for scientific reasons in writing by the investigator[10]. Given the nature of regenerative medicine research, animals are frequently subjected to surgical injury in order to observe the healing process. Potential experimental confounders include the impact of opioids on wound healing[1] and immune function.

Morphine, the prototypical μ receptor agonist, increases corticosteroid secretion and decreases natural killer cell activity[8,11]. Overall, morphine administration leads to suppression of inflammatory cell proliferation, with an increase in proinflammatory mediators and decrease in anti-inflammatory mediators[11]. However, studies have demonstrated that buprenorphine can be safely used in models of sepsis in mice[8]. It has been demonstrated that the immune response is directly involved in healing and regeneration in axolotls[5,6]. Extrapolating from studies in mice,

buprenorphine has been shown to have less impact on the immune system compared with other opioid analgesics (morphine). However, this relationship has not been established in amphibians. Since our model is dependent upon a robust immune response, the impact opioids may have on tissue regeneration must be established.

The few studies which are available concerning antinociception in amphibians have used frogs (*Xenopus laevis* and *Rana pipiens*) and newts (*Notophthalmus viridescens*). A recent book chapter[4] cautioned the direct application of amphibian protocols and findings in different species to procedures for axolotls (*Ambystoma mexicanum*), citing that although they are all amphibians, the different species are not closely related to each other. This divergence is evidenced by the fact that newt regeneration and axolotl regeneration after limb injury is driven by different mechanisms[14]. With sufficient differences in physiology, a study on the appropriate antinociceptives and their administration (dosage and frequency) in axolotls is needed.

While there are several demonstrated difference between these disparate groups it has been shown that A and C nociceptive fibers are present in most vertebrate animals, including amphibians[2,7,15]. Although axolotls are classified in a different family and order from newts and frogs respectively, it is expected that pain receptors are likely conserved within the class. However, nociceptor fiber distribution and number may vary[15]. Previous studies in frogs (*Rana pipiens and Xenopus laevis)* have described mechanical, thermal, and chemical methods to assess pain and analgesic efficacy[18]. In addition, a recent study in newts (*Notophthalmus viridescens*)[9] used qualitative behavioral observations to show the efficacy of opioids (buprenorphine and butorphanol) after limb amputation. Therefore, quantitative assessment methods (vF and acetic acid test [AAT]) may work in axolotls, but will likely need to be modified to produce a repeatable result within this species. In addition, behavioral assessments (provoked/unprovoked movement, body posture, food consumption) can be applied to the axolotl to monitor general health and welfare. Our laboratory has performed preliminary studies with a small number of axolotls using vF aesthesiometers to evaluate response to mechanical stimuli and video tracking software to quantify movement. These studies have shown a repeatable response to the vF fibers. The mechanical vF evaluators have provided useful data, but an electronic vF evaluator will provide further refinement and increase the accuracy of our quantitative assessment. In addition, we propose to evaluate a modified AAT to determine if this can be used as a quantitative assessment of pain in axolotls. Based upon the results of this work, quantitative measurements will be used to optimize an opioid analgesic regimen to use in a surgical model in axolotls.

Specific Aim 1: Determine optimal analgesic dosing in a surgical model in axolotls: *Design:*

Experiment 1: *Validate quantitative methods using naïve animals.* For this experiment two different quantitative techniques, von Frey fibers and a modified acetic-acid wiping test, will be evaluated in naïve axolotls to determine which method produces more consistent responses. Each technique (vF or AAT) will be evaluated with a different group of six animals. The animals' response to noxious mechanical and chemical stimulation will be measured with an electronic vF aesthesiometer or different concentrations of acetic acid, respectively, to establish a baseline response. The quantitative method which produces the most repeatable results will determine which technique will be utilized in subsequent experiments.

Experiment 2: *Using validated quantitative methods, determine optimized analgesic doses.* We will evaluate the effects of different doses of butorphanol and buprenorphine on quantitative and behavioral parameters (see Table 2). Six animals will be assigned to each analgesic group, buprenorphine or butorphanol (low [L], medium [M], or high [H] dosage).

Experiment 3: *Evaluate optimal analgesic dose in a surgical model in axolotls.* Three surgical groups of animals (6 per group, receiving either butorphanol, buprenorphine, no analgesic) will undergo mechanical induction of cardiac ischemia. Using data from Experiment 2, animals will receive optimized analgesic doses. The same evaluation criteria and schedule (behavioral and quantitative methods) that were used in Experiment 2 will be used in Experiment 3 however the 0-hour time point will be designated as the point of recovery from anesthesia.

Table 2: Study schedule for each dose (L,M, and H) in Experiment 2.

	Baseline	Analgesia	Assessments			Analgesia	Assessments			
Test	-24h	0h	1h	6h	12h	24h	25h	31h	36h	48h
Quantitative test (vF or AAT)	✓		✓	✓	✓	✓	✓	✓		✓
Cageside	✓		✓	✓			✓	✓		
Video	✓ (x2)*		✓		✓	✓			✓	✓
Feeding	✓			✓				✓		

Two measures in 24 hours

Specific Aim 2: Determine whether, and to what degree, opioid analgesics affect tissue healing and regeneration in an axolotl surgical model. *Design:* ***Experiment 4:*** *Compare the histologic differences in healing response after mechanically inducing ischemia in an axolotl heart, with and without the administration of opioid analgesia.* Three surgical experimental groups (buprenorphine, butorphanol, and no analgesia) of naïve axolotls will undergo mechanical induction of cardiac ischemia using the same doses utilized in Experiment 3. Each experimental group will consist of 18 animals; 6 will be humanely euthanized at each of three post-operative timepoints (12 hr, 2 days, 7 days). These timepoints were selected based upon observations from pilot studies we have performed examining cardiac histology in axolotls following mechanical ischemic injury. Following euthanasia, cardiac tissue will be collected for histologic processing and analysis. Quantitative and behavioral assessments will be performed as described in Table 2 for each group as allowed until the time of euthanasia.

Detailed Methods: ***Experimental animals:*** Male and female, wild-type (WT) axolotls (Ambystoma Genetic Stock Center, University of Kentucky, Lexington, KY) will be individually housed in large, polypropylene rat cages in a vivarium controlled between 60-60°F (15.6-18.9°C) maintained at a 12:12-h light:dark cycle. Water will be treated to remove ammonia, chlorine, and metals and then mixed with appropriate salts to create 50% Holtfreter's solution (homogenous mixture of ionic particles). The animals will be fed (Soft Moist Salmon Diet, Rangen, Inc., Buhl, ID) three days per week (MWF). All animals will be acclimated for 5-7 days before any experiments are conducted. All procedures are approved by the Institutional Animal Care and Use Committee (IACUC) of Wayne State University (WSU). ***Justification of numbers:*** A sample size of 6 animals per group was determined by assuming an α=0.05 and a β=0.05, while estimating a large effect size (σ=0.25 for laboratory-bred animals and assuming clear behavioral differences with and without antinociceptives[3]). When possible, animals will be used in multiple experiments however no animals will undergo more than one major surgical procedure. ***Analgesics:*** Two antinociceptives will be compared. Buprenorphine (Penro Specialty Compounding, Colchester, VT) shall be administered at one of three doses (low=25 mg/kg, medium=50 mg/kg, high=75 mg/kg) as an intracoelomic (IC) injection every 24-hours for 48 hours. Butorphanol (MWI Veterinary Supply, Boise, ID) shall be administered at one of three concentrations (low=0.25 mg/L, medium=0.50 mg/L, high=0.75 mg/L) directly into the 50% Holtfreter's solution of the animal's cage every 24-hours for 48 hours. The medium dose is based upon a published dose that

was effective in newts and the low and high doses are 50% lower or higher, respectively. When animals are used in more than one experiment, they will be provided a minimum of 1 week washout between treatments and must return to baseline behavior. ***Behavioral assessment:*** Feeding: At least one week of food consumption will be measured to establish a baseline intake. Also, feeding behavior (latency to feed) will be measured using a highly palatable treat, such as black worms. Additionally, the animals will be weighed 3 times a week at cage change (M,W,F) to assess body weight changes. Cageside Assessment: The animals will be assessed cageside by blinded operators at least twice daily at predetermined timepoints. Assessment methods will include observing body posture, responses after gently tapping on cage, squirting 3-5 mL of water from a syringe into the water surface to assess response to water disruption, and touching the animal. The animals will be scored using a binary system (response/no response)[9]. Video assessment: Animals will be videotaped in one hour segments at defined intervals during each experiment (See Table 2). Videos are quantitatively analyzed (EthoVision XT, Noldus, Leesburg, VA) to assess spontaneous movement. Behavior such as total distance moved, tail curling, gill position, any abnormal signs of posture, spurts of movement, and any flipping/rolling around the body axes will be noted. ***Quantitative tools to measure pain:*** Stimulation with vF filaments: . Using electronic vF device, Increasing pressure is applied at the site of evaluation (lateral to dorsal fin, inline with forelimb) until nociceptive behavior is observed at which point the applied force is recorded. Acetic acid test: Axolotls will be placed in a polypropylene mouse cage with enough 50% Holtfreter's solution to cover half of its body, leaving the dorsal surface above the waterline. The AAT is performed according to previously published reports in frogs[18]. Glacial acetic acid is serially diluted to produce 10 dilutions evenly spaced on a logarithmic scale. Testing is performed by placing a single drop of the weakest concentration acetic acid on the same location described above for the vF Fibers. The animal will be observed for a repeatable behavioral response (wiping, turning, escape behavior). If a response is not observed within 5 seconds the area is rinsed using 50% Holtfreter's solution. Testing on the opposite side using the next highest concentration will occur. The testing continues until the nociceptive threshold is reached which is the highest concentration to produce a response. If no response is observed with the highest concentration the nociceptive threshold will be designated at 10, consistent with the highest concentration of acetic acid. ***Mechanically induced cardiac ischemia:*** Surgical procedure: Animals will be fasted for at least 24 hours in order to avoid emesis during anesthesia induction and to reduce stomach volume for organ movement. Anesthesia will be induced by placing the animal in a water bath with 0.1% tricaine methanesulfonate (MS-222). Though aseptic surgical technique will be used, a single dose of enrofloxacin will be administered pre-operatively as amphibian procedures are considered "clean-contaminated" at best. Analgesics shall be administered up to 1h prior to surgery. Anesthesia will be maintained by covering the animal in gauze sponges moistened with MS-222 in 50% Holtfreter's solution. The ventral surface of the thorax will be disinfected by placing sterile gauze soaked in chlorhexidine solution (0.75%) or benzalkonium solution (2 mg/L) for 5-10 minutes at the intended site of incision followed by irrigation with sterile normal saline (0.9% NaCl). The heart will be exposed and the apex of the ventricle will be mechanically clamped for at least 30 minutes to reduce the blood flow to the region to ensure irreversible cellular damage[13], inducing myocardial injury by ischemia. The cardiac cavity will be lavaged with saline and the body wall and skin will be individually closed with a monofilament, non-absorbable suture. All surgeries will be performed by a single surgeon and all surgeries will be completed in the morning on any given day. For 3-5 days following surgery (as allowed by each experimental schedule), the animals shall be given daily IC injections of enrofloxacin. Post-operative care: Food shall be offered starting on

postoperative day 1 (surgical procedure is day 0). The surgical wound will be assessed daily for any complications until suture removal (5-7 days) and for a few days afterwards. For nuclei labeling index studies in Experiment 4, each animal will be injected with BrdU [30 mg/kg, intracoelomic] three hours prior to collecting the heart. ***Tissue staining:*** Harvested hearts will be fixed in formalin, dehydrated in 20% sucrose, and embedded in Tissue Freezing Medium. Mounted sections will be stained using Goldner's Trichrome or Picrosirius Red methods. Tissue will be processed by the graduate student co-investigator using staining supplies and protocols from Electron Microscopy Sciences (Hatfield, PA). Staining times are optimized to ensure good contrast in axolotl tissue. ***Tissue Analysis:*** Tissue staining will identify areas of necrotic, perinecrotic and penumbral tissue. Cellular proliferation activity in the penumbra will be indexed by staining with antibodies specific for BrdU. Studies of cardiac myofibrillogenesis describe the myofibril assembly process as a transition through three types of fibrils: premyofibrils containing non-muscle myosin IIB; nascent myofibrils containing both non-muscle myosin IIB and muscle-specific myosin II; and mature myofibrils containing only muscle-specific myosin II[12]. All tissue samples will be stained with antibodies for proteins of myofibrillogenesis and stem cell markers; 10 high-powered views will be evaluated under microscopy to observe statistical differences in histology. ***Data analysis and statistics:*** With each animal serving as its own control, self-paired, two-tailed t-test statistics can be used to compare the means of quantitative behavior assessments. A one-way ANOVA will be used to assess differences across time points. If the data cannot be appropriately assessed by assuming a normal distribution (or are non-interval data), the non-parametric equivalent of the t-test and ANOVA shall be used. When data cannot be evaluated by parametric methods, the Mann-Whitney/Wilcoxon Rank Sum test will be used to evaluate differences from baseline, while the Kruskal-Wallis analysis of variance will be used to evaluate differences across time points. SPSS (IBM Corporation©, Version 23) software will be used to compute statistics.

Study Timeline: *Specific Aim 1:* Q3 2016 – Q4 2016; *Specific Aim 2:* Q4 2016 – Q1 2017. Studies will be completed by the graduate student (co-investigator) and DLAR staff, with the veterinarians (PI and co-investigator) providing oversight on animal welfare and data analysis. A manuscript and national presentation of data will be completed within 18 months of funding.

Anticipated Outcome(s): The immediate expected outcomes will be the reduction of pain and stress in axolotls planned for higher-powered studies in regenerative medicine at WSU. For the field in regenerative medicine, the long-term results will have a significant impact in establishing pain control in axolotls, ultimately guiding future studies that use this novel animal in studies in regenerative medicine. Characterization of the affects of opioid analgesics on tissue regeneration will be useful for investigators when determining which analgesic may have the fewest impacts on their specific models.

Anticipated Pitfall(s): The current approach to elicit a nociceptive response in axolotls relies on stimulating the animal just lateral to the dorsal fin, in line with its forelimb. However, in the integumentary system of salamanders, in contrast to the cold/heat receptors and tactile receptors located in the epidermis, the pain and pressure receptors are situated in the dermis. Thus, the vF anesthesiometers may be stimulating tactile receptors and not pain receptors. Additionally, while several behaviors observed in newts may be useful in evaluating analgesic efficacy in that species, it is unclear whether these same behaviors will be useful in axolotls. Given the lack of any established pain related ethograms specific to axolotls, the published data in newts is the most promising starting point.

Section E. Facilities and Equipment
1 page maximum

Describe the facilities to be used and the available equipment.

Laboratory: The co-investigator's sponsor has dedicated wet laboratory space (~1000 square feet in size with ~450 square feet of bench space) located in the Integrative Biosciences Center (IBio) at Wayne State University. The laboratory is designed for DNA cloning; Southern blot and PCR genotyping; expression analyses in mammalian cells/tissues by RNA and protein characterization, immunocytochemistry, immunohistochemistry, histology, and radiochemical labeling. Dedicated areas are defined for working with tissue samples for fixing, sectioning, staining, and performing immunohistochemistry, along with a dedicated room for cell-cultures. The following are dedicated equipment in the Sponsor's laboratory. This equipment caters to tissue sample preparation:

- Shel Lab Vacuum Oven: This oven/incubator is used to hold reagents at a certain temperature for proper staining of tissue samples.
- Hacker Instruments & Industries (H/I) Bright OTF5000 Cyrostat/Microtome: This cryo-microtome is used to prepare tissue sections for histology staining and immunohistochemical studies.
- Premiere® XH-2001 Slide Warmer: Slide warmer to attach tissue sections to slides after slicing.
- Olympus IMT Inverted Tissue Culture Microscope: This microscope is used for checking slides before scanning.
- EVOS® FL Auto Imaging System: This is a fully-automated, inverted, transmitted-light imaging system. This is used to perform and record high-resoltion scans of prepared tissue sections.
- Adjustable Pipettes (multiple volume limits): These are used to prepare solutions, drugs, and reagents.

Animal Facilities: Axolotls are housed in an Association of Assessment and Accreditation for Laboratory Animal Care- (AAALAC) accredited vivarium located in facilities supervised by Animal Facilities Core/Division of Laboratory Animal Resources (DLAR) located in the basement of the new Integrative Biosciences Center. The vivarium is 15,328 gsf and contains 12 animal rooms, a procedure room with fume hood, a behavioral suite, a telemetry suite, an embryo transfer suite, and a surgical suite. The WSU Division of Laboratory Animal Resources (DLAR) staffs and manages all animal facilities. Animal care is directed by an ACLAM board-certified veterinarian who serves as the Attending Veterinarian and the Senior Director of DLAR. The two DLAR clinical veterinarians are board certified by the American College of Laboratory Animal Medicine (ACLAM). Veterinarians are on-site during normal working hours, and are available by pager 24 hours a day, 7 days a week, 365 days a year. Licensed Veterinary Technologists provide animal husbandry, technical assistance, and training. Many DLAR staff members hold certification by the American Association of Laboratory Animal Science (AALAS).

Video recording hardware, purchased as a commercially available, home-based security surveillance system (Lorex, Model No. LH03081TC4), has been installed on the axolotl caging rack. Each day/night camera is positioned to record up to three animals. Video files are downloaded and edited/spliced with Windows® Movie Maker.

Section F. Budget

Animals, Supplies, and Equipment (Itemize by category)	TOTALS
Animal Numbers: ***Experiment 1:*** 6 axolotls/group x 2 groups = **12 axolotls** ***Experiment 2:*** 6 axolotls/group x 6 drug/dose groups (Re-use 12 animals from Experiment 1 + **24 additional animals**) ***Experiment 3:*** 6 axolotls/group x 3 groups (Re-use 12 animals from the low dose groups in Experiment 1 + **6 additional axolotls** for no the analgesic group) ***Experiment 4:*** 6 axolotls/group x 3 groups x 3 sample endpoints = **54 animals** Total Animals = (12 + 24 + 6 + 54) x 10% (unexpected attrition) = 106	
Animals:	
Axolotls, Wild Type, Adult, Non-Breeding, Quantity of 106 ($25/each)	$2650
Shipping/Handling ($7/animal) = $7 x 106	$742
Per Diem: - Acclimation: 5 days x $0.88 animal/day x 106 animals - Daily Care: - Experiment 1 = 2 days - Experiment 2 = 5 days - Experiment 3 = 10 days (Including time for drug washout for non-naïve animals) - Experiment 4 = (9 x 1d) + (9 x 2d)+(9 x 7d)=90 animal-days - Cost: [2 days x $0.88/animal-day x 12 animals]+[5 days x 36 animals x $0.88/animal-day]+[10 days x 18 animals x $0.88/animal-day] + [$0.88/animal-day x 90 animal-days]	$467
Supplies:	$418
Buprenorphine (10 mg/mL, $340 per 12-mL multi-dose vial), Quantity of 3	$1020
Butorphanol (10 mg/mL, $70 per 10-mL multi-dose vial), Quantity of 2	$140
Sodium Chloride, 5kg bottle, Quantity 2 ($178/each)	$356
Potassium Chloride, 1 kg bottle, Quantity 2 ($115/each)	$230
Calcium Chloride, 0.5 kg bottle, Quantity of 4 ($210/each)	$840
Sodium Bicarbonate, 5 kg bottle, Quantity 2 ($175/each)	$350
BrDU, 3 mg/mL, 15 mL bottle, Quantity 5 ($69.00 each)	$345
Rangen Sinking Pellets, 0.5lb bag, Quantity of 40 ($5.50 each)	$220
Black Worms, 16 oz ($20)	$20
Tricaine-S (MS-222, Aquatic animal anesthesia), 1 kg bottle, Quantity 2 ($650/each)	$1350
Tissue Preparation/Histology Supplies (Stains, Xylene, Anhydrous Ethanol)	$1500
Pathology Core Immunohistochemistry Service: $25/slide x 3 slides/axolotl x 54 axolotls	$4050
Equipment:	
Electronic von Frey Aesthesiometer	$5990
Noldus EthoVision XT (Video Tracking Software)	$9100
Dell Laptop (For Video Tracking Software)	$1000

Personnel				
Name	Position Title	Salary	% Effort	N/A
N/A	N/A	N/A	N/A	N/A

Other Expenses (Itemize by category)	
Travel: Travel allowance to AALAS National Meeting	$1000
Budget Total (USD): **Funds Requested (USD):**	$31,788 $31,788

Section G. Supporting Information

References (1 page maximum this section)

1. **Chrastil J, Sampson C, Jones KB, Higgins TF**. 2013. Postoperative opioid administration inhibits bone healing in an animal model. Clin Orthop Relat Res **471**:4076-4081.
2. **Coble DJ, Taylor DK, Mook DM**. 2011. Analgesic effects of meloxicam, morphine sulfate, flunixin meglumine, and xylazine hydrochloride in African-clawed frogs (Xenopus laevis). J Am Assoc Lab Anim Sci **50**:355-360.
3. **Drăghici S**. 2012. Statistics and data analysis for microarrays using R and Bioconductor. Boca Raton, FL: CRC Press.
4. **Farkas JE, Monaghan JR**. 2015. Housing and maintenance of Ambystoma mexicanum, the Mexican axolotl. Methods Mol Biol **1290**:27-46.
5. **Godwin JW, Pinto AR, Rosenthal NA**. 2013. Macrophages are required for adult salamander limb regeneration. Proc Natl Acad Sci U S A **110**:9415-9420.
6. **Godwin JW, Rosenthal N**. 2014. Scar-free wound healing and regeneration in amphibians: immunological influences on regenerative success. Differentiation **87**:66-75.
7. **Hamamoto DT, Simone DA**. 2003. Characterization of cutaneous primary afferent fibers excited by acetic acid in a model of nociception in frogs. J Neurophysiol **90**:566-577.
8. **Hugunin KM, Fry C, Shuster K, Nemzek JA**. 2010. Effects of tramadol and buprenorphine on select immunologic factors in a cecal ligation and puncture model. Shock **34**:250-260.
9. **Koeller CA**. 2009. Comparison of buprenorphine and butorphanol analgesia in the eastern red-spotted newt (Notophthalmus viridescens). J Am Assoc Lab Anim Sci **48**:171-175.
10. **National Research Council (U.S.). Committee for the Update of the Guide for the Care and Use of Laboratory Animals., Institute for Laboratory Animal Research (U.S.), National Academies Press (U.S.)**. Guide for the care and use of laboratory animals, pp. xxv, 220 p. Washington, D.C.: National Academies Press,.
11. **Odunayo A, Dodam JR, Kerl ME, DeClue AE**. 2010. Immunomodulatory effects of opioids. J Vet Emerg Crit Care (San Antonio) **20**:376-385.
12. **Rhee D, Sanger JM, Sanger JW**. 1994. The premyofibril: evidence for its role in myofibrillogenesis. Cell Motil Cytoskeleton **28**:1-24.
13. **Robbins SL, Kumar V, Cotran RS**. 2010. Robbins and Cotran pathologic basis of disease, 8th ed. Philadelphia, PA: Saunders/Elsevier.
14. **Sandoval-Guzman T, Wang H, Khattak S, Schuez M, Roensch K, Nacu E, Tazaki A, Joven A, Tanaka EM, Simon A**. 2014. Fundamental differences in dedifferentiation and stem cell recruitment during skeletal muscle regeneration in two salamander species. Cell Stem Cell **14**:174-187.
15. **Sneddon LU, Elwood, R.W., Adama, S.A., Leach M.C.** 2014. Review: Defining and assessing animal pain. Anim Behav **97**:12
16. **Stevens CW**. 1996. Relative analgesic potency of mu, delta and kappa opioids after spinal administration in amphibians. J Pharmacol Exp Ther **276**:440-448.
17. **Stevens CW, Klopp AJ, Facello JA**. 1994. Analgesic potency of mu and kappa opioids after systemic administration in amphibians. J Pharmacol Exp Ther **269**:1086-1093.
18. **Willenbring S, Stevens CW**. 1996. Thermal, mechanical and chemical peripheral sensation in amphibians: opioid and adrenergic effects. Life Sci **58**:125-133.

1. **Biographical Sketches.** Complete parts a-d for the principal investigator and co-investigators. **(2 pages maximum per person)**

Principal Investigator

a. General Information
Name: Tara Cotroneo, DVM, DACLAM
Position Title: Sr. Clinical Veterinarian / Director, Veterinary Technical Service

b. Education
Add rows to the table below to list all post high school education including residency training.

Institution/City	Degree (if applicable)	Date Completed (MM/DD/YYYY)	Field of Study
University of Pittsburgh	BS	05/2004	Biology
Western University of Health Sciences	DVM	05/2008	DVM
University of Michigan		07/01/2011	Laboratory Animal Medicine Residency

c. Personal Statement of Qualifications
Please identify each person's role on the project and briefly summarize the experience and qualifications related to this role.
My role in this project will be to oversee experimental design and clinical aspects of the project. I will be directly involved in performing or training individuals on the monitoring methods. My primary research interests are refinement of animal models and improving animal welfare in research a setting. This current project allows me to determine effective analgesic recommendations in a surgical model of regeneration. This information is currently not published in the literature and would provide significant refinement to axolotl pain management. I have the background and training necessary to complete the proposed research study. I completed a three year residency in laboratory animal medicine which provided a solid background in both clinical veterinary care of a variety of laboratory animal species and primary research. During this time I worked on several projects which involved assessment of analgesic impact on research models. Specifically, I completed a project involving the impact of analgesics in a surgical mouse model of sepsis. I am board certified in laboratory animal medicine and have a broad knowledge of medical and surgical care for laboratory animal species. During my residency and as a clinical veterinarian I have provided veterinary care and reviewed IACUC protocols for amphibian and aquatic species including zebrafish, African clawed frogs (xenopus laevis), and Axolotls. My clinical veterinary background combined with my research experience and interest in pain management aligns well with my current proposed research project.

d. Selected Peer-reviewed Publications
AALAS encourages applicants to submit citations for up to 15 peer reviewed publications or manuscripts. The applicant may choose to include selected publications based on importance to the field, recency, and or relevancy to the proposed research. Publications

should be cited per *Comparative Medicine* and *JAALAS* format (http://www.aalas.org/publications/cm_jaalas_info_for_au.aspx).

Cotroneo TM, Hugunin KM, Shuster KA, Hwang HJ, Kakaraparthi BN, Nemzek-Hamlin JA. 2012. Effects of buprenorphine on a cecal ligation and puncture model in C57BL/6 mice. J Am Assoc Lab Anim Sci **51**:357-365.

Cotroneo TM, Nemzek-Hamlin JA, Bayliss J, Su GL. 2012. Lipopolysaccharide binding protein inhibitory peptide alters hepatic inflammatory response post-hemorrhagic shock. Innate Immun **18**:866-875.

Cotroneo TM, Colby LA, Bergin IL. 2011. Hemophagocytic syndrome in a pancytopenic simian retrovirus-infected male rhesus macaque (Macaca mulatta). Vet Pathol **48**:1138-1143.

Co-Investigator

a. General Information
Name: Gerald Hish, DVM
Position Title: Sr. Surgical Service Veterinarian / Director, Veterinary Surgical Services

b. Education
Add rows to the table below to list all post high school education including residency training.

Institution/City	Degree (if applicable)	Date Completed (MM/DD/YYYY)	Field of Study
VA Tech Blacksburg VA	BS	05/1995	Wildlife Biology
VMRCVM Blacksburg, VA	DVM	05/1999	Veterinarian
University of Michigan Ann Arbor, MI		06/30/2013	Laboratory Animal Medicine Residency

c. Personal Statement of Qualifications
My role in this project is to contribute to experimental design, perform and train laboratory personnel to complete quantitative and behavioral assessments, and provide veterinary care to the animals on this study. I practiced companion animal and exotic animal clinical medicine for 11 years before completing a residency in laboratory animal medicine in 2013. I have always had a strong interest in surgery, anesthesia and analgesia that I have been able to apply to both my clinical and research activities. Specifically, I have been involved with projects and have experience with several pain assessment modalities including grimace scales and scoring according to behavioral ethograms. As an IACUC member and reviewer of animal use protocols, I am also very interested in exploring and documenting the impact that commonly used analgesics may have on animal surgical models and have published on this topic. I believe that my clinical experience, research training, and demonstrated interest are a good fit with the currently proposed project.

d. Selected Peer-reviewed Publications
Hish GA, Diaz JA, Hawley AE, Myers DD, Lester PA. 2014. Effects of analgesic use on inflammation and hematology in a murine model of venous thrombosis. J Am Assoc Lab Anim Sci **53**:485-93.

Hampton AL, Aslam MN, Naik MK, Bergin IL, Allen RM, Craig RA, Kunkel SL, Veerapaneni I, Paruchuri T, Patterson KA, Rothman ED, Hish GA, Varani J, Rush HG. 2015. Ulcerative dermatitis in C57BL/6NCrl mice on a low-fat or high-fat diet with or without a mineralized red-algae supplement. J Am Assoc Lab Anim Sci **54**:487-96.
Hampton AL, Hish GA, Aslam MN, Rothman ED, Bergin IL, Patterson KA, Naik M, Paruchuri T, Varani J, Rush HG. 2012. Progression of ulcerative dermatitis lesions in C57BL/6Crl mice and the development of a scoring system for dermatitis lesions. J Am Assoc Lab Anim Sci **51**:586-93.
Shuster KA, Hish GA, Selles LA,Chowdhury MA, Wiggins RC, Dysko RC, Bergin IL. 2013. Naturally occurring disseminated group B streptococcus infections in postnatal rats. Comp Med **63**:55-61.

Co-Investigator

a. General Information
Name: Jeremy T. Llaniguez, MS
Position Title: MD/PhD Candidate, Graduate Research Assistant

b. Education
Add rows to the table below to list all post high school education including residency training.

Institution/City	Degree (if applicable)	Date Completed (MM/DD/YYYY)	Field of Study
University of California, Berkeley (Berkeley, CA)	BS	05/2001	Mechanical Engineering
Massachusetts Institute of Technology (Cambridge, MA)	MS	09/2003	Mechanical Engineering
Wayne State University, School of Medicine (Detroit, MI)	MD/PhD (In progress)	05/2019	Medicine/Biomedical Engineering

c. Personal Statement of Qualifications
Project Role: As a co-investigator, J. Llaniguez will perform all of the animal experiments listed in the experimental design. However, cageside assessments will be passed on to trained DLAR veterinary technicians (trained by J. Llaniguez) to record data in a blinded manner.
Experience and qualifications: The axolotl is a novel model animal used in basic science research. Other than the DLAR procedures required by WSU Institutional Animal Care and Use Committee (IACUC) for working with animals, all of the surgical procedures have been developed by the co-investigator. For animal husbandry, the co-investigator visited the axolotl colony (Ambystoma Genetic Stock Center, AGSC) maintained at the University

of Kentucky for informal training. Additionally, the Axolotl Newsletter, a publication started in 1976 by the AGSC, was used to guide the development of axolotl care at WSU.

d. Selected Peer-reviewed Publications
None in the field of veterinary medicine.

2. **Disclosures of Business or Financial Interest in the Project (1 page maximum this section)**

None

3. **Support from Other Funding Agencies (1 page maximum this section)**

All funding thus far has been internal to WSU. Preliminary studies have been funded by the co-investigator's sponsor's departmental funds. DLAR have helped with funding for animals, analgesics, and the video surveillance system.

BIBLIOGRAPHY AND REFERENCES CITED

Abraham, M.R., Henrikson, C.A., Tung, L., Chang, M.G., Aon, M., Xue, T., Li, R.A., B, O.R., Marban, E., 2005. Antiarrhythmic engineering of skeletal myoblasts for cardiac transplantation. Circ Res 97, 159-167.

Akazawa, H., Komazaki, S., Shimomura, H., Terasaki, F., Zou, Y., Takano, H., Nagai, T., Komuro, I., 2004. Diphtheria toxin-induced autophagic cardiomyocyte death plays a pathogenic role in mouse model of heart failure. J Biol Chem 279, 41095-41103.

Alberts, B., 2002. Molecular biology of the cell, 4th ed. Garland Science, New York.

Ali, S.R., Hippenmeyer, S., Saadat, L.V., Luo, L., Weissman, I.L., Ardehali, R., 2014. Existing cardiomyocytes generate cardiomyocytes at a low rate after birth in mice. Proc Natl Acad Sci U S A 111, 8850-8855.

Alworth, L.C., Harvey, S.B., 2007. IACUC issues associated with amphibian research. ILAR J 48, 278-289.

Ambardekar, A.V., Buttrick, P.M., 2011. Reverse remodeling with left ventricular assist devices: a review of clinical, cellular, and molecular effects. Circ Heart Fail 4, 224-233.

Andersen, D.C., Ganesalingam, S., Jensen, C.H., Sheikh, S.P., 2014. Do neonatal mouse hearts regenerate following heart apex resection? Stem cell reports 2, 406-413.

Anversa, P., Hiler, B., Ricci, R., Guideri, G., Olivetti, G., 1986. Myocyte cell loss and myocyte hypertrophy in the aging rat heart. J Am Coll Cardiol 8, 1441-1448.

Anversa, P., Kajstura, J., 1998. Myocyte cell death in the diseased heart. Circ Res 82, 1231-1233.

Anversa, P., Palackal, T., Sonnenblick, E.H., Olivetti, G., Meggs, L.G., Capasso, J.M., 1990. Myocyte cell loss and myocyte cellular hyperplasia in the hypertrophied aging rat heart. Circ Res 67, 871-885.

Armstrong, J.B., Malacinski, G.M., 1989. Developmental biology of the axolotl. Oxford University Press, New York.

Azhar, G., Gao, W., Liu, L., Wei, J.Y., 1999. Ischemia-reperfusion in the adult mouse heart influence of age. Exp Gerontol 34, 699-714.

Balsam, L.B., Wagers, A.J., Christensen, J.L., Kofidis, T., Weissman, I.L., Robbins, R.C., 2004. Haematopoietic stem cells adopt mature haematopoietic fates in ischaemic myocardium. Nature 428, 668-673.

Barja, G., Herrero, A., 2000. Oxidative damage to mitochondrial DNA is inversely related to maximum life span in the heart and brain of mammals. FASEB J 14, 312-318.

Barsky, S.H., Hannah, J.B., 1987. Extracellular hyaline bodies are basement membrane accumulations. Am J Clin Pathol 87, 455-460.

Battey, J., Jordan, E., Cox, D., Dove, W., 1999. An action plan for mouse genomics. Nat Genet 21, 73-75.

Bayat, H., Swaney, J.S., Ander, A.N., Dalton, N., Kennedy, B.P., Hammond, H.K., Roth, D.M., 2002. Progressive heart failure after myocardial infarction in mice. Basic Res Cardiol 97, 206-213.

Becker, R.O., Chapin, S., Sherry, R., 1974. Regeneration of the ventricular myocardium in amphibians. Nature 248, 145-147.

Begemann, G., Gibert, Y., Meyer, A., Ingham, P.W., 2002. Cloning of zebrafish T-box genes tbx15 and tbx18 and their expression during embryonic development. Mech Dev 114, 137-141.

Beltrami, A.P., Urbanek, K., Kajstura, J., Yan, S.M., Finato, N., Bussani, R., Nadal-Ginard, B., Silvestri, F., Leri, A., Beltrami, C.A., Anversa, P., 2001. Evidence that human cardiac myocytes divide after myocardial infarction. N Engl J Med 344, 1750-1757.

Bergmann, O., Bhardwaj, R.D., Bernard, S., Zdunek, S., Barnabe-Heider, F., Walsh, S., Zupicich, J., Alkass, K., Buchholz, B.A., Druid, H., Jovinge, S., Frisen, J., 2009. Evidence for cardiomyocyte renewal in humans. Science 324, 98-102.

Bergmann, O., Jovinge, S., 2014. Cardiac regeneration in vivo: mending the heart from within? Stem Cell Res 13, 523-531.

Bergmann, O., Zdunek, S., Felker, A., Salehpour, M., Alkass, K., Bernard, S., Sjostrom, S.L., Szewczykowska, M., Jackowska, T., Dos Remedios, C., Malm, T., Andra, M., Jashari, R., Nyengaard, J.R., Possnert, G., Jovinge, S., Druid, H., Frisen, J., 2015. Dynamics of cell generation and turnover in the human heart. Cell 161, 1566-1575.

Bernal, J., Baldwin, M., Gleason, T., Kuhlman, S., Moore, G., Talcott, M., 2009. Guidelines for rodent survival surgery. J Invest Surg 22, 445-451.

Berridge, M.J., Bootman, M.D., Roderick, H.L., 2003. Calcium signalling: dynamics, homeostasis and remodelling. Nat Rev Mol Cell Biol 4, 517-529.

Bersell, K., Arab, S., Haring, B., Kuhn, B., 2009. Neuregulin1/ErbB4 signaling induces cardiomyocyte proliferation and repair of heart injury. Cell 138, 257-270.

Bollini, S., Smart, N., Riley, P.R., 2011. Resident cardiac progenitor cells: at the heart of regeneration. J Mol Cell Cardiol 50, 296-303.

Bond, J.M., Harper, I.S., Chacon, E., Reece, J.M., Herman, B., Lemasters, J.J., 1994. The pH Paradox in the Pathophysiology of Reperfusion Injury to Rat Neonatal Cardiac Myocytes a. Ann N Y Acad Sci 723, 25-37.

Booz, G.W., Baker, K.M., 1995. Molecular signalling mechanisms controlling growth and function of cardiac fibroblasts. Cardiovasc Res 30, 537-543.

Bornstein, P., 2001. Thrombospondins as matricellular modulators of cell function. The Journal of clinical investigation 107, 929-934.

Bornstein, P., Sage, E.H., 2002. Matricellular proteins: extracellular modulators of cell function. Curr Opin Cell Biol 14, 608-616.

Boulton, D.W., Duncan, G.F., Vachharajani, N.N., 2002. Validation and application of a sensitive assay for butorphanol in human plasma by high-performance liquid chromatography with tandem mass spectrometry detection. J Chromatogr B Analyt Technol Biomed Life Sci 775, 57-62.

Brockes, J.P., 1997. Amphibian limb regeneration: rebuilding a complex structure. Science 276, 81-87.

Bryant, D.M., O'Meara, C.C., Ho, N.N., Gannon, J., Cai, L., Lee, R.T., 2015. A systematic analysis of neonatal mouse heart regeneration after apical resection. J Mol Cell Cardiol 79, 315-318.

Burggren, W.W., Warburton, S., 2007. Amphibians as animal models for laboratory research in physiology. ILAR J 48, 260-269.

Cai, M.X., Shi, X.C., Chen, T., Tan, Z.N., Lin, Q.Q., Du, S.J., Tian, Z.J., 2016. Exercise training activates neuregulin 1/ErbB signaling and promotes cardiac repair in a rat myocardial infarction model. Life Sci 149, 1-9.

Cano-Martinez, A., Vargas-Gonzalez, A., Guarner-Lans, V., Prado-Zayago, E., Leon-Oleda, M., Nieto-Lima, B., 2010. Functional and structural regeneration in the axolotl heart (Ambystoma mexicanum) after partial ventricular amputation. Arch Cardiol Mex 80, 79-86.

Castellan, R.F.P., Meloni, M., 2018. Mechanisms and Therapeutic Targets of Cardiac Regeneration: Closing the Age Gap. Front Cardiovasc Med 5, 7.

Chablais, F., Jaźwińska, A., 2012. The regenerative capacity of the zebrafish heart is dependent on TGFβ signaling. Development 139, 1921-1930.

Chablais, F., Veit, J., Rainer, G., Jazwinska, A., 2011. The zebrafish heart regenerates after cryoinjury-induced myocardial infarction. BMC Dev Biol 11, 21.

Chalkley, D.T., 1954. A quantitative histological analysis of forelimb regeneration in Triturus viridescens. J Morphol 94, 21-70.

Chang, M.P., Bramhall, J., Graves, S., Bonavida, B., Wisnieski, B.J., 1989. Internucleosomal DNA cleavage precedes diphtheria toxin-induced cytolysis. Evidence that cell lysis is not a simple consequence of translation inhibition. J Biol Chem 264, 15261-15267.

Chen, Z., Li, T., Zhang, B., 2008. Morphine postconditioning protects against reperfusion injury in the isolated rat hearts. J Surg Res 145, 287-294.

Cheng, W., Li, B., Kajstura, J., Li, P., Wolin, M.S., Sonnenblick, E.H., Hintze, T.H., Olivetti, G., Anversa, P., 1995. Stretch-induced programmed myocyte cell death. J Clin Invest 96, 2247-2259.

Chico, T.J., Ingham, P.W., Crossman, D.C., 2008. Modeling cardiovascular disease in the zebrafish. Trends Cardiovasc Med 18, 150-155.

Choi, W.Y., Poss, K.D., 2012. Cardiac regeneration. Curr Top Dev Biol 100, 319-344.

Chrastil, J., Sampson, C., Jones, K.B., Higgins, T.F., 2013. Postoperative opioid administration inhibits bone healing in an animal model. Clin Orthop Relat Res 471, 4076-4081.

Christia, P., Frangogiannis, N.G., 2013. Targeting inflammatory pathways in myocardial infarction. Eur J Clin Invest 43, 986-995.

Christian, L.M., Graham, J.E., Padgett, D.A., Glaser, R., Kiecolt-Glaser, J.K., 2006. Stress and wound healing. Neuroimmunomodulation 13, 337-346.

Claver, J.A., Quaglia, A.I., 2009. Comparative morphology, development, and function of blood cells in nonmammalian vertebrates. Journal of Exotic Pet Medicine 18, 87-97.

Coble, D.J., Taylor, D.K., Mook, D.M., 2011. Analgesic effects of meloxicam, morphine sulfate, flunixin meglumine, and xylazine hydrochloride in African-clawed frogs (Xenopus laevis). J Am Assoc Lab Anim Sci 50, 355-360.

Cohen, G.M., 1997. Caspases: the executioners of apoptosis. Biochem J 326 (Pt 1), 1-16.

Collinson, P.O., Gaze, D.C., 2007. Biomarkers of cardiovascular damage and dysfunction--an overview. Heart Lung Circ 16 Suppl 3, S71-82.

Committee, I.R.A., 1985. US Government Principles for the Utilization and Care of Vertebrate Animals Used in Testing, Federal Register Vol. 50, No. 97 [FR Doc. 85-12059]. Office of Science and Technology Policy.

Cooper, G.M., 2000. The Cell: A Molecular Approach, 2nd ed. Sinauer Associates Inc.

Council, N.R., 2011. Guide for the Care and Use of Laboratory Animals: Eighth Edition. The National Academies Press, Washington, DC.

Crompton, M., 1999. The mitochondrial permeability transition pore and its role in cell death. Biochem J 341 (Pt 2), 233-249.

D'Uva, G., Aharonov, A., Lauriola, M., Kain, D., Yahalom-Ronen, Y., Carvalho, S., Weisinger, K., Bassat, E., Rajchman, D., Yifa, O., Lysenko, M., Konfino, T., Hegesh, J., Brenner, O., Neeman, M., Yarden, Y., Leor, J., Sarig, R., Harvey, R.P., Tzahor, E., 2015. ERBB2 triggers mammalian heart regeneration by promoting cardiomyocyte dedifferentiation and proliferation. Nat Cell Biol 17, 627-638.

Dams, R., Benijts, T., Lambert, W.E., De Leenheer, A.P., 2002. Simultaneous determination of in total 17 opium alkaloids and opioids in blood and urine by fast liquid chromatography-diode-array detection-fluorescence detection, after solid-phase extraction. J Chromatogr B Analyt Technol Biomed Life Sci 773, 53-61.

Darehzereshki, A., Rubin, N., Gamba, L., Kim, J., Fraser, J., Huang, Y., Billings, J., Mohammadzadeh, R., Wood, J., Warburton, D., Kaartinen, V., Lien, C.L., 2015. Differential regenerative capacity of neonatal mouse hearts after cryoinjury. Dev Biol 399, 91-99.

de Haan, J.J., Smeets, M.B., Pasterkamp, G., Arslan, F., 2013. Danger signals in the initiation of the inflammatory response after myocardial infarction. Mediators Inflamm 2013, 206039.

Dooley, K., Zon, L.I., 2000. Zebrafish: a model system for the study of human disease. Curr Opin Genet Dev 10, 252-256.

Drăghici, S., 2012. Statistics and data analysis for microarrays using R and Bioconductor. CRC Press, Boca Raton, FL.

Draper, R.K., Simon, M.I., 1980. The entry of diphtheria toxin into the mammalian cell cytoplasm: evidence for lysosomal involvement. The Journal of cell biology 87, 849-854.

Dubin, A.E., Patapoutian, A., 2010. Nociceptors: the sensors of the pain pathway. J Clin Invest 120, 3760-3772.

Duchrow, M., Schluter, C., Key, G., Kubbutat, M.H., Wohlenberg, C., Flad, H.D., Gerdes, J., 1995. Cell proliferation-associated nuclear antigen defined by antibody Ki-67: a new kind of cell cycle-maintaining proteins. Arch Immunol Ther Exp (Warsz) 43, 117-121.

Duellman, W.E., Trueb, L., 1994. Biology of amphibians. Johns Hopkins University Press, Baltimore.

Dumesnil, J.G., Dion, D., Yvorchuk, K., Davies, R.A., Chan, K., 1995. A new, simple and accurate method for determining ejection fraction by Doppler echocardiography. Can J Cardiol 11, 1007-1014.

Earnshaw, W.C., Martins, L.M., Kaufmann, S.H., 1999. Mammalian caspases: structure, activation, substrates, and functions during apoptosis. Annu Rev Biochem 68, 383-424.

Easton, H.S., Armstrong, J.B., Smith, S.C., 1994. Heart specification in the Mexican axolotl (Ambystoma mexicanum). Dev Dyn 200, 313-320.

Ebner, B., Lange, S.A., Eckert, T., Wischniowski, C., Ebner, A., Braun-Dullaeus, R.C., Weinbrenner, C., Wunderlich, C., Simonis, G., Strasser, R.H., 2013. Uncoupled eNOS annihilates neuregulin-1beta-induced cardioprotection: a novel mechanism in pharmacological postconditioning in myocardial infarction. Mol Cell Biochem 373, 115-123.

Edler, I., Hertz, C.H., 2004. The Use of Ultrasonic Reflectoscope for the Continuous Recording of the Movements of Heart Walls, 1954. Clinical physiology and functional imaging 24, 118-136.

Ellison, G.M., Galuppo, V., Vicinanza, C., Aquila, I., Waring, C.D., Leone, A., Indolfi, C., Torella, D., 2010. Cardiac stem and progenitor cell identification: different markers for the same cell? Front Biosci (Schol Ed) 2, 641-652.

Ellison, G.M., Vicinanza, C., Smith, A.J., Aquila, I., Leone, A., Waring, C.D., Henning, B.J., Stirparo, G.G., Papait, R., Scarfo, M., Agosti, V., Viglietto, G., Condorelli, G., Indolfi, C., Ottolenghi, S., Torella, D., Nadal-Ginard, B., 2013. Adult c-kit(pos) cardiac stem cells are necessary and sufficient for functional cardiac regeneration and repair. Cell 154, 827-842.

Eltzschig, H.K., Eckle, T., 2011. Ischemia and reperfusion--from mechanism to translation. Nat Med 17, 1391-1401.

Endl, E., Gerdes, J., 2000. The Ki-67 protein: fascinating forms and an unknown function. Exp Cell Res 257, 231-237.

Engel, F.B., 2005. Cardiomyocyte proliferation: a platform for mammalian cardiac repair. Cell Cycle 4, 1360-1363.

Fabiato, A., Fabiato, F., 1979. Calcium and cardiac excitation-contraction coupling. Annu Rev Physiol 41, 473-484.

Falnes, P.Ø., Sandvig, K., 2000. Penetration of protein toxins into cells. Current opinion in cell biology 12, 407-413.

Farkas, J.E., Monaghan, J.R., 2015. Housing and maintenance of Ambystoma mexicanum, the Mexican axolotl. Methods Mol Biol 1290, 27-46.

Fernandes, S., Amirault, J.C., Lande, G., Nguyen, J.M., Forest, V., Bignolais, O., Lamirault, G., Heudes, D., Orsonneau, J.L., Heymann, M.F., Charpentier, F., Lemarchand, P., 2006.

Autologous myoblast transplantation after myocardial infarction increases the inducibility of ventricular arrhythmias. Cardiovasc Res 69, 348-358.

Field, L.J., 1993. Transgenic mice in cardiovascular research. Annu Rev Physiol 55, 97-114.

Fischer, A.H., Jacobson, K.A., Rose, J., Zeller, R., 2008. Hematoxylin and eosin staining of tissue and cell sections. Cold Spring Harbor Protocols 2008, pdb. prot4986.

Francis, E.T.B., 1934. The anatomy of the salamander. The Clarendon Press, Oxford,.

Frangogiannis, N.G., 2012. Regulation of the inflammatory response in cardiac repair. Circ Res 110, 159-173.

Frangogiannis, N.G., 2015. The reparative function of cardiomyocytes in the infarcted myocardium. Cell Metab 21, 797-798.

Fransen, M.E., Lemanski, L.F., 1990. Epicardial development in the axolotl, Ambystoma mexicanum. Anat Rec 226, 228-236.

Gage, A.A., Baust, J., 1998. Mechanisms of tissue injury in cryosurgery. Cryobiology 37, 171-186.

Galvez, A.S., Diwan, A., Odley, A.M., Hahn, H.S., Osinska, H., Melendez, J.G., Robbins, J., Lynch, R.A., Marreez, Y., Dorn, G.W., 2nd, 2007. Cardiomyocyte degeneration with calpain deficiency reveals a critical role in protein homeostasis. Circ Res 100, 1071-1078.

Gentz, E.J., 2007. Medicine and surgery of amphibians. ILAR J 48, 255-259.

Gerdes, J., Lemke, H., Baisch, H., Wacker, H.H., Schwab, U., Stein, H., 1984. Cell cycle analysis of a cell proliferation-associated human nuclear antigen defined by the monoclonal antibody Ki-67. J Immunol 133, 1710-1715.

Glaser, R., Kiecolt-Glaser, J.K., 2005. Stress-induced immune dysfunction: implications for health. Nat Rev Immunol 5, 243-251.

Gnecchi, M., Zhang, Z., Ni, A., Dzau, V.J., 2008. Paracrine mechanisms in adult stem cell signaling and therapy. Circ Res 103, 1204-1219.

Godbout, J.P., Glaser, R., 2006. Stress-induced immune dysregulation: implications for wound healing, infectious disease and cancer. J Neuroimmune Pharmacol 1, 421-427.

Godwin, J., Debuque, R., Salimova, E., Rosenthal, N., 2017a. Heart regeneration in the salamander relies on macrophage-mediated control of fibroblast activation and the extracellular landscape. npj Regenerative Medicine 2, 22.

Godwin, J., Debuque, R., Salimova, E., Rosenthal, N., 2017b. Heart regeneration in the salamander relies on macrophage-mediated control of fibroblast activation and the extracellular landscape. NPJ Regen Med 2.

Godwin, J.W., Pinto, A.R., Rosenthal, N.A., 2013. Macrophages are required for adult salamander limb regeneration. Proc Natl Acad Sci U S A 110, 9415-9420.

Godwin, J.W., Rosenthal, N., 2014. Scar-free wound healing and regeneration in amphibians: immunological influences on regenerative success. Differentiation 87, 66-75.

Goldner, J., 1938. A modification of the Masson trichrome technique for routine laboratory purposes. The American journal of pathology 14, 237.

Gonzalez-Rosa, J.M., Martin, V., Peralta, M., Torres, M., Mercader, N., 2011. Extensive scar formation and regression during heart regeneration after cryoinjury in zebrafish. Development 138, 1663-1674.

González-Rosa, J.M., Mercader, N., 2012. Cryoinjury as a myocardial infarction model for the study of cardiac regeneration in the zebrafish. Nature protocols 7, 782-788.

Goto, H., Tomono, Y., Ajiro, K., Kosako, H., Fujita, M., Sakurai, M., Okawa, K., Iwamatsu, A., Okigaki, T., Takahashi, T., Inagaki, M., 1999. Identification of a novel phosphorylation site on histone H3 coupled with mitotic chromosome condensation. J Biol Chem 274, 25543-25549.

Grabowski, M.W., Buckman, R.F., Jr., Goldberg, A., Badellino, M.M., 1995. Clamp control of the right ventricular angle to facilitate exposure and repair of cardiac wounds. Am J Surg 170, 399-400.

Groban, L., Vernon, J.C., Butterworth, J., 2004. Intrathecal morphine reduces infarct size in a rat model of ischemia-reperfusion injury. Anesth Analg 98, 903-909.

Guo, S., Dipietro, L.A., 2010. Factors affecting wound healing. J Dent Res 89, 219-229.

Gurley, L.R., Walters, R.A., Tobey, R.A., 1973. Histone phosphorylation in late interphase and mitosis. Biochem Biophys Res Commun 50, 744-750.

Halestrap, A.P., Clarke, S.J., Javadov, S.A., 2004. Mitochondrial permeability transition pore opening during myocardial reperfusion--a target for cardioprotection. Cardiovasc Res 61, 372-385.

Hamamoto, D.T., Simone, D.A., 2003. Characterization of cutaneous primary afferent fibers excited by acetic acid in a model of nociception in frogs. J Neurophysiol 90, 566-577.

Hamburger, V., 1942. A manual of experimental embryology. Univ. of Chicago Press, Chicago,.

Han, P., Zhou, X.H., Chang, N., Xiao, C.L., Yan, S., Ren, H., Yang, X.Z., Zhang, M.L., Wu, Q., Tang, B., Diao, J.P., Zhu, X., Zhang, C., Li, C.Y., Cheng, H., Xiong, J.W., 2014. Hydrogen peroxide primes heart regeneration with a derepression mechanism. Cell Res 24, 1091-1107.

Haubner, B.J., Adamowicz-Brice, M., Khadayate, S., Tiefenthaler, V., Metzler, B., Aitman, T., Penninger, J.M., 2012. Complete cardiac regeneration in a mouse model of myocardial infarction. Aging (Albany NY) 4, 966-977.

Hausenloy, D.J., Yellon, D.M., 2013. Myocardial ischemia-reperfusion injury: a neglected therapeutic target. J Clin Invest 123, 92-100.

Hay, E.D., Fischman, D.A., 1961. Origin of the blastema in regenerating limbs of the newt Triturus viridescens. An autoradiographic study using tritiated thymidine to follow cell proliferation and migration. Dev Biol 3, 26-59.

Heallen, T., Morikawa, Y., Leach, J., Tao, G., Willerson, J.T., Johnson, R.L., Martin, J.F., 2013. Hippo signaling impedes adult heart regeneration. Development 140, 4683-4690.

Heallen, T., Zhang, M., Wang, J., Bonilla-Claudio, M., Klysik, E., Johnson, R.L., Martin, J.F., 2011. Hippo pathway inhibits Wnt signaling to restrain cardiomyocyte proliferation and heart size. Science 332, 458-461.

Hendzel, M.J., Wei, Y., Mancini, M.A., Van Hooser, A., Ranalli, T., Brinkley, B.R., Bazett-Jones, D.P., Allis, C.D., 1997. Mitosis-specific phosphorylation of histone H3 initiates primarily within pericentromeric heterochromatin during G2 and spreads in an ordered fashion coincident with mitotic chromosome condensation. Chromosoma 106, 348-360.

Hoffmann, N.E., Bischof, J.C., 2002. The cryobiology of cryosurgical injury. Urology 60, 40-49.

Hotchkiss, R.S., Strasser, A., McDunn, J.E., Swanson, P.E., 2009. Cell death. N Engl J Med 361, 1570-1583.

Hronowski, L., Armstrong, J.B., 1977. Ionic composition of the plasma of Ambystoma mexicanum. Comparative Biochemistry and Physiology Part A: Physiology 58, 181-183.

Hsieh, P.C., Segers, V.F., Davis, M.E., MacGillivray, C., Gannon, J., Molkentin, J.D., Robbins, J., Lee, R.T., 2007. Evidence from a genetic fate-mapping study that stem cells refresh adult mammalian cardiomyocytes after injury. Nat Med 13, 970-974.

Hu, N., Yost, H.J., Clark, E.B., 2001. Cardiac morphology and blood pressure in the adult zebrafish. Anat Rec 264, 1-12.

Hugunin, K.M., Fry, C., Shuster, K., Nemzek, J.A., 2010. Effects of tramadol and buprenorphine on select immunologic factors in a cecal ligation and puncture model. Shock 34, 250-260.

Huotari, J., Helenius, A., 2011. Endosome maturation. EMBO J 30, 3481-3500.

Iismaa, S.E., Kaidonis, X., Nicks, A.M., Bogush, N., Kikuchi, K., Naqvi, N., Harvey, R.P., Husain, A., Graham, R.M., 2018. Comparative regenerative mechanisms across different mammalian tissues. NPJ Regen Med 3, 6.

Ikeda, S., Sadoshima, J., 2016. Regulation of Myocardial Cell Growth and Death by the Hippo Pathway. Circ J 80, 1511-1519.

Ivaska, J., Pallari, H.M., Nevo, J., Eriksson, J.E., 2007. Novel functions of vimentin in cell adhesion, migration, and signaling. Exp Cell Res 313, 2050-2062.

Jackson, K.A., Majka, S.M., Wang, H., Pocius, J., Hartley, C.J., Majesky, M.W., Entman, M.L., Michael, L.H., Hirschi, K.K., Goodell, M.A., 2001. Regeneration of ischemic cardiac muscle and vascular endothelium by adult stem cells. J Clin Invest 107, 1395-1402.

Jacobson, A.G., Sater, A.K., 1988. Features of embryonic induction. Development 104, 341-359.

Jakob, P., Landmesser, U., 2013. Current status of cell-based therapy for heart failure. Curr Heart Fail Rep 10, 165-176.

Jesty, S.A., Steffey, M.A., Lee, F.K., Breitbach, M., Hesse, M., Reining, S., Lee, J.C., Doran, R.M., Nikitin, A.Y., Fleischmann, B.K., Kotlikoff, M.I., 2012. c-kit+ precursors support postinfarction myogenesis in the neonatal, but not adult, heart. Proc Natl Acad Sci U S A 109, 13380-13385.

Jhamb, D., Rao, N., Milner, D.J., Song, F., Cameron, J.A., Stocum, D.L., Palakal, M.J., 2011. Network based transcription factor analysis of regenerating axolotl limbs. BMC Bioinformatics 12, 80.

Jones, P.L., Jones, F.S., 2000. Tenascin-C in development and disease: gene regulation and cell function. Matrix Biol 19, 581-596.

Jopling, C., Sleep, E., Raya, M., Marti, M., Raya, A., Izpisua Belmonte, J.C., 2010. Zebrafish heart regeneration occurs by cardiomyocyte dedifferentiation and proliferation. Nature 464, 606-609.

Judd, J., Xuan, W., Huang, G.N., 2016. Cellular and molecular basis of cardiac regeneration. Turkish Journal of Biology 40, 265-275.

Junqueira, L.C.U., Bignolas, G., Brentani, R., 1979. Picrosirius staining plus polarization microscopy, a specific method for collagen detection in tissue sections. The Histochemical journal 11, 447-455.

Kajstura, J., Cheng, W., Sarangarajan, R., Li, P., Li, B., Nitahara, J.A., Chapnick, S., Reiss, K., Olivetti, G., Anversa, P., 1996. Necrotic and apoptotic myocyte cell death in the aging heart of Fischer 344 rats. Am J Physiol 271, H1215-1228.

Kari, G., Rodeck, U., Dicker, A.P., 2007. Zebrafish: an emerging model system for human disease and drug discovery. Clin Pharmacol Ther 82, 70-80.

Kempf, T., Zarbock, A., Widera, C., Butz, S., Stadtmann, A., Rossaint, J., Bolomini-Vittori, M., Korf-Klingebiel, M., Napp, L.C., Hansen, B., Kanwischer, A., Bavendiek, U., Beutel, G., Hapke, M., Sauer, M.G., Laudanna, C., Hogg, N., Vestweber, D., Wollert, K.C., 2011. GDF-15 is an inhibitor of leukocyte integrin activation required for survival after myocardial infarction in mice. Nat Med 17, 581-588.

Khattak, S., Schuez, M., Richter, T., Knapp, D., Haigo, S.L., Sandoval-Guzman, T., Hradlikova, K., Duemmler, A., Kerney, R., Tanaka, E.M., 2013. Germline transgenic methods for tracking cells and testing gene function during regeneration in the axolotl. Stem Cell Reports 1, 90-103.

Kijima, Y., Saito, A., Jetton, T.L., Magnuson, M.A., Fleischer, S., 1993. Different intracellular localization of inositol 1,4,5-trisphosphate and ryanodine receptors in cardiomyocytes. J Biol Chem 268, 3499-3506.

Kikuchi, K., Holdway, J.E., Werdich, A.A., Anderson, R.M., Fang, Y., Egnaczyk, G.F., Evans, T., Macrae, C.A., Stainier, D.Y., Poss, K.D., 2010. Primary contribution to zebrafish heart regeneration by gata4(+) cardiomyocytes. Nature 464, 601-605.

Kinsella, T.J., Dobson, P.P., Mitchell, J.B., Fornace, A.J., Jr., 1987. Enhancement of X ray induced DNA damage by pre-treatment with halogenated pyrimidine analogs. Int J Radiat Oncol Biol Phys 13, 733-739.

Kinsella, T.J., Mitchell, J.B., Russo, A., Morstyn, G., Glatstein, E., 1984. The use of halogenated thymidine analogs as clinical radiosensitizers: rationale, current status, and future prospects: non-hypoxic cell sensitizers. Int J Radiat Oncol Biol Phys 10, 1399-1406.

Klocke, R., Tian, W., Kuhlmann, M.T., Nikol, S., 2007. Surgical animal models of heart failure related to coronary heart disease. Cardiovasc Res 74, 29-38.

Kochi, S.K., Collier, R.J., 1993. DNA fragmentation and cytolysis in U937 cells treated with diphtheria toxin or other inhibitors of protein synthesis. Experimental cell research 208, 296-302.

Koeller, C.A., 2009. Comparison of buprenorphine and butorphanol analgesia in the eastern red-spotted newt (Notophthalmus viridescens). J Am Assoc Lab Anim Sci 48, 171-175.

Kojima, T., Takagi, A., Maeda, M., Segawa, T., Shimizu, A., Yamamoto, K., Matsushita, T., Saito, H., 2001. Plasma levels of syndecan-4 (ryudocan) are elevated in patients with acute myocardial infarction. Thromb Haemost 85, 793-799.

Komatsu, N., Oda, T., Muramatsu, T., 1998. Involvement of both caspase-like proteases and serine proteases in apoptotic cell death induced by ricin, modeccin, diphtheria toxin, and pseudomonas toxin. The Journal of Biochemistry 124, 1038-1044.

Konfino, T., Landa, N., Ben-Mordechai, T., Leor, J., 2015. The type of injury dictates the mode of repair in neonatal and adult heart. J Am Heart Assoc 4, e001320.

Korecky, B., Rakusan, K., 1978. Normal and hypertrophic growth of the rat heart: changes in cell dimensions and number. Am J Physiol 234, H123-128.

Kostin, S., Pool, L., Elsasser, A., Hein, S., Drexler, H.C., Arnon, E., Hayakawa, Y., Zimmermann, R., Bauer, E., Klovekorn, W.P., Schaper, J., 2003. Myocytes die by multiple mechanisms in failing human hearts. Circ Res 92, 715-724.

Kowaltowski, A.J., de Souza-Pinto, N.C., Castilho, R.F., Vercesi, A.E., 2009. Mitochondria and reactive oxygen species. Free Radic Biol Med 47, 333-343.

Kraus, F., Haenig, B., Kispert, A., 2001. Cloning and expression analysis of the mouse T-box gene Tbx18. Mech Dev 100, 83-86.

Laflamme, M.A., Murry, C.E., 2005. Regenerating the heart. Nat Biotechnol 23, 845-856.

Lafontant, P.J., Burns, A.R., Grivas, J.A., Lesch, M.A., Lala, T.D., Reuter, S.P., Field, L.J., Frounfelter, T.D., 2012. The giant danio (D. aequipinnatus) as a model of cardiac remodeling and regeneration. Anat Rec (Hoboken) 295, 234-248.

Laurie, G.W., Leblond, C.P., Martin, G.R., 1982a. Localization of type IV collagen, laminin, heparan sulfate proteoglycan, and fibronectin to the basal lamina of basement membranes. J Cell Biol 95, 340-344.

Laurie, G.W., Leblond, C.P., Martin, G.R., Silver, M.H., 1982b. Intracellular localization of basement membrane precursors in the endodermal cells of the rat parietal yolk sac. III. Immunostaining for laminin and its precursors. J Histochem Cytochem 30, 991-998.

Lecker, S.H., Goldberg, A.L., Mitch, W.E., 2006. Protein degradation by the ubiquitin-proteasome pathway in normal and disease states. J Am Soc Nephrol 17, 1807-1819.

Lemanski, L.F., 1973a. Heart development in the Mexican salamander, Ambystoma mexicanum. I. Gross anatomy, histology and histochemistry. J Morphol 139, 301-327.

Lemanski, L.F., 1973b. Heart development in the Mexican salamander, Ambystoma mexicanum. II. Ultrastructure. Developmental Dynamics 136, 487-525.

Lemasters, J.J., Bond, J.M., Chacon, E., Harper, I.S., Kaplan, S.H., Ohata, H., Trollinger, D.R., Herman, B., Cascio, W.E., 1996. The pH paradox in ischemia-reperfusion injury to cardiac myocytes. EXS 76, 99-114.

Leone, M., Magadum, A., Engel, F.B., 2015. Cardiomyocyte proliferation in cardiac development and regeneration: a guide to methodologies and interpretations. Am J Physiol Heart Circ Physiol 309, H1237-1250.

Lepilina, A., Coon, A.N., Kikuchi, K., Holdway, J.E., Roberts, R.W., Burns, C.G., Poss, K.D., 2006. A dynamic epicardial injury response supports progenitor cell activity during zebrafish heart regeneration. Cell 127, 607-619.

Leslie, C.C., 1997. Properties and regulation of cytosolic phospholipase A2. J Biol Chem 272, 16709-16712.

Lewandoski, M., 2001. Conditional control of gene expression in the mouse. Nat Rev Genet 2, 743-755.

Lieschke, G.J., Currie, P.D., 2007. Animal models of human disease: zebrafish swim into view. Nat Rev Genet 8, 353-367.

Lilly, L.S., 2011. Pathophysiology of heart disease : a collaborative project of medical students and faculty, 5th ed. Wolters Kluwer/Lippincott Williams & Wilkins, Baltimore, MD.

Limana, F., Zacheo, A., Mocini, D., Mangoni, A., Borsellino, G., Diamantini, A., De Mori, R., Battistini, L., Vigna, E., Santini, M., Loiaconi, V., Pompilio, G., Germani, A., Capogrossi, M.C., 2007. Identification of myocardial and vascular precursor cells in human and mouse epicardium. Circ Res 101, 1255-1265.

Loffredo, F.S., Steinhauser, M.L., Gannon, J., Lee, R.T., 2011. Bone marrow-derived cell therapy stimulates endogenous cardiomyocyte progenitors and promotes cardiac repair. Cell Stem Cell 8, 389-398.

Lovell, M.J., Mathur, A., 2010. Cardiac stem cell therapy: progress from the bench to bedside. Heart 96, 1531-1537.

Lutfy, K., Cowan, A., 2004. Buprenorphine: a unique drug with complex pharmacology. Curr Neuropharmacol 2, 395-402.

Madri, J.A., Roll, F.J., Furthmayr, H., Foidart, J.M., 1980. Ultrastructural localization of fibronectin and laminin in the basement membranes of the murine kidney. J Cell Biol 86, 682-687.

Mahajan, V.S., Jarolim, P., 2011. How to interpret elevated cardiac troponin levels. Circulation 124, 2350-2354.

Mahmoud, A.I., Porrello, E.R., Kimura, W., Olson, E.N., Sadek, H.A., 2014. Surgical models for cardiac regeneration in neonatal mice. Nat Protoc 9, 305-311.

Major, R.J., Poss, K.D., 2007. Zebrafish Heart Regeneration as a Model for Cardiac Tissue Repair. Drug Discov Today Dis Models 4, 219-225.

Malliaras, K., Zhang, Y., Seinfeld, J., Galang, G., Tseliou, E., Cheng, K., Sun, B., Aminzadeh, M., Marban, E., 2013. Cardiomyocyte proliferation and progenitor cell recruitment underlie therapeutic regeneration after myocardial infarction in the adult mouse heart. EMBO Mol Med 5, 191-209.

Marcu, L., 2010. Fluorescence lifetime in cardiovascular diagnostics. J Biomed Opt 15, 011106.

Marla, S.S., Lee, J., Groves, J.T., 1997. Peroxynitrite rapidly permeates phospholipid membranes. Proc Natl Acad Sci U S A 94, 14243-14248.

Martin, G.R., Timpl, R., 1987. Laminin and other basement membrane components. Annual review of cell biology 3, 57-85.

Martinez-Hernandez, A., Chung, A.E., 1984. The ultrastructural localization of two basement membrane components: entactin and laminin in rat tissues. J Histochem Cytochem 32, 289-298.

Mayfield, A.E., Tilokee, E.L., Davis, D.R., 2014. Resident cardiac stem cells and their role in stem cell therapies for myocardial repair. Can J Cardiol 30, 1288-1298.

Mazur, P., 1970. Cryobiology: the freezing of biological systems. Science 168, 939-949.

Mazur, P., 1984. Freezing of living cells: mechanisms and implications. Am J Physiol 247, C125-142.

McGuire, L., Heffner, K., Glaser, R., Needleman, B., Malarkey, W., Dickinson, S., Lemeshow, S., Cook, C., Muscarella, P., Melvin, W.S., Ellison, E.C., Kiecolt-Glaser, J.K., 2006. Pain and wound healing in surgical patients. Ann Behav Med 31, 165-172.

Menasche, P., Alfieri, O., Janssens, S., McKenna, W., Reichenspurner, H., Trinquart, L., Vilquin, J.T., Marolleau, J.P., Seymour, B., Larghero, J., Lake, S., Chatellier, G., Solomon, S., Desnos, M., Hagege, A.A., 2008. The Myoblast Autologous Grafting in Ischemic Cardiomyopathy (MAGIC) trial: first randomized placebo-controlled study of myoblast transplantation. Circulation 117, 1189-1200.

Michael, L.H., Entman, M.L., Hartley, C.J., Youker, K.A., Zhu, J., Hall, S.R., Hawkins, H.K., Berens, K., Ballantyne, C.M., 1995. Myocardial ischemia and reperfusion: a murine model. Am J Physiol 269, H2147-2154.

Mihatsch, M.J., Bremer, J., 1978. Acid fuchsin orange G-stain (AFOG) for glomerular protein deposits. Clin Nephrol 9, 259.

Milasinovic, D., Mohl, W., 2015. Contemporary perspective on endogenous myocardial regeneration. World J Stem Cells 7, 793-805.

Moens, A.L., Claeys, M.J., Timmermans, J.P., Vrints, C.J., 2005. Myocardial ischemia/reperfusion-injury, a clinical view on a complex pathophysiological process. Int J Cardiol 100, 179-190.

Mollova, M., Bersell, K., Walsh, S., Savla, J., Das, L.T., Park, S.Y., Silberstein, L.E., Dos Remedios, C.G., Graham, D., Colan, S., Kuhn, B., 2013. Cardiomyocyte proliferation contributes to heart growth in young humans. Proc Natl Acad Sci U S A 110, 1446-1451.

Monaghan, J.R., Maden, M., 2012. Visualization of retinoic acid signaling in transgenic axolotls during limb development and regeneration. Dev Biol 368, 63-75.

Moore, J.F., Mayr, W., Hougie, C., 1976. Number, location and severity of coronary arterial changes in steelhead trout (Salmo gairdnerii). Atherosclerosis 24, 381-386.

Mor-Vaknin, N., Punturieri, A., Sitwala, K., Markovitz, D.M., 2003. Vimentin is secreted by activated macrophages. Nature cell biology 5, 59.

Murphy, S.L., Xu, J., Kochanek, K.D., 2013. Deaths: final data for 2010. Natl Vital Stat Rep 61, 1-117.

Murphy, S.L., Xu, J., Kochanek, K.D., Curtin, S.C., Arias, E., 2017. Deaths: Final Data for 2015. Natl Vital Stat Rep 66, 1-75.

Murry, C.E., Soonpaa, M.H., Reinecke, H., Nakajima, H., Nakajima, H.O., Rubart, M., Pasumarthi, K.B., Virag, J.I., Bartelmez, S.H., Poppa, V., Bradford, G., Dowell, J.D., Williams, D.A., Field, L.J., 2004. Haematopoietic stem cells do not transdifferentiate into cardiac myocytes in myocardial infarcts. Nature 428, 664-668.

Murry, C.E., Wiseman, R.W., Schwartz, S.M., Hauschka, S.D., 1996. Skeletal myoblast transplantation for repair of myocardial necrosis. J Clin Invest 98, 2512-2523.

Nadal-Ginard, B., Ellison, G.M., Torella, D., 2014. The cardiac stem cell compartment is indispensable for myocardial cell homeostasis, repair and regeneration in the adult. Stem Cell Res 13, 615-630.

Narula, J., Haider, N., Virmani, R., DiSalvo, T.G., Kolodgie, F.D., Hajjar, R.J., Schmidt, U., Semigran, M.J., Dec, G.W., Khaw, B.A., 1996. Apoptosis in myocytes in end-stage heart failure. N Engl J Med 335, 1182-1189.

National Research Council (U.S.). Committee for the Update of the Guide for the Care and Use of Laboratory Animals., Institute for Laboratory Animal Research (U.S.), National Academies Press (U.S.), 2011. Guide for the care and use of laboratory animals, 8th ed. National Academies Press,, Washington, D.C., pp. xxv, 220 p.

Neff, A.W., Dent, A.E., Armstrong, J.B., 1996. Heart development and regeneration in urodeles. Int J Dev Biol 40, 719-725.

Nelson, D.L., Cox, M.M., Lehninger, A.L., 2017. Lehninger principles of biochemistry, Seventh edition. ed. W.H. Freeman and Company; Macmillan Higher Education, New York, NY.

Newton, K., Dixit, V.M., 2012. Signaling in innate immunity and inflammation. Cold Spring Harb Perspect Biol 4.

Nguyen, P.K., Rhee, J.W., Wu, J.C., 2016. Adult Stem Cell Therapy and Heart Failure, 2000 to 2016: A Systematic Review. JAMA Cardiol 1, 831-841.

Nicotera, P., Bellomo, G., Orrenius, S., 1990. The role of Ca2+ in cell killing. Chem Res Toxicol 3, 484-494.

Nicotera, P., Bellomo, G., Orrenius, S., 1992. Calcium-mediated mechanisms in chemically induced cell death. Annu Rev Pharmacol Toxicol 32, 449-470.

Nicotera, P., Zhivotovsky, B., Orrenius, S., 1994. Nuclear calcium transport and the role of calcium in apoptosis. Cell Calcium 16, 279-288.

Northcutt, R.G., 1984. Evolution of the vertebrate central nervous system: patterns and processes. American Zoologist 24, 701-716.

Nygren, J.M., Jovinge, S., Breitbach, M., Sawen, P., Roll, W., Hescheler, J., Taneera, J., Fleischmann, B.K., Jacobsen, S.E., 2004. Bone marrow-derived hematopoietic cells generate cardiomyocytes at a low frequency through cell fusion, but not transdifferentiation. Nat Med 10, 494-501.

Oberpriller, J.O., Oberpriller, J.C., 1974. Response of the adult newt ventricle to injury. J Exp Zool 187, 249-253.

Odelberg, S.J., Kollhoff, A., Keating, M.T., 2000. Dedifferentiation of mammalian myotubes induced by msx1. Cell 103, 1099-1109.

Odunayo, A., Dodam, J.R., Kerl, M.E., DeClue, A.E., 2010. Immunomodulatory effects of opioids. J Vet Emerg Crit Care (San Antonio) 20, 376-385.

Olivetti, G., Abbi, R., Quaini, F., Kajstura, J., Cheng, W., Nitahara, J.A., Quaini, E., Di Loreto, C., Beltrami, C.A., Krajewski, S., Reed, J.C., Anversa, P., 1997. Apoptosis in the failing human heart. N Engl J Med 336, 1131-1141.

Olivetti, G., Quaini, F., Sala, R., Lagrasta, C., Corradi, D., Bonacina, E., Gambert, S.R., Cigola, E., Anversa, P., 1996. Acute myocardial infarction in humans is associated with activation of

programmed myocyte cell death in the surviving portion of the heart. J Mol Cell Cardiol 28, 2005-2016.

Omland, T., de Lemos, J.A., Sabatine, M.S., Christophi, C.A., Rice, M.M., Jablonski, K.A., Tjora, S., Domanski, M.J., Gersh, B.J., Rouleau, J.L., Pfeffer, M.A., Braunwald, E., Prevention of Events with Angiotensin Converting Enzyme Inhibition Trial, I., 2009. A sensitive cardiac troponin T assay in stable coronary artery disease. N Engl J Med 361, 2538-2547.

Organization, W.H., 2017. The Top 10 Causes of Death.

Orlic, D., Kajstura, J., Chimenti, S., Jakoniuk, I., Anderson, S.M., Li, B., Pickel, J., McKay, R., Nadal-Ginard, B., Bodine, D.M., Leri, A., Anversa, P., 2001. Bone marrow cells regenerate infarcted myocardium. Nature 410, 701-705.

Ornitz, D.M., Itoh, N., 2001. Fibroblast growth factors. Genome Biol 2, REVIEWS3005.

Pappenheimer, A.M., Jr., 1977. Diphtheria toxin. Annu Rev Biochem 46, 69-94.

Piper, H.M., Meuter, K., Schafer, C., 2003. Cellular mechanisms of ischemia-reperfusion injury. Ann Thorac Surg 75, S644-648.

Polizzotti, B.D., Ganapathy, B., Haubner, B.J., Penninger, J.M., Kuhn, B., 2016. A cryoinjury model in neonatal mice for cardiac translational and regeneration research. Nat Protoc 11, 542-552.

Polizzotti, B.D., Ganapathy, B., Walsh, S., Choudhury, S., Ammanamanchi, N., Bennett, D.G., dos Remedios, C.G., Haubner, B.J., Penninger, J.M., Kuhn, B., 2015. Neuregulin stimulation of cardiomyocyte regeneration in mice and human myocardium reveals a therapeutic window. Sci Transl Med 7, 281ra245.

Pollack, M., Phaneuf, S., Dirks, A., Leeuwenburgh, C., 2002. The role of apoptosis in the normal aging brain, skeletal muscle, and heart. Ann N Y Acad Sci 959, 93-107.

Porrello, E.R., Mahmoud, A.I., Simpson, E., Hill, J.A., Richardson, J.A., Olson, E.N., Sadek, H.A., 2011. Transient regenerative potential of the neonatal mouse heart. Science 331, 1078-1080.

Porrello, E.R., Mahmoud, A.I., Simpson, E., Johnson, B.A., Grinsfelder, D., Canseco, D., Mammen, P.P., Rothermel, B.A., Olson, E.N., Sadek, H.A., 2013. Regulation of neonatal and adult mammalian heart regeneration by the miR-15 family. Proc Natl Acad Sci U S A 110, 187-192.

Poss, K.D., 2007. Getting to the heart of regeneration in zebrafish. Semin Cell Dev Biol 18, 36-45.

Poss, K.D., Wilson, L.G., Keating, M.T., 2002. Heart regeneration in zebrafish. Science 298, 2188-2190.

Prabhu, S.D., Frangogiannis, N.G., 2016. The Biological Basis for Cardiac Repair After Myocardial Infarction: From Inflammation to Fibrosis. Circ Res 119, 91-112.

Quinones, M.A., Waggoner, A.D., Reduto, L.A., Nelson, J.G., Young, J.B., Winters, W.L., Jr., Ribeiro, L.G., Miller, R.R., 1981. A new, simplified and accurate method for determining ejection fraction with two-dimensional echocardiography. Circulation 64, 744-753.

Radi, R., 2004. Nitric oxide, oxidants, and protein tyrosine nitration. Proc Natl Acad Sci U S A 101, 4003-4008.

Radi, R., Beckman, J.S., Bush, K.M., Freeman, B.A., 1991. Peroxynitrite-induced membrane lipid peroxidation: the cytotoxic potential of superoxide and nitric oxide. Arch Biochem Biophys 288, 481-487.

Raya, A., Consiglio, A., Kawakami, Y., Rodriguez-Esteban, C., Izpisua-Belmonte, J.C., 2004. The zebrafish as a model of heart regeneration. Cloning Stem Cells 6, 345-351.

Reese, D.E., Mikawa, T., Bader, D.M., 2002. Development of the coronary vessel system. Circ Res 91, 761-768.

Rhee, D., Sanger, J.M., Sanger, J.W., 1994. The premyofibril: evidence for its role in myofibrillogenesis. Cell Motil Cytoskeleton 28, 1-24.

Rich, L., Whittaker, P., 2005. Collagen and picrosirius red staining: a polarized light assessment of fibrillar hue and spatial distribution. Braz J Morphol Sci 22, 97-104.

Robbins, S.L., Kumar, V., Cotran, R.S., 2010. Robbins and Cotran pathologic basis of disease, 8th ed. Saunders/Elsevier, Philadelphia, PA.

Rodriguez, M., Schaper, J., 2005. Apoptosis: measurement and technical issues. J Mol Cell Cardiol 38, 15-20.

Rohr, S., 2011. Cardiac fibroblasts in cell culture systems: myofibroblasts all along? J Cardiovasc Pharmacol 57, 389-399.

Rose, S.M., 1948. Epidermal dedifferentiation during blastema formation in regenerating limbs of Triturus viridescens. J Exp Zool 108, 337-361.

Rose, S.M., Rose, F.C., 1952. Tumor agent transformations in Amphibia. Cancer Res 12, 1-12.

Roy, S., Gatien, S., 2008. Regeneration in axolotls: a model to aim for! Exp Gerontol 43, 968-973.

Rumyantsev, P.P., 1977. Interrelations of the proliferation and differentiation processes during cardiact myogenesis and regeneration. Int Rev Cytol 51, 186-273.

Rumyantsev, P.P., Carlson, B.M., 1991. Growth and hyperplasia of cardiac muscle cells. Harwood Academic Publishers, London, U.K. ; New York, N.Y., U.S.A.

Saito, M., Iwawaki, T., Taya, C., Yonekawa, H., Noda, M., Inui, Y., Mekada, E., Kimata, Y., Tsuru, A., Kohno, K., 2001. Diphtheria toxin receptor-mediated conditional and targeted cell ablation in transgenic mice. Nat Biotechnol 19, 746-750.

Salto-Tellez, M., Yung Lim, S., El-Oakley, R.M., Tang, T.P., ZA, A.L., Lim, S.K., 2004. Myocardial infarction in the C57BL/6J mouse: a quantifiable and highly reproducible experimental model. Cardiovasc Pathol 13, 91-97.

Sandoval-Guzman, T., Wang, H., Khattak, S., Schuez, M., Roensch, K., Nacu, E., Tazaki, A., Joven, A., Tanaka, E.M., Simon, A., 2014. Fundamental differences in dedifferentiation and stem cell recruitment during skeletal muscle regeneration in two salamander species. Cell Stem Cell 14, 174-187.

Sandvig, K., Olsnes, S., 1980. Diphtheria toxin entry into cells is facilitated by low pH. The Journal of cell biology 87, 828-832.

Santiago, J.J., Dangerfield, A.L., Rattan, S.G., Bathe, K.L., Cunnington, R.H., Raizman, J.E., Bedosky, K.M., Freed, D.H., Kardami, E., Dixon, I.M., 2010. Cardiac fibroblast to myofibroblast differentiation in vivo and in vitro: expression of focal adhesion components in neonatal and adult rat ventricular myofibroblasts. Dev Dyn 239, 1573-1584.

Sarrazin, S., Lamanna, W.C., Esko, J.D., 2011. Heparan sulfate proteoglycans. Cold Spring Harb Perspect Biol 3.

Schindelin, J., Arganda-Carreras, I., Frise, E., Kaynig, V., Longair, M., Pietzsch, T., Preibisch, S., Rueden, C., Saalfeld, S., Schmid, B., 2012. Fiji: an open-source platform for biological-image analysis. Nature methods 9, 676.

Schindelin, J., Rueden, C.T., Hiner, M.C., Eliceiri, K.W., 2015. The ImageJ ecosystem: An open platform for biomedical image analysis. Molecular reproduction and development 82, 518-529.

Schnabel, K., Wu, C.C., Kurth, T., Weidinger, G., 2011. Regeneration of cryoinjury induced necrotic heart lesions in zebrafish is associated with epicardial activation and cardiomyocyte proliferation. PLoS One 6, e18503.

Schneider, C.A., Rasband, W.S., Eliceiri, K.W., 2012. NIH Image to ImageJ: 25 years of image analysis. Nature methods 9, 671.

Schnellbacher, R., 2010. Butorphanol. Journal of Exotic Pet Medicine 19, 192-195.

Scholzen, T., Gerdes, J., 2000. The Ki-67 protein: from the known and the unknown. J Cell Physiol 182, 311-322.

Schwartz, E., Fleischmajer, R., 1986. Association of elastin with oxytalan fibers of the dermis and with extracellular microfibrils of cultured skin fibroblasts. Journal of Histochemistry & Cytochemistry 34, 1063-1068.

Segers, V.F., Tokunou, T., Higgins, L.J., MacGillivray, C., Gannon, J., Lee, R.T., 2007. Local delivery of protease-resistant stromal cell derived factor-1 for stem cell recruitment after myocardial infarction. Circulation 116, 1683-1692.

Senyo, S.E., Lee, R.T., Kuhn, B., 2014. Cardiac regeneration based on mechanisms of cardiomyocyte proliferation and differentiation. Stem Cell Res 13, 532-541.

Senyo, S.E., Steinhauser, M.L., Pizzimenti, C.L., Yang, V.K., Cai, L., Wang, M., Wu, T.D., Guerquin-Kern, J.L., Lechene, C.P., Lee, R.T., 2013. Mammalian heart renewal by pre-existing cardiomyocytes. Nature 493, 433-436.

Serhan, C.N., 2014. Pro-resolving lipid mediators are leads for resolution physiology. Nature 510, 92-101.

Serluca, F.C., 2008. Development of the proepicardial organ in the zebrafish. Dev Biol 315, 18-27.

Shelton, G., Jones, D.R., 1968. A comparative study of central blood pressures in five amphibians. J Exp Biol 49, 631-643.

Shrout, P.E., Fleiss, J.L., 1979. Intraclass correlations: uses in assessing rater reliability. Psychol Bull 86, 420-428.

Simon, H.G., 2012. Salamanders and fish can regenerate lost structures--why can't we? BMC Biol 10, 15.

Simonot, L., Hebert, M., 2014. Between additive and subtractive color mixings: intermediate mixing models. J Opt Soc Am A Opt Image Sci Vis 31, 58-66.

Singh, B.N., Koyano-Nakagawa, N., Garry, J.P., Weaver, C.V., 2010. Heart of newt: a recipe for regeneration. J Cardiovasc Transl Res 3, 397-409.

Singh, S., Goyal, A., 2007. The origin of echocardiography: a tribute to Inge Edler. Tex Heart Inst J 34, 431-438.

Smart, N., Bollini, S., Dube, K.N., Vieira, J.M., Zhou, B., Davidson, S., Yellon, D., Riegler, J., Price, A.N., Lythgoe, M.F., Pu, W.T., Riley, P.R., 2011. De novo cardiomyocytes from within the activated adult heart after injury. Nature 474, 640-644.

Smith, E.S., Lewin, G.R., 2009. Nociceptors: a phylogenetic view. J Comp Physiol A Neuroethol Sens Neural Behav Physiol 195, 1089-1106.

Sneddon, L.U., Elwood, R.W., Adama, S.A., Leach M.C., 2014. Review: Defining and assessing animal pain. Anim Behav 97, 12

Sobkow, L., Epperlein, H.H., Herklotz, S., Straube, W.L., Tanaka, E.M., 2006. A germline GFP transgenic axolotl and its use to track cell fate: dual origin of the fin mesenchyme during development and the fate of blood cells during regeneration. Dev Biol 290, 386-397.

Solomon, V., Goldberg, A.L., 1996. Importance of the ATP-ubiquitin-proteasome pathway in the degradation of soluble and myofibrillar proteins in rabbit muscle extracts. J Biol Chem 271, 26690-26697.

Soon, K., Acton, C., 2006. Pain-induced stress: a barrier to wound healing. Wounds UK 2, 92.

Spalding, K.L., Bhardwaj, R.D., Buchholz, B.A., Druid, H., Frisen, J., 2005. Retrospective birth dating of cells in humans. Cell 122, 133-143.

Stainier, D.Y., 2001. Zebrafish genetics and vertebrate heart formation. Nat Rev Genet 2, 39-48.

States, U., 2013. Animal Welfare Act as Amended, United States Code, Title 7 (Agriculture), Chapter 54 (Transportation, Sale, and Handling of Certain Animals), §§ 2131-2159 (2013), United States.

Steinhauser, M.L., Lee, R.T., 2011. Regeneration of the heart. EMBO Mol Med 3, 701-712.

Stevens, C.W., 1996. Relative analgesic potency of mu, delta and kappa opioids after spinal administration in amphibians. J Pharmacol Exp Ther 276, 440-448.

Stevens, C.W., 2004. Opioid research in amphibians: an alternative pain model yielding insights on the evolution of opioid receptors. Brain Res Brain Res Rev 46, 204-215.

Stevens, C.W., Klopp, A.J., Facello, J.A., 1994. Analgesic potency of mu and kappa opioids after systemic administration in amphibians. J Pharmacol Exp Ther 269, 1086-1093.

Stevens, C.W., Rothe, K.S., 1997. Supraspinal administration of opioids with selectivity for mu-, delta- and kappa-opioid receptors produces analgesia in amphibians. Eur J Pharmacol 331, 15-21.

Stewart, R., Rascon, C.A., Tian, S., Nie, J., Barry, C., Chu, L.F., Ardalani, H., Wagner, R.J., Probasco, M.D., Bolin, J.M., Leng, N., Sengupta, S., Volkmer, M., Habermann, B., Tanaka, E.M., Thomson, J.A., Dewey, C.N., 2013. Comparative RNA-seq analysis in the unsequenced axolotl: the oncogene burst highlights early gene expression in the blastema. PLoS Comput Biol 9, e1002936.

Stocum, D.L., 2006. Regenerative biology and medicine. Elsevier Academic Press, Amsterdam ; Boston.

Strauer, B.E., Brehm, M., Zeus, T., Gattermann, N., Hernandez, A., Sorg, R.V., Kogler, G., Wernet, P., 2001. [Intracoronary, human autologous stem cell transplantation for myocardial regeneration following myocardial infarction]. Dtsch Med Wochenschr 126, 932-938.

Strungs, E.G., Ongstad, E.L., O'Quinn, M.P., Palatinus, J.A., Jourdan, L.J., Gourdie, R.G., 2013. Cryoinjury models of the adult and neonatal mouse heart for studies of scarring and regeneration. Methods Mol Biol 1037, 343-353.

Subramanian, S.V., Fitzgerald, M.L., Bernfield, M., 1997. Regulated shedding of syndecan-1 and-4 ectodomains by thrombin and growth factor receptor activation. Journal of Biological Chemistry 272, 14713-14720.

Sucov, H.M., Gu, Y., Thomas, S., Li, P., Pashmforoush, M., 2009. Epicardial control of myocardial proliferation and morphogenesis. Pediatr Cardiol 30, 617-625.

Sullivan, K.E., Quinn, K.P., Tang, K.M., Georgakoudi, I., Black, L.D., 3rd, 2014. Extracellular matrix remodeling following myocardial infarction influences the therapeutic potential of mesenchymal stem cells. Stem Cell Res Ther 5, 14.

Sun, Y., Weber, K.T., 1996. Angiotensin converting enzyme and myofibroblasts during tissue repair in the rat heart. J Mol Cell Cardiol 28, 851-858.

Suvarna, K.S., Layton, C., Bancroft, J.D., 2012. Bancroft's Theory and Practice of Histological Techniques E-Book. Elsevier Health Sciences.

Sweat, F., Puchtler, H., Rosenthal, S.I., 1964. Sirius Red F3ba as a Stain for Connective Tissue. Arch Pathol 78, 69-72.

Symes, K., Smith, E.M., Mitsi, M., Nugent, M.A., 2010. Sweet cues: How heparan sulfate modification of fibronectin enables growth factor guided migration of embryonic cells. Cell Adh Migr 4, 507-510.

Takata, H., Hanafusa, T., Mori, T., Shimura, M., Iida, Y., Ishikawa, K., Yoshikawa, K., Yoshikawa, Y., Maeshima, K., 2013. Chromatin compaction protects genomic DNA from radiation damage. PLoS One 8, e75622.

Takemura, G., Kanoh, M., Minatoguchi, S., Fujiwara, H., 2013. Cardiomyocyte apoptosis in the failing heart--a critical review from definition and classification of cell death. Int J Cardiol 167, 2373-2386.

Tarnavski, O., McMullen, J.R., Schinke, M., Nie, Q., Kong, S., Izumo, S., 2004. Mouse cardiac surgery: comprehensive techniques for the generation of mouse models of human diseases and their application for genomic studies. Physiol Genomics 16, 349-360.

Taylor, B.N., Kuyatt, C.E., 1994. Guidelines for evaluating and expressing the uncertainty of NIST measurement results, 1994 ed. U.S. Department of Commerce, Technology Administration, National Institute of Standards and Technology, Gaithersburg, MD.

Taylor, D.A., Atkins, B.Z., Hungspreugs, P., Jones, T.R., Reedy, M.C., Hutcheson, K.A., Glower, D.D., Kraus, W.E., 1998. Regenerating functional myocardium: improved performance after skeletal myoblast transplantation. Nat Med 4, 929-933.

Taylor, D.A., Silvestry, S.C., Bishop, S.P., Annex, B.H., Lilly, R.E., Glower, D.D., Kraus, W.E., 1997. Delivery of primary autologous skeletal myoblasts into rabbit heart by coronary infusion: a potential approach to myocardial repair. Proc Assoc Am Physicians 109, 245-253.

Timpl, R., Dziadek, M., 1986. Structure, development, and molecular pathology of basement membranes. Int Rev Exp Pathol 29, 1-112.

Tompkins, A.J., Burwell, L.S., Digerness, S.B., Zaragoza, C., Holman, W.L., Brookes, P.S., 2006. Mitochondrial dysfunction in cardiac ischemia-reperfusion injury: ROS from complex I, without inhibition. Biochim Biophys Acta 1762, 223-231.

Tune, J.D., Gorman, M.W., Feigl, E.O., 2004. Matching coronary blood flow to myocardial oxygen consumption. J Appl Physiol (1985) 97, 404-415.

Ushiki, T., 2002. Collagen fibers, reticular fibers and elastic fibers. A comprehensive understanding from a morphological viewpoint. Archives of histology and cytology 65, 109-126.

van Amerongen, M.J., Harmsen, M.C., van Rooijen, N., Petersen, A.H., van Luyn, M.J., 2007. Macrophage depletion impairs wound healing and increases left ventricular remodeling after myocardial injury in mice. Am J Pathol 170, 818-829.

van Berlo, J.H., Kanisicak, O., Maillet, M., Vagnozzi, R.J., Karch, J., Lin, S.C., Middleton, R.C., Marban, E., Molkentin, J.D., 2014. c-kit+ cells minimally contribute cardiomyocytes to the heart. Nature 509, 337-341.

van Berlo, J.H., Molkentin, J.D., 2014. An emerging consensus on cardiac regeneration. Nat Med 20, 1386-1393.

van den Bos, E.J., Mees, B.M., de Waard, M.C., de Crom, R., Duncker, D.J., 2005. A novel model of cryoinjury-induced myocardial infarction in the mouse: a comparison with coronary artery ligation. Am J Physiol Heart Circ Physiol 289, H1291-1300.

Van Ness, B.G., Howard, J.B., Bodley, J.W., 1980a. ADP-ribosylation of elongation factor 2 by diphtheria toxin. Isolation and properties of the novel ribosyl-amino acid and its hydrolysis products. J Biol Chem 255, 10717-10720.

Van Ness, B.G., Howard, J.B., Bodley, J.W., 1980b. ADP-ribosylation of elongation factor 2 by diphtheria toxin. NMR spectra and proposed structures of ribosyl-diphthamide and its hydrolysis products. J Biol Chem 255, 10710-10716.

Vesselkin, N., Agayan, A., Nomokonova, L., 1971. A study of thalamo-telencephalic afferent systems in frogs. Brain, Behavior and Evolution 4, 295-306.

Vidal, B.D.C., Mello, M.L.S., Pimentel, É.R., 1982. Polarization microscopy and microspectrophotometry of Sirius Red, Picrosirius and Chlorantine Fast Red aggregates and of their complexes with collagen. The Histochemical Journal 14, 857-878.

Vileikyte, L., 2007. Stress and wound healing. Clin Dermatol 25, 49-55.

Vivien, C.J., Hudson, J.E., Porrello, E.R., 2016. Evolution, comparative biology and ontogeny of vertebrate heart regeneration. NPJ Regen Med 1, 16012.

Voss, S.R., Epperlein, H.H., Tanaka, E.M., 2009. Ambystoma mexicanum, the axolotl: a versatile amphibian model for regeneration, development, and evolution studies. Cold Spring Harb Protoc 2009, pdb emo128.

Voss, S.R., Kump, D.K., Putta, S., Pauly, N., Reynolds, A., Henry, R.J., Basa, S., Walker, J.A., Smith, J.J., 2011. Origin of amphibian and avian chromosomes by fission, fusion, and retention of ancestral chromosomes. Genome Res 21, 1306-1312.

Wadugu, B., Kuhn, B., 2012. The role of neuregulin/ErbB2/ErbB4 signaling in the heart with special focus on effects on cardiomyocyte proliferation. Am J Physiol Heart Circ Physiol 302, H2139-2147.

Waldhoer, M., Bartlett, S.E., Whistler, J.L., 2004. Opioid receptors. Annu Rev Biochem 73, 953-990.

Walter, P., Johnson, A.E., 1994. Signal sequence recognition and protein targeting to the endoplasmic reticulum membrane. Annu Rev Cell Biol 10, 87-119.

Wang, J., Bo, H., Meng, X., Wu, Y., Bao, Y., Li, Y., 2006. A simple and fast experimental model of myocardial infarction in the mouse. Tex Heart Inst J 33, 290-293.

Wang, J., Cao, J., Dickson, A.L., Poss, K.D., 2015. Epicardial regeneration is guided by cardiac outflow tract and Hedgehog signalling. Nature 522, 226.

Wang, J., Panakova, D., Kikuchi, K., Holdway, J.E., Gemberling, M., Burris, J.S., Singh, S.P., Dickson, A.L., Lin, Y.F., Sabeh, M.K., Werdich, A.A., Yelon, D., Macrae, C.A., Poss, K.D., 2011. The regenerative capacity of zebrafish reverses cardiac failure caused by genetic cardiomyocyte depletion. Development 138, 3421-3430.

Welfare, O.o.L.A., 2015. Public Health Service Policy on Humane Care and Use of Laboratory Animals, NIH Publication No. 15-8013. National Institutes of Health

U.S. Department of Health and Human Services

Whited, J.L., Lehoczky, J.A., Tabin, C.J., 2012. Inducible genetic system for the axolotl. Proc Natl Acad Sci U S A 109, 13662-13667.

Whited, J.L., Tabin, C.J., 2010. Regeneration review reprise. J Biol 9, 15.

Whited, J.L., Tsai, S.L., Beier, K.T., White, J.N., Piekarski, N., Hanken, J., Cepko, C.L., Tabin, C.J., 2013. Pseudotyped retroviruses for infecting axolotl in vivo and in vitro. Development 140, 1137-1146.

Whitmarsh, A.J., 2007. Regulation of gene transcription by mitogen-activated protein kinase signaling pathways. Biochim Biophys Acta 1773, 1285-1298.

Whittaker, P., Kloner, R., Boughner, D., Pickering, J., 1994. Quantitative assessment of myocardial collagen with picrosirius red staining and circularly polarized light. Basic research in cardiology 89, 397-410.

Willenbring, S., Stevens, C.W., 1996. Thermal, mechanical and chemical peripheral sensation in amphibians: opioid and adrenergic effects. Life Sci 58, 125-133.

Williamson, J.R., 1966. Glycolytic control mechanisms. II. Kinetics of intermediate changes during the aerobic-anoxic transition in perfused rat heart. J Biol Chem 241, 5026-5036.

Witman, N., Murtuza, B., Davis, B., Arner, A., Morrison, J.I., 2011. Recapitulation of developmental cardiogenesis governs the morphological and functional regeneration of adult newt hearts following injury. Dev Biol 354, 67-76.

Woods, A., Oh, E.S., Couchman, J.R., 1998. Syndecan proteoglycans and cell adhesion. Matrix Biol 17, 477-483.

Wright, K.M., 2000. Surgery of amphibians. Vet Clin North Am Exot Anim Pract 3, 753-758, viii.

Wright, K.M., Whitaker, B.R., 2001. Amphibian medicine and captive husbandry, Original ed. Krieger Pub. Co., Malabar, Fla.

Xin, M., Olson, E.N., Bassel-Duby, R., 2013. Mending broken hearts: cardiac development as a basis for adult heart regeneration and repair. Nat Rev Mol Cell Biol 14, 529-541.

Xu, J., Murphy, S.L., Kochanek, K.D., Bastian, B.A., 2016. Deaths: Final Data for 2013. Natl Vital Stat Rep 64, 1-119.

Yamamoto, A., Hen, R., Dauer, W.T., 2001. The ons and offs of inducible transgenic technology: a review. Neurobiol Dis 8, 923-932.

Yang, F., Liu, Y.H., Yang, X.P., Xu, J., Kapke, A., Carretero, O.A., 2002. Myocardial infarction and cardiac remodelling in mice. Exp Physiol 87, 547-555.

Yang, W.J., Li, S.H., Weisel, R.D., Liu, S.M., Li, R.K., 2012. Cell fusion contributes to the rescue of apoptotic cardiomyocytes by bone marrow cells. J Cell Mol Med 16, 3085-3095.

Yue, X., Yu, H., Lin, X., Liu, K., Wang, X., Zhou, F., Zhao, J., Zou, B., 2013. Investigation into the optimal surgical conditions for coronary artery ligation for establishing a myocardial infarction model in mice. Exp Ther Med 6, 341-346.

Zacchigna, S., Giacca, M., 2014. Extra- and intracellular factors regulating cardiomyocyte proliferation in postnatal life. Cardiovasc Res 102, 312-320.

Zemljic-Harpf, A., Manso, A.M., Ross, R.S., 2009. Vinculin and talin: focus on the myocardium. J Investig Med 57, 849-855.

Zhang, R., Han, P., Yang, H., Ouyang, K., Lee, D., Lin, Y.F., Ocorr, K., Kang, G., Chen, J., Stainier, D.Y., Yelon, D., Chi, N.C., 2013. In vivo cardiac reprogramming contributes to zebrafish heart regeneration. Nature 498, 497-501.

Zhao, B., Li, L., Lei, Q., Guan, K.L., 2010. The Hippo-YAP pathway in organ size control and tumorigenesis: an updated version. Genes Dev 24, 862-874.

Zhen, J., Lu, H., Wang, X.Q., Vaziri, N.D., Zhou, X.J., 2008. Upregulation of endothelial and inducible nitric oxide synthase expression by reactive oxygen species. Am J Hypertens 21, 28-34.

Zhivotovsky, B., Orrenius, S., 2011. Calcium and cell death mechanisms: a perspective from the cell death community. Cell Calcium 50, 211-221.

Zhou, Q., Li, L., Zhao, B., Guan, K.L., 2015. The hippo pathway in heart development, regeneration, and diseases. Circ Res 116, 1431-1447.

Zielonko, J., 1875. Pathologisch-anatomische und experimentelle Studien über Hypertrophie des Herzens. Archiv für pathologische Anatomie und Physiologie und für klinische Medicin 62, 29-57.

Zimmermann, R., Muller, L., Wullich, B., 2006. Protein transport into the endoplasmic reticulum: mechanisms and pathologies. Trends Mol Med 12, 567-573.

ABSTRACT

DEVELOPMENT OF A NOVEL CARDIAC ISCHEMIA-REPERFUSION MODEL IN THE AXOLOTL

by

JEREMY (JAY) T. LLANIGUEZ

August 2018

Advisor: Dr. Juri G. Gelovani

Major: Biomedical Engineering

Degree: Doctor of Philosophy

The Center for Disease Control's National Center for Health Statistics data on mortality from diseases of the heart show the age-adjusted death rate has fallen from almost 600 deaths in the 1950s to just over 190 deaths per 100,000 U.S. residents today. With the recognized limitations of pharmacotherapy of myocardial infarction (MI), cell-based therapies have been undergoing rapid development and clinical testing. However, there is still no consensus about cell types, delivery routes, dosing and treatment schedules and pretreatment conditioning of cells prior to administration. Furthermore, a fundamental question remains unanswered about the reasons for the poor capacity for myocardial tissue regeneration in humans (mammals in general) as compared to robust myocardial regeneration in non-mammalian vertebrates (i.e., axolotl [*Ambystoma mexicanum*] and zebrafish [*Danio rerio*]). This lack in understanding the mechanisms behind the cell-cycle of cardiomyocytes and or cardiac progenitor cells, both during times of normal homeostasis and after pathologic insults, is central to the lack of progress in

stimulating the regeneration of cardiac tissue. To understand the differences in cardiac tissue response after an MI, developing a true model of ischemia-reperfusion injury in an animal known for epimorphic regeneration in the adult life stage like the axolotl will help reframe the direction of research in the field of tissue engineering and regenerative medicine in the realm of cardiology. To understand how the axolotl will respond to an MI, this research focuses on two Specific Aims:

Specific Aim 1: Develop a cardiac injury model in the axolotl that mimics the pathophysiology of a myocardial infarction in the mammalian heart. Cardiac injury models used to study heart regeneration in non-mammalian vertebrates known for robust healing responses have used novel approaches to induce major cardiomyocyte death. However, these novel injury models do not recapitulate the cellular signaling mechanisms present during ischemia and ischemia-reperfusion injuries. Thus, to study the epimorphic regeneration of heart tissue in axolotls, a novel model of inducing ischemia needs to be developed.

Specific Aim 2: Determine the spatiotemporal progression of axolotl cardiac tissue histopathology over time. Once a novel cardiac injury model produces the expected pathophysiological tissue response, chronic follow-up of surviving animals will help develop the spatiotemporal response to an MI. Data on functional recovery will require the development of regular, non-invasive techniques for monitoring heart function. After long-term recovery, appropriate harvesting of heart samples for histologic study is required to determine if the axolotl can completely regenerate cardiac injuries after an MI.

AUTOBIOGRAPHICAL STATEMENT

Before joining the MD/PhD. program at Wayne State University's (WSU) School of Medicine (SOM), Jay (née: Jeremy) spent time working as an engineer in the automotive, aerospace, and medical device industries. In the medical device field, the "language" barrier between physician consultants and engineers presented a hurdle in product development. Thus, his overall career goal is to bridge the clinical, scientific and engineering aspects of medicine and medical technology to accelerate advances in medical knowledge and therapeutic approaches. Ideally, his career goals include working as a practicing physician, continually learning about and applying medicine, to better understand what areas of medicine need improvement. This will inform his involvement as a scientist-engineer in the research, design and delivery of therapeutics that can benefit scores of patients, hoping to rein in the exploding costs of healthcare today.

As a student leader of WSUSOM's student senate and nationally with the American Medical Association Medical Student Section, Jay involves himself in accelerating changes in medical education, the social responsibility of medicine and medical practice, and the social justice of equal access to healthcare for all patients.

EDUCATION

Wayne State University School of Medicine, Detroit, MI
MD/PhD; PhD Candidate in Biomedical Engineering 2011 – 2020 (est)
Dissertation: "Development of a Novel Ischemia-Reperfusion Model in the Axolotl"
Sub-Study: "Efficacy of buprenorphine and butorphanol in relieving pain using a novel cardiac injury model in axolotls"
Sub-Study: "Qualitative and quantitative behavioral measurements to assess pain in axolotls"

Massachusetts Institute of Technology, Cambridge, MA
MS in Mechanical Engineering 2001-2003
Thesis: "A Fundamental Study of Relationships Among Fuel Properties, Combustion Characteristics, and Emissions with Normal and Synthetic Diesel Fuel"

University of California at Berkeley, Berkeley, CA
BS (With Honors) in Mechanical Engineering 1997-2001
Area of Concentration: Combustion theory and application.
Minor: Chemical Engineering

AWARDS

AALAS – Grant for Laboratory Animal Science **2016**
WSU SOM Board of Governors Full Tuition Scholarship **January 2011 – January 2013**
WSU SOM Medical Student Research Scholarship **January 2011 – January 2013**
Outstanding Abstract, Univ. of Mich.-WSU Physiology Symposium **January 2011**